Metabolic and Respiratory Control of Absence Epilepsy

Kathryn Anne Salvati

Roselle Park, NJ

Bachelor of Science in Biology

Washington and Lee University, 2012

A Dissertation presented to the Graduate Faculty

of the University of Virginia in Candidacy for the Degree of

Doctor of Philosophy

Neuroscience Graduate Program

Department of Pharmacology

University of Virginia

December 2021

Abstract

Metabolic and Respiratory Control of Absence Epilepsy

Kathryn A. Salvati

Advisor: Mark P. Beenhakker, Ph.D.

Absence epilepsy is a pediatric seizure disorder characterized by brief, stereotyped electrographic patterns that often rapidly spread across the brain. Decades of work demonstrate that absence seizures arise from paroxysmal activity within neural networks connecting the thalamus and cortex. How these seizures *spontaneously* occur remains unknown. Herein, I provide evidence to advance the argument that absence seizures are not simply random events, but are, in fact, events that emerge following disruptions in metabolism and respiration.

First, I present data that supports a long-storied observation that absence seizures worsen during episodes of acute hypoglycemia. I demonstrate that this effect is likely linked to the interaction between the cellular energy sensor AMPK and postsynaptic $GABA_B$ receptors expressed by thalamocortical neurons. Next, I summarize the history and scientific findings that detail hyperventilation-induced absence seizures and describe work on existing pH-sensitive elements expressed by neurons of the thalamus. Lastly, I adapt the clinical tool of voluntary hyperventilation in human absence patients to an inbred, rodent model of absence seizures, the WAG/Rij rat. I show that seizure occurrence is sensitive to fluctuations in PCO_2.

In sum, my work highlights how two factors, metabolism and respiration, enhance the probability that the brain enters a state permissive for the expression of absence seizures. Armed with this foundational knowledge, future work can now identify strategies to suppress the underlying mechanisms to develop better treatments for absence epilepsy, the most common pediatric seizure disorder.

Acknowledgements

My Family: Mom, Dad, Meghan and Walker, thank you for all your love and support. I am not sure this would have been possible without you.

The Igloo: Annie (Will & Lexington), Lauren, and Dana, you all have helped me stay motivated to reach my goals since college. Thank you for always being a shoulder to cry on or a phone call away when I needed you most. Friends like you last a lifetime.

Mark: What a wild ride. You taught me everything I know about how to be a successful scientist. Thank you for your mentorship, holding my hand through the difficult times, celebrating my achievements, and endless patience. I hope we remain colleagues and, most importantly, friends throughout our careers.

Peter and Adi: My lab brothers. Peter, thank you for being the best lab mate and friend. You taught me how to be a great graduate student. I learned so much from you. I am so happy we are still neighboring epilepsy researchers in California. Adi, **y**our friendship has been invaluable. I know you will be an amazing surgeon and I cannot wait for you to achieve your goals.

My Committee: Jaideep, Howard, Doug, Paula, and Patrice, thank you for guiding me along my scientific journey. I have learned so much from you during our meetings and informal chats throughout the years. You helped me believe in myself and gain the self-confidence necessary to be a PhD. Your support and advice (scientific and personal) will continue to influence my scientific career.

The Pharmacology Department and NGP: I cannot summarize in words how much I appreciate everything you have helped me achieve. It truly takes a village.

Funding

The work enclosed was funded by intramural support from the NIH funding agencies NINDS (R01 NS099586), NIAMS (R01 AR050429), NIDDK (K99/R00-AG057825), NIGMS (T32G007055), and the American Heart Association (#19POST34430205).

Glossary of Terms:

Thalamus: a subcortical brain structure comprised of many nuclei that is organized into three divisions: the epithalamus, the dorsal thalamus, and the ventral thalamus. These nuclei function as major relay sites for sensory and motor information among the cortex and other subcortical brain structures. Thalamocortical and intrathalamic circuits are implicated as critical seizure nodes in absence epilepsy.

Specific Nuclei: refers to the major sensory relay nuclei of the dorsal thalamus, including the ventral anterior nucleus (VA), ventral posterior lateral nucleus (VPL), ventral posterior medial nucleus (VPM), lateral geniculate nucleus (LGN), medial lateral geniculate nucleus (MGN).

Non-Specific Nuclei: refers to nuclei of the thalamus that are not considered major sensory relay nuclei. The midline and intralaminar nuclei are members of the non-specific thalamic projection system (NSTPS).

Midline Nuclei: refers to thalamic nuclei along the midline, including the nucleus centré median (NCM), mediodorsal nucleus (MD), reunions (Re), rhomboid (Rh), posterior thalamic nucleus (Po), and the intralaminar nuclei.

Intralaminar Nuclei: refers to a collection of nuclei in the midline thalamus, including the central lateral nucleus (CL), paracentral nucleus (PC), parafasicular nucleus (Pf) as well as the nucleus centré median (NCM).

Reticular Thalamic Nucleus (RT): a population of inhibitory interneurons surrounding the dorsal thalamus. The RT is often referred to as the "keeper of the gateway" to the thalamus, as all projections to and from the cortex pass through the RT. The RT is an intrinsic thalamic pacemaker, thought to be responsible for generating intrathalamic oscillations important during sleep (sleep spindles) and wake states.

Sleep Spindles: 10-12 Hz oscillations thalamic oscillations that occur in non-REM sleep. These oscillations are thought to be important for memory consolidation.

Spike-and-Wave Discharge: 3 Hz oscillations (5-7 Hz in rodents), considered the electrographic signature of an absence seizure.

Recruiting Response: a high-voltage negative potential elicited in the cortex following direct, repetitive electrical stimulation of the midline thalamus.

Primary Response: a multifaceted electrical potential elicited in the cortex after low-voltage stimulation of a specific thalamic nucleus. The first phase of the primary response consists of an initial surface positive potential followed by a small amplitude negative potential. Repetitive stimulation evokes a second negative potential, larger amplitude, known as the augmenting response.

Feline Generalized Penicillin Epilepsy (FGPE): a model of absence epilepsy introduced by Prince and Farrell (1969). Intramuscular injection of penicillin, a $GABA_A$ receptor antagonist, elicits cortical SWD activity. The FGPE was a widely used model in studies investigating the underlying mechanisms of SWDs. Later, the FGPE was phased out by the use of in-bred genetic rat models of absence epilepsy.

I_h current: hyperpolarization-activated cation current encoded by the HCN channel. An important ionic conductance setting the resting membrane potential of thalamocortical neurons.

I_T current: low-threshold Ca^{2+} current encoded by the T-type Ca^{2+} channel. Another critical ionic conductance setting the resting membrane potential of thalamocortical neurons. Also, important for low threshold calcium bursts of activity.

Retrotrapezoid Nucleus (RTN): a thin layer of densely packed neurons between the facial nucleus and ventral surface of the medulla. The RTN acts as a CO_2^+ and H^+ sensor regulating respiration.

Respiratory Alkalosis: a disturbance in acid and base balance due to alveolar hyperventilation. Hyperventilation is defined by a decreased partial pressure of carbon dioxide ($PaCO_2$) in the blood. A consequent decrease in PCO_2 leads to an increase in bicarbonate concentration, relative to PCO_2, thereby, increasing pH (alkalosis).

Hypocapnia: a state of reduced carbon dioxide in the blood. Also known as hypocarbia.

Hypercapnia: a state of increase carbon dioxide in the blood. Also known as hypercarbia.

Table of Contents

Chapter 1: Introduction - Childhood Absence Epilepsy

"*Les absences ne sont pas rares chez les épileptiques ; elles ne paraissent point dangereuses, mais au moins constituent-elles un phénomène curieux* (Calmeil, 1824)*"*

Overview

The following pages provide a clinical history of childhood absence epilepsy (CAE) as well as a survey of the relevant literature that details the underlying neural circuitry intimately associated with absence seizures. **Section I** will highlight the clinical features of absence epilepsy. Then, **Section II** will detail the current known genetic etiology of childhood absence epilepsy in humans and rodent models. Current treatments and outcomes for CAE patients follows in **Section III**. Special attention will be given to animal models, in **Section IV**, used to study absence seizures. I will underscore the important contributions that animal models have provided in elucidating the mechanisms at the core of absence seizures. **Section V** will describe the thalamus and the thalamocortical circuit. Therein, this section will discuss the origin of the spike-wave discharge (SWD), the electrographic signature of absence seizures. A closer examination of the canonical thalamocortical circuit will be broached in **Section VI.** Next, in **Section VII,** I will summarize the intrinsic properties of thalamic neurons and how these properties facilitate absence seizure generation**.** Lastly, **Section VIII** will provide a brief synopsis of how two factors, metabolism and respiration, modulate absence seizures. My dissertation work on these two topics will be highlighted in **Chapters 2** through **Chapter 4**.

I. Clinical history

In 1770, a Swiss physician, Samuel Tissot, reported his observations of a young girl who lost consciousness multiple times a day (Tissot, 1770). Although impairment of consciousness was already a known symptom of epilepsy, the lack of any concomitant convulsions led Tissot to conclude that the girl's epilepsy was distinct (Tissot, 1770). Tissot's instincts were correct and he is credited with coining these events as *petit mal* seizures. Only much later, in 1939, did we discover the dramatic, highly-stereotyped, electrical activity patterns that likely pulsed within the little girl's brain during her brief episodes of unconsciousness. It was Gibbs et al. who used newly developed electroencephalogram (EEG) recording techniques to describe the characteristic 3-Hz, spike-wave discharge (SWD) now synonymous with absence epilepsy (Figure 1) (F. Gibbs & Davis, 1935). Over 80 years later, clinicians still use the electrographic signature of the SWD, accompanied by a loss of consciousness, as diagnostic criteria for absence epilepsy.

In 1989, the International League Against Epilepsy (ILAE) partitioned absence epilepsy into two distinct epilepsy syndromes: *Childhood Absence Epilepsy* (CAE) and *Juvenile Absence Epilepsy* (JAE) (Commission on Classification and Terminology of the International League Against Epilepsy, 1989). While seizures associated with CAE and JAE are both characterized by impaired consciousness and 3-4 Hz SWDs, differences between the two syndromes exist. Trinka et al. retrospectively examined 163 patients to identify pyknoleptic absences and non-pyknoleptic absences (Trinka et al., 2004). While such terminology has generally fallen out of favor, *pyknoleptic absences* refer to seizures that occur in clusters, often hundreds per day, while *non-pyknoleptic absences* occur less frequently (i.e. <1 per day). Pyknoleptic absences are also associated with an abrupt and severe state of unconsciousness, while the state of unconsciousness associated with non-pyknoleptic absences is often less pronounced.

When the operational distinction between pyknoleptic and non-pyknoleptic absences is applied to patients, absence epilepsy appears to subdivide into two syndromes with differing onset ages (Trinka et al., 2004). CAE has a peak onset between 5-7 years of age (Matricardi et al., 2014) and associates with frequent, abrupt absences (i.e. pyknoleptic). In contrast, JAE diagnosis occurs in early adolescence (mean age of onset: 15 years) and typically presents with infrequent absences (i.e. non-pyknoleptic). Moreover, JAE patients present with additional, different seizure types at the time of diagnosis. Specifically, Trinka et al. reported that nearly 95% of JAE patients eventually develop generalized tonic-clonic seizures (GTCS), compared to 69% of CAE patients; other reports suggest that GTCS prevalence in the CAE population may be much lower (Shinnar et al., 2015).

In aggregate, the data indicate that two distinct absence epilepsy syndromes exist. In CAE, relatively young patients present with frequent, abrupt seizures of a singular form that generally subside with age. In JAE, older children have fewer, less pronounced absence seizures, and exhibit other seizure subtypes that, collectively, are less likely to remit. Despite these differences, much overlap between CAE and JAE exists, leading some to argue that absence epilepsy represents a continuum of syndromes primarily characterized by SWDs (Guilhoto, 2017; Reutens DC, 1995). Moreover, absence seizures are not unique to children and juveniles. Absence seizures occur in adults, more often in women (Gastaut, 1981; Panayiotopoulos et al., 1992). Sometimes these seizures recur in patients who had absence seizures in their youth (Berkovic & Bladin, 1983; Michelucci et al., 1996). Usually, these absence episodes arise in conjunction with other idiopathic generalized epilepsies (IGE) (Marini et al., 2003) or psychoses (Iivanainen et al., 1984). Thus, while CAE represents the prototypical form of the epileptic disorder, absence seizures consisting of SWDs with concomitant impaired consciousness are observed in wide-ranging clinical contexts.

Finally, electrographic SWDs and unconsciousness are not the only feature of absence epilepsy; associated comorbidities include attentional problems, depression, anxiety and memory impairments (Tenney & Glauser, 2013). Although treated absence patients have cognitive functioning within a normal range, these children have been found to be on the lower end of normalcy (Fonseca Wald et al., 2019). Significantly, many analyses of cognitive function represent the performance of CAE patients amid the active stage of their epilepsy (Fonseca Wald et al., 2019). Few studies exist that detail the long-term cognitive deficits after CAE remission (Fonseca Wald et al., 2019). Future work should focus on long-term observational studies of patients into adulthood. Thus, clinicians must give due consideration to treatment plans that address cognitive developmental deficits *and* seizure management.

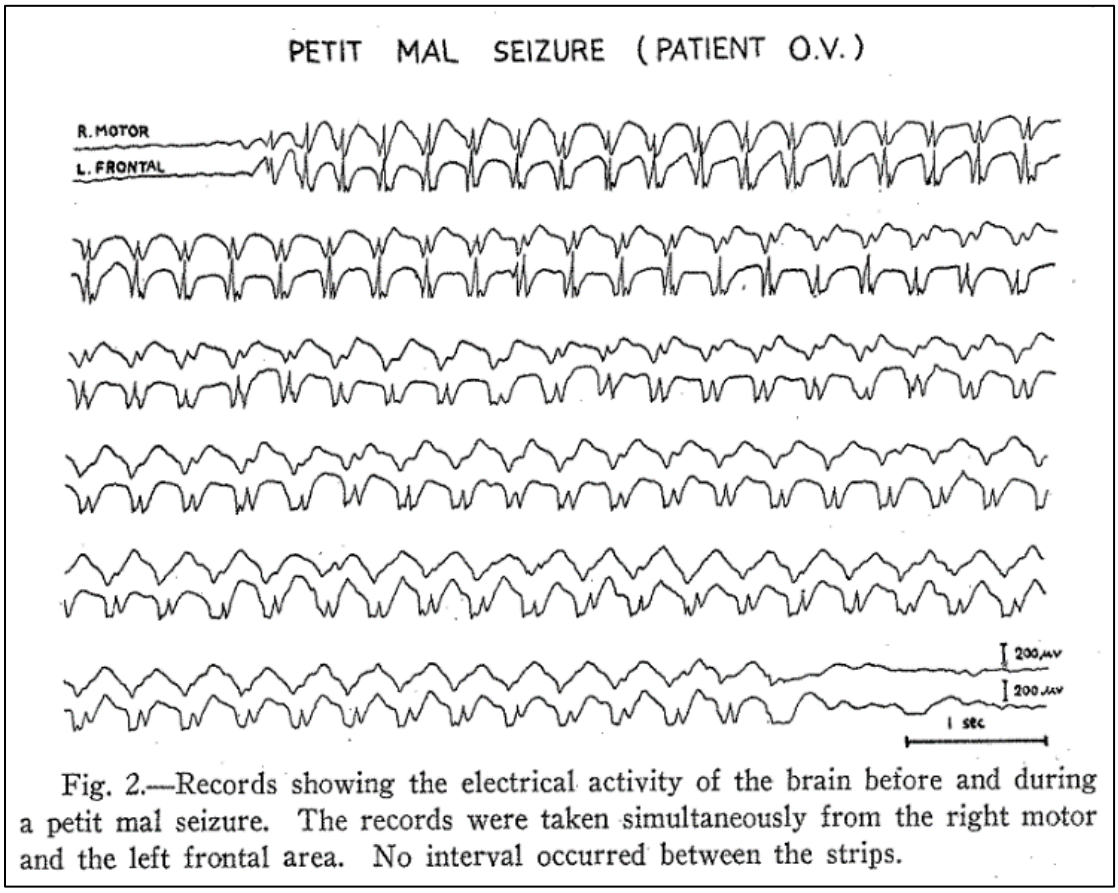

Fig. 2.—Records showing the electrical activity of the brain before and during a petit mal seizure. The records were taken simultaneously from the right motor and the left frontal area. No interval occurred between the strips.

Figure 1. Example absence seizure, from Gibbs et al., 1935. The above EEG recording was performed using electrodes placed in the right motor and left frontal cortices of an absence epilepsy patient. The 3Hz, spike-wave discharge appears on both recording channels, indicating that absence seizures generalize throughout the entire cortex.

II. Etiology

The causes of absence epilepsy are complex and varied, but primarily involve genetic mutations. While many rodent studies highlight potential mechanisms underlying absence epilepsy (Coenen, 2003; Cortez et al., 2016; Depaulis et al., 2016; Depaulis & Charpier, 2017; Felix, 2002), herein, I focus on human genetic mutations associated with the disorder. To date, identified human mutations include genes encoding for specific subunits of *(1)* the primary ionotropic receptor for γ-aminobutyric acid (GABA), the main inhibitory neurotransmitter in the brain, and *(2)* the low threshold, T-type calcium channel. The primary ionotropic receptor for GABA, also called the A-type GABA ($GABA_A$) receptor, is a pentameric structure, wherein each of the 5 subunits corresponds to one of four subunit subtypes: α, β, δ, γ (Cortez et al., 2016; Jones-Davis & Macdonald, 2003; Macdonald et al., 2010; Rudolph et al., 2001). Identified, CAE-associated mutations have been localized to the γ2 (Tan et al., 2007), α1 (Cossette et al., 2002; Lachance-Touchette et al., 2011; Maljevic et al., 2006) and β3 (Holopainen et al., 2001; Huntsman et al., 1999; Roden et al., 2010) subunits of the $GABA_A$ receptor.

While more studies are required, the aforementioned $GABA_A$ receptor subunit mutations generally appear to reduce the ability of the receptor to traffic to the plasma membrane of neurons (Kang & Macdonald, 2004). For example, mice heterozygous for the R43Q point mutation in the γ2 subunit produce SWDs (Kang & Macdonald, 2004). Cortical neurons in these mice receive reduced GABAergic inhibition, an effect attributed to reduced surface expression of the receptor; GABAergic inhibition was largely spared in other brain structures involved in SWD generation. Similar to the R43Q mutation in the γ2 subunit, α1 subunit mutations are also associated with both increased SWDs (Cossette et al., 2002; Maljevic et al., 2006) and reduced $GABA_A$ receptor expression at the cell membrane (Lachance-Touchette et al., 2011; Maljevic et al., 2006). Finally, mutations in

the β3 subunit of the $GABA_A$ receptor are also associated with SWDs. And again, the emerging picture indicates that β3 subunit mutations reduce the number of functional $GABA_A$ receptors and, generally, reduce inhibition (Huntsman et al., 1999; Jones-Davis & Macdonald, 2003; Roden et al., 2010).

In contrast to the aforementioned, loss-of-function mutations in the $GABA_A$ receptor, gain of function T-type Ca^{2+} channel mutations associate with absence epilepsy. Chen et al. originally identified missense mutations in *CACNA1H*, the gene encoding the α1H subunit of the T-type channel complex, in a Han Chinese cohort (Chen et al., 2003). Subsequent studies on other, non-Chinese populations confirm that *CACNA1H* mutations are associated with CAE (Heron et al., 2007). Consistent with these observations, several studies have demonstrated that CAE-associated *CACNA1H* mutations generally lead to greater calcium influx through the channel following activation (Khosravani & Zamponi, 2006; Peloquin et al., 2006; Vitko et al., 2005). Greater Ca^{2+} influx, in turn, is thought to support robust low-threshold Ca^{2+} spikes that sustain SWDs (see **Section IV**). The induction of absence seizure-like SWDs in otherwise normal rats by the introduction of the human-associated, C456S, gain-of-function *CACNA1H* mutation supports this hypothesis (G. Wang et al., 2015). However, this conclusion warrants a word of caution. Epilepsy-associated variants in *CACNA1H* are also observed in *unaffected* individuals (Heron et al., 2007), suggesting that T-type Ca^{2+} channel mutations appear to increase CAE susceptibility, but alone do not cause CAE. Indeed, the emerging paradigm is that most epilepsies are complex disorders that do not arise from a single, clear biological origin (Heron et al., 2007; Staley, 2015). Instead, the *Genetic Generalized Epilepsies* are multifactorial disorders that likely involve mutations in several proteins (i.e. polygenic), and are disorders often influenced by the environment (Saul A. Mullen & Berkovic, 2018).

III. Outcome and treatment

As remission often occurs by early adulthood, absence epilepsy is frequently described as a mild seizure disorder. Such a designation requires reconsideration (Tenney & Glauser, 2013). *First*, reported remission rates are variable and generally not as high as commonly perceived. Several studies report that approximately 60% of subjects remit by 20 years of age (Loiseau et al., 1983; Trinka et al., 2004; Wirrell et al., 1997), although the number of seizure-free subjects no longer requiring medication is likely lower (Sillanpää et al., 1998). *Second*, prior to possible remission, a cocktail of anti-seizure drugs (ASDs) – Ethosuximide, Valproate and Lamotrigine – is sometimes recommended to manage seizures (Glauser et al., 2013). While ASD cocktails are at times effective, the treatment strategy also often contributes to additive and intolerable side-effects (Matricardi et al., 2014). Moreover, little is known regarding the effects of such a blunt pharmacological strategy on the developing brain. *Third,* long-term cognitive and psychosocial problems are prominent in absence patients. Comorbidities include social anxiety disorder, depression, attention deficit disorder and behavioral/linguistic problems (Caplan, 2015; Caplan et al., 2008; Fonseca Wald et al., 2019; Tenney & Glauser, 2013; Wirrell et al., 1997). Considering remission rates, available treatment methods and comorbidities, labeling absence seizures as *benign* appears inappropriate.

IV. Animal models

Decades of research highlight how reciprocal interactions between cortical and thalamic circuits act as critical architects of absence seizure generation (Avoli, 2012). Greater discussion of the thalamocortical network will be presented in **Section V**. Before highlighting this work, it is important to define terms used when characterizing seizures. First, seizures are largely either *focal* or *generalized*. Focal seizures are marked by aberrant electrical activity localized to a singular (or few) brain structure(s). In contrast,

generalized seizures are associated with aberrant activity throughout the brain, usually excluding the cerebellum. The nature and extent to which aberrant electrical activity is generalized throughout the brain often provide critical insights into the underlying *ictogenic* (i.e. seizure generating) mechanisms. Thus, when early clinical investigators noted a lack of cortical focus in the EEG of absence seizures, they postulated that subcortical structure(s) are responsible for the widespread cortical discharges (Jasper & Kershman, 1941; Penfield & Erickson, 1942). These hypotheses were largely tested and confirmed in non-primate animals.

Insights into the neural circuits associated with CAE were largely derived from the use of several animal models. The earliest studies utilized anesthetized cat preparations to study the thalamocortical circuitry engaged in sleep and wake cycles. Eventually, these preparations led to studies probing how paroxysmal activity in thalamocortical networks generates SWDs. In the late 1970s, the introduction of the feline generalized model of epilepsy (FGPE) enabled researchers to model absence seizures without invasive electrical stimulation (Prince & Farrell, 1969). Instead, an intramuscular injection of penicillin, a $GABA_A$ receptor antagonist, evokes the behavioral and electrophysiological features of human absence seizures. The FGPE model demonstrated that removing the cortex, thalamus, or intrathalamic connections abolished the 3-4 Hz SWDs (Fisher & Prince, 1977), highlighting the significance of thalamocortical circuits in CAE.

The FGPE was the predominant animal model of absence epilepsy until it was largely replaced by two inbred rat strains with spontaneous SWDs: (1) the Genetic Absence Epilepsy Rat from Strasbourg (Danober et al., 1998), and (2) the Wister Albino-Glaxo/Rij rat (WAG/Rij) (van Luijtelaar & Coenen, 1986). Both inbred rat strains arose independently but share a common ancestor, the Wistar rat. Evidence supporting the utility of these absence seizure models include (1) the involvement of thalamocortical networks to produce large-amplitude SWDs comparable to those observed in human absence

patients, (2) the associated behavioral arrest and decreased responsiveness in behavioral tasks, and (3) the efficacy of valproate and ethosuximide in reducing SWD expression (Blumenfeld, 2005). While both rat models have enabled researchers to glean a general understanding of SWD mechanisms, they have not provided much insight into the genetic etiology of this disorder.

Both rat models express generalized cortical SWDs with accompanying thalamic hypersynchrony (van Luijtelaar & Coenen, 1986; Vergnes et al., 1987). However, SWDs in the GAERS are limited to the sensory-motor regions of the cortex and primary thalamic nuclei, and SWDs do not appear in the midline nuclei (Vergnes et al., 1987). Moreover, SWDs in GAERS originate in the thalamus or simultaneously in the thalamus and cortex; cortical SWDs never precede those of the thalamus (Vergens et al., 1984). However, a potential reason that cortical SWDs were not captured before thalamic SWDs was due to cortical electrode placement (M. Vergnes et al., 1987). Nonetheless, the progression of seizure activity in the GAERs rat suggests that the thalamus is the site of SWD initiation. However, the absence of SWDs in the midline nuclei directly conflicted with earlier studies in anesthetized cats (Hanbery & Jasper, 1953; Kostopoulos & Avoli, 1983).

Electrographic recordings in the WAG/Rij rat identified the presence of two types of paroxysmal SWDs. The first type occurs predominantly during slow-wave sleep and at sleep-to-wake transitions, whereas the second type appears during periods of wakefulness (van Luijtelaar & Coenen, 1986). In contrast to SWD progression in the GAERS model, a persistent focus in the peri-oral region of the somatosensory cortex precedes all SWDs in the WAG/Rij model (Meeren et al., 2002). Moreover, SWD activity in this focal site occurs before SWDs in the thalamus. Thalamic SWDs often disappear prior to cessation of cortical SWDs. Additionally, cortical SWDs can be observed in the absence of thalamic spikes. In conclusion, the authors proposed that during the first 500msec of a SWD, the cortex initiates and drives the paroxysmal oscillation within the

thalamocortical network (Meeren et al., 2002) While the authors provide strong evidence for this conclusion, it is noteworthy that activity in the midline/intralaminar nuclei was not recorded in the animals. I will address this shortcoming in **Chapter 3**.

In contrast to the rat models, mouse SWD models have provided researchers with genetic tools to understand SWD generation. Several mouse models demonstrate that defects in thalamic inhibition or thalamocortical excitation precipitate the occurrence of absence seizures (Blumenfeld, 2005). For example, a study in which the β3 subunit of the $GABA_A$ receptor was knocked-out demonstrated that defects in GABAergic mediated inhibition in the thalamus leads to hypersynchronous, SWD-associated activity (Huntsman et al., 1999). Additionally, *stargazer*, *tottering*, and *lethargic* mouse models have demonstrated that mutations in voltage-gated Ca^{2+} channels (as well as secondary abnormalities in other proteins) can promote SWDs (Crunelli & Leresche, 2002).

In sum, both rat and mouse models of CAE have their benefits and drawbacks. Currently, the GAERs and WAG/Rij offer a more "organic" approach to understand the etiology of SWDs, but lack the genetic power afforded by mice. As genetic tools continually advance, greater opportunities will be available to explore the mechanisms underlying CAE pathophysiology in both species.

V. The thalamus and the thalamocortical circuit

The thalamus is a subcortical structure referred to as the sensory gateway to the cortex. It is responsible for processing all sensory inputs, excluding olfaction (Jones, 2007). Besides its role as a sensory structure, the thalamus has reciprocal connections with cortical areas critical for executive function and learning (Jones, 2007). Several midline thalamic nuclei work in concert with the basal ganglia to orchestrate motor function (Jones, 2007). Critically, the thalamus produces electrical oscillations during sleep-states, known as sleep spindles, which are likely important for memory consolidation (Steriade &

Llinás, 1988). Moreover, the thalamus is a member of the reticular activating system, a group of subcortical brain structures promoting awake and aroused brain states (Steriade, 1996; Steriade et al., 1993).

In 70 years of research into the mechanisms driving absence seizures, three theories emerged to explain how thalamocortical circuitry is hijacked to produce seizures: the *centrencephalic theory*, the *corticoreticular theory* and the *cortical focus theory* (Figure 2). Each theory presents different hypotheses for SWD-generating mechanisms.

Centrencephalic Theory (Figure 2A): In the 1940s and 1950s, Jasper and colleagues used the anesthetized cat preparation to identify specific thalamic structure(s) capable of acting as a pacemaker for absence seizures (Jasper & Droogleever-Fortuyn, 1947). The authors used electrodes to stimulate various thalamic nuclei to ultimately demonstrate that *repetitive* midline stimulation evokes generalized SWDs comparable to those observed in human absence seizures. Shortly thereafter, Hunter and Jasper demonstrated in the *awake cat* that repetitive stimulation of the midline also elicits behavioral arrest accompanied by SWDs in the EEG (Hunter & Jasper, 1949). Electrical stimulation of sensory thalamic nuclei did not elicit the same features as the midline nuclei.

Following the discovery that the midline thalamus uniquely precipitates SWDs, there was great interest in more precisely delineating the contributions of each thalamic nuclei during an absence seizure. Hanbery and Jasper utilized thermocoagulation techniques to lesion several nuclei of the sensory thalamus to determine whether the cortical recruiting response (detailed in **Chapter 3**) could be maintained after electrical stimulation of the midline (Hanbery & Jasper, 1953). Striking results from their work reveal that midline stimulation still evokes a recruiting response in the absence of the sensory nuclei. Indeed, this outcome proved to be a remarkable finding as it was *the* fundamental discovery demonstrating how the midline thalamic nuclei modulates cortical activity independent of the sensory nuclei and suggests that the midline nuclei serve as the

primary orchestrators that can sustain cortical oscillations. While these landmark studies provide little evidence to define how the entire duration of the SWD is sustained, the *centrencephalic theory* presumed that the thalamus is an intrinsic pacemaker and perpetuates synchronous activity independent of cortical inputs (Avoli, 2012).

Corticoreticular Theory (Figure 2B): Several years after Jasper and colleagues introduced the centrencephalic theory, Pierre Gloor offered a different perspective in his "*cortico-reticular*" theory. Gloor argued that one cannot neatly dichotomize the contributions of the cortex and thalamus to SWD generation. Rather, the two structures depend on each other. His hypothesis stemmed from his attempt to assess whether a SWD occurs first in the cortex or in the thalamic/reticular system (Gloor, 1968). To do so, he injected metrazol, a $GABA_A$ receptor agonist, into either the carotid arteries or vertebral artery of the cat and examined SWD activity. Gloor argued that metrazol injection into the carotid arteries selectively targets the cortex, whereas vertebral artery injections target the thalamus and the brainstem. Only carotid injections elicited generalized SWDs; intravertebral injection failed to activate any bilateral SWDs. His results implicate the cortex in initiating SWDs. However, intracarotid injection-induced SWDs were not consistent among patients (Gloor, 1968). When he administered a unilateral injection of PTZ in patients with generalized seizures prolonged the appearance of spike-wave discharges in the EEG. Intravertebral injection of PTZ attenuated the spike-wave discharges. Therefore, Gloor hypothesized that the thalamus and brainstem must also be recruited to modulate the appearance of SWDs. He concluded that these "general cortico-reticular epilepsies" result from underlying pathophysiological disturbances involving both the cortex and reticular projections of the brainstem and thalamus (Gloor, 1968).

To further characterize cortical participation in SWDs, Gloor and Avoli modified the FGPE to include a 5-10 Hz stimulation of the midline thalamus to transform spindle like activity (10-12Hz) into SWDs (Avoli & Gloor, 1982). The authors show that SWDs

initially appear in the cortex yet only occur when thalamocortical connections are intact. In addition, the authors observe that penicillin fails to induce SWD-like activity in the thalamus of decorticated cats; however, unilateral decortication does not prevent SWD-like activity from generalizing throughout the intact corticothalamic hemisphere (Avoli & Gloor, 1982). Only severing the anterior commissure ablated cross-hemisphere migration. Thus, the authors conclude that the cortex may act first to induce SWD activity, but the thalamus is necessary for continuous seizure propagation. Kostopoulos and Gloor later show that SWD generalization in the cortex depends on enhanced activation of the midline thalamus (Kostopoulos & Avoli, 1983). Therein, the authors provide evidence that midline thalamus exclusively evokes long-lasting SWDs in the cortex, whereas stimulation of the lateral, sensory thalamic nuclei elicit short-lasting SWDs constricted to their respective, topographically mapped sensory cortices.

Cortical Focus Theory (Figure 2C): Provocative studies in a feline model of Lennox-Gastaut, an absence-like epilepsy syndrome, indicate that thalamic burst-firing follows cortical SWDs (Timofeev & Steriade, 2004). A similar finding was observed in WAG/Rij rats (Meeren et al., 2002). Simultaneous field recordings from multiple cortices and thalamic sites uncover a focus within the peri-oral subregion of the somatosensory cortex (Meeren et al., 2002). SWD appearance in other cortical sites and sites within the thalamus lag behind this region (Meeren et al., 2002). As such, a *cortical focus theory* of CAE has emerged (Meeren et al., 2005; Meeren et al., 2002). Observations in human absence patients also support the cortical focus theory (Niedermeyer, 1996). Specifically, a cortical focus localized in the frontal lobe occurs in humans during SWD onset (Holmes et al., 2004; Niedermeyer, 1996; Tucker et al., 2007). Detailed functional magnetic resonance (fMRI) and magnetoencephalography (MEG) studies have corroborated the notion of a “focus” in the frontal cortex in recruiting generalized SWDs in humans (Holmes et al., 2004; Hu et al., 2011; Tucker et al., 2007). Significantly, insights gained from fMRI

and MEG studies in CAE patients have motivated a reexamination of key observations made by Morison and Dempsey (Dempsey, 1942a, 1942b; Morison & Dempsey, 1942) and Bancaud (Bancaud, 1969), who collectively argue that the midline nuclei are necessary to trigger SWDs. In contrast to the somatosensory focus documented in the WAG/Rij rat (Meeren et al., 2002), the frontal distribution of SWDs in humans seems to parallel that of the cat and may be indicative of the innate difference in cognitive function and anatomy separating rodents, cats and humans. Such conclusions warrant a word of caution because, as stated earlier, Meeren et al. did not record the midline thalamus.

As new achievements in neuroanatomy, activity-based reporters and *in vivo* recording techniques emerge, all will be instrumental in mapping the temporal progression of absence seizures across the brain. Already, recent studies have begun to unravel the circuit architecture and real-time activity of cortical and thalamic neurons during an absence seizure (McCafferty et al., 2018; Paz et al., 2013). Nevertheless, these studies primarily focus on populations of thalamic neurons already known to associate with absence seizures. Future investigations on the contribution of midline thalamic nuclei and other cell populations outside the reticular and somatosensory thalami are necessary. Potentially, new revelations from such investigation may either support or counter the currently accepted cortical focus theory of absence seizures.

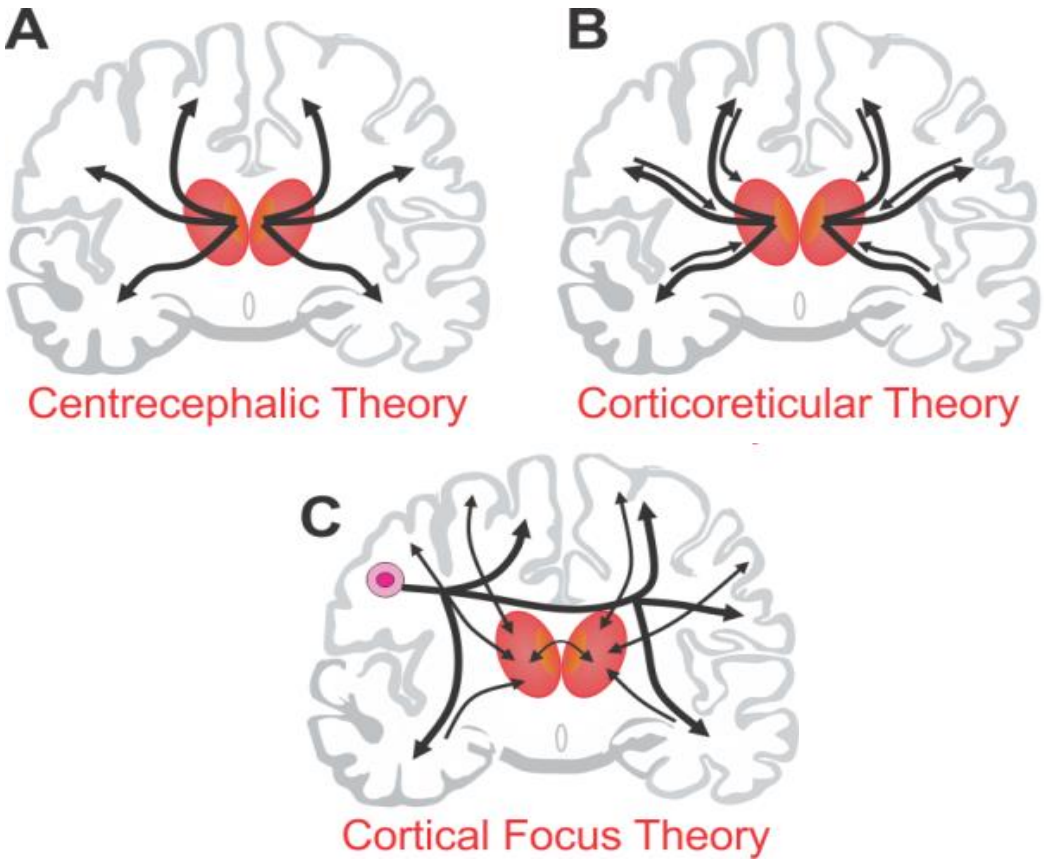

Figure 2. Illustration of three theories regarding the origin and propagation of generalized spike-wave discharges. (A) As illustrated, the centrencephalic theory hypothesizes that the origin of spike-wave seizures stems solely from nuclei of the midline thalamus (red). Midline afferent projections subsequently engage other thalamic nuclei and the cortex to generalize the seizure. **(B)** Evidence from studies using the FGPE demonstrate an interdependency between the cortex and thalamus to precipitate a spike-wave seizure (i.e. Corticoreticular Theory). **(C)** An illustration of the cortical focus theory highlighting the site of spike-wave seizure initiation at a singular cortical focus (pink dot). Focal epileptic activity recruits the thalamus via its efferent corticothalamic projections that in turn excite thalamocortical projection that feedback throughout the entire cortex. Data that illustrate the ability of the spike-wave seizure to generalize through cortico-cortical connections distinguishes aspects of this theory from the corticoreticular theory.

VII. Rhythmic microcircuits in the thalamus

The decades leading up to the 1980s provided invaluable insights into key brain structures associated with absence epilepsy. The decades that followed this era provided a much deeper, mesoscopic understanding of thalamocortical circuit dynamics that produce the SWD. A number of studies from the 1980-90s support the hypothesis that thalamic circuits underlie the rhythmic nature of the SWD (Bal et al., 1995; Contreras et al., 1996; Destexhe, 1998; J. R. Huguenard & McCormick, 1992; Jahnsen & Llinás, 1984a; Llinás & Jahnsen, 1982; McCormick & Bal, 1997; McCormick & Huguenard, 1992; Sherman & Guillery, 1996; Steriade et al., 1993). Three neuronal populations are likely critical for orchestrating thalamocortical rhythms: glutamatergic thalamocortical relay (TC) neurons, glutamatergic corticothalamic (CT) neurons, and GABAergic neurons of the reticular thalamus (RT). The interactions among these three neuron subpopulations have been extensively described in several excellent review articles (Beenhakker & Huguenard, 2009; Huguenard & McCormick, 2007; McCormick & Contreras, 2001); therefore, I only briefly highlight salient aspects of the circuitry.

As depicted in Figure 3, CT neurons send excitatory projections to both RT neurons and TC neurons. RT neurons provide feedforward inhibition to TC neurons. TC neurons, in turn, provide recurrent excitation back to RT neurons. The populations of reciprocally connected RT and TC neurons constitute a critical circuit for generating rhythmic activity patterns in the thalamus. As TC neurons project to the cortex, such rhythmicity is imposed on cortical neurons. Circuit rhythmicity is primarily observed during sleep and seizure states. In contrast, during wakefulness, most thalamic neurons fire action potentials in tonic mode, a firing property in which a neuron produces action potentials at a relatively low and arrhythmic rate. More detail on the firing properties of thalamic neurons and thalamocortical circuit connectivity can be found in **Section VII**.

Several hypotheses attempt to account for the abrupt onset of highly rhythmic circuit activity observed during a SWD. Many of these hypotheses ultimately depend on the activation of robust burst firing in RT and TC neurons. In contrast to the aforementioned tonic firing mode, *burst* firing mode in thalamic neurons, first described by Jahnsen and Llinas (Jahnsen & Llinás, 1984a, 1984b; Llinás & Jahnsen, 1982), is a firing property in which a neuron produces a brief, high-frequency burst of action potentials. Thalamic burst firing depends on low threshold, T-type Ca^{2+} channels (T channel), and is proposed to play a critical role in sustaining thalamic circuit rhythmicity during SWDs (Chen et al., 2003; Cheong & Shin, 2013; Choi et al., 2015). Indeed, as described above, gain-of-function mutations in this channel are associated with absence epilepsy and ethosuximide, a T channel blocker, is used clinically to treat absence epilepsy.

As enhanced T channel activity represents a common thread in most hypotheses regarding SWD generation, many studies have focused on mechanisms that promote thalamic burst firing. We briefly highlight two. *First*, strengthened feedforward, RT neuron-mediated inhibition of TC neurons (see Fig. 3C) is known to promote robust burst firing in TC neurons. The T-type Ca^{2+} channel-mediated mechanism known as *post-inhibitory rebound bursting* drives this TC neuron behavior. Proposed mechanisms that account for augmented feedforward, RT-mediated inhibition include a breakdown of processes that normally dampen RT neuron activity (Castro-Alamancos, 1999; Destexhe, 1998; Huntsman et al., 1999) (see Fig. 3C). *Second*, diminished glutamatergic excitation of RT neurons is proposed to promote SWD generation (Menuz & Nicoll, 2008; Paz et al., 2011) and can lead to enhanced T channel-mediated bursting (Paz et al., 2011). Thus, perturbations in several nodes of the thalamocortical circuit likely contribute to SWD generation.

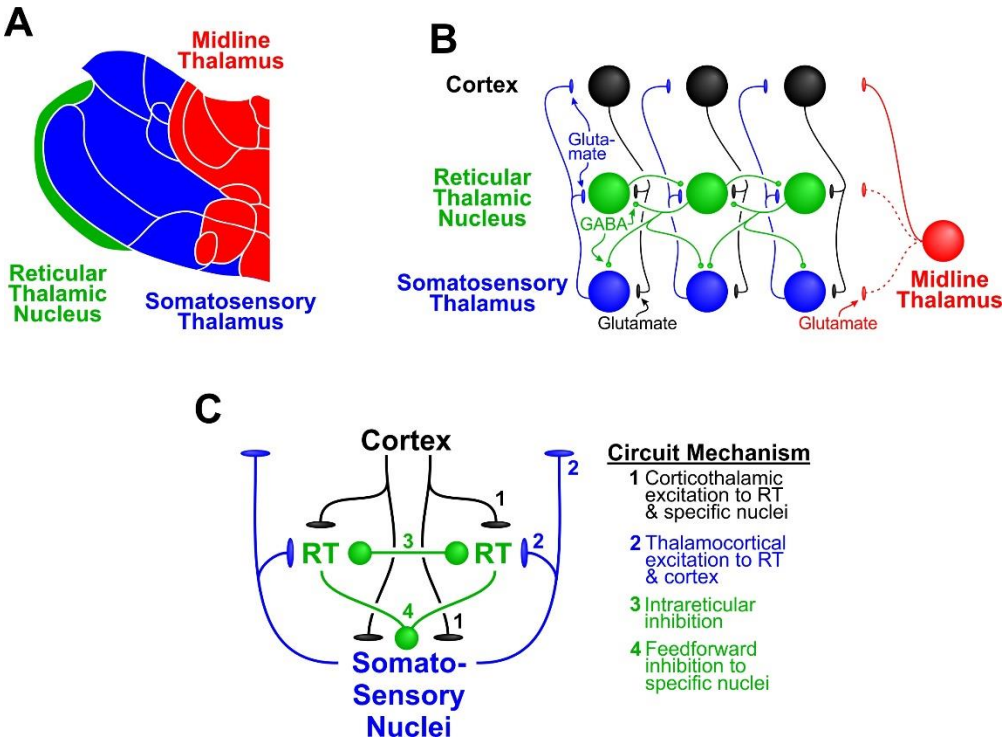

Figure 3. Rhythm generating circuits of the thalamus. (A) Schematic representation of thalamic nuclei likely involved in electrical oscillations produced by the thalamus. Several hypotheses propose that circuit rhythmicity can be achieved through interactions between the reticular thalamic (RT, green) nucleus and somatosensory thalamic nuclei (blue). **(B)** Circuit diagram representing connections among cortical and RT neurons, as well as neurons of the somatosensory nuclei. Cortical neurons (black) provide direct, glutamatergic excitation to both RT neurons (green) and somatosensory thalamic neurons (blue). Somatosensory thalamic neurons provide direct, glutamatergic excitation to both RT and cortical neurons. RT neurons provide GABAergic inhibition to other RT neurons and neurons of the specific nuclei. Based on the conclusions of Purpura and Cohen (Purpura & Cohen, 1962), neurons of the midline thalamic nuclei (red) putatively excite neurons of the lateral, sensory nuclei and the cortex. As there is little anatomical evidence for this conclusion, we represent such connectivity with a red dashed line. There is limited

evidence demonstrating that the midline thalamic nuclei project to the RT (red dash line). **(C)** Simplified representation of circuit dynamics shown in B to highlight nodes proposed to regulate SWD generation. Studies that have discovered these nodes have primarily focused on the somatosensory nuclei. Therefore, the non-specific connections were omitted for simplicity. Elements highlighted in 1 & 2 represent excitatory, glutamatergic nodes. Intrareticular inhibition node (node 3) represents inhibition among RT neurons proposed to desynchronize thalamic circuit activity and limit seizure activity (Sohal et al., 2000). RT-mediated, feedforward inhibition (node 4) is proposed to promote burst firing and seizure-related activity patterns (Kim et al., 1997; Sanchez-Vives & McCormick, 1997).

VIII. Regulating thalamic neuron activity

The ability of thalamic neurons to rapidly alternate between tonic and burst modes hinges mainly on the voltage-dependent activity of two essential ionic conductances, I_T and I_h (Soltesz et al., 1991). Each current works to set the resting membrane potential of thalamocortical neurons. The first current, I_T, encoded by the T channel, is active at membrane potentials positive to approximately -65mV (Soltesz et al., 1991) and often leads to the generation of a relatively long-lasting, low-threshold calcium spikes (LTSs) (D. Kim et al., 2001, 2003; Porcello et al., 2003). Second, the hyperpolarization-activated cationic *I*h current, encoded by the hyperpolarization-activated cyclic nucleotide-gated (HCN) channel*,* is a slowly developing, non-inactivating mixed Na^+-K^+ inward current. I_h activates at hyperpolarized membrane potentials (negative to approximately -55 mV) and reaches maximum activation at around -95 mV (Soltesz et al., 1991). At rest, I_h is partially activated, whereas, the I_T current activity is minimal. To keep matters simple, only TC neuron, not RT neuron, activity is detailed below.

In the awake state, under normal conditions, TC neurons fire tonically in response to incoming excitatory synaptic transmission. During non-REM sleep, burst-mode firing synchronizes TC neurons and facilitates thalamocortical network oscillations, like sleep spindles (Beenhakker & Huguenard, 2009; Huguenard & McCormick, 2007; McCormick & Bal, 1997; McCormick & Contreras, 2001). Many hypothesize that the 3 Hz spike-wave discharge, the electrographic pattern of spike-wave seizures, is a paroxysmal offshoot of

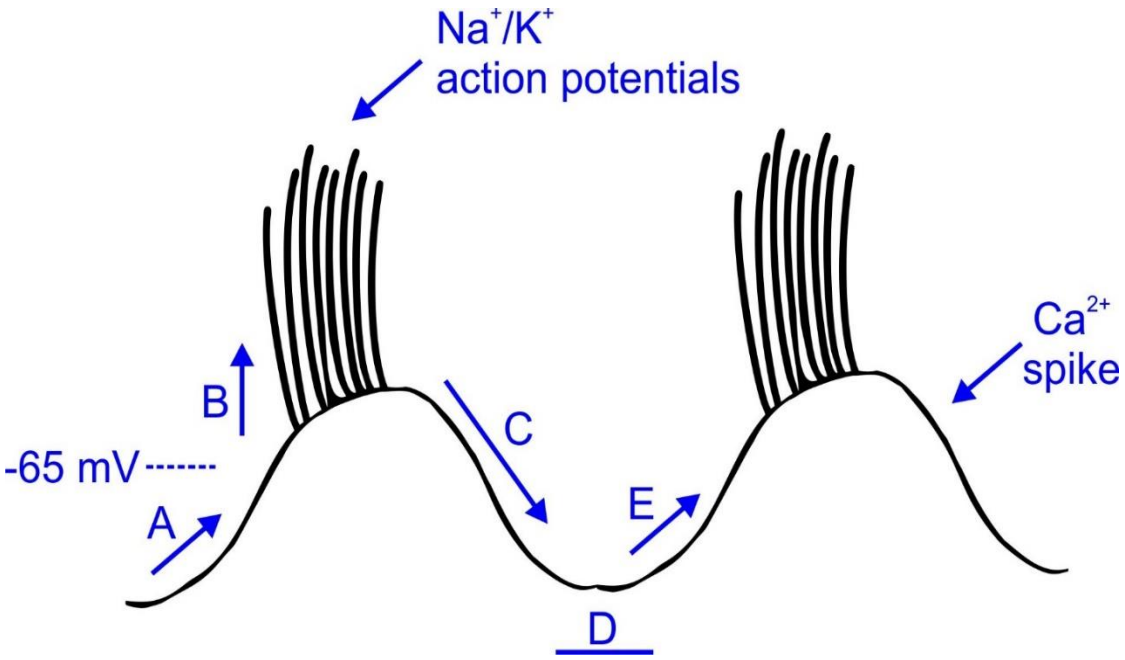

Figure 4. Illustration of the currents underlying oscillatory, burst-mode activity in thalamocortical neurons. (A) Hyperpolarized membrane potential activates I_h encoded by the HCN channel. I_h activation causes the membrane potential to slowly depolarize. **(B)** The slow depolarization results in I_T activation and, if sufficient depolarization is achieved, a low-threshold Ca^{2+} spike (LTS) occurs. Subsequently, the LTS depolarizes the membrane potential to cross the threshold for Na^+/K^+ action potentials. **(C)** Membrane repolarization back to rest leads to I_h de-activation and I_T inactivation. The burst-firing cycle begins again upon hyperpolarization that causes I_T de-inactivation **(D)** and I_h activation **(E)**. (based on Figure 2B, McCormick and Bal., 1997).

the sleep spindle (detailed in Beenhakker and Huguenard, 2009). Oscillatory burst-mode activity occurs under the following conditions. TC neuron membrane hyperpolarization activates I_h. I_h activation causes a slow ramping depolarization. As the membrane potential slowly depolarizes, T channels begin to activate. If sufficient depolarization is achieved, a low-threshold Ca^{2+} spike occurs. The LTS drives the membrane potential to become even more depolarized and reaches the threshold for Na^+/K^+ action potentials. Figure 4 illustrates the LTS "crowned" with Na^+/K^+ spikes. As firing activity ceases, TC neuron membrane repolarization causes I_h deactivation and I_T inactivation. Another bout of burst firing can ensue when the neuron, again, hyperpolarizes. The membrane hyperpolarization of TC neurons largely stems from feed-forward inhibition from GABAergic RT neurons. Altogether, the interplay between these two conductances acts to maintain a tight handle on thalamic activity and establishes a preventative threshold to block paroxysmal activity that may lead to events like an absence seizure.

Returning to the significance of the T channel, the magnitude of inhibitory synaptic transmission largely influences T channel activity. Particularly, expression of extra-synaptic $GABA_A$ (Cope et al., 2009) and $GABA_B$ receptor activity (Bortolato et al., 2010; Kulik et al., 2002; Liu et al., 1992; Marguerite Vergnes et al., 1997) drive membrane hyperpolarization that causes T channel de-inactivation. In turn, such de-inactivation promotes burst-firing in thalamocortical neurons upon receiving excitatory inputs. Computational models from our lab demonstrate that $GABA_B$ receptor-mediated inhibition is the predominant conductance that regulates T channel activity and seizure-like oscillations in the thalamus (Lu et al., 2020). My data, in **Chapter 2**, again links heightened $GABA_B$ receptor function as a potential mechanism to increase seizure-like activity *in vitro* and spike-wave seizures *in vivo* during instances of acute hypoglycemia.

Lastly, Klein et al., reported how the K^+-Cl^- co-transporter, KCC2, serves to regulate intracellular chloride $[Cl^-]_i$ in neurons of the reticular thalamus (RT) (Klein et al.,

2018). $GABA_A$-receptor mediated inhibition among reticular thalamic neurons is essential to maintain intra-RT inhibition and is considered a major seizure chokepoint (Huntsman et al., 1999; Makinson et al., 2017; Paz & Huguenard, 2015; Sohal & Huguenard, 2003). The breakdown of intra-RT inhibition leads to excessive feed-forward inhibition onto thalamocortical neurons, which promotes synchronous activity that is permissive to spike-wave seizures. Klein et al., demonstrated that excessive chloride loading from heightened inhibitory synaptic transmission causes the net action of the $GABA_A$ receptor to become excitatory rather than inhibitory (Klein et al., 2018). As a result, the RT inhibitory seizure-chokepoint breaks down. The authors conclude that KCC2 activity, although weakly expressed, acts to prevent the accumulation of excessive intracellular chloride and protects against the potential weakening of an important seizure chokepoint, relying on intra-RT inhibition.

Later, in **Chapter 3,** discussion of the participation of TASK channels and their role in setting thalamic neuron resting membrane potential will be explored. TASK channels are pH-sensitive and I hypothesize that TASK channel activity is likely mobilized during pH changes that occur during hyperventilation-induced absence seizures. Indeed, many other mechanisms exist that control thalamic neuron activity. The cellular properties I discuss here are likely the most relevant for our work. There are many expert reviews that can be consulted with more insight on this topic (Fogerson & Huguenard, 2016; Huguenard, 2019).

IX. A glimpse into metabolism, respiration and spike-wave-seizures

Clinical observations that document the impact of hypoglycemia and hyperventilation in absence epilepsy extend almost 80 and 100 years, respectively. Beginning with hypoglycemia, in 1939, Gibbs et al., observed that the “wave and spike of petit mal seizures” appears to increase in frequency during hypoglycemia (Gibbs et al.,

1939). Subsequently, they began to use this observation as an approach to differentially diagnose various epilepsy syndromes (Gibbs et al., 1939). In more recent history, the definition of the *Genetic Generalized Epilepsies* expanded to include the spike-wave like seizures found in patients with GLUT1 deficiency syndrome (Mullen et al., 2010; Suls et al., 2009). GLUT1 deficiency syndrome is caused by a mutation in *SLC2A1* that leads to an autosomal-dominant deficiency in GLUT1, the main glucose transporter lining the blood-brain-barrier (Wang et al., 1993). Interestingly, there is roughly a 10% overlap in children diagnosed with childhood absence epilepsy and GLUT1 deficiency syndrome (Arsov et al., 2012; Mullen et al., 2010). Reports of seizures in a GLUT1 deficiency mouse model support the notion that this phenomenon is conserved across species. Moreover, the observation that patients with either childhood absence epilepsy or GLUT1 deficiency syndrome present with similar electrographic seizure patterns suggests that both syndromes recruit a common neural circuit that is sensitive to low glucose. In **Chapter 2**, my study proposes a mechanism that addresses how hypoglycemia recruits the thalamocortical network to instigate spike-wave seizures.

In addition to hypoglycemia-aggravated spike-wave seizures, it has likewise long been appreciated that voluntary hyperventilation in absence epilepsy patients produces an absence seizure (Abubakr et al., 2010; Foerster, 1924; Watemberg et al., 2015) . The clinical use of this technique precludes protracted EEG recordings in children to confirm a diagnosis (Adams & Lueders, 1981). Importantly, voluntary hyperventilation is distinct from hyperpnoea, which is involuntary hyperventilation experienced during exercise; hyperpnoea does not evoke absence seizures in absence patients (Esquivel et al., 1991). One major difference that distinguishes voluntary hyperventilation from hyperpnoea is the change in blood pH. Voluntary hyperventilation induces respiratory alkalosis, a term that describes the drop in the partial pressure of CO_2 (PCO_2) in the blood. Consequently, the decrease in PCO_2 leads to an increase in bicarbonate concentration, relative to PCO_2,

resulting in an alkaline blood pH (alkalosis). Simply put, a drop in PCO_2 causes the blood pH to become more alkaline. On the other hand, hyperpnoea does not cause respiratory alkalosis. Despite exhaling more CO_2 during exercise, an increase in metabolic activity produces more CO_2 as a by-product, thereby replacing exhaled CO_2. Thus, there is no net change in PCO_2.

The sensitivity of absence seizures to CO_2 has been explored in a few clinical studies (Son et al., 2012; Wirrell et al., 1996; Yang et al., 2014). As hyperventilation results in hypocapnia, these clinical studies begin to address whether there is a threshold of hypocapnia a patient must achieve to induce a seizure, or if absence patients have an intrinsic difference in regulating their blood pH relative to non-epileptic people. Recently, one group has demonstrated that hypercapnia suppresses hyperventilation-induced absence seizures (Yang et al., 2014). Collectively, these results suggest that the respiratory alkalosis resulting from voluntary hyperventilation likely invokes some CO_2-dependent factor within thalamocortical networks to produce an absence seizure.

Exploration of a potential mechanism for hyperventilation-induced absence seizures in animal models is limited. Only two studies from Ira Sherwin provide evidence for hyperventilation modulating cortico-thalamocortical circuit activity (Sherwin, 1965, 1967). Sherwin showed that the thalamus is likely necessary to produce hyperventilation-induced high-amplitude rhythmic slowing (HIHARS) in the cortex of cats (Sherwin, 1967). HIHARS is not unique to cats; this electrographic pattern also appears in humans upon voluntary hyperventilation (Lum et al., 2002). After creating a lesion within the central lateral nucleus of the midline thalamus, the hyperventilation no longer evoked HIHARS (Sherwin, 1967). Sherwin concluded that (1) HIHARS can only be evoked in an intact thalamocortical network and (2) the thalamocortical network must possess some, currently unknown, pH-sensitive factor. Few, if any, studies have followed-up on the findings of Sherwin. My thesis work is the first to create a rodent model of hyperventilation-induced

absence seizures. Significantly, this rodent model allows one to systematically analyze spike-wave seizure expression under various respiratory conditions. Greater examination of the link between hyperventilation and respiration will be reviewed in **Chapters 3** and **4**. First, **Chapters 3** will delve into a broader discussion of the clinical history of hyperventilation-induced absence seizures. Additionally, **Chapter 3** will discuss evidence suggesting that thalamic nuclei recruited during hyperventilation-induced absence seizures are more consistent with the corticoreticular theory of absences seizures, not the currently accepted dogma outlined by the cortical focus theory. Then, **Chapter 4** will explore the relationship between PCO_2 and absence seizures in a rat model of absence epilepsy.

X. Conclusion

Absence epilepsy remains a common pediatric disorder affecting 10% to 17% of all school-age children diagnosed with epilepsy (Albuja & Murphy, 2020). Although remission remains high for absence epilepsy patients, many continue to be affected by either long-term behavioral issues or the development of a more complex seizure disorder. Few absence seizure therapies exist, and those that do are decades-old and associated with significant side effects. These anti-seizure drugs either target a singular ion channel (ethosuximide) or act in a non-specific fashion commensurate with an assortment of short-term and potential long-term adverse side-effects (lamotrigine and valproate). The value in investigating the underlying mechanisms that cause acute hypoglycemia and respiratory alkalosis to aggravate absence seizures may not be immediate; however, we can use these conditions as leverage to understand the basic underpinnings of thalamic neuron function and thalamocortical network activity. It is my hope that knowledge gained from my and similar approaches will uncover novel properties of thalamocortical circuit function and, therefore, lead to the development of better absence seizure therapies.

XI. References

Abubakr, A., Ifeayni, I., & Wambacq, I. (2010). The efficacy of routine hyperventilation for seizure activation during prolonged video-electroencephalography monitoring. *Journal of Clinical Neuroscience*, *17*(12), 1503–1505. https://doi.org/10.1016/j.jocn.2009.12.037

Adams, D. J., & Lueders, H. (1981). Hyperventilation and 6-hour EEG recording in evaluation of absence seizures. *Neurology*, *31*(9), 1175–1177. https://doi.org/10.1212/wnl.31.9.1175

Albuja, A. C., & Murphy, P. B. (2020). Absence Seizure. In *StatPearls*. StatPearls Publishing. http://www.ncbi.nlm.nih.gov/books/NBK499867/

Arsov, T., Mullen, S. A., Rogers, S., Phillips, A. M., Lawrence, K. M., Damiano, J. A., Goldberg-Stern, H., Afawi, Z., Kivity, S., Trager, C., Petrou, S., Berkovic, S. F., & Scheffer, I. E. (2012). Glucose transporter 1 deficiency in the idiopathic generalized epilepsies. *Annals of Neurology*, *72*(5), 807–815. https://doi.org/10.1002/ana.23702

Avoli, M. (2012). A brief history on the oscillating roles of thalamus and cortex in absence seizures. *Epilepsia*, *53*(5), 779–789. https://doi.org/10.1111/j.1528-1167.2012.03421.x

Avoli, M., & Gloor, P. (1982). Interaction of cortex and thalamus in spike and wave discharges of feline generalized penicillin epilepsy. *Experimental Neurology*, *76*(1), 196–217. http://dx.doi.org/10.1016/0014-4886(82)90112-1

Bal, T., Krosigk, M. von, & McCormick, D. A. (1995). Role of the ferret perigeniculate nucleus in the generation of synchronized oscillations in vitro. *The Journal of Physiology*, *483*(3), 665–685. https://doi.org/10.1113/jphysiol.1995.sp020613

Bancaud, J. (1969). The physiopathogenesis of generalized epilepsies of organic nature. In *Physiopathogenesis of the epilepsies* (pp. 158–185).

Beenhakker, M. P., & Huguenard, J. R. (2009). Neurons that Fire Together Also Conspire Together: Is Normal Sleep Circuitry Hijacked to Generate Epilepsy? *Neuron*, *62*(5), 612–632. http://dx.doi.org/10.1016/j.neuron.2009.05.015

Berkovic, S. F., & Bladin, P. F. (1983). Absence status in adults. *Clinical and Experimental Neurology*, *19*, 198–207.

Blumenfeld, H. (2005). Cellular and Network Mechanisms of Spike-Wave Seizures. *Epilepsia*, *46*, 21–33. https://doi.org/10.1111/j.1528-1167.2005.00311.x

Bortolato, M., Frau, R., Orrù, M., Fà, M., Dessì, C., Puligheddu, M., Barberini, L., Pillolla, G., Polizzi, L., Santoni, F., Mereu, G., & Marrosu, F. (2010). GABAB receptor activation exacerbates spontaneous spike-and-wave discharges in DBA/2J mice. *Seizure*, *19*(4), 226–231. http://dx.doi.org/10.1016/j.seizure.2010.02.007

Caplan, R. (2015). A call to arms against “The Phantom of Epilepsy.” *Epilepsia*, *56*(11), 1710–1711. https://doi.org/10.1111/epi.13197

Caplan, R., Siddarth, P., Stahl, L., Lanphier, E., Vona, P., Gurbani, S., Koh, S., Sankar, R., & Shields, W. D. (2008). Childhood absence epilepsy: Behavioral, cognitive, and linguistic comorbidities. *Epilepsia*, *49*(11), 1838–1846. https://doi.org/10.1111/j.1528-1167.2008.01680.x

Castro-Alamancos, M. A. (1999). Neocortical Synchronized Oscillations Induced by Thalamic Disinhibition In Vivo. *The Journal of Neuroscience*, *19*(18), RC27.

Chen, Y., Lu, J., Pan, H., Zhang, Y., Wu, H., Xu, K., Liu, X., Jiang, Y., Bao, X., Yao, Z., Ding, K., Lo, W. H. Y., Qiang, B., Chan, P., Shen, Y., & Wu, X. (2003). Association between genetic variation of CACNA1H and childhood absence epilepsy. *Annals of Neurology*, *54*(2), 239–243. https://doi.org/10.1002/ana.10607

Cheong, E., & Shin, H.-S. (2013). T-type Ca2 + channels in absence epilepsy. *Biochimica et Biophysica Acta (BBA) - Biomembranes*, *1828*(7), 1560–1571. https://doi.org/10.1016/j.bbamem.2013.02.002

Choi, S., Yu, E., Lee, S., & Llinás, R. R. (2015). Altered thalamocortical rhythmicity and connectivity in mice lacking CaV3.1 T-type Ca2+ channels in unconsciousness. *Proceedings of the National Academy of Sciences*, *112*(25), 7839–7844. https://doi.org/10.1073/pnas.1420983112

Coenen, A. M. (2003). Genetic animal models for absence epilepsy: A review of the WAG/Rij strain of rats. *Behavior Genetics*, *33*(6), 635–655.

Commision on Classification and Terminology of the International League Against Epilepsy. (1989). Proposal for revised classification of epilepsies and epileptic syndromes. *Epilepsia*, *30*, 389–399.

Contreras, D., Destexhe, A., Sejnowski, T. J., & Steriade, M. (1996). Control of Spatiotemporal Coherence of a Thalamic Oscillation by Corticothalamic Feedback. *Science*, *274*(5288), 771–774. https://doi.org/10.1126/science.274.5288.771

Cope, D. W., Di Giovanni, G., Fyson, S. J., Orbán, G., Errington, A. C., Lőrincz, M. L., Gould, T. M., Carter, D. A., & Crunelli, V. (2009). Enhanced tonic GABAA inhibition in typical absence epilepsy. *Nature Medicine*, *15*(12), 1392–1398. https://doi.org/10.1038/nm.2058

Cortez, M. A., Kostopoulos, G. K., & Snead, O. C. (2016). Acute and chronic pharmacological models of generalized absence seizures. *Journal of Neuroscience Methods*, *260*, 175–184. https://doi.org/10.1016/j.jneumeth.2015.08.034

Cossette, P., Liu, L., Brisebois, K., Dong, H., Lortie, A., Vanasse, M., Saint-Hilaire, J.-M., Carmant, L., Verner, A., Lu, W.-Y., Wang, Y. T., & Rouleau, G. A. (2002).

Mutation of GABRA1 in an autosomal dominant form of juvenile myoclonic epilepsy. *Nature Genetics*, *31*(2), 184–189. https://doi.org/10.1038/ng885

Crunelli, V., & Leresche, N. (2002). Childhood absence epilepsy: Genes, channels, neurons and networks. *Nat Rev Neurosci*, *3*(5), 371–382.

Danober, L., Deransart, C., Depaulis, A., Vergnes, M., & Marescaux, C. (1998). Pathophysiological mechanisms of genetic absence epilepsy in the rat. *Progress in Neurobiology*, *55*(1), 27–57. https://doi.org/10.1016/S0301-0082(97)00091-9

Dempsey, E. and M. (1942a). The interaction of certain spontaneous and induced cortical potentials. *American Journal of Physiology*, *135*, 301–308.

Dempsey, E. and M. (1942b). The production of rhythmically recurrent cortical potentials after localized thalamic stimulation. *American Journal of Physiology*, *135*, 293–300.

Depaulis, A., & Charpier, S. (2017). Pathophysiology of absence epilepsy: Insights from genetic models. *Neuroscience Letters*. http://dx.doi.org/10.1016/j.neulet.2017.02.035

Depaulis, A., David, O., & Charpier, S. (2016). The genetic absence epilepsy rat from Strasbourg as a model to decipher the neuronal and network mechanisms of generalized idiopathic epilepsies. *Journal of Neuroscience Methods*, *260*, 159–174. https://doi.org/10.1016/j.jneumeth.2015.05.022

Destexhe, A. (1998). Spike-and-Wave Oscillations Based on the Properties of GABAB Receptors. *The Journal of Neuroscience*, *18*(21), 9099–9111.

Esquivel, E., Chaussain, M., Plouin, P., Ponsot, G., & Arthuis, M. (1991). Physical exercise and voluntary hyperventilation in childhood absence epilepsy. *Electroencephalography and Clinical Neurophysiology*, *79*(2), 127–132. http://dx.doi.org/10.1016/0013-4694(91)90050-E

Felix, R. (2002). Insights from mouse models of absence epilepsy into Ca2+ channel physiology and disease etiology. *Cellular and Molecular Neurobiology*, *22*(2), 103–120. https://doi.org/10.1023/a:1019807719343

Fisher, R. S., & Prince, D. A. (1977). Spike-wave rhythms in cat cortex induced by parenteral penicillin. I. Electroencephalographic features. *Electroencephalography and Clinical Neurophysiology*, *42*(5), 608–624.

Foerster, O. (1924). Hyperventilationsepilepsie. *Deut Ztschr Nervenheilk*, *83*, 347–356.

Fogerson, P. M., & Huguenard, J. R. (2016). Tapping the Brakes: Cellular and Synaptic Mechanisms that Regulate Thalamic Oscillations. *Neuron*, *92*(4), 687–704. http://dx.doi.org/10.1016/j.neuron.2016.10.024

Fonseca Wald, E. L. A., Hendriksen, J. G. M., Drenthen, G. S., Kuijk, S. M. J. V., Aldenkamp, A. P., Vles, J. S. H., Vermeulen, R. J., Debeij-van Hall, M. H. J. A., & Klinkenberg, S. (2019). Towards a Better Understanding of Cognitive Deficits in Absence Epilepsy: A Systematic Review and Meta-Analysis. *Neuropsychology Review*, *29*(4), 421–449. https://doi.org/10.1007/s11065-019-09419-2

Gastaut, H. (1981). [Individualization of so-called benign and functional epilepsy at different ages. Appraisal of variations corresponding the predisposition for epilepsy at these ages]. *Rev Electroencephalogr Neurophysiol Clin*, *11*(3–4), 346–366.

Gibbs, F. A., Gibbs, E. L., & Lennox, W. G. (1939). Influence of the blood sugar on the wave and spike formation in petit mal epilepsy. *Archives of Neurology & Psychiatry*, *41*(6), 1111–1116. https://doi.org/10.1001/archneurpsyc.1939.02270180039002

Gibbs, F., & Davis, H. (1935). The electroencephalogram in epilepsy and in conditions of impaired consciousness. *Arch Neurol Psychiatry*, *34*, 1133–1148.

Glauser, T. A., Cnaan, A., Shinnar, S., Hirtz, D. G., Dlugos, D., Masur, D., Clark, P. O., Adamson, P. C., & for the Childhood Absence Epilepsy Study, T. (2013). Ethosuximide, valproic acid, and lamotrigine in childhood absence epilepsy: Initial monotherapy outcomes at 12 months. *Epilepsia*, *54*(1), 141–155. https://doi.org/10.1111/epi.12028

Gloor, P. (1968). Generalized Cortico-Reticular Epilepsies Some COnsideration on the Pathophysiology of Generalized Bilaterally Synchronous Spike and Wave Discharge. *Epilepsia*, *9*, 249–263.

Guilhoto, L. M. (2017). Absence epilepsy: Continuum of clinical presentation and epigenetics? *Seizure*, *44*, 53–57. https://doi.org/10.1016/j.seizure.2016.11.031

Hanbery, J., & Jasper, H. H. (1953). Independence of diffuse thalamocortical projection system shown by specific nuclear destructions. *Journal of Neurophysiology*, *16*(3), 252–271. https://doi.org/10.1152/jn.1953.16.3.252

Heron, S. E., Khosravani, H., Varela, D., Bladen, C., Williams, T. C., Newman, M. R., Scheffer, I. E., Berkovic, S. F., Mulley, J. C., & Zamponi, G. W. (2007). Extended spectrum of idiopathic generalized epilepsies associated with CACNA1H functional variants. *Annals of Neurology*, *62*(6), 560–568. https://doi.org/10.1002/ana.21169

Holmes, M. D., Brown, M., & Tucker, D. M. (2004). Are “Generalized” Seizures Truly Generalized? Evidence of Localized Mesial Frontal and Frontopolar Discharges in Absence. *Epilepsia*, *45*(12), 1568–1579. https://doi.org/10.1111/j.0013-9580.2004.23204.x

Holopainen, I. E., Metsähonkala, E. L., Kokkonen, H., Parkkola, R. K., Manner, T. E., Någren, K., & Korpi, E. R. (2001). Decreased binding of [11C]flumazenil in Angelman syndrome patients with GABAA receptor β3 subunit deletions. *Annals*

of Neurology, *49*(1), 110–113. https://doi.org/10.1002/1531-8249(200101)49:1<110::AID-ANA17>3.0.CO;2-T

Hu, X., Dong, J., Wang, X., Wu, T., Yang, L., & Lu, X. (2011). Localization of epileptic foci in Children with childhood absence epilepsy by magnetoencephalography combined with synthetic aperture magnetometry(). *Journal of Biomedical Research*, *25*(4), 259–265. https://doi.org/10.1016/S1674-8301(11)60035-3

Huguenard, J. (2019). Current Controversy: Spikes, Bursts, and Synchrony in Generalized Absence Epilepsy: Unresolved Questions Regarding Thalamocortical Synchrony in Absence Epilepsy. *Epilepsy Currents*, *19*(2), 105–111. https://doi.org/10.1177/1535759719835355

Huguenard, J. R., & McCormick, D. A. (1992). Simulation of the currents involved in rhythmic oscillations in thalamic relay neurons. *Journal of Neurophysiology*, *68*(4), 1373–1383.

Huguenard, J. R., & McCormick, D. A. (2007). Thalamic synchrony and dynamic regulation of global forebrain oscillations. *Trends Neurosci*, *30*(7), 350–356. http://dx.doi.org/10.1016/j.tins.2007.05.007

Hunter, J., & Jasper, H. H. (1949). Effects of thalamic stimulation in unanaesthetised animals: The arrest reaction and petit Mal-like seizures, activation patterns and generalized convulsions. *Electroencephalography and Clinical Neurophysiology*, *1*(1–4), 305–324. http://dx.doi.org/10.1016/0013-4694(49)90196-0

Huntsman, M. M., Porcello, D. M., Homanics, G. E., DeLorey, T. M., & Huguenard, J. R. (1999). Reciprocal inhibitory connections and network synchrony in the mammalian thalamus. *Science (New York, N.Y.)*, *283*(5401), 541–543. https://doi.org/10.1126/science.283.5401.541

Iivanainen, M., Bergström, L., Nuutila, A., & Viukari, M. (1984). Psychosis-like absence status of elderly patients: Successful treatment with sodium valproate. *Journal of*

Neurology, Neurosurgery & Psychiatry, *47*(9), 965–969. https://doi.org/10.1136/jnnp.47.9.965

Jahnsen, H., & Llinás, R. (1984a). Electrophysiological properties of guinea-pig thalamic neurones: An in vitro study. *The Journal of Physiology*, *349*(1), 205–226. https://doi.org/10.1113/jphysiol.1984.sp015153

Jahnsen, H., & Llinás, R. (1984b). Ionic basis for the electro-responsiveness and oscillatory properties of guinea-pig thalamic neurones in vitro. *The Journal of Physiology*, *349*(1), 227–247. https://doi.org/10.1113/jphysiol.1984.sp015154

Jasper, H. H., & Droogleever-Fortuyn, J. (1947). Experimental studies of the functional anatomy of petit mal epilepsy. *Res. Publ. Assoc. Res. Nerve Ment. Dis.*, *26*, 272–298.

Jasper, H. H., & Kershman, J. (1941). Electroencephalographic classification of the epilepsies. *Arch Neurol Psychiatry*, *45*, 903–943.

Jones, E. G. (2007). *The Thalamus* (Vol. 1). Cambridge University Press.

Jones-Davis, D. M., & Macdonald, R. L. (2003). GABAA receptor function and pharmacology in epilepsy and status epilepticus. *Current Opinion in Pharmacology*, *3*(1), 12–18. https://doi.org/10.1016/S1471-4892(02)00015-2

Kang, J., & Macdonald, R. L. (2004). The GABAA Receptor γ2 Subunit R43Q Mutation Linked to Childhood Absence Epilepsy and Febrile Seizures Causes Retention of α1β2γ2S Receptors in the Endoplasmic Reticulum. *Journal of Neuroscience*, *24*(40), 8672–8677. https://doi.org/10.1523/JNEUROSCI.2717-04.2004

Khosravani, H., & Zamponi, G. W. (2006). Voltage-Gated Calcium Channels and Idiopathic Generalized Epilepsies. *Physiological Reviews*, *86*(3), 941–966. https://doi.org/10.1152/physrev.00002.2006

Kim, D., Park, D., Choi, S., Lee, S., Sun, M., Kim, C., & Shin, H.-S. (2003). Thalamic Control of Visceral Nociception Mediated by T-Type Ca2+ Channels. *Science*, *302*(5642), 117–119. https://doi.org/10.1126/science.1088886

Kim, D., Song, I., Keum, S., Lee, T., Jeong, M.-J., Kim, S.-S., McEnery, M. W., & Shin, H.-S. (2001). Lack of the Burst Firing of Thalamocortical Relay Neurons and Resistance to Absence Seizures in Mice Lacking α1G T-Type Ca2+ Channels. *Neuron*, *31*(1), 35–45. https://doi.org/10.1016/S0896-6273(01)00343-9

Kim, U., Sanchez-Vives, M. V., & McCormick, D. A. (1997). Functional Dynamics of GABAergic Inhibition in the Thalamus. *Science*, *278*(5335), 130–134. https://doi.org/10.1126/science.278.5335.130

Klein, P. M., Lu, A. C., Harper, M. E., McKown, H. M., Morgan, J. D., & Beenhakker, M. P. (2018). Tenuous Inhibitory GABAergic Signaling in the Reticular Thalamus. *The Journal of Neuroscience: The Official Journal of the Society for Neuroscience*, *38*(5), 1232–1248. https://doi.org/10.1523/JNEUROSCI.1345-17.2017

Kostopoulos, G., & Avoli, M. (1983). Enhanced response of cortical neurons to thalamic stimuli precedes the appearance of spike and wave discharges in feline generalized penicillin epilepsy. *Brain Research*, *278*(1–2), 207–217. http://dx.doi.org/10.1016/0006-8993(83)90239-1

Kulik, Á., Nakadate, K., Nyíri, G., Notomi, T., Malitschek, B., Bettler, B., & Shigemoto, R. (2002). Distinct localization of GABAB receptors relative to synaptic sites in the rat cerebellum and ventrobasal thalamus. *European Journal of Neuroscience*, *15*(2), 291–307. https://doi.org/10.1046/j.0953-816x.2001.01855.x

Lachance-Touchette, P., Brown, P., Meloche, C., Kinirons, P., Lapointe, L., Lacasse, H., Lortie, A., Carmant, L., Bedford, F., Bowie, D., & Cossette, P. (2011). Novel α1 and γ2 GABAA receptor subunit mutations in families with idiopathic generalized

epilepsy. *The European Journal of Neuroscience*, *34*(2), 237–249. https://doi.org/10.1111/j.1460-9568.2011.07767.x

Liu, Z., Vergnes, M., Depaulis, A., & Marescaux, C. (1992). Involvement of intrathalamic GABAb neurotransmission in the control of absence seizures in the rat. *Neuroscience*, *48*(1), 87–93. https://doi.org/10.1016/0306-4522(92)90340-8

Llinás, R., & Jahnsen, H. (1982). Electrophysiology of mammalian thalamic neurones in vitro. *Nature*, *297*(5865), 406–408. https://doi.org/10.1038/297406a0

Loiseau, P., Pestre, M., Dartigues, J. F., Commenges, D., Barberger-Gateau, C., & Cohadon, S. (1983). Long-term prognosis in two forms of childhood epilepsy: Typical absence seizures and epilepsy with rolandic (centrotemporal) EEG foci. *Annals of Neurology*, *13*(6), 642–648. https://doi.org/10.1002/ana.410130610

Lu, A. C., Lee, C. K., Kleiman-Weiner, M., Truong, B., Wang, M., Huguenard, J. R., & Beenhakker, M. P. (2020). Nonlinearities between inhibition and T-type calcium channel activity bidirectionally regulate thalamic oscillations. *ELife*, *9*, e59548. https://doi.org/10.7554/eLife.59548

Lum, L. M., Connolly, M. B., Farrell, K., & Wong, P. K. H. (2002). Hyperventilation-induced High-amplitude Rhythmic Slowing with Altered Awareness: A Video-EEG Comparison with Absence Seizures. *Epilepsia (Series 4)*, *43*(11), 1372–1378. https://doi.org/10.1046/j.1528-1157.2002.35101.x

Macdonald, R. L., Kang, J.-Q., & Gallagher, M. J. (2010). *Mutations in GABAA receptor subunits associated with genetic epilepsies*. https://www.ncbi.nlm.nih.gov/pmc/articles/PMC2901974/

Makinson, C. D., Tanaka, B. S., Sorokin, J. M., Wong, J. C., Christian, C. A., Goldin, A. L., Escayg, A., & Huguenard, J. R. (2017). Regulation of Thalamic and Cortical Network Synchrony by Scn8a. *Neuron*, *93*(5), 1165-1179.e6. https://doi.org/10.1016/j.neuron.2017.01.031

Maljevic, S., Krampfl, K., Cobilanschi, J., Tilgen, N., Beyer, S., Weber, Y., Schlesinger, F., Ursu, D., Melzer, W., Cossette, P., Bufler, J., Lerche, H., & Heils, A. (2006). A mutation in the GABAA receptor α1-subunit is associated with absence epilepsy. *Annals of Neurology*, *59*(6), 983–987.

Marini, C., King, M. A., Archer, J. S., Newton, M. R., & Berkovic, S. F. (2003). Idiopathic generalised epilepsy of adult onset: Clinical syndromes and genetics. *Journal of Neurology, Neurosurgery & Psychiatry*, *74*(2), 192–196. https://doi.org/10.1136/jnnp.74.2.192

Matricardi, S., Verrotti, A., Chiarelli, F., Cerminara, C., & Curatolo, P. (2014). Current Advances in Childhood Absence Epilepsy. *Pediatric Neurology*, *50*(3), 205–212. http://dx.doi.org/10.1016/j.pediatrneurol.2013.10.009

McCafferty, C., David, F., Venzi, M., Lőrincz, M. L., Delicata, F., Atherton, Z., Recchia, G., Orban, G., Lambert, R. C., Di Giovanni, G., Leresche, N., & Crunelli, V. (2018). Cortical drive and thalamic feed-forward inhibition control thalamic output synchrony during absence seizures. *Nature Neuroscience*, *21*(5), 744–756. https://doi.org/10.1038/s41593-018-0130-4

McCormick, D. A., & Bal, T. (1997). SLEEP AND AROUSAL: Thalamocortical Mechanisms. *Annual Review of Neuroscience*, *20*(1), 185–215. https://doi.org/10.1146/annurev.neuro.20.1.185

McCormick, D. A., & Contreras, D. (2001). On The Cellular and Network Bases of Epileptic Seizures. *Annual Review of Physiology*, *63*(1), 815–846. https://doi.org/10.1146/annurev.physiol.63.1.815

McCormick, D. A., & Huguenard, J. R. (1992). A model of the electrophysiological properties of thalamocortical relay neurons. *Journal of Neurophysiology*, *68*(4), 1384–1400.

Meeren, H. K. M., Pijn, J. P. M., Van Luijtelaar, E. L. J. M., Coenen, A. M. L., & Lopes da Silva, F. H. (2002). Cortical Focus Drives Widespread Corticothalamic Networks during Spontaneous Absence Seizures in Rats. *The Journal of Neuroscience*, *22*(4), 1480–1495.

Meeren, H., van Luijtelaar, G., Lopes da Silva, F., & Coenen, A. (2005). Evolving concepts on the pathophysiology of absence seizures: The cortical focus theory. *Archives of Neurology*, *62*(3), 371–376. https://doi.org/10.1001/archneur.62.3.371

Menuz, K., & Nicoll, R. A. (2008). Loss of Inhibitory Neuron AMPA Receptors Contributes to Ataxia and Epilepsy in Stargazer Mice. *Journal of Neuroscience*, *28*(42), 10599–10603. https://doi.org/10.1523/JNEUROSCI.2732-08.2008

Michelucci, R., Rubboli, G., Passarelli, D., Riguzzi, P., Volpi, L., Parmeggiani, L., Rizzi, R., Gardella, E., & Tassinari, C. A. (1996). Electroclinical features of idiopathic generalised epilepsy with persisting absences in adult life. *Journal of Neurology, Neurosurgery, and Psychiatry*, *61*(5), 471–477.

Morison, R., & Dempsey, E. (1942). Mechanism of Thalamocortical Augmentation and Repetition. *Amer J Physiology*.

Mullen, S. A., Suls, A., Jonghe, P. D., Berkovic, S. F., & Scheffer, I. E. (2010). Absence epilepsies with widely variable onset are a key feature of familial GLUT1 deficiency. *Neurology*, *75*(5), 432–440. https://doi.org/10.1212/WNL.0b013e3181eb58b4

Mullen, Saul A., & Berkovic, S. F. (2018). Genetic generalized epilepsies. *Epilepsia*, *59*(6), 1148–1153. https://doi.org/10.1111/epi.14042

Niedermeyer, E. (1996). Primary (idiopathic) generalized epilepsy and underlying mechanisms. *Clinical EEG (Electroencephalography)*, *27*(1), 1–21.

Panayiotopoulos, C. P., Chroni, E., Daskalopoulos, C., Baker, A., Rowlinson, S., & Walsh, P. (1992). Typical absence seizures in adults: Clinical, EEG, video-EEG findings and diagnostic/syndromic considerations. *Journal of Neurology, Neurosurgery, and Psychiatry*, *55*(11), 1002–1008.

Paz, J. T., Bryant, A. S., Peng, K., Fenno, L., Yizhar, O., Frankel, W. N., Deisseroth, K., & Huguenard, J. R. (2011). A new mode of corticothalamic transmission revealed in the Gria4-/- model of absence epilepsy. *Nat Neurosci*, *14*(9), 1167–1173. http://www.nature.com/neuro/journal/v14/n9/abs/nn.2896.html#supplementary-information

Paz, J. T., Davidson, T. J., Frechette, E. S., Delord, B., Parada, I., Peng, K., Deisseroth, K., & Huguenard, J. R. (2013). Closed-loop optogenetic control of thalamus as a tool for interrupting seizures after cortical injury. *Nat Neurosci*, *16*(1), 64–70. http://www.nature.com/neuro/journal/v16/n1/abs/nn.3269.html#supplementary-information

Paz, J. T., & Huguenard, J. R. (2015). Microcircuits and their interactions in epilepsy: Is the focus out of focus? *Nat Neurosci*, *18*(3), 351–359. https://doi.org/10.1038/nn.3950

Peloquin, J. B., Khosravani, H., Barr, W., Bladen, C., Evans, R., Mezeyova, J., Parker, D., Snutch, T. P., McRory, J. E., & Zamponi, G. W. (2006). Functional analysis of Ca3.2 T-type calcium channel mutations linked to childhood absence epilepsy. *Epilepsia*, *47*(3), 655–658. https://doi.org/10.1111/j.1528-1167.2006.00482.x

Penfield, W., & Erickson, T. C. (1942). Epilepsy and cerebral localization. A Study of the Mechanisms, Treatment and Prevention of Epileptic Seizures. *BJS (British Journal of Surgery)*, *30*(118), 184–184. https://doi.org/10.1002/bjs.18003011823

Porcello, D. M., Smith, S. D., & Huguenard, J. R. (2003). Actions of U-92032, a T-Type Ca2+ Channel Antagonist, Support a Functional Linkage Between I T and Slow

Intrathalamic Rhythms. *Journal of Neurophysiology*, *89*(1), 177–185. https://doi.org/10.1152/jn.00667.2002

Prince, D. A., & Farrell, D. (1969). “Centrencephalic” spike-wave discharges following parenteral penicillin injection in the cat. *Neurology*, *19*, 309–310.

Purpura, D. P., & Cohen, B. (1962). INTRACELLULAR RECORDING FROM THALAMIC NEURONS DURING RECRUITING RESPONSES. *Journal of Neurophysiology*, *25*(5), 621–635.

Reutens DC, B. (1995). Idiopathic generealized epilepsy of adolescence: Are the syndromes clinically distinct? *Neurology*, *45*(8), 1469–1476.

Roden, W. H., Peugh, L. D., & Jansen, L. A. (2010). Altered GABA(A) receptor subunit expression and pharmacology in human Angelman syndrome cortex. *Neuroscience Letters*, *483*(3), 167–172. https://doi.org/10.1016/j.neulet.2010.08.001

Rudolph, U., Crestani, F., & Möhler, H. (2001). GABAA receptor subtypes: Dissecting their pharmacological functions. *Trends in Pharmacological Sciences*, *22*(4), 188–194. https://doi.org/10.1016/S0165-6147(00)01646-1

Sanchez-Vives, M. V., & McCormick, D. A. (1997). Functional Properties of Perigeniculate Inhibition of Dorsal Lateral Geniculate Nucleus Thalamocortical Neurons In Vitro. *The Journal of Neuroscience*, *17*(22), 8880–8893.

Sherman, S. M., & Guillery, R. W. (1996). Functional organization of thalamocortical relays. *Journal of Neurophysiology*, *76*(3), 1367–1395.

Sherwin, I. (1965). Differential effects of hyperventillation on the excitability of intact and isolated cortex. *Electroencephalography and Clinical Neurophysiology*, *18*(6), 599–607. https://doi.org/10.1016/0013-4694(65)90077-5

Sherwin, I. (1967). Alterations in the non-specific cortical afference during hyperventilation. *Electroencephalography and Clinical Neurophysiology*, *23*(6), 532–538. https://doi.org/10.1016/0013-4694(67)90019-3

Shinnar, S., Cnaan, A., Hu, F., Clark, P., Dlugos, D., Hirtz, D. G., Masur, D., Mizrahi, E. M., Moshé, S. L., Glauser, T. A., & For the Childhood Absence Epilepsy Study Group. (2015). Long-term outcomes of generalized tonic-clonic seizures in a childhood absence epilepsy trial. *Neurology*, *85*(13), 1108–1114. https://doi.org/10.1212/wnl.0000000000001971

Sillanpää, M., Jalava, M., Kaleva, O., & Shinnar, S. (1998). Long-term prognosis of seizures with onset in childhood. *The New England Journal of Medicine*, *338*(24), 1715–1722. https://doi.org/10.1056/NEJM199806113382402

Sohal, V. S., & Huguenard, J. R. (2003). Inhibitory Interconnections Control Burst Pattern and Emergent Network Synchrony in Reticular Thalamus. *Journal of Neuroscience*, *23*(26), 8978–8988.

Sohal, V. S., Huntsman, M. M., & Huguenard, J. R. (2000). Reciprocal Inhibitory Connections Regulate the Spatiotemporal Properties of Intrathalamic Oscillations. *Journal of Neuroscience*, *20*(5), 1735–1745.

Soltesz, I., Lightowler, S., Leresche, N., Jassik-Gerschenfeld, D., Pollard, C. E., & Crunelli, V. (1991). Two inward currents and the transformation of low-frequency oscillations of rat and cat thalamocortical cells. *The Journal of Physiology*, *441*(1), 175–197. https://doi.org/10.1113/jphysiol.1991.sp018745

Son, S., Kwon, O.-Y., Jung, S., Kim, Y.-S., Choi, N.-C., & Lim, B. H. (2012). Relationship between Hyperventilation-Induced Electroencephalographic Changes and PCO2 Level. *Journal of Epilepsy Research*, *2*(1). https://doi.org/10.14581/jer.12002

Staley, K. (2015). Molecular mechanisms of epilepsy. *Nature Neuroscience*, *18*(3), 367–372. https://doi.org/10.1038/nn.3947

Steriade, M. (1996). Awakening the brain. *Nature*, *383*(6595), 24–25. https://doi.org/10.1038/383024a0

Steriade, M., & Llinás, R. R. (1988). The functional states of the thalamus and the associated neuronal interplay. *Physiological Reviews*, *68*(3), 649–742.

Steriade, M., McCormick, D. A., & Sejnowski, T. J. (1993). Thalamocortical oscillations in the sleeping and aroused brain. *Science*, *262*(5134), 679–685. https://doi.org/10.1126/science.8235588

Suls, A., Mullen, S. A., Weber, Y. G., Verhaert, K., Ceulemans, B., Guerrini, R., Wuttke, T. V., Salvo-Vargas, A., Deprez, L., Claes, L. R. F., Jordanova, A., Berkovic, S. F., Lerche, H., De Jonghe, P., & Scheffer, I. E. (2009). Early-onset absence epilepsy caused by mutations in the glucose transporter GLUT1. *Annals of Neurology*, *66*(3), 415–419. https://doi.org/10.1002/ana.21724

Tan, H. O., Reid, C. A., Single, F. N., Davies, P. J., Chiu, C., Murphy, S., Clarke, A. L., Dibbens, L., Krestel, H., Mulley, J. C., Jones, M. V., Seeburg, P. H., Sakmann, B., Berkovic, S. F., Sprengel, R., & Petrou, S. (2007). Reduced cortical inhibition in a mouse model of familial childhood absence epilepsy. *Proceedings of the National Academy of Sciences*, *104*(44), 17536–17541. https://doi.org/10.1073/pnas.0708440104

Tenney, J. R., & Glauser, T. A. (2013). The Current State of Absence Epilepsy: Can We Have Your Attention? *Epilepsy Currents*, *13*(3), 135–140. https://doi.org/10.5698/1535-7511-13.3.135

Timofeev, I., & Steriade, M. (2004). Neocortical seizures: Initiation, development and cessation. *Neuroscience*, *123*(2), 299–336. https://doi.org/10.1016/j.neuroscience.2003.08.051

Tissot, S. A. D. (1770). *Traité de l'epilepsie: Faisant le tome troisieme du Traite des nerfs et de leurs maladies*.

Trinka, E., Baumgartner, S., Unterberger, I., Unterrainer, J., Luef, G., Haberlandt, E., & Bauer, G. (2004). Long-term prognosis for childhood and juvenile absence epilepsy. *Journal of Neurology*, *251*(10), 1235–1241. https://doi.org/10.1007/s00415-004-0521-1

Tucker, D. M., Brown, M., Luu, P., & Holmes, M. D. (2007). Discharges in ventromedial frontal cortex during absence spells. *Epilepsy & Behavior*, *11*(4), 546–557. http://dx.doi.org/10.1016/j.yebeh.2007.04.023

van Luijtelaar, E. L., & Coenen, A. M. (1986). Two types of electrocortical paroxysms in an inbred strain of rats. *Neuroscience Letters*, *70*(3), 393–397.

Vergens, M., Marescaux, C., Micheletti, G., Depaulis, A., Rumbach, L., & Warter, J. M. (1984). Enhancement of spike and wave discharges by GABAmimetic drugs in rats with spontaneous petit-mallike epilepsy. *Neuroscience Letters*, *44*(1), 91–94. https://doi.org/10.1016/0304-3940(84)90226-X

Vergnes, M., Marescaux, C., Depaulis, A., Micheletti, G., & Warter, J. M. (1987). Spontaneous spike and wave discharges in thalamus and cortex in a rat model of genetic petit mal-like seizures. *Experimental Neurology*, *96*(1), 127–136. https://doi.org/10.1016/0014-4886(87)90174-9

Vergnes, Marguerite, Boehrer, A., Simler, S., Bernasconi, R., & Marescaux, C. (1997). Opposite effects of GABAB receptor antagonists on absences and convulsive seizures. *European Journal of Pharmacology*, *332*(3), 245–255. http://dx.doi.org/10.1016/S0014-2999(97)01085-6

Vitko, I., Chen, Y., Arias, J. M., Shen, Y., Wu, X.-R., & Perez-Reyes, E. (2005). Functional characterization and neuronal modeling of the effects of childhood absence epilepsy variants of CACNA1H, a T-type calcium channel. *The Journal of Neuroscience: The Official Journal of the Society for Neuroscience*, *25*(19), 4844–4855. https://doi.org/10.1523/JNEUROSCI.0847-05.2005

Wang, D., Pascual, J. M., & De Vivo, D. (1993). Glucose Transporter Type 1 Deficiency Syndrome. In M. P. Adam, H. H. Ardinger, R. A. Pagon, S. E. Wallace, L. J. Bean, K. Stephens, & A. Amemiya (Eds.), *GeneReviews*®. University of Washington, Seattle. http://www.ncbi.nlm.nih.gov/books/NBK1430/

Wang, G., Bochorishvili, G., Chen, Y., Salvati, K. A., Zhang, P., Dubel, S. J., Perez-Reyes, E., Snutch, T. P., Stornetta, R. L., Deisseroth, K., Erisir, A., Todorovic, S. M., Luo, J.-H., Kapur, J., Beenhakker, M. P., & Zhu, J. J. (2015). CaV3.2 calcium channels control NMDA receptor-mediated transmission: A new mechanism for absence epilepsy. *Genes & Development*, *29*(14), 1535–1551. https://doi.org/10.1101/gad.260869.115

Watemberg, N., Farkash, M., Har-Gil, M., Sezer, T., Goldberg-Stern, H., & Alehan, F. (2015). Hyperventilation During Routine Electroencephalography: Are Three Minutes Really Necessary? *Pediatric Neurology*, *52*(4), 410–413. https://doi.org/10.1016/j.pediatrneurol.2014.12.003

Wirrell, E. C., Camfield, C. S., Camfield, P. R., Dooley, J. M., Gordon, K. E., & Smith, B. (1997). Long-term psychosocial outcome in typical absence epilepsy: Sometimes a wolf in sheeps clothing. *Archives of Pediatrics & Adolescent Medicine*, *151*(2), 152–158. https://doi.org/10.1001/archpedi.1997.02170390042008

Wirrell, E. C., Camfield, P. R., Gordon, K. E., Camfield, C. S., Dooley, J. M., & Hanna, B. D. (1996). Will a Critical Level of Hyperventilation-Induced Hypocapnia Always Induce an Absence Seizure. *Epilepsia*, *37*(5), 459–462.

Yang, X.-F., Shi, X.-Y., Ju, J., Zhang, W.-N., Liu, Y.-J., Li, X.-Y., & Zou, L.-P. (2014). 5% CO2 inhalation suppresses hyperventilation-induced absence seizures in children. Epilepsy Research, 108(2), 345–348. http://dx.doi.org/10.1016/j.eplepsyres.2013.11.012

Chapter 2: AMPK activation increases spike-and-wave seizures

Kathryn A. Salvati

Matthew L. Ritger

Pasha A. Davoudian

Finnegan O'Dell

George M.P.R. Souza

Adam C. Lu

Joshua C. Drake

Daniel R. Wyskiel

Zhen Yan

Mark P. Beenhakker

KAS and MPB designed the study and experiments. KAS and MPB wrote the manuscript and analyzed the data. All authors provided commentary on the primary draft of the manuscript. KAS performed experiments in Figs. 1, 2, 3, 4, 5, and Supp. Fig. 3C, H-M. MLR performed experiments Fig. 5I-J and in Supp. Fig. 3F-G, Supp. Fig. 4C-E. PAD performed immunohistochemistry in Supp. Fig. 3A-C. FO performed oscillation experiments in Supp. Fig. 5. DRW performed patch-clamp electrophysiology in Supp. Fig 3D-E. GMPRS helped with catheter surgery and blood sample collection for lactate measurements in Fig. 5F-G and Supp. Fig. 6C, F. ACL provided custom-code in MATLAB for Fig. 4B-N and Fig. 5H-J. EPR cloned AAV9-UPCamAMPKAR in Fig. 3A. JCD preformed western blot experiments and analysis in Supp. Fig. 4A-B. MPB collected data in Fig. 3A-D and Supp. Fig. 5.

Abstract

Metabolism regulates neuronal activity and modulates the occurrence of epileptic seizures. Here, using two rodent models of absence epilepsy, we show that hypoglycemia increases the occurrence of spike-wave seizures. We then show that selectively disrupting glycolysis in the thalamus, a structure implicated in absence epilepsy, is sufficient to increase spike-wave seizures. We propose that activation of thalamic AMP-activated protein kinase (AMPK), a sensor of cellular energetic stress and potentiator of metabotropic $GABA_B$ receptor function, is a significant driver of hypoglycemia-induced spike-wave seizures. We show that AMPK augments postsynaptic $GABA_B$ receptor-mediated currents in thalamocortical neurons and strengthens epileptiform network activity evoked in thalamic brain slices. Selective thalamic AMPK activation also increases spike-wave seizures. Finally, systemic administration of metformin, an AMPK agonist and common diabetes treatment, profoundly increased spike-wave seizures. These results advance the decades-old observation that glucose metabolism regulates thalamocortical circuit excitability by demonstrating that AMPK and $GABA_B$ receptor cooperativity is sufficient to provoke spike-wave seizures.

Introduction

Epilepsy is a disorder defined by spontaneously recurring seizures. Identifying factors that drive neural circuits to very rapidly, yet transiently, seize remains a major challenge. The *Genetic Generalized Epilepsies* (GGEs) comprise one-third of all epilepsy syndromes and stem from complex, polygenic insults whose mechanisms remain poorly understood. Absence seizures are commonly observed in the GGEs and appear as bursts of rhythmic, high amplitude spike-wave-discharges that arise from synchronous activity among cortical and subcortical circuits (Huguenard & McCormick, 2007; Kandel &

Buzsáki, 1997; McCafferty et al., 2018). Cortical structures are thought to initiate spike-wave seizures, whereas thalamic structures serve as critical nodes for seizure generalization and maintenance (Avoli, 2012; Beenhakker & Huguenard, 2009; Blumenfeld, 2005; Meeren et al., 2002a).

The brain consumes 20% of dietary glucose to sustain normal function (Mergenthaler et al., 2013). Unsurprisingly, glucose availability has a considerable effect on seizures(Arsov et al., 2012; Leiva-Salinas et al., 2017; Mullen & Berkovic, 2018; Reid et al., 2011). Over eighty years ago, Gibbs et al. (Gibbs et al., 1939) showed that hypoglycemia precipitates seizures in children with absence epilepsy. Since then, we have learned that nearly 10% of patients diagnosed with early-onset childhood absence epilepsy are deficient in glucose transporter-1 (GLUT1) (Leary et al., 2003; Mullen & Berkovic, 2018), the singular glucose transporter that shuttles glucose across the blood brain barrier (Simpson et al., 1999, 2007). Hypoglycemia-sensitive seizures are also observed in GLUT1 deficient mice (Furuse et al., 2019) and a mouse model of spike-wave seizures (Reid et al., 2011). The cellular mechanisms that transduce glucose availability into spike-wave seizures are unknown.

The conversion of cellular energy state into neural activity is complex (Dienel, 2018; López-Gambero et al., 2018). The canonical transduction pathway involves the ATP-sensitive potassium (K_{ATP}) channel. Largely regulated by ATP, the K_{ATP} channel adjusts the membrane voltage of the cell in response to cellular energy state; ATP depletion activates the channel, causing membrane voltage hyperpolarization (Ashford et al., 1990; Yellen, 2008). K_{ATP} channels modulate neuronal activity in the hippocampus, (Giménez-Cassina et al., 2012; Tanner et al., 2011) hypothalamus (Ashford et al., 1990; Lee et al., 1999) and brainstem (Karschin et al., 1998), and are proposed to regulate limbic seizures (Giménez-Cassina et al., 2012; Martínez-François et al., 2018). Metabolic regulation of neural activity can also arise from the cooperative action between the

metabotropic, B-type GABA receptor ($GABA_B$) and the energy-sensitive AMP kinase (AMPK). During cellular stress, activated AMPK (p-AMPK) phosphorylates the $GABA_B$ receptor and potentiates $GABA_B$ receptor-mediated potassium currents (Kuramoto et al., 2007). Thalamocortical neurons are enriched in postsynaptic $GABA_B$ receptors (Kulik et al., 2002) and exert substantial control over thalamocortical oscillations and spike-wave seizures (Bal et al., 2000; Blumenfeld & McCormick, 2000; Bortolato et al., 2010; Destexhe, 1998; Hosford et al., 1992; Krosigk et al., 1993; Lu et al., 2020; Vergnes et al., 1997).

Here, we aimed to identify mechanisms that underlie hypoglycemia-provoked spike-wave seizures. We show that despite thalamocortical neuron expression, K_{ATP} channels play a minimal role in regulating thalamic neural activity during hypoglycemia. We therefore tested the hypothesis that hypoglycemia promotes functional coupling between AMPK and $GABA_B$ receptors to provoke spike-wave seizures. In support of this model, we demonstrate that AMPK activation strengthens $GABA_B$ receptor-associated currents in thalamocortical neurons and escalates thalamic network oscillations *in vitro*. Direct, thalamic AMPK activation also increases spike-wave seizures. Metformin, a well-established diabetes treatment and AMPK activator, produced a profound increase in spike-wave seizures that often progressed into lethal convulsive seizures. Collectively, we propose the first mechanistic framework to understand the long-established, clinical observation that low blood glucose exacerbates spike-wave seizures.

Results

Overnight fasting increases spike-wave seizures

Acute food withdrawal increases the number of spontaneous spike-wave seizures (SWSs) recorded in the DBA/2J strain of mouse (Reid et al., 2011). We first confirmed this

result (Supp. Fig. 1C-G) and then determined if acute hypoglycemia also provokes SWSs in the WAG/Rij rat, a long-standing, validated model of absence epilepsy (Coenen, 2003; van Luijtelaar & Coenen, 1986). We performed electrocorticogram (ECoG) recordings in adult WAG/Rij rats for three consecutive days (Fig. 1A). Animals received food and water *ad libitum* for two days. On day three, animals fasted for 18 hours, a duration required to achieve at least a 30% drop in blood glucose. We quantified SWSs during a four-hour period beginning at the same time of day for fed and fasted experiments. SWSs in WAG/Rij rats had an abrupt onset and occurred during behavioral arrest (Fig. 1B). Consistent with the efficacy of ethosuximide in treating human absence epilepsy, ethosuximide reduced SWSs in the rats (Fig. 1C). One hour prior to fed and fasted recording sessions, we collected peripheral blood samples for blood glucose and serum ketone body (i.e. β-hydroxybutyrate) measurements. Ketone bodies represent an alternative fuel source for the brain during hypoglycemia (Rehni & Dave, 2018) and are hypothesized to modulate seizures (Lutas & Yellen, 2013).

Raster plots of individual SWSs (Figs. 1D-E) show that fasting increased SWSs relative to the fed state. Below each raster, we quantified the total number of SWSs per hour across the population; stacked histograms reveal the contribution of each animal to total SWS count for each hour-long bin. SWS count was nearly 2-fold higher during the fast versus fed recording sessions for WAG/Rij rats (p = 0.0078, n = 13; Fig. 1F). Seizure burden, measured as % duration seizing per recording session, was nearly 2-fold higher in WAG/Rij rats (p = 0.00061, n = 13; Fig. 1H) during fast versus fed sessions. The increased seizure burden was largely driven by an elevated seizure count, not an increase in SWS duration (p = 0.17, n = 13; Fig. 1G).

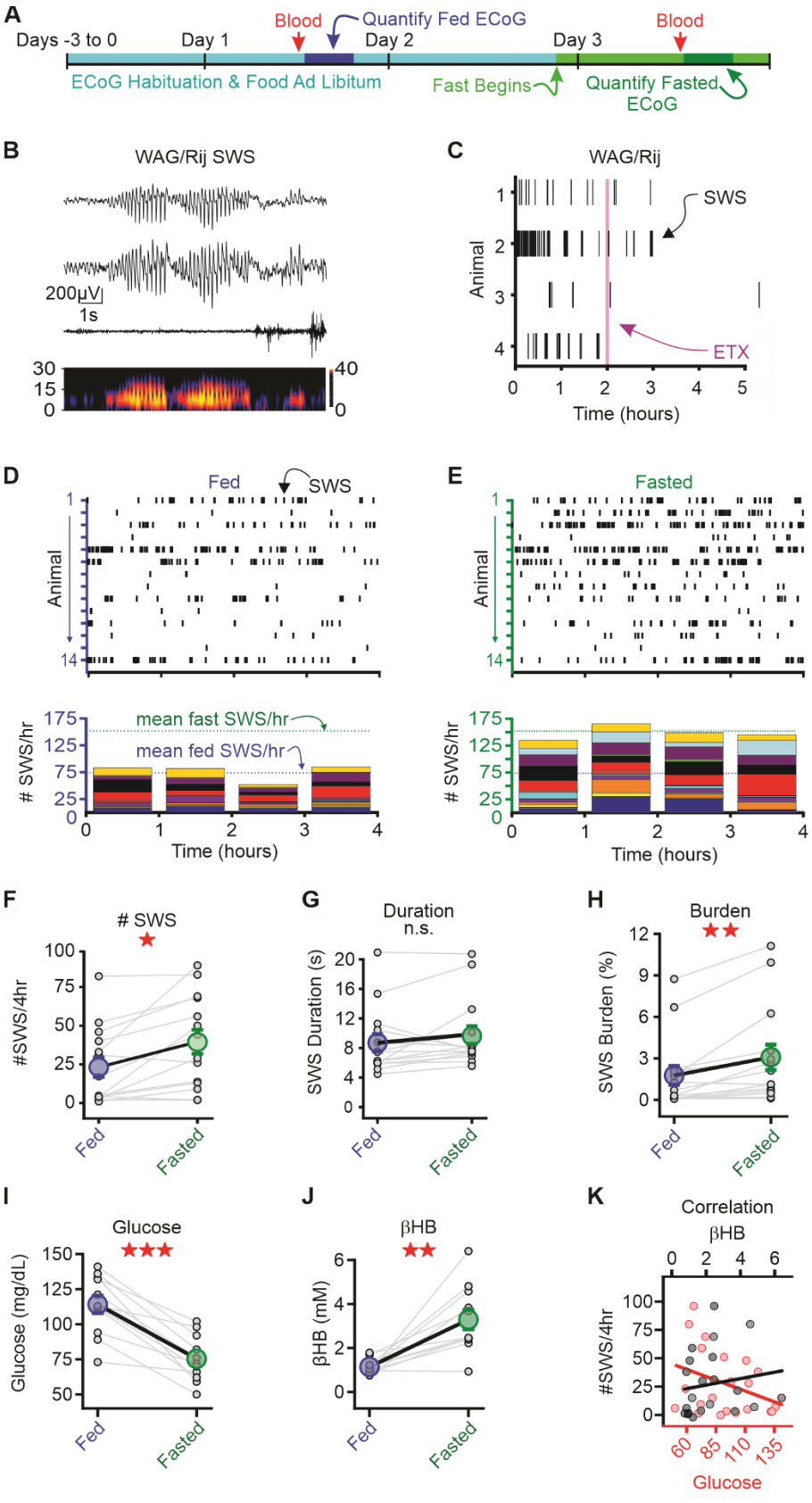
A
Days -3 to 0
Day 1
Blood
Quantify Fed ECoG
Day 2
Day 3
Blood
ECoG Habituation & Food Ad Libitum
Fast Begins
Quantify Fasted ECoG
B
WAG/Rij SWS
200μV
1s
30
15
0
40
0
C
WAG/Rij
SWS
ETX
Animal
Time (hours)
D
Fed
SWS
Animal
SWS/hr
mean fast SWS/hr
mean fed SWS/hr
Time (hours)
E
Fasted
Animal
SWS/hr
Time (hours)
F
SWS
#SWS/4hr
Fed
Fasted
G
Duration
n.s.
SWS Duration (s)
H
Burden
SWS Burden (%)
I
Glucose
Glucose (mg/dL)
J
βHB
βHB (mM)
K
Correlation
βHB
#SWS/4hr
Glucose

Figure 1. Overnight fasting increases spike-and-wave discharges. (A) Seizure activity was evaluated for multiple days. Animals had access to food *ad libitum* prior to the overnight fast on Day 3. Prior to control and fasting experiments, blood was drawn for glucose and β-hydroxybutyrate measurements. **(B)** *Top:* Representative SWS from a WAG/Rij rat (*right*). CTX1 and CTX2 are cortical ECoG recordings while EMG recording is from the neck. EMG activity was suppressed during the SWS, corresponding to behavioral arrest. *Bottom:* Spectrograms from CTX1 showing increased power in the 5-8 Hz frequency band during the SWS. **(C)** Ethosuximide (ETX; 200 mg/kg) suppressed SWSs in the WAG/Rij rat. Purple line indicates i.p. injection of ETX. **(D and E)** *Top:* SWS rasters during fed **(D)** and fasted **(E)** conditions in rats (n = 13). *Bottom:* Stacked histograms showing hourly SWS count for each rat during fed and fasted conditions. Blue and green dashed lines represent mean of the total SWS count per bin during fed and fasted conditions, respectively. **(F-H)** Fasting increased SWS count, duration and burden. **(I, J)** Fasting decreased blood glucose and increased β-hydroxybutyrate, relative to the fed state (n = 11). **(K)** Blood glucose (red) or serum β-hydroxybutyrate (black) versus SWS count. For each panel, small circles represent data from one animal, while large circles represent the sample mean (± SE). * $p < 0.05$, ** $p < 0.01$, ***$p < 0.001$ or not significant (n.s.) from the Wilcoxon sign rank test. See Table S1 for details.

Acute fasting elicited predictable changes in both blood glucose and β-hydroxybutyrate. Fasting decreased blood glucose (p = 0.00097, n = 11; Fig 1I) and increased β-hydroxybutyrate (p = 0.002, n = 11; Fig. 1J), relative to the fed sessions. Fasting had similar effects on the DBA/2J mice (Supp. Fig 1H-J). We evaluated the correlation between SWS counts and glucose/β-hydroxybutyrate levels across both fed and fasted recording sessions. While correlation coefficients were not statistically significant, SWS count and β-hydroxybutyrate trended towards a positive correlation, whereas SWS count and blood glucose trended towards an inverse correlation (Fig. 1K). The observed trends suggested that either hypoglycemia or ketosis – or both – might underlie the increase in SWS count following an acute fast.

Elevated SWS count consistently associates with low glucose, not elevated ketone bodies.

We next employed a blunt manipulation – insulin injection – to disambiguate the effects of glucose and β-hydroxybutyrate on SWSs. In fed animals, insulin reduces blood sugar (Titchenell et al., 2017; Tokarz et al., 2018) without, presumably, affecting serum ketone bodies; although insulin can inhibit ketogenesis, this effect is primarily observed in fasted or diabetic animals (Bieberdorf et al., 1970; Sherwin et al., 1976). We therefore tested the capacity of acute insulin administration in fed animals to reduce blood glucose and increase SWSs, without elevating serum β-hydroxybutyrate. We recorded SWSs in WAG/Rij rats during two, four-hour recording sessions, each separated by a day of rest. One hour into the recording session, the animals received either insulin injection (3 IU, i.p.) or volume-matched saline injection (Fig. 2A); we opted for a high insulin dose to induce a rapid and precipitous drop in glucose levels. We obtained peripheral blood samples 90 minutes after insulin injection to measure blood glucose and β-hydroxybutyrate (Fig. 2A). The 90 minute time point aimed to capture the peak

hypoglycemic response induced by insulin (Vinué & González-Navarro, 2015). SWS count, represented in stacked histograms, shows the contribution of each rat following either saline (Fig. 2B) or insulin (Fig. 2C) injection. To evaluate the effect of insulin on SWS count, we compared the mean number of SWSs observed during the three hours following saline versus insulin injection. Relative to saline, insulin increased SWS count (p = 0.036, n = 12; Fig. 2D) and SWS burden in the rats (p = 0.012, n = 12; Fig. 2F); SWS duration was not affected (p = 0.92, n = 12; Fig. 2E). Insulin injection produced a large reduction in blood glucose (p = 0.0039, n = 9; Fig. 2G), whereas β-hydroxybutyrate remained unchanged relative to saline injection (p = 0.36, n = 9; Fig. 2H). We made similar observations for SWSs, blood glucose and β-hydroxybutyrate in DBA/2J mice (Supp. Fig. 2C-G). As in Figure 1K, we evaluated the correlation between SWS count and glucose or β-hydroxybutyrate levels. This analysis revealed that SWS count and blood glucose were significantly and inversely correlated (R = -0.48, p = 0.046), similar to the trend we observed during acute fasting (c.f. Fig. 2I and Fig. 1K). As the inverse relationship between SWS count and blood glucose was consistent across fasting and insulin experiments, we concluded that hypoglycemia is sufficient to increase SWSs.

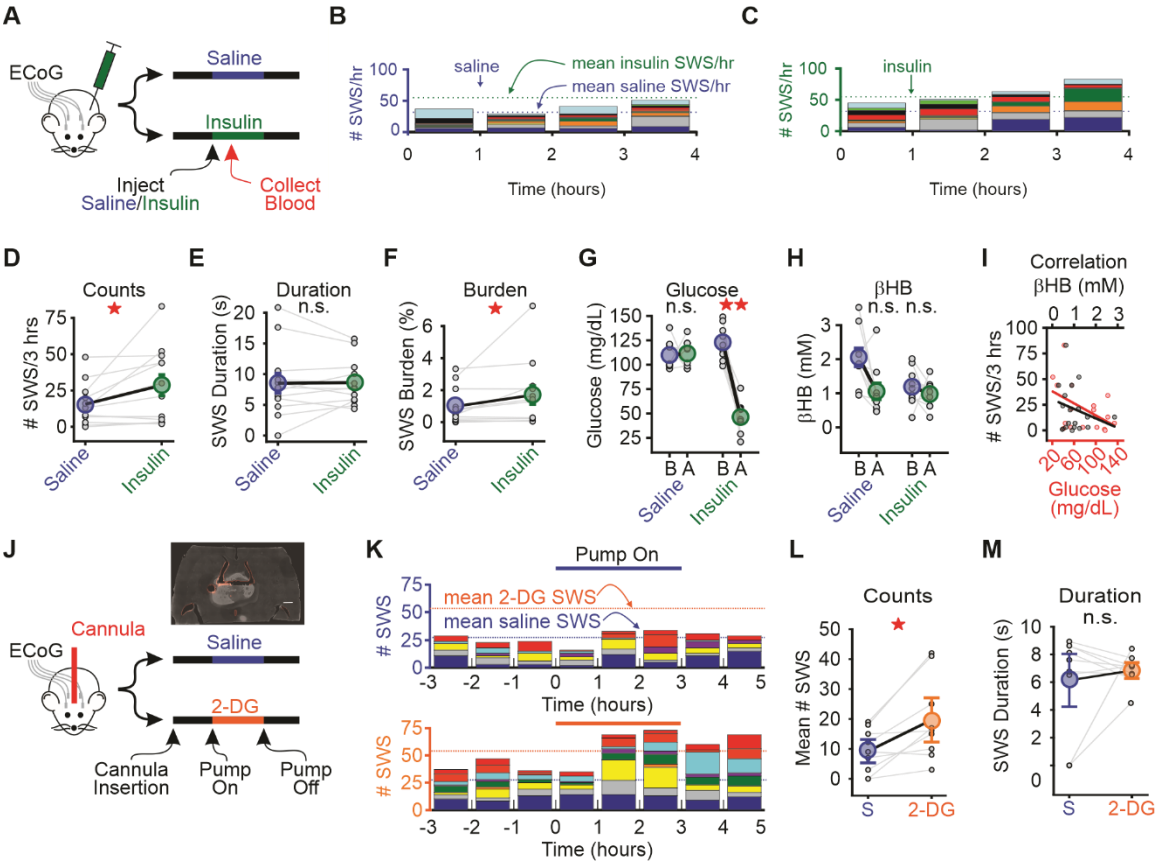

Figure 2. Elevated SWS count tracks with low blood glucose. (A) Animals received either saline or insulin (3 IUs) one hour into a 4-hour recording session (n = 12). Blood was collected at 90 minutes post-injection for glucose and serum β-hydroxybutyrate analysis. **(B, C)** Stacked histograms showing SWS counts for WAG/Rij rats after saline **(B)** or insulin **(C)** injection. Blue dashed lines represent the mean total SWS count per bin after saline. Green dashed lines represent the mean SWS total count per bin after insulin. **(D-F)** Insulin increased mean SWS count and burden, but not duration, relative to saline injection. **(G, H)** In rats, insulin significantly decreased blood glucose but had no effect on serum β-hydroxybutyrate concentration. B, before injection; A, after injection. **(I)** Plot comparing SWS count to blood glucose (red) and serum β-hydroxybutyrate (black) in rats (n = 9). **(J)** Rats implanted with ECoG electrodes and unilateral cannulae in somatosensory thalamus received either saline or 2-DG on separate days. Pump was

automatically turned on after a 4-hour baseline recording and turned off three hours later. Inset shows example of cannula placement in thalamus. 100 µm horizontal section from rat following injection of DiI (scale = 1mm). **(K)** Stacked histograms showing SWS count per hour for saline infusion (*top*) and 2-DG (*bottom*). Blue and orange dotted lines represent the mean of the total SWS count per bin during the infusion of saline and 2-DG, respectively. **(L, M)** 2-DG infusion increased mean SWS count during the infusion period (i.e., 0-3 hr) whereas duration was unaffected. In each panel, small circles represent data from one animal, whereas large circles represent the sample mean (± SE). * $p < 0.05$, ** $p < 0.01$ or not significant (n.s.) from Wilcoxon sign rank test or paired t-test. See Table S2 for details.

Intra-thalamic 2-DG increases SWSs in WAG/Rij rats

Reduced peripheral blood glucose also reduces cerebral glucose (Routh et al., 2014). Moreover, neural activity in the human thalamus, a structure critical for SWS generation, is particularly susceptible to moderate levels of acute hypoglycemia.(Arbeláez et al., 2012a) Therefore, we tested the hypothesis that selective disruption of thalamic glycolysis is sufficient to provoke SWSs. We used a local drug delivery system to infuse 2-deoxyglucose (2-DG) into the thalamus of WAG/Rij rats. 2-DG disrupts glycolysis by competing with native glucose as a substrate for glycolytic metabolism.(Wick et al., 1957) We targeted our local, unilateral 2-DG delivery to the somatosensory thalamus, a well-characterized SWS node,(Fogerson & Huguenard, 2016) while recording ECoG signals (Fig. 2J). After positioning a solution-filled cannula into the thalamus and recording basal activity for three hours, we delivered either 2-DG [27 μM (Slusser & Ritter, 1980)] or saline for an additional three hours. Figure 2K shows the number of SWSs contributed by each animal to total SWS count per hour during intrathalamic infusion of saline or 2-DG. Comparing total SWS count during active delivery (i.e., pump turned on) showed that 2-DG infusion doubled SWS count, relative to saline (p = 0.010, n = 9; Fig. 2L). 2-DG did not affect SWS duration (p = 0.56, n = 9; Fig. 2M). Thus, targeted disruption of thalamic glycolysis is sufficient to provoke SWSs.

K_{ATP} channels are well-characterized, glucose-sensitive ion channels(Ashford et al., 1990; Lee et al., 1999) implicated in epilepsy.(Giménez-Cassina et al., 2012; Martínez-François et al., 2018) Therefore, we determined whether thalamic neurons express K_{ATP} channels, and whether these channels confer glucose-sensitivity to thalamic neurons. Whereas immunohistochemical (Supp. Fig. 3A-B), qPCR (Supp. Fig. 3C) and electrophysiological (Supp. Fig. 3D) assays support the conclusion that thalamocortical neurons express K_{ATP} channels, low glucose challenges did not affect the intrinsic excitability of these neurons in either WAG/Rij rats (Supp. Fig. 3H-I) or DBA/2J mice

(Supp. Fig. 3J,K), indicating that ion channel activity in thalamocortical neurons is unaffected during hypoglycemic conditions. We therefore turned our attention to possible changes in synaptic properties induced by hypoglycemia.

Activated AMPK rescues attenuation of $GABA_B$ receptor-mediated currents

AMP-activated protein kinase (AMPK) serves as a master metabolic regulator(Herzig & Shaw, 2018; Kahn et al., 2005) in many tissues, including brain (Culmsee et al., 2001; Kim et al., 2004; Lee et al., 2005; McCrimmon et al., 2004; Ramamurthy & Ronnett, 2006), by responding to the ratio of AMP or ADP to ATP within cells. As ATP levels drop, AMP or ADP activates AMPK, which is rapidly mobilized to restore the balance of cellular energy (Herzig & Shaw, 2018). The kinase, therefore, functions specifically as a sensor of low levels of intracellular ATP and, more generally, as a sensor of energetic stress in the cell. Reliable cellular stressors that activate (i.e. phosphorylate) AMPK include hypoxia (Jun et al., 2007; Ramamurthy & Ronnett, 2006) and hypoglycemia (Culmsee et al., 2001; Kong et al., 2016). We first used western blots to determine if AMPK activation is inducible in acute WAG/Rij rat, thalamic brain slices. We applied two indirect activators of AMPK, 2-DG and metformin, as well as the potent, direct activator A-769662, to thalamic slices and measured phosphorylated AMPK (p-AMPK) levels. Consistent with previous studies (Konagaya et al., 2017; Tsou et al., 2011), a 30 minute bath application of 2-DG, metformin or A-769662 each produced a noticeable trend toward increased p-AMPK expression in a thalamic slice preparation, relative to a standard ACSF solution (Supp. Fig. 4A-B). However, we also observed significant differences in baseline p-AMPK signal across slices. As AMPK activation and deactivation are rapid signaling events, our variable p-AMPK signals likely reflect the challenge in mitigating the cellular stress imposed during thalamic tissue extraction. Consequently, we

used a FRET-based AMPK activity reporter, AMPKAR (Konagaya et al., 2017), that allows within slice comparisons and offers better temporal resolution. Previous studies using AMPKAR show that AMPK activation occurs within 10-20 minutes following application of 2-DG, metformin or A-769662 (Konagaya et al., 2017; Tsou et al., 2011). We generated a virally deliverable AMPK activity reporter driven by the excitatory neuron CaMKII promoter (Fig. 3A); thalamocortical neurons express CaMKII. AAV.Camk2a.AMPKAR.WPRE.Rbg was stereotaxically delivered to the somatosensory nucleus of the thalamus of WAG/Rij rats. Following expression, we extracted acute brain slices containing the thalamus and measured AMPKAR FRET efficiency. Within 20 minutes, application of either metformin (10 mM; p = 0.0002, n = 13; Figure 3B, C) or A-769662 (100 nM; p = 0.0129, n = 10; Figure 3B, D) increased FRET efficiency relative to baseline, indicating elevated AMPK activity.

Next, we tested whether AMPK activation by metformin alters the intrinsic excitability of WAG/Rij rat thalamocortical neurons. We recorded individual thalamocortical neurons in the current clamp configuration while injecting a family of hyperpolarizing and depolarizing current steps (Supp. Fig. 4C-E). Hyperpolarizing current injection was used to evaluate post-inhibitory rebound burst firing by thalamocortical neurons, a firing mode associated with SWSs (Beenhakker & Huguenard, 2009). Depolarizing current injection was used to evaluate general neuronal excitability. Rebound burst strength following a 2-second, -140pA, hyperpolarizing current injection was unaltered during 10 mM metformin application (p = 0.70, n = 13; Supp. Fig. 4D). In contrast, 10 mM metformin produced a modest increase in excitability during depolarizing current injections [repeated-measures two-way ANOVA: $F(1,245) = 15.3$, p = 0.0001, n = 13; Supp. Fig. 4E]. The physiological relevance of the observed increase in spike count during a sustained, depolarizing current injection remains unclear as rebound burst firing

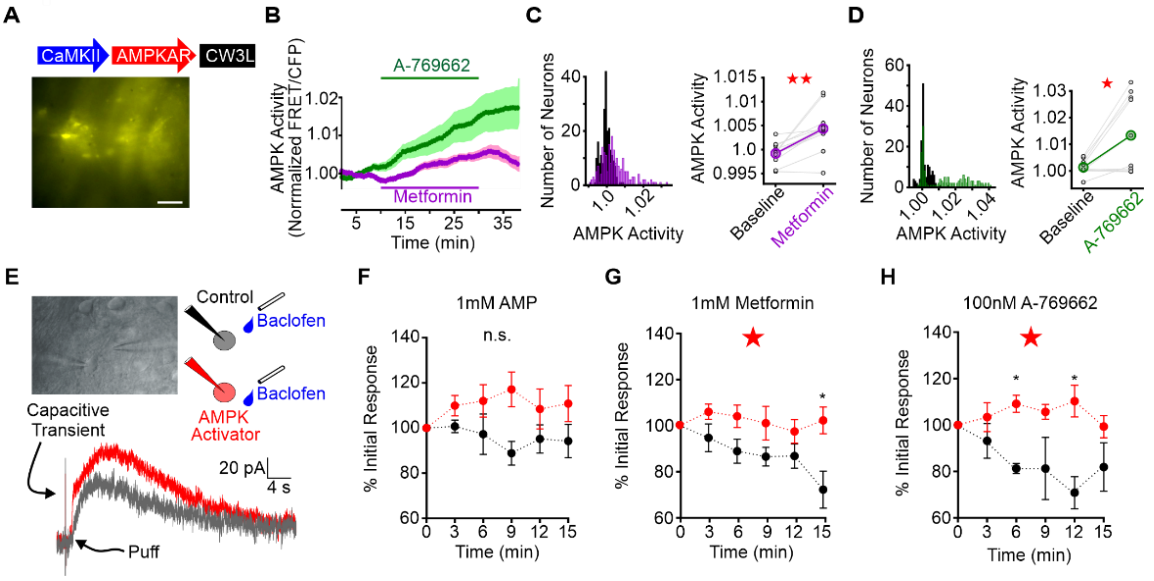

Figure 3. Thalamic p-AMPK expression and GIRK currents following AMPK activation. (A) Thalamocortical neuron AMPKAR expression based on construct developed by Tsou et al. (Tsou et al., 2011) and Konagaya et al. (Konagaya et al., 2017). Scale bar = 50 µM. **(B)** Thalamocortical neuron AMPKAR FRET efficiency increased during application of metformin (10mM, purple), A-769662 (100nM, green). FRET values are normalized to the three-minute baseline period prior to drug application. **(C)** Histogram (*left*) of FRET values for all neurons during baseline (black) and metformin (purple) application. Pairwise comparison (right) of mean FRET per slice in baseline and metformin application. **(D)** Histogram of FRET values (*left*) and mean pairwise comparisons (*right*) for A-769662 application. **(E)** *Top, left*: Whole cell patch-clamp recording in an acute thalamic brain slice. Baclofen application pipette is on the right. *Top, right:* Schematic of experiment. Whole cell patch-clamp recordings were performed using recording pipettes containing either control internal solution (black) or internal solution supplemented with an AMPK activator (red). A second pipette, placed proximal to the patched neuron, contained 100 µM baclofen (blue). *Bottom*: Representative traces of evoked $GABA_B$ currents (gray: control; red: AMPK activator). Arrows point to capacitive transient of a voltage-step used to measure access resistance and puff onset. **(F)** AMP (1 mM) stabilized, but did not

significantly mitigate (p = 0.06), $GABA_B$ receptor current rundown. **(G)** Metformin (1 mM) significantly prevented $GABA_B$ current rundown relative to control. **(H)** A-769662 (100 nM) similarly attenuated $GABA_B$ current rundown relative to control. For **(F-H)**, response amplitude of $GABA_B$-receptor mediated K^+ current was normalized to the current amplitude at 3 min (t = 1); data are mean ± SE; **p* <0.05, **p <0.01 or not significant (n.s.). Repeated-measures two-way ANOVA; Unpaired t-test for pairwise comparison. See Table S3 for data values.

mode, not tonic firing mode, is proposed to drive SWSs (Beenhakker & Huguenard, 2009; McCormick & Contreras, 2001). AMPK-mediated enhancement of inhibitory $GABA_B$ receptor signaling serves to curtail the damaging effects of ischemia, a stressor that activates the kinase (Kuramoto et al., 2007; Jun et al., 2007). AMPK phosphorylates S783 of the R2, $GABA_B$ receptor subunit that, in turn, potentiates receptor coupling to G-protein inwardly rectifying K^+ channels (GIRKs) (Kuramoto et al., 2007; Padgett & Slesinger, 2010). The slow, long-lasting hyperpolarizing current that results from GIRK channel activation counters ischemia-associated excitotoxicity (Kuramoto et al., 2007). As enhanced postsynaptic $GABA_B$ receptor function increases SWS occurrence (Bortolato et al., 2010; Liu et al., 1992), we hypothesized that hypoglycemia-provoked SWSs rely on similar AMPK-$GABA_B$ receptor cooperativity during energetic stress.

We evaluated the effects of AMPK on postsynaptic $GABA_B$ receptor function by manipulating the internal pipette solution of voltage-clamped neurons recorded in the whole-cell patch clamp configuration. We evoked $GABA_B$ receptor-mediated GIRK currents in WAG/Rij thalamocortical neurons by pressure ejecting the $GABA_B$ receptor agonist baclofen (100 μM, 5 msec) proximal to the recorded neuron every three minutes (Fig. 3E). Similar to observations made in cultured hippocampal neurons (Kuramoto et al., 2007), successive baclofen applications produced progressively smaller responses in thalamocortical neurons recorded under control conditions (i.e. internal solution containing 2 mM ATP; Fig. 3F-H, black), a response rundown attributed to cell surface instability of the receptor (Couve et al., 2002; Kuramoto et al., 2007). AMPK activation in cultured hippocampal neurons increases cell surface $GABA_B$ receptor stability and counteracts baclofen response rundown (Couve et al., 2002; Kuramoto et al., 2007). Similarly, when included in the internal pipette solution of recorded thalamocortical neurons, AMPK activators metformin (Zhou et al., 2001) and A-769662 (Göransson et al., 2007) eliminated rundown to repeated baclofen application (Fig. 3G-H, red); inclusion of AMP produced a

non-significant trend of this rundown elimination (Fig. 3F). We quantified these observations by normalizing the amplitude of all baclofen responses to the amplitude of the first baclofen response. Thus, under control conditions, baclofen-activated GIRK currents exhibited rundown, relative to starting responses, while inclusion of AMP in the recording pipette produced responses that trended larger [repeated-measures two-way ANOVA: $F(5,65) = 2.21$, $p = 0.06$; Fig. 3F]. Rundown was significantly mitigated when 1 mM metformin [repeated-measures two-way ANOVA: $F(5,75) = 2.79$, $p = 0.022$; Fig. 3G] or 100 nM A-769662 [repeated-measures two-way ANOVA: $F(5,65) = 2.83$, $p = 0.022$; Fig. 3H] was added to the internal pipette solution. Thus, AMPK activation potentiates post-synaptic $GABA_B$ receptor-mediated GIRK currents in thalamocortical neurons.

AMPK agonists intensify $GABA_B$ receptor-dependent epileptiform oscillations

We next tested whether thalamic circuit oscillations recorded *in vitro* are also sensitive to AMPK activation. Electrical stimulation of corticothalamic afferents in acute brain slices containing somatosensory thalamus is a well-established model of both sleep spindles and SWSs (Bal et al., 1995; Kleiman-Weiner et al., 2009; von Krosigk et al., 1993) and provides a measure of thalamic circuit excitability. Several studies demonstrate that spindle-like activity evoked in the thalamic slice preparation relies on A-type GABA ($GABA_A$) receptor-mediated signaling, whereas SWS-associated epileptiform activity relies on robust activation of $GABA_B$ receptors expressed by thalamocortical neurons (Bal et al., 2000; Blumenfeld & McCormick, 2000; Destexhe, 1998). Using this model, we tested the sensitivity of both $GABA_B$ receptor-dependent and -independent activity to AMPK activation.

Pilot studies suggested that A-769662 potentiates evoked oscillations generated in slices wherein $GABA_A$ and $GABA_B$ receptors are both functional (Supp. Fig. 5A). Next,

to dissect the contribution of $GABA_A$ and $GABA_B$ receptors to this effect, we evoked thalamic, SWS-like oscillations in WAG/Rij brain slices by stimulating neurons of the reticular thalamic nucleus in the presence of the $GABA_A$ receptor antagonist, bicuculline (10 μM; Fig. 4A-B). Oscillations were evoked once per minute and action potential activity was recorded with extracellular field electrodes placed within somatosensory thalamus. In the absence of any additional pharmacological manipulation, oscillations evoked during bicuculline application are generally stable(Lu et al., 2020) but can exhibit some rundown(Bryant et al., 2009) (Supp. Figure 5B). Following a baseline period wherein oscillations were evoked 10 μM bicuculline, we co-applied either metformin (5 mM) or A-769662 (10 μM) to the perfusate for 40 minutes, followed by a 20-minute washout period. Both metformin (Fig. 4C) and A-769662 (Fig. 4G) prolonged evoked oscillations. Plotting binned spikes in a grayscale heat map showed that oscillation prolongation occurred within 10 minutes of metformin (Fig. 4D) or A-769662 (Fig. 4H) application. Such was also the case when pooling all slice experiments and tracking oscillation duration across time (metformin: Fig. 4E; A-769662: Fig. 4I). The pooled data showed that oscillation duration increased by 20% during metformin application (p = 0.0027, n = 11; Fig. 4F) and 12% during A-769662 application (p = 0.0082, n =15; Fig. 4J). These results suggest that AMPK-$GABA_B$ cooperativity modulates thalamic oscillations.

We also evaluated the sensitivity of evoked network activity during AMPK activation when $GABA_B$, not $GABA_A$, receptors were blocked. $GABA_B$ receptor blockade produces oscillations that are disorganized and short in duration (Bal et al., 2000; Blumenfeld & McCormick, 2000). Nonetheless, activity evoked during $GABA_B$ receptor blockade provides an opportunity to evaluate the sensitivity of thalamic circuits to AMPK activity in the absence of $GABA_B$ receptor activity. We recorded thalamic network activity in the presence of 20 nM CGP-54626, a potent $GABA_B$ receptor blocker (Beenhakker &

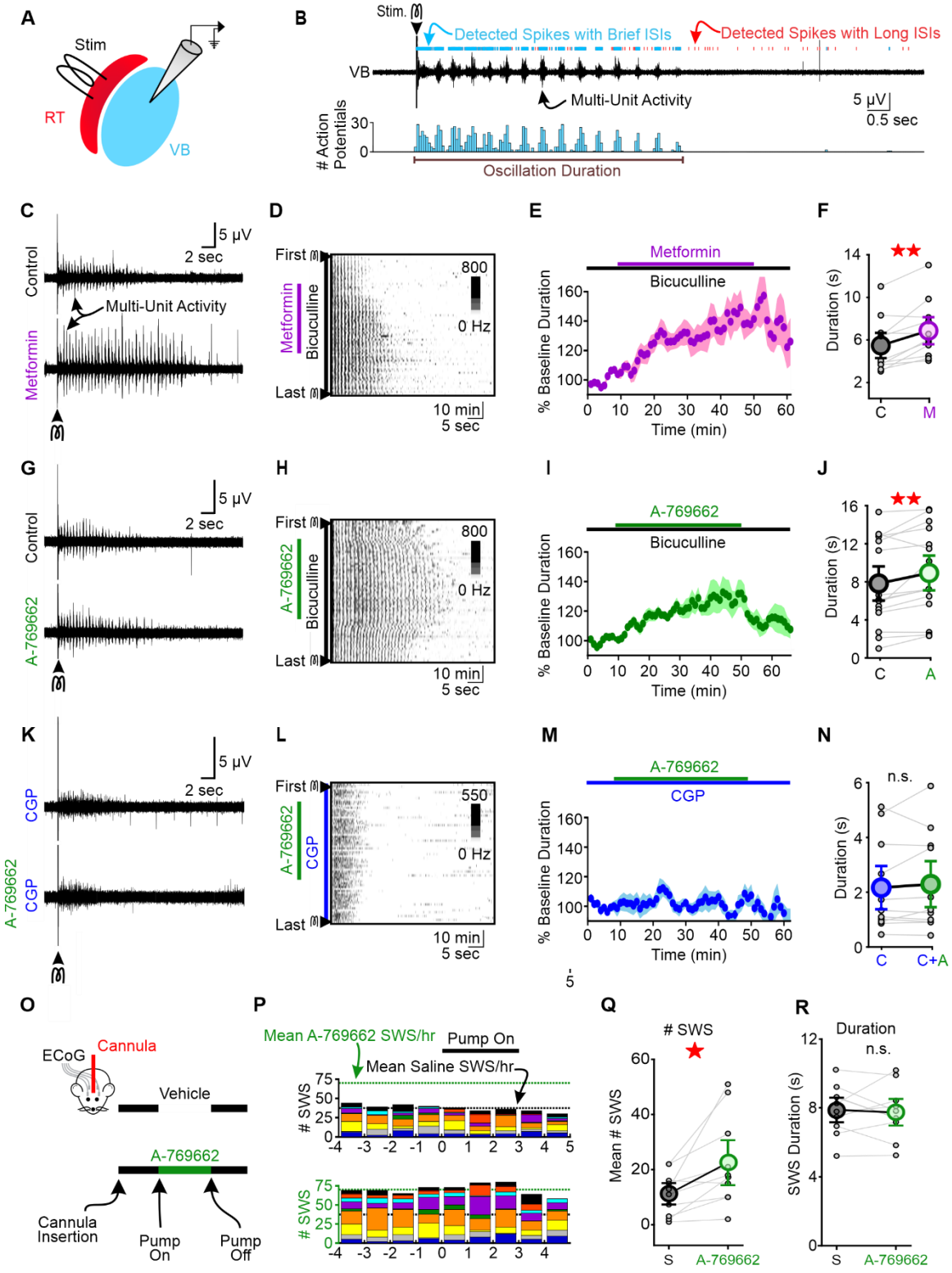

Figure 4. AMPK activators intensify thalamocortical oscillations *in vitro* and SWS *in vivo*. (A) Thalamocortical oscillations were electrically evoked in acute brain slices

containing RT and VB thalamus. **(B)** *Top:* A single stimulus evoked seconds-long bursting activity in VB that was evaluated by measuring interspike intervals (ISIs, see methods). **(C)** Representative oscillations and **(D)** spike raster during control and 5 mM metformin. Oscillations were evoked once every 60 seconds. **(E)** Normalized oscillation duration versus time for all metformin experiments. Durations were normalized to baseline values per slice. **(F)** Metformin increased oscillation duration relative to baseline. **(G)** Representative oscillations and **(H)** spike raster during control and 10 µM A-769662. **(I)** Normalized oscillation duration versus time for all A-769662 experiments. **(J)** A-769662 increased oscillation duration relative to baseline. **(K)** Representative oscillations and **(L)** spike raster during control (20 nM CGP-54626) and 20 nM CGP-54626 + 10 µM A-769662. Blocking $GABA_B$ receptors with CGP resulted in briefer and more disorganized spiking activity. **(M)** Normalized oscillation duration versus time for all CGP experiments. **(N)** Mean duration of evoked activity was not different between CGP-54626 and CGP-54626 + A-769662 co-application. **(O)** Direct infusion of A-769662 in somatosensory thalamus increased SWSs. WAG/Rij rats implanted with ECoG electrodes and unilateral cannulae in somatosensory thalamus received either saline or 10 µM A-769662 for 3-hours on separate days. **(P)** Stacked histograms showing SWS counts for each animal [saline (*top*) and A-769662 (*bottom*)]. Black and green dotted lines represent mean of the total SWS count per bin after infusion start for saline and A-769662, respectively. **(Q)** A-769662 infusion increased mean SWS count during the infusion period (i.e., 0-3 hr) but not **(R)** SWS duration. All data are represented as mean ± SE. *p < 0.05, ** p<0.01 or not significant (n.s.) from paired student's t-test or Wilcoxon sign rank test. Each circle in the figure represents one slice (**C-N**) or animal (**Q-R**). See Table S4 for details.

Huguenard, 2010), using the same stimulation paradigm described above. As expected, evoked activity was less oscillatory and shorter in duration, relative to oscillations evoked during $GABA_A$ receptor blockade (c.f. Fig. 4K and Fig. 4C, G). Importantly, application of the potent, direct AMPK activator A-769662 did not affect activity duration (p = 0.43, n=11; Fig. 4K-N). Thus, prolongation of oscillations evoked in the acute thalamic slice requires functional $GABA_B$ receptors.

The observation that AMPK activation specifically modulated SWS-like activity in the WAG/Rij rat thalamic slice motivated us to determine if A-769662 is sufficient to provoke SWSs recorded *in vivo*. We compared the actions of saline and 10 μM A-769662 on SWS occurrence in cannulated (somatosensory thalamus, unilateral) WAG/Rij rats (Fig. 4O). Figure 4P shows the contribution of each rat to total SWS count per hour before, during and after intrathalamic infusion of saline or A-769662. Relative to saline infusion, A-769662 infusion produced more SWSs (p = 0.017, n = 10; Fig. 4Q), but did not change SWS duration (p = 0.72, n = 10; Fig. 4R). These data demonstrate that like fasting (Fig. 1), insulin injection (Fig. 2B-F), and thalamic 2-DG infusion (Fig. 2K-M), thalamic AMPK activation is sufficient to increase SWSs in WAG/Rij rats.

Metformin increases SWSs and causes Status Epilepticus in WAG/Rij rats

Similar to A-769662, metformin potentiated postsynaptic $GABA_B$ receptor function in thalamocortical neurons and strengthened SWS-like oscillations. We therefore hypothesized that metformin would also exacerbate SWSs. To test this hypothesis, we administered metformin systemically (i.p.) to WAG/Rij rats and monitored SWSs. We delivered metformin systemically as this route is more comparable to its oral administration in patients. We tested metformin at 150 mg/kg and 200 mg/kg, two doses used in previous rat studies (Mehrabi et al., 2018; Rubio Osornio et al., 2018; Zhao et al., 2014). While the lower dose of metformin produced a trend towards increased SWSs (see below), WAG/Rij

rats injected with 200 mg/kg metformin advanced through a stereotyped progression of worsening seizure phenotype. Within 20 minutes of 200 mg/kg metformin injection, SWS count increased by several-fold and the rats quickly entered a state of nearly continuous SWSs for 30 minutes (i.e. absence status epilepticus, Fig. 5A). Within 70 minutes of metformin injection, all animals experienced generalized tonic-clonic seizures (convulsive status epilepticus, Fig. 5A) for approximately 20 minutes, after which five of six animals died. The one surviving rat remained in convulsive status epilepticus for 11 hours before seizures subsided. Figure 5B shows binned SWS counts for baseline (i.e. no injection) and saline injection, whereas Figure 5C shows SWS counts before/after 150 mg/kg and 200 mg/kg metformin injections, respectively. Binned SWS counts for non-epileptic Wistar rats, the strain of rat from which WAG/Rij rats are derived (Festing, 1979), are shown in Figures 5D-E.

We compared the total SWS count for each animal during the two hours following saline versus metformin injection (Fig. 5F-G). WAG/Rij rats injected with 200 mg/kg metformin produced more SWSs, relative to saline (p = 0.036, n = 6; Fig. 5F). 200 mg/kg metformin did not provoke seizures in non-epileptic Wistar rats (Fig. 5G). 150 mg/kg metformin produced a trend towards increased SWSs in WAG/Rij rats (p = 0.22, n = 6; Supp. Fig. 6B) relative to saline. In Wistar rats, 150 mg/kg metformin did not affect SWS count (Supp. Fig. 6E).

At high doses, metformin causes lactic acidosis.(Huang et al., 2017) Therefore, we measured blood lactate after metformin/saline injection in a separate cohort of WAG/Rij and Wistar rats. The one-hour time point aligned with the pronounced change in SWSs and the emergence of tonic-clonic seizures in the WAG/Rij rat. Lactate did not increase in WAG/Rij rats injected with 150 mg/kg metformin (p = 0.16, n = 7; Supp. Fig. 6C). After 200 mg/kg injection, we observed a 3-fold increase in lactate (p = 0.016; n = 7;

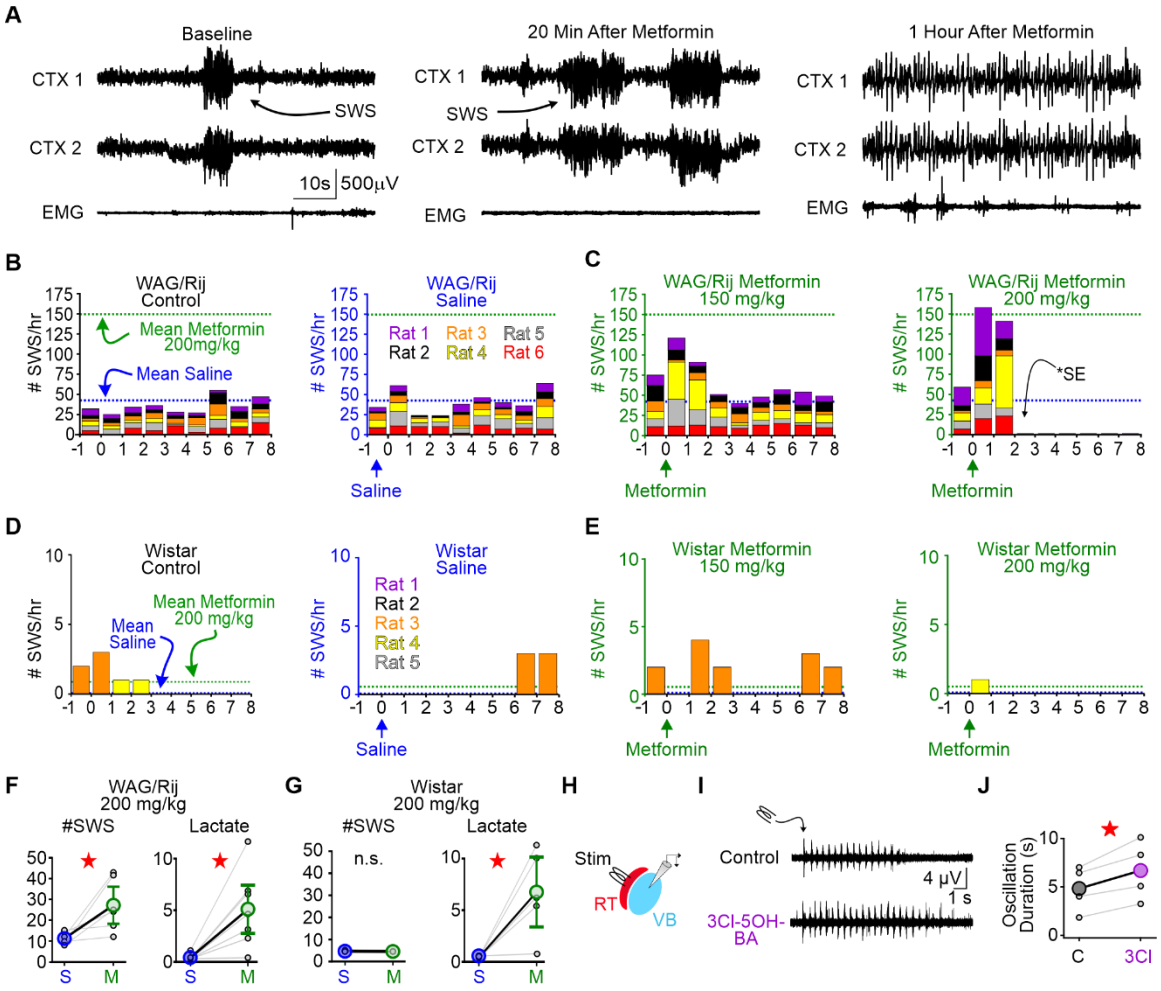

Figure 5. Metformin elevates SWSs and can cause Status Epileptics in WAG/Rij rats.

(A) Representative recording of WAG/Rij rat injected with 200 mg/kg metformin. *Left*: ECoG/EMG activity before metformin injection. Arrow indicates spontaneous SWS. *Center*: 20 minutes after metformin injection, SWSs occurred frequently and marked the beginning of continual SWSs. *Right*: ECoG/EMG recording 1 hour after metformin injection, wherein the transition from SWSs to convulsive status epilepticus (SE) has occurred. Heightened muscle activity is recorded in the EMG, consistent with motor activity induced by tonic-clonic seizures. **(B)** WAG/Rij rat SWS counts for control and saline. **(C)** SWS counts in same WAG/Rij rats after 150 mg/kg and 200 mg/kg metformin. Stacked histograms showing SWS counts per animal for all conditions. Dotted lines indicate the mean of the total SWS count per bin following saline (blue) and 200 mg/kg

metformin (green) injection, respectively. **(D)** Non-epileptic Wistar rat SWS counts for control and saline. **(E)** Wistar rat SWS counts in stacked histogram format for 150 mg/kg and 200 mg/kg metformin. **(F)** 200 mg/kg metformin increased WAG/Rij SWS counts, while lactate (mmoL/L) levels trended higher. **(G)** 200 mg/kg metformin did not evoke any seizure activity in Wistar rats despite comparable changes in lactate (mmol/L). **(H)** Schematic of experiment used to evaluate effect of HCAR1 agonist 3-Chloro-5-hydroxybenzoic acid (3Cl-5OH-BA) on network activity. **(I)** Representative multi-unit recordings of evoked thalamocortical oscillations in VB thalamus following electrical stimulation of RT. *Top*: Control trace showing oscillation evoked during baseline conditions. *Bottom*: Oscillation evoked during 3Cl-5OH-BA application. **(J)** 3Cl-5OH-BA significantly prolonged the duration of evoked oscillations. In each panel, data are represented as mean ± SE. Each dot presents one animal **(F, G)** or slice **(J).** *$p < 0.05$ or not significant (n.s.) from paired, t-test or Wilcoxon sign rank pairwise comparison. See Table S5 for details.

Fig. 5F), and all rats perished within one hour. 200 mg/kg metformin also increased lactate in Wistar rats (p = 0.03; n = 5; Fig. 5G).

As the WAG/Rij seizure response to lactate-producing doses of metformin is complex, we speculate that lactate's actions on WAG/Rij neural circuits are likewise complex. Nonetheless, we tested whether $GABA_B$ receptor-dependent oscillations evoked in acute thalamic slices from WAG/Rij rats were sensitive to activation of HCAR1, a receptor for lactate that, like AMPK, has recently been shown to augment $GABA_B$ receptor function (Abrantes et al., 2019). 3Cl-5OH-BA, a selective HCAR1 receptor agonist, prolonged evoked oscillations by 40% (p = 0.025, n = 4; Figs. 5H-J). Thus, both p-AMPK and lactate are sufficient to augment $GABA_B$ receptor function and exacerbate thalamic network oscillations associated with SWSs. However, it remains formally possible that p-AMPK actions on $GABA_B$ receptor function are indirect, resulting from its ability to elevate lactate.

Discussion

Here, we first advance the observation that hypoglycemia provokes spike-wave seizures by showing that selective blockade of thalamic glycolysis in the WAG/Rij rat is sufficient to provoke spike-wave seizures. Specifically, we show that hypoglycemia likely activates AMPK in the thalamus, and that activated AMPK augments postsynaptic $GABA_B$ receptor signaling in thalamocortical neurons. AMPK-$GABA_B$ receptor enhancement strengthens epileptiform, $GABA_B$ receptor-dependent oscillations in acute thalamic slices and elevates spike-wave seizures *in vivo*. Lastly, we report that metformin, a common diabetes treatment and AMPK activator (Pernicova & Korbonits, 2014), powerfully instigates spike-wave seizures in the WAG/Rij rat. These findings provide the first

molecular framework for understanding how glucose availability regulates generalized spike-wave seizures.

Hypoglycemia and spike-wave seizures

Glucose fuels the brain and is the most robust energy source for generating ATP. Moreover, glucose-derived metabolites are required for the synthesis of several neurotransmitters that regulate neuronal excitability, including glutamate and GABA (Dienel, 2018; Schousboe et al., 2007). Spike-wave seizure exacerbation by hypoglycemia was first reported nearly eighty-years ago (Gibbs et al., 1939), and impaired glucose handling continues to associate with the genetic generalized epilepsies today. Mutations in *SLC2A1*, the gene encoding glucose transporter-1 (GLUT1), are found in 1% of all genetic generalized epilepsy patients and specifically account for 10% of early-onset childhood absence epilepsies (Mullen & Berkovic, 2018). Moreover, nearly half of GLUT1 deficient patients produce 2.5-4 Hz spike-wave discharges (Leary et al., 2003), electrographic patterns similar to spike-wave seizures associated with the absence epilepsies. The *SLC2A1* mutation impairs glucose transport across the blood-brain barrier. As GLUT1-deficient patients present with cerebrospinal fluid containing less than 60 mg/dL glucose (Wang et al., 1993), these patients lack the necessary cerebral glucose to maintain proper brain function.

An effective therapy for GLUT1 deficiency syndrome is the ketogenic diet (Soto-Insuga et al., 2019), a high-fat, low carbohydrate diet that switches the body's fuel source from glucose to ketone bodies (Kristopher & Carl, 2010). As the brain shifts towards a reliance on ketone bodies for fuel, a change that takes several days, seizures in GLUT1 patients on the diet eventually abate. Indeed, the anti-convulsant effects of the ketogenic diet extend well beyond GLUT1 deficiency (D'Andrea Meira et al., 2019; H. Liu et al., 2018; Lutas & Yellen, 2013; McNally & Hartman, 2012). Several studies specifically attribute the

anti-seizure effects of the diet to elevated ketone bodies (Kadowaki et al., 2017; W. Ma et al., 2007; McNally & Hartman, 2012). And yet, here we report that acute fasting – a manipulation that elevates ketone bodies – exacerbates spike-wave seizures. We speculate that during acute hypoglycemia, the pro-spike-wave seizure actions of hypoglycemia outweigh the anti-spike-wave seizure mechanisms of ketosis, if any, to provoke spike-wave seizures; notably, the diet is considered only moderately effective in treating the absence epilepsies (Groomes et al., 2011; Thammongkol et al., 2012). If true, then evaluating whether absence seizure occurrence in patients correlates with normal, diurnal fluctuations in blood glucose may ultimately provide novel insights into improving seizure control.

Curiously, our observations that hypoglycemia, 2-DG and metformin can aggravate seizures appear to contradict the proposed, seizure-suppressing utility of these drugs. Indeed, both 2-DG (Garriga-Canut et al., 2006) and metformin (Mehrabi et al., 2018) show great promise in treating temporal lobe seizures. However, both 2-DG and metformin may ultimately belong to a sizeable list of anti-seizure drugs that counterintuitively worsen absence epilepsy. Drugs in this list – carbamazepine, oxcarbazepine, phenytoin, vigabatrin and tiagabine are used to treat temporal lobe seizures and yet aggravate absence seizures (French & Pedley, 2009; Gelisse et al., 2004; L. Liu et al., 2006; Osorio et al., 2000; Panayiotopoulos, 1999; Panayiotopoulos et al., 1997; Parker et al., 1998; Schapel & Chadwick, 1996). Indeed, both vigabatrin (Panayiotopoulos et al., 1997) and tiagabine (Knake et al., 1999) can induce *absence status epilepticus*, a state of continuous and prolonged spike-wave seizures and the EEG pattern we observed in WAG/Rij rats following a high metformin dose. Both vigabatrin and tiagabine increase the availability of extracellular GABA and are hypothesized to exacerbate absence seizures by promoting $GABA_B$ receptor activation (Beenhakker & Huguenard, 2010; Lu et al., 2020; Panayiotopoulos, 1999). Thus, the finding that 2-DG

and metformin may in fact both reduce temporal lobe seizures and aggravate absence seizures may ultimately align with our current understanding of some anti-seizure drugs.

$GABA_B$ receptor mediated inhibition in the thalamus

Our results support the hypothesis that energetic stress activates thalamic AMPK that, in turn, upregulates $GABA_B$ receptor function. Promoting $GABA_B$ receptor function elevates spike-wave seizure counts (Liu et al., 1992; Smith & Fisher, 1996; Vergnes et al., 1997), whereas inhibiting $GABA_B$ receptor function dampens spike-wave seizures (Bortolato et al., 2010; Liu et al., 1992; Stewart et al., 2009). The long-lasting and powerful inhibition produced by postsynaptic $GABA_B$ receptors recruits low threshold, T-type calcium channel activity to produce robust post-inhibitory rebound bursts that likely sustain spike-wave seizures (Beenhakker & Huguenard, 2009; McCormick & Contreras, 2001). Consistent with these observations, we show that activated AMPK potentiates postsynaptic $GABA_B$ receptor signaling in thalamocortical neurons, strengthens $GABA_B$ receptor-dependent, epileptiform oscillations recorded in thalamic brain slice preparations, and increases spike-wave seizures. Postsynaptic $GABA_B$ receptors have a moderate affinity for GABA [1μM (Sodickson & Bean, 1996)] and are largely localized to extrasynaptic dendritic regions of thalamocortical neurons (Kulik et al., 2002). Thus, the receptors are largely inactive during basal conditions or during moderate synaptic activity (Dutar & Nicoll, 1988; U. Kim et al., 1997; Scanziani, 2000). However, if GABAergic inputs are sufficiently active, then released GABA can spillover to extrasynaptic regions to activate $GABA_B$ receptors (Beenhakker & Huguenard, 2010). We propose that AMPK-mediated potentiation of thalamic $GABA_B$ receptor activity during hypoglycemia reduces the threshold for such receptor activation.

Herein, we focused on the potential contribution of the thalamus to hypoglycemia-provoked spike-wave seizures. Notably, however, spike-wave seizures result from

complex interactions between multiple structures, including the cortex and thalamus. According to the *Cortical Focus Theory*, the somatosensory cortex provides the initiating drive to thalamic circuits that then generate hypersynchronous, rhythmic activity that is rapidly generalized throughout widespread regions of the cortex (Manning et al., 2004; Meeren et al., 2002b). While our findings demonstrate that selective disruption of glucose metabolism in the thalamus is sufficient to elevate spike-wave seizures in the seizure-prone animal, future studies are warranted to determine whether selective cortical disruption is likewise sufficient. Nonetheless, our current observations suggest that glucose-sensitive mechanisms in the thalamus might establish a threshold necessary to produce generalized spike-wave seizures, and that hypoglycemia reduces this threshold by enhancing thalamic $GABA_B$ receptor function. This hypothesis is consistent with the observation that the human thalamus is uniquely sensitive to even moderate levels of hypoglycemia (Arbeláez et al., 2012b).

Metformin and spike-wave seizures

Metformin exacerbated spike-wave seizures and, at high doses, evoked a profound and fatal seizure response in seizure-prone animals. Metformin inhibits complex I of the mitochondrial electron transport chain, an effect that reduces ATP production and elevates AMP levels that facilitate AMPK activation (Pernicova & Korbonits, 2014). Metformin increases insulin sensitivity, enhances glucose uptake in muscle tissue, and blocks gluconeogenesis in the liver; collectively, all actions result in lower blood glucose (Pernicova & Korbonits, 2014) and make metformin the most common and highly effective pharmacological treatment for type 2 diabetes (Flory & Lipska, 2019; Pernicova & Korbonits, 2014). With its ability to pass the blood-brain barrier, metformin also has potential therapeutic effects in Huntington's disease (Ma et al., 2007), Alzheimer's disease (Li et al., 2012) and some forms of epilepsy (Mehrabi et al., 2018; Rubio Osornio et al.,

2018; Yang et al., 2017; Zhao et al., 2014). While adverse actions of metformin on absence epilepsy are not reported, several reasons may obscure any possible links. First, the high metformin dose used in our study was roughly twice that of the equivalent dose used in humans and therefore may not have a clinical equivalence; however, metformin overdose occurs in humans (Chiew et al., 2018; Flory & Lipska, 2019). Second, despite the drug's ubiquity, metformin is generally not prescribed to children; the mean age of onset for childhood absence epilepsy is 4-7 years of age (Matricardi et al., 2014). Thus, future studies are required to fully resolve the clinical ramifications of our unexpected observations.

Herein, the effects of metformin on spike-wave seizures likely result from a combination of actions. We propose that lower doses of metformin activate AMPK to augment $GABA_B$ receptor mediated signaling and increase spike-wave seizures. The actions of high doses of metformin are likely multifaceted. Following a high dose of metformin, spike-wave seizure counts not only increased, but all animals quickly transitioned into a state of near-continuous spike-wave activity (i.e., *absence status epilepticus*). We speculate that metformin-induced absence status epilepticus in rats results from the converging and enhancing actions of AMPK (Kuramoto et al., 2007) and lactate (Abrantes et al., 2019) on thalamic $GABA_B$ receptor function. The subsequent progression into convulsive, tonic-clonic seizures (status epilepticus) and death likely results from the actions of elevated lactate on multiple brain structures. Indeed, the drug's capacity to produce lactic acidosis provides the basis for the FDA's black box warning. Nevertheless, the intense seizure response was not observed in non-epileptic Wistar rats. Thus, spike-wave seizure predisposition appears necessary for a metformin-provoked seizure response. Clearly, the actions of metformin are complex and varied and fully testing this hypothesis will ultimately benefit from transgenic approaches that modify AMPK's activation capability.

Conclusions

In aggregate, our study addresses a growing number of observations that glucose availability regulates spike-wave seizures. Despite such conclusions, the mechanisms that enable hypoglycemia to regulate spike-wave seizures remain entirely unknown. We now provide data in support of the hypothesis that glucose-mediated regulation of spike-wave seizures results from p-AMPK potentiation of $GABA_B$ receptor-mediated signaling.

Materials and Methods

Animals

All procedures followed the National Institutes of Health *Guide for Care and Use of Laboratory Animals* and were approved by the University of Virginia Animal Care and Use Committee (Charlottesville, VA, USA). Unless otherwise stated, animals were housed at 23-25°C under an artificial 12 hr light-dark cycle with food and water provided *ad libitum*. Wistar Albino Glaxo/from Rijswijk (WAG/Rij rats) were kindly provided by Dr. Edward Bertram (University of Virginia). Non-epileptic Wistar IGS rats (stock #: 003) were purchased from Charles River (Wilmington, MA, USA). Wild type DBA/2J mice (stock #: 000671) were purchased from The Jackson Laboratory (Bar Harbor, ME, USA). Both sexes were used in all experiments and no differences were observed. In total, 44 DBA/2J mice and 141 WAG/Rij rats were used.

Simultaneous Video-Electrocorticography (ECoG)/Electromyographic (EMG) recordings

Rat ECoG devices were purchased from Plastics One (Roanoke, VA, USA). Mouse devices were assembled from parts purchased at Digikey (Thief River, MN, USA). Stainless-steel recording electrodes were implanted bilaterally in the cortex while a

reference electrode was placed in the cerebellum; EMG recordings were obtained from neck muscles. One week after surgery, animals were habituated to recording cages for 48 hrs. Filtered ECoG (0.3-100Hz) and EMG (>100Hz) signals were amplified with a Model 3500 amplifier (A-M Systems Sequim, WA, USA) and sampled (200Hz) with a PowerLab digitizer (ADI Instruments, Colorado Springs, CO, USA). All experiments occurred between hours 2-10 of the 12h dark cycle (i.e., Zeitgeber time 14-22). Spike-wave seizures were scored manually by blinded individuals.

Fast blood measurements

In both rats and mice, tail vein blood was collected and glucose levels were measured with a human glucometer (Nova Max Plus, Nova Biomedical Corporation, Waltham, MA, USA). Serum was separated from the same blood sample to quantify β-hydroxybutyrate levels using a colorimetric assay kit (Cayman Chemical, Item Number 700190, Ann Arbor, Michigan, USA).

Insulin Injection

Animals were injected intraperitoneally with either saline or insulin (3IU/kg). Blood samples were collected in WAG/Rij rats 90 min prior to experiment start, 90 min after injection and at experiment conclusion. Blood draws were not performed in mice during ECoG/EMG recordings due to elevated stress and casualty.

Combined ECoG/EMG and Drug Infusion

A custom length guide cannula (Plastics One) was implanted in the left ventral basal nucleus of the thalamus (AP: -2.7mm/ML: -2.7mm). Prior to experimentation, the dummy cannula was removed and replaced with a delivery cannula. Vehicle, 2-

deoxyglucose [(2-DG); Millipore-Sigma, USA, Cat# D8375] or A-769662 (Tocris, Minneapolis, MN, USA; Cat# 3336) solution was infused (50nL/min) into the ventrobasal thalamus with a Microdialysis Syringe Pump (Harvard Apparatus, Holliston, MA, USA).

Lactate Measurements

An incision in the leg of anesthetized rats exposed the femoral artery, enabling the insertion of a catheter (Clay Adams, Parsippany, NJ, USA) that was pushed towards the abdominal aorta. Arterial lactate blood samples were measured using an iSTAT instrument (Abbott Instruments, Lake Bluff, IL, USA).

Immunohistochemistry

Anesthetized animals were transcardially perfused with 4% paraformaldehyde in 0.1M phosphate buffer (PB, pH 7.4). 40µm sections were cut from fixed brains with a Leica VT 1000S microtome (Leica Biosystems, Buffalo Grove, IL). All blocking and antibody solutions were prepared in an incubation buffer of 0.1% sodium azide and 2% normal goat serum. Primary antibody solutions containing rabbit anti-Kir6.2 (1:2000, Alomone Labs Cat# APC-020, RRID: AB_2040124) and mouse anti-parvalbumin (1:2000, Sigma-Aldrich Cat# P3088, RRID: AB_477329) were prepared and incubated for 2 days at 4°C. After PBS washes, sections were incubated overnight in secondary antibody solutions containing donkey anti-rabbit Cy3 (1:1000, Jackson ImmunoResearch Labs Cat# 711-165-152, RRID: AB_2307443) and donkey anti-mouse AlexaFluor 488 (1:1000, Jackson ImmunoResearch Labs Cat# 715-545-151, RRID: AB_2341099). Sections were imaged with a Z1 Axio Imager (Zeiss Microscopy, Thornwood, NY, USA) and captured with consistent exposure settings.

Quantitative RT-PCR

400 µm brain sections were cut with a Leica VT 1200S microtome. Thalamus and somatosensory cortex were dissected and placed in sterile tubes containing RNA*later* (Life Technologies, Carlsbad, CA, USA). RNA was isolated using the RNAqueous 4PCR kit (Applied Biosystems, Foster City, CA, USA) and/or RNAeasy mini kit (Qiagen, Gaithersburg, MD, USA) and DNAse-treated. cDNA was prepared with the iScript cDNA Synthesis Kit (Bio-Rad, Hercules, CA, USA) and PCR was used to assess levels of Kcnj11 (Ensemble gene ID: ENSMUSG00000096146) mRNA expression using the PrimePCR™ Assay (Bio-Rad). The amplicon context sequence was designed to detect the Ensemble transcript ID: ENSMUST00000180081 (Kcnj11). Quantification of mRNA was performed with SsoAdvanced™ SYBR® Green Supermix (Bio-Rad) that was compared to a standard curve generated by the PrimePCR™ Template for SYBR® Green. Only experiments with an R^2 value ≥ 0.95 were included. Kcnj11 transcript values were normalized to the control transcript provided by the PrimePCR™ Assay.

Western Blot Analysis

Whole thalamus lysates were subjected to SDS-PAGE and transferred for 2 hours onto nitrocellulose membranes(Laker et al., 2017) with antibodies (1:1000) against AMPKα1/2 (C Cell Signaling Technology Cat# 2532, RRID: AB_330331), p-AMPKα1/2[T172] (Cell Signaling Technology Cat# 2535, RRID: AB_331250), and Gapdh (Cell Signaling Technology Cat# 2118, RRID: AB_561053CST). Goat anti-rabbit IR800 (LI-COR Biosciences Cat# 926-32211, RRID: AB_621843 LICOR, Lincoln, NE, USA) served as the secondary antibody. Blots were scanned using Odyssey CLx infrared imaging system (LICOR). A common protein standard consisting of whole tissue lysate

mixture of liver, heart, and skeletal muscle was used to calculate phospho: total AMPK ratio.

Acute slice preparation

Animals were transcardially perfused with an ice-cold protective recovery solution containing the following in (mM): 92 NMDG, 26 $NaHCO_3$, 25 glucose, 20 HEPES, 10 $MgSO_4$m, 5 Na-ascorbate, 3 Na-pyruvate, 2.5 KCl, 2 thiourea, 1.25 NaH_2PO_4, 0.5 $CaCl_2$, titrated to a pH of 7.3-7.4 with HCl.(Ting et al., 2014) Horizontal slices containing the RT and VB were cut with a Leica VT1200 vibratome and then kept at room temperature in oxygenated (95% O_2, 5% CO_2) ACSF containing (in mM): 126 NaCl, 26 $NaHCO_3$, 10 glucose, 2.5 KCl, 2 $CaCl_2$, 1.25 NaH_2PO_4, 1 $MgSO_4$.

Patch-clamp recordings

Thalamic neuron recordings (31-33°C) were performed in 250 µm slices visualized with a Zeiss Axio Examiner microscope and an ORCA Flash4.0 camera (Hamamatsu, Bridgewater, NJ, USA). Borosilicate glass recording electrodes were fabricated using a P1000 puller (Sutter Instruments, Novato, CA, USA). Whole-cell recording electrodes contained (in mM): 128 K-gluconate, 10 HEPES, 1 EGTA, 10 KCl, 1 $MgCl_2$, 0.3 $CaCl_2$, 0.3 Na-GTP, 2 ATP. Recordings were acquired using a Multiclamp 700B amplifier (Axon Instruments, Molecular Devices, San Jose, CA, USA), low-pass filtered at 2 kHz and digitized at 10 kHz with a Digidata 1440A (Molecular Devices) and visualized with pClamp software (Molecular Devices). Data analyses were performed using custom code written in MATLAB (MathWorks, Natick, MA, USA). $GABA_B$ receptor-activated K^+ currents were evoked by pressure ejecting (Picospritzer, Parker Hannifin, Hollis, New Hampshire, USA) 100 µM baclofen (Millipore Sigma, Cat# B5399) adjacent to the soma of cells. To isolate

these currents, kynurenic acid (1mM, Millipore Sigma, Cat# K3375) and bicuculline methiodide (10 µM; Tocris, Cat# 2503, Bio-Techne Corporation, Minneapolis, MN, USA, RRID: SCR_003689) were added to the ACSF. Internal solution included QX-314 (5µM, Tocris, Cat# 1014) to suppress action potentials. AMPK-activating drugs were dissolved in the internal pipette solution and included: metformin (Millipore Sigma, Cat# D150959), AMP (Millipore Sigma, Cat# A1752), and A-769662 (Tocris). To assess K_{ATP} currents in VB neurons, glibenclamide (Abcam, Cambridge, MA, USA, Cat# ab120267) and/or diazoxide (Abcam, Cat# ab120266) was dissolved in the ACSF. Sucrose was added to low glucose-containing ACSF to compensate for osmolality changes.

Extracellular Multiunit Recordings

Network activity was recorded in 400 µM thalamic slices within an interface chamber supplied with warm, oxygenated ACSF (31-33°C, 95% O_2/5% CO_2). Electrical stimuli were delivered to RT with bipolar tungsten electrodes (FHC, Bowdoinham, ME, USA), while single tungsten electrodes placed in VB recorded extracellular activity. Filtered activity (0.1-3-kHz) was digitized and recorded with a Digidata 1440A and pClamp software. AMPK agonists and CGP-54626 (Tocris, Cat# 1088) were dissolved in the ACSF perfusate. Activity was quantified with custom MATLAB scripts.(Lu et al., 2020) Voltage amplitude thresholds were applied to detect action potentials and were set at 3-4x the root mean square of the trace prior to stimulation. Oscillation duration was defined as the period between the stimulus onset and the last activity burst to occur within the specified inter-burst interval of 1 second.

AMPKAR FRET Imaging

We cloned AAV9-UPCamAMPKAR by moving the AMPKAR coding region from pPBbsr2-4031NES [gift from Michiyuki Matsuda (Addgene_105241)] into the plasmid pENN.AAV.CamKII0.4.eGFP.WPRE.rBG [gift from James M. Wilson (RRID: Addgene_105541)]. The insert was amplified by PCR using primers that added AgeI and BsrGI sites. The vector was digested with the same enzymes, thereby excising GFP and providing compatible restriction enzyme sites for the insert. Packaging in serotype AAV9 particles was performed by Vigene Biosciences (titer 3.58 x 10^{13} VG/ml). P14-P21 rats received bilateral stereotaxic injection of AAV.Camk2a.AMPKAR.WPRE.Rbg targeted to somatosensory thalamus (300 nL per injection site). Acute thalamic brain slices (250 µM) were prepared 2-4 weeks later and widefield imaged. ROIs were drawn in ImageJ and CFP/YFP signal intensities were measured using the FRETOffline plugin developed for ImageJ.(Sprenger et al., 2012)

Data analysis and statistics

Statistical analyses were performed in MATLAB. Data normality was tested using a combination of the Lilliefors test, the Anderson-Darling test and the Jarque-Bera test. Statistical details are described in the results section and corresponding supplemental tables. Either parametric or non-parametric statistical analyses were performed, as indicated in the figure legends. A significance level was set at 0.05. Data are expressed as mean ± SEM. Error bars reflect 95% confidence intervals.

Supplementary Materials

Data Tables

Table S1 SWSs during acute fasting. *N* refers to animal number. Data correspond to those in Figure 1 and Supplementary Figure 1. Data values are rounded to the nearest tenth.

	Parameter	Fed	Fasted	N	p Value
DBA	SWS Count	3.2 ± 1.1	9.4 ± 1.7	10	0.0078
	SWS Duration (s)	2.6 ± 0.7	3.4 ± 0.4	10	0.375
	Seizure Burden (%)	0.08 ± 0.03	0.2 ± 0.03	10	0.0098
	Blood Glucose (mg/dL)	165.6 ± 14.3	132.1 ± 10.8	10	0.048
	β-hydroxybutyrate (mM)	2.0 ± 0.2	8.2 ± 0.8	10	0.002
	Blood Glucose (mg/dL) vs SWS Counts	r = -0.23	r^2 = 0.053		p = 0.31
	β-hydroxybutyrate (mM) vs SWS Counts	r = 0.52	r^2 = 0.27		p = 0.020
WAG	SWS Count	21.9 ± 7.10	34.9 ± 9.7	13	0.0044
	SWS Duration (s)	8.2 ± 1.7	10.1 ± 1.5	13	0.17
	Seizure Burden (%)	1.8 ± 0.7	3.1 ± 0.9	13	0.0006
	Blood Glucose (mg/dL)	114.1 ± 6.2	75.4 ± 4.8	11	0.00097
	β-hydroxybutyrate (mM)	1.1 ± 0.9	3.3 ± 0.4	11	0.002
	Blood Glucose (mg/dL) vs SWS Counts	r = -0.37	r^2 = 0.14		p = 0.094
	β-hydroxybutyrate (mM) vs SWS Counts	r = 0.15	r^2 = 0.023		p = 0.49

Table S2 SWSs during acute insulin and 2-DG. *N* refers to animal number. Data correspond to those found in Figure 2 and Supplementary Figure 2. Data values are rounded to the nearest tenth.

	Parameter	Saline	Insulin	N	p Value
DBA	SWS Count	6.1 ± 1.8	13.4 ± 2.9	11	0.0195
	SWS Duration (s)	2.8 ± 0.4	3.3 ± 0.2	11	0.83
	Seizure Burden (%)	0.10 ± 0.03	0.3 ± 0.06	11	0.049
	Blood Glucose (mg/dL)	157.3 ± 17.3	63.0 ± 4.0	4	0.13
	β-hydroxybutyrate (mM)	1.7 ± 0.2	1.2 ± 0.07	4	0.13
	Blood Glucose (mg/dL) vs SWS Counts	r = -0.31	r^2 = 0.096		p = 0.45
	β-hydroxybutyrate (mM) vs SWS Counts	r = -0.34	r^2 = 0.12		p = 0.42
WAG	SWS Count	15.6 ± 4.1	28.6 ± 7.5	12	0.036
	SWS Duration (s)	8.5 ± 1.6	8.6 ± 1.8	12	0.92
	Seizure Burden (%)	0.98 ± 0.3	1.7 ± 0.6	12	0.012
	Blood Glucose (mg/dL)	111.6 ± 4.3	46.4 ± 5.1	9	0.0039
	β-hydroxybutyrate (mM)	1.1 ± 0.2	1.0 ± 0.1	9	0.36
	Blood Glucose (mg/dL) vs SWS Counts	r = -0.48	r^2 = 0.23		p = 0.046
	β-hydroxybutyrate (mM) vs SWS Counts	r = -0.24	r^2 = 0.058		p = 0.33
	Parameter	**Saline**	**2-DG**	**N**	**p Value**
	SWS Count	9.2 ± 2.4	19.7 ± 4.6	9	0.01
	SWS Duration (s)	6.1 ± 1.9	6.8 ± 0.36	9	0.56

Table S3 Neuron excitability, AMPKAR-FRET and baclofen application. *n* refers to cell number. *N* refers to animal number. Data correspond to those found in Figure 3 and Supplementary Figure 4. Data values are rounded to the nearest tenth.

	Manipulation		Control	Metformin	n (N)	p Value
Rebound Action Potentials (#)	10 mM Metformin	-140 pA	5.7 ± 0.8	6.5 ± 1.0	13 (7)	0.70
Depolarization-Evoked Action Potentials (#)	10 mM Metformin	+20 pA	0 ± 0	0 ± 0	13 (7)	-
		+40 pA	0.8 ± 0.7	2.6 ± 1.2		0.11
		+60 pA	2.6 ± 2.4	9.7 ± 4.3		0.054
		+80 pA	6.7 ± 3.5	21.4 ± 8.5		0.039
		+100 pA	29.1 ± 15.4	36.8 ± 12.4		0.36
		+120 pA	29.3 ± 12.3	49.6 ± 15.7		0.023
		+140 pA	39.2 ± 15.3	64.8 ± 20.3		0.023
		+160 pA	48.8 ± 16.9	80.8 ± 25.2		0.009
		+180 pA	61.6 ± 19.7	101.2 ± 7.0		0.016
		+200 pA	74.6 ± 23.1	113.2 ± 28.5		.018
AMPKAR-FRET	10 mM Metformin		1.00 ± 0.0021	1.004 ± 0.0042	13(3)	0.0002
	100 nM A-769662		1.001 ± 0.0028	1.013 ± 0.014	10(5)	0.0129

	Manipulation	Control	n (N)	Drug	n (N)	p Value
Baclofen Puff	1 mM AMP	96% ± 4%	5 (6)	110% ± 6%	9 (8)	0.06
	1 mM Metformin	88% ± 9%	7 (6)	102% ± 3%	9 (6)	0.02
	100 nM A-769662	85% ± 10%	5 (6)	104% ± 4%	10 (6)	0.02

Table S4 AMPK activation and thalamic oscillations. *n* refers to slice number. *N* refers to animal number. Data correspond to those found in Figure 4 and Supplementary Figure 5. Data values are rounded to the nearest tenth.

Experiment	Baseline Duration (sec)	Drug Duration (sec)	n (N)	p-Value
Oscillations Metformin (5 mM)	5.5 ± 0.8	6.9 ± 0.8	11 (7)	0.0027
Oscillations A-769662 (10 µM)	7.8 ± 1.2	8.9 ± 1.2	15 (11)	0.0082
Oscillations CGP-54626 (20 nM)	2.2 ± 0.51	2.3 ± 0.54	11 (6)	0.43
Oscillations A-769662 (Fig. S5)	4.8 ± 1.3	6.1 ± 1.7	5 (3)	0.06
Oscillations Bicuculline (Fig. S5)	7.7 ± 0.8	7.1 ± 0.8	6 (3)	0.23

A-769662 (10 µM) EEG and Infusion	**# Saline SWSs**	**#A-769662 SWSs**	**p – Value**	**Saline SWS Duration**	**A-769662 SWS Duration**	**p - Value**	**N**
	11.2 ± 4.5	22.5 ± 5.2	0.017	7.9 ± 0.5	7.75 ± 0.5	0.72	10

Table S5 SWSs and metformin. *n* refers to cell number. *N* refers to animal number. Data correspond to Figure 5 and Supplemental Figure 6. Most data values are rounded to the nearest tenth.

	Rat Strain	# Saline SWSs	# Met SWSs	N	p Value	Lactate Saline (mmol/L)	Lactate Metformin (mmol/L)	N	p Value
150 mg/kg	WAG/Rij	1.5 ± 4.6	32.7 ± 5.8	6	0.22	0.46 ± 0.1	0.88 ± 0.2	7	0.16
	Wistar	0 ± 0	0.2 ± 0	5	1	0.51 ± 0.1	2.7 ± 1.4	5	0.19
200 mg/kg	WAG/Rij	14.2 ± 2.8	49.8 ± 11.5	6	0.036	0.42 ± 0.11	5.1 ± 1.4	7	0.016
	Wistar	0 ± 0	0.2 ± 0	5	1	0.49 ± 0.04	6.8 ± 1.9	5	0.03

	Baseline Duration (sec)	3Cl-OH-BA Duration (sec)	n (N)	p Value
Evoked Oscillations	4.8 ± 1.2	6.7 ± 1.5	4 (4)	0.025

Table S6 KATP channel expression and glucose responsivity. *n* refers to cell number. *N* refers to animal number. Data correspond to those found in Supplementary Figure 3.

		Cortex	Dentate Gyrus	Reticular Thalamus		Ventrobasal Thalamus
Immunohisto-Chemistry (A.U.)		23 ± 4.6	40.5 ± 0.6	32.0 ± 3.2		23.0 ± 2.3
		Cortex	**Thalamus**			
qPCR (Copy #) ΔCt		4.1 ± 0.2 10.9 ± 0.7	4.1 ± 0.2 10.2 ± 0.2			
		Manipulation	**Control**		**n (N)**	**p Value**
DBA/2J Mouse	**Holding Current (pA)**	10 µM Diazoxide	-0.67 ± 2.3	2.3 ± 7.9	8 (2)	0.57
		100 µM Diazoxide	-2.11 ± 2.0	56.9 ± 22.7	7 (4)	0.038
		250 µM Diazoxide	-0.35 ± 2.3	123.7 ± 19.7	8 (4)	0.0016
		500 µM Diazoxide	-1.4 ± 2.7	172.7 ± 34.6	6 (5)	0.022
		100 nM Glibenclamide + 500 µM Diazoxide	-0.57 ± 0.49	-1.8 ± 1.0	4 (2)	0.69
		Low Glucose	1.1 ± 0.55	15.2 ± 10.6	14 (12)	0.18
	Membrane Resistance (MΩ)	Low Glucose	218.5 ± 20.4	210.1 ± 23.5	14 (12)	0.77
WAG/Rij Rat	**Holding Current (pA)**	500 µM Diazoxide	2.8 ± 1.3	69.2 ± 9.4	8 (5)	0.00016
		1 µM Glibenclamide + 500 µM Diazoxide	-0.57 ± 0.49	-1.8 ± 1.0	8 (4)	0.69
		Low Glucose	1.2 ± 1.1	-1.4 ± 13.7	11 (5)	0.29
	Membrane Resistance (MΩ)	Low Glucose	151.3 ± 23.6	147.0 ± 20.0	11 (5)	0.95

Supplemental Figures

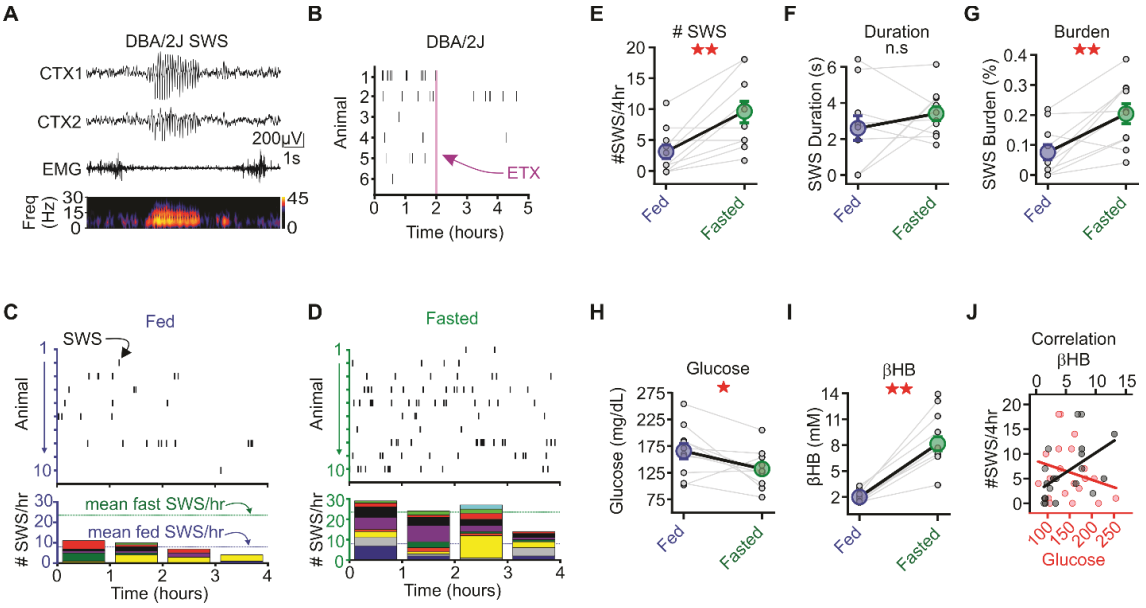

Supplemental Figure 1. Overnight fasting increases spike-and-wave discharges in DBA/2J mice. (A) *Top:* Representative SWS from DBA/2J mouse. CTX1 and CTX2 are cortical ECoG recordings while EMG recording is from the neck. EMG activity was suppressed during the SWS, corresponding to behavioral arrest. *Bottom:* Spectrograms from CTX1 showing increased power in the 5-8 Hz frequency band during the SWS. **(B)** Ethosuximide (ETX; 200 mg/kg) suppressed SWSs in the DBA/2J mouse. Purple line indicates i.p. injection of ETX. **(C, D)** *Top:* SWS rasters during the fed and fasted conditions. *Bottom:* Stacked histograms showing hourly SWS count for each mouse during fed **(C)** and fasted **(D)** conditions. Blue and green dashed lines represent mean SWSs count during fed and fasted conditions, respectively. **(E)** The number of SWSs was 3-fold higher during the fasted period than during the fed period ($p = 0.0078$, $n = 10$; Table S1). **(F)** Fasting did not affect SWS duration ($p = 0.375$, $n=10$; Table S1). Mice that had no SWSs were assigned a duration value = 0 sec. **(G)** SWS burden was 2.5-fold higher post-fast relative to the fed state ($p = 0.0098$, $n=10$; Table S1). **(H)** Fasting decreased blood

glucose ($p = 0.048$, $n = 10$; Table S1). **(I)** Fasting increased β-hydroxybutyrate ($p = 0.002$, $n = 10$; Table S1) relative to the fed state. **(J)** Blood glucose (red) or serum β-hydroxybutyrate (black) versus SWS count in mice. For each panel, small circles represent data from one animal, while large circles represent the sample mean (± SE). * $p < 0.05$, ** $p < 0.01$ or not significant (n.s.) from the Wilcoxon sign rank test. See Table S1 for details.

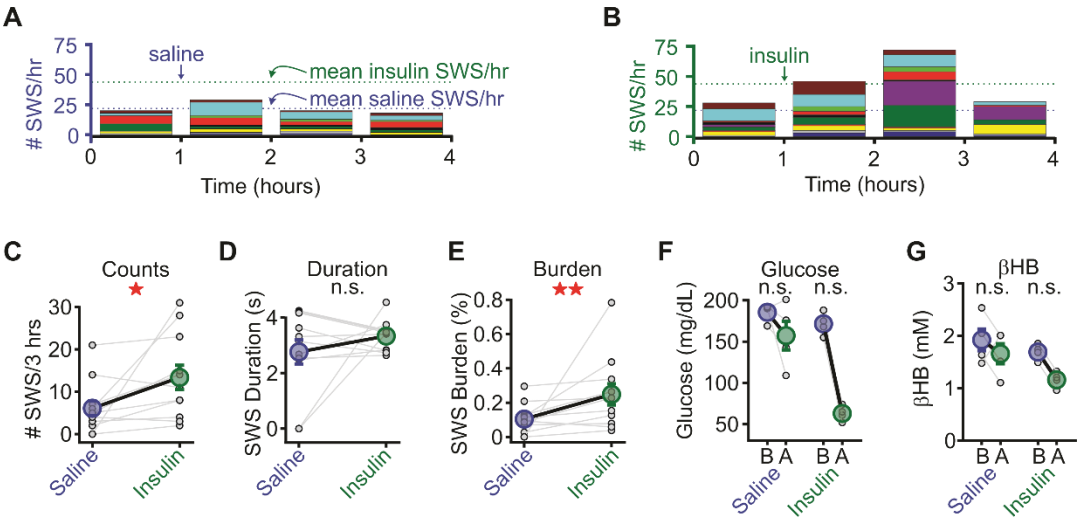

Supplemental Figure 2. Elevated SWS count tracks with low blood glucose in DBA/2J mice. (A, B) Stacked histograms showing SWS counts for DBA/2J mice after saline **(A)** or insulin **(B)** injection. Blue dashed lines represent the mean SWS count after saline. Green dashed lines represent the mean SWS count after insulin. **(C)** Insulin increased mean SWS count ($p = 0.0195$, $n = 11$; Table S2). **(D)** SWS duration did not change after insulin injection ($p = 0.83$, $n = 11$; Table S2). Mice that had no SWSs were assigned a duration value = 0 sec. **(E)** Insulin increased SWS burden ($p = 0.049$, $n = 11$; Table S2). **(F)** Insulin produced a trend towards decreased blood glucose ($p = 0.13$, $n = 4$; Table S2). **(G)** Insulin had no effect on β-hydroxybutyrate ($p = 0.13$, $n = 4$; Table S2). In each panel, small circles represent data from one animal, while large circles represent the sample mean (± SE). * $p < 0.05$, ** $p < 0.01$ or not significant (n.s.) from paired t-test. See Table S2 for details.

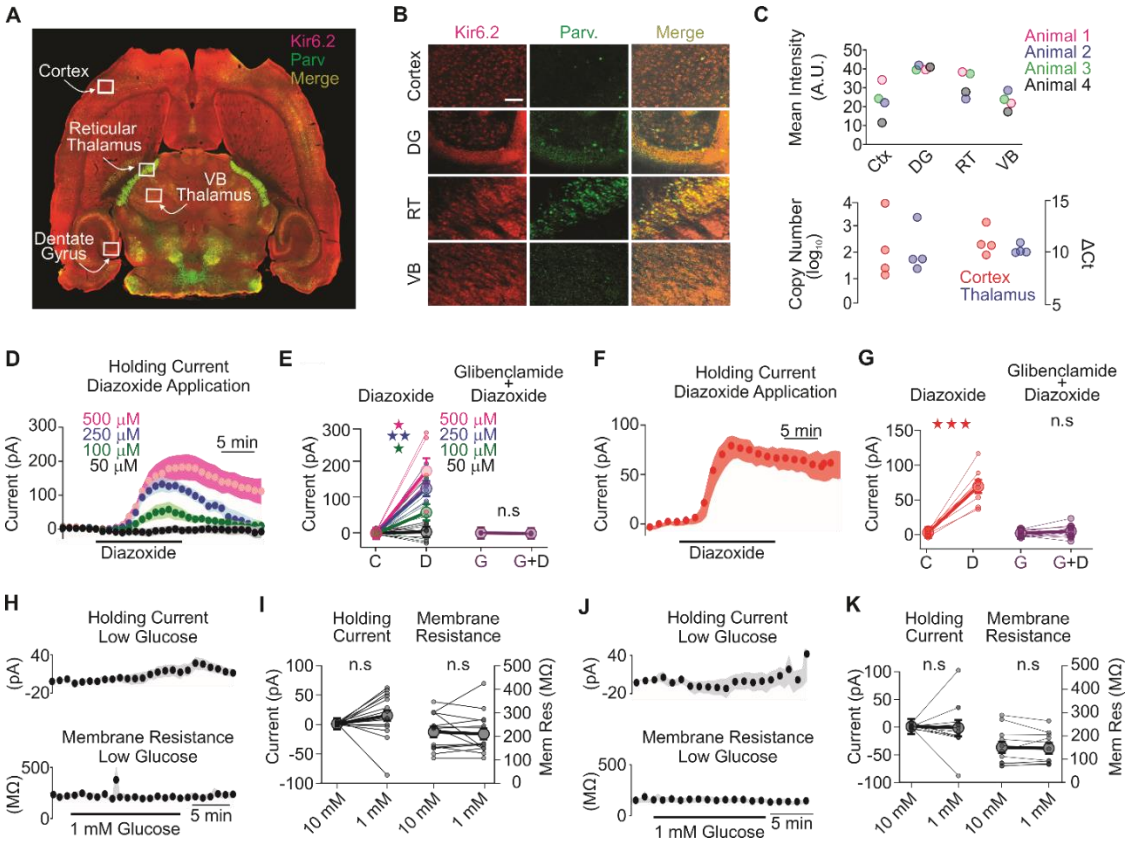

Supplemental Figure 3. K_{ATP} channel expression in thalamocortical neurons.

(A) Kir6.2 (magenta) and parvalbumin (green) expression in the mouse brain. White boxes indicate structures shown in Fig. 3B. Scale bar = 500 µM. **(B)** Kir6.2 expression in cortex, dentate gyrus (DG), reticular (RT) and ventrobasal (VB) thalamus was qualitatively similar. Scale bar = 50 µM. **(C)** *Top:* Mean Kir6.2 intensity in each structure across four mice. Each circle represents one animal. *Bottom*: Absolute and relative Kir6.2 mRNA expression in mouse thalamus and cortex. *Bottom, left axis*: total Kir6.2 copy number. *Bottom, right axis*: Kir6.2 mRNA expression relative to cyclophilin A. Each circle represents one sample. **(D)** Diazoxide induced a dose-dependent inward current in mouse thalamocortical neurons, indicating functional channel expression. **(E)** *Left*: Mean holding current change at each diazoxide dose. *Right*: Mean holding current in 500 µM diazoxide + 100 nM glibenclamide. **(F, G)** As in mice, 500 µM diazoxide application induced a glibenclamide-sensitive outward current in WAG/Rij thalamocortical neurons. **(H)** Low

glucose did not alter thalamocortical neuron activity in DBA/2J mice. *Top*: holding current; *Bottom:* membrane resistance. **(I)** Mean holding current (*left*) and mean membrane resistance (*right*) did not change in 1 mM glucose relative to 10 mM glucose for DBA/2J mouse. **(J, K)** Likewise, low glucose did not affect these parameters in WAG/Rij rat thalamocortical neurons. In each panel, small circles represent data from one animal, whereas large circles represent the sample mean (± SE). * $p < 0.05$, ** $p < 0.01$, *** $p<0.001$ or not significant (n.s.) from paired t-test. See Table S6 for details.

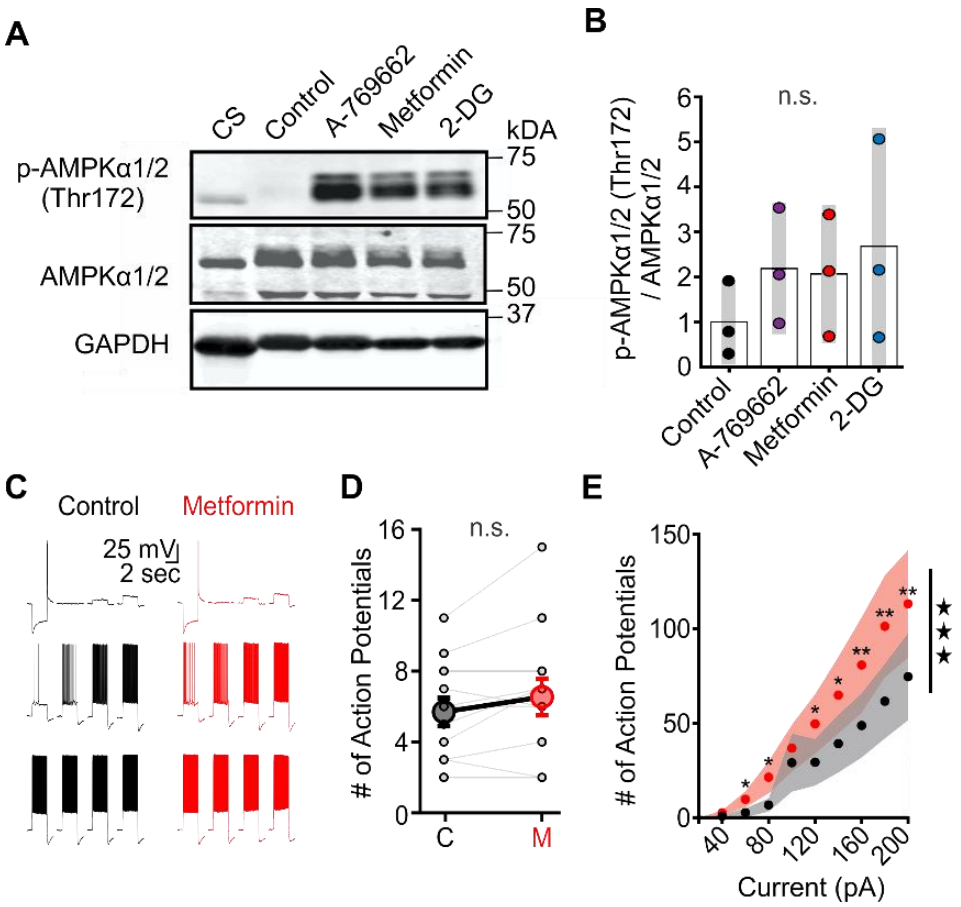

Supplemental Figure 4. P-AMPK protein expression and firing properties in thalamocortical neurons with pharmacological activation of AMPK.

(A) Relative p-AMPK/total AMPK protein expression in acute thalamic slices incubated with AMPK agonists. Representative western blot illustrating p-AMPK expression after 30-minute exposure to control (standard ACSF) or solutions containing AMPK activators (*left* to *right*): ACSF + 100 nM A-769662, 10 mM metformin or 27 µM 2-DG. CS lane represents a standard sample of a whole tissue lysate mixture of liver, heart, and skeletal muscle. **(B)** Fold change in p-AMPK expression relative to total AMPK across conditions normalized to mean control p-AMPK values. Results of one-way ANOVA: $F(3,8) = 0.63$, $p = 0.62$. Each circle represents an experiment. **(C)** Representative recording of WAG/Rij thalamocortical neuron during hyperpolarizing and depolarizing current injections (black: ACSF; red: ACSF + 10 mM metformin). **(D)** Metformin did not significantly alter the number

of rebound burst action potentials relative to saline following hyperpolarizing current injections. **(E)** Metformin altered the number of action potentials evoked by depolarizing current injection. The F-I plot shows the effect metformin had on thalamocortical neuron firing activity during depolarizing current steps (+20 pA increments). Each circle represents mean ± SE current responses at each step; *p <0.05, **p< 0.01, ***p<0.001 or not significant (n.s.); Friedman's test, Wilcoxon sign rank test for pairwise comparison. See Table S4 for details.

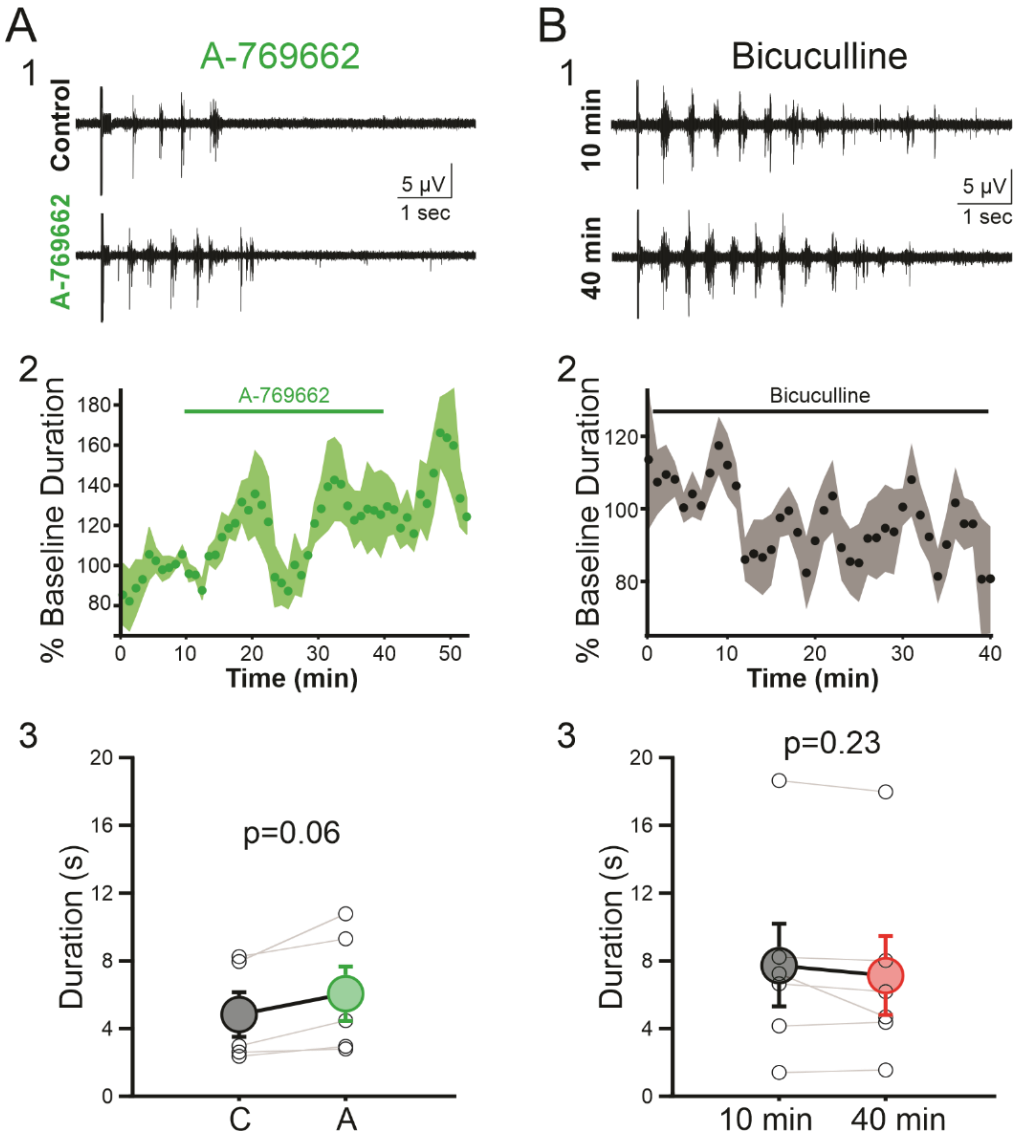

Supplemental Figure 5. Oscillations evoked in the naïve thalamic slice trend towards longer durations during AMPK activation. (A) 400 µm slices from WAG/Rij rats were recorded in the absence of any GABA receptor (A or B) blockade. (1) Oscillatory activity was evoked with a 20Hz burst of 10 electrical stimuli and AMPK was activated with A-769662. (2) AMPK activation produced a trend towards longer duration oscillations (n=5). This trend was not significant (p=0.06). **(B)** The duration of thalamic oscillations evoked only in the presence of $GABA_A$ receptor blockade (i.e., 10 µM bicuculline, (1) are generally stable (2) insofar the duration evoked at 10 minutes is similar to the duration evoked at 40 minutes (3). See Table S4 for further details.

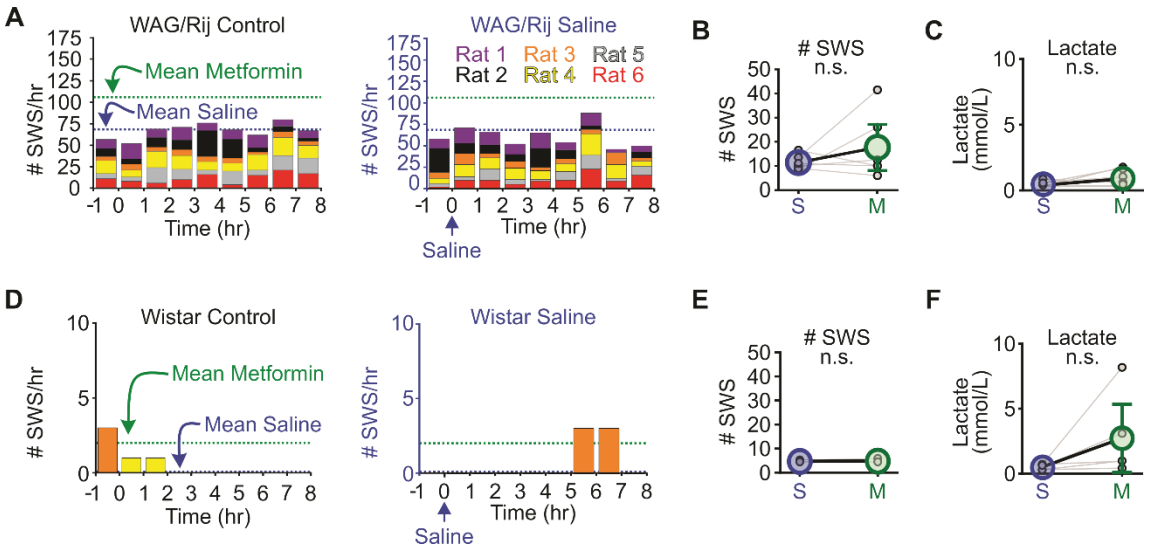

Supplemental Figure 6. SWSs and lactate measurements at 150 mg/kg metformin

(A) WAG/Rij rat SWS counts for control and saline injections for the 150 mg/kg metformin experiment. Saline injection did not affect SWS occurrence relative spontaneous (i.e. not injected) epochs. Stacked histograms showing SWS counts per animal for all conditions. Dotted lines indicate mean SWS count following saline (blue) and 150 mg/kg metformin (green) injection, respectively. **(B, C)** SWS counts and lactate (mmoL/L) trended higher two hours after 150 mg/kg metformin injection. **(D)** Non-epileptic Wistar rat SWS counts for control and saline injections for the 150 mg/kg metformin experiment. **(E, F)** 150 mg/kg metformin did not change SWS counts in Wistar rats despite similar changes in lactate (mmol/L) between the two strains. In each panel, small circles represent data from one animal, whereas large circles represent the sample mean (± SE); not significant (n.s.) from Wilcoxon test (WAGs) and paired student's t-test (Wistars). See Table S5 for details.

References

Abrantes, H. de C., Briquet, M., Schmuziger, C., Restivo, L., Puyal, J., Rosenberg, N., Rocher, A.-B., Offermanns, S., & Chatton, J.-Y. (2019). The Lactate Receptor HCAR1 Modulates Neuronal Network Activity through the Activation of Gα and Gβγ Subunits. Journal of Neuroscience, 39(23), 4422–4433. https://doi.org/10.1523/JNEUROSCI.2092-18.2019

Arbeláez, A. M., Rutlin, J. R., Hershey, T., Powers, W. J., Videen, T. O., & Cryer, P. E. (2012a). Thalamic Activation During Slightly Subphysiological Glycemia in Humans. Diabetes Care. https://doi.org/10.2337/dc12-0297

Arbeláez, A. M., Rutlin, J. R., Hershey, T., Powers, W. J., Videen, T. O., & Cryer, P. E. (2012b). Thalamic Activation During Slightly Subphysiological Glycemia in Humans. Diabetes Care. https://doi.org/10.2337/dc12-0297

Arsov, T., Mullen, S. A., Rogers, S., Phillips, A. M., Lawrence, K. M., Damiano, J. A., Goldberg-Stern, H., Afawi, Z., Kivity, S., Trager, C., Petrou, S., Berkovic, S. F., & Scheffer, I. E. (2012). Glucose transporter 1 deficiency in the idiopathic generalized epilepsies. Annals of Neurology, 72(5), 807–815. https://doi.org/10.1002/ana.23702

Ashford, M. L., Boden, P. R., & Treherne, J. M. (1990). Glucose-induced excitation of hypothalamic neurones is mediated by ATP-sensitive K+ channels. Pflugers Arch, 415(4), 479–483.

Avoli, M. (2012). A brief history on the oscillating roles of thalamus and cortex in absence seizures. Epilepsia, 53(5), 779–789. https://doi.org/10.1111/j.1528-1167.2012.03421.x

Bal, T., Debay, D., & Destexhe, A. (2000). Cortical Feedback Controls the Frequency and Synchrony of Oscillations in the Visual Thalamus. The Journal of Neuroscience, 20(19), 7478–7488.

Bal, T., von Krosigk, M., & McCormick, D. A. (1995). Synaptic and membrane mechanisms underlying synchronized oscillations in the ferret lateral geniculate nucleus in vitro. The Journal of Physiology, 483(3), 641–663. https://doi.org/10.1113/jphysiol.1995.sp020612

Beenhakker, M. P., & Huguenard, J. R. (2009). Neurons that Fire Together Also Conspire Together: Is Normal Sleep Circuitry Hijacked to Generate Epilepsy? Neuron, 62(5), 612–632. http://dx.doi.org/10.1016/j.neuron.2009.05.015

Beenhakker, M. P., & Huguenard, J. R. (2010). Astrocytes as Gatekeepers of GABAB Receptor Function. Journal of Neuroscience, 30(45), 15262–15276. https://doi.org/10.1523/JNEUROSCI.3243-10.2010

Bieberdorf, F. A., Chernick, S. S., & Scow, R. O. (1970). Effect of insulin and acute diabetes on plasma FFA and ketone bodies in the fasting rat. The Journal of Clinical Investigation, 49(9), 1685–1693. https://doi.org/10.1172/JCI106386

Blumenfeld, H. (2005). Cellular and Network Mechanisms of Spike-Wave Seizures. Epilepsia, 46, 21–33. https://doi.org/10.1111/j.1528-1167.2005.00311.x

Blumenfeld, H., & McCormick, D. A. (2000). Corticothalamic Inputs Control the Pattern of Activity Generated in Thalamocortical Networks. Journal of Neuroscience, 20(13), 5153–5162. https://doi.org/10.1523/JNEUROSCI.20-13-05153.2000

Bortolato, M., Frau, R., Orrù, M., Fà, M., Dessì, C., Puligheddu, M., Barberini, L., Pillolla, G., Polizzi, L., Santoni, F., Mereu, G., & Marrosu, F. (2010). GABAB receptor activation exacerbates spontaneous spike-and-wave discharges in DBA/2J mice. Seizure, 19(4), 226–231. http://dx.doi.org/10.1016/j.seizure.2010.02.007

Bryant, A. S., Li, B., Beenhakker, M. P., & Huguenard, J. R. (2009). Maintenance of thalamic epileptiform activity depends on the astrocytic glutamate-glutamine cycle. Journal of Neurophysiology, 102(5), 2880–2888. https://doi.org/10.1152/jn.00476.2009

Chiew, A. L., Wright, D. F. B., Dobos, N. M., McArdle, K., Mostafa, A. A., Newth, A., Roberts, M. S., & Isbister, G. K. (2018). “Massive” metformin overdose. British Journal of Clinical Pharmacology, 84(12), 2923–2927. https://doi.org/10.1111/bcp.13582

Coenen, A. M. (2003). Genetic animal models for absence epilepsy: A review of the WAG/Rij strain of rats. Behavior Genetics, 33(6), 635–655.

Couve, A., Thomas, P., Calver, A. R., Hirst, W. D., Pangalos, M. N., Walsh, F. S., Smart, T. G., & Moss, S. J. (2002). Cyclic AMP–dependent protein kinase phosphorylation facilitates GABAB receptor–effector coupling. Nature Neuroscience, 5(5), 415–424. https://doi.org/10.1038/nn833

Culmsee, C., Monnig, J., Kemp, B. E., & Mattson, M. P. (2001). AMP-activated protein kinase is highly expressed in neurons in the developing rat brain and promotes neuronal survival following glucose deprivation. Journal of Molecular Neuroscience, 17(1), 45–58. https://doi.org/10.1385/JMN:17:1:45

D’Andrea Meira, I., Romão, T. T., Pires do Prado, H. J., Krüger, L. T., Pires, M. E. P., & da Conceição, P. O. (2019). Ketogenic Diet and Epilepsy: What We Know So Far. Frontiers in Neuroscience, 13. https://doi.org/10.3389/fnins.2019.00005

Destexhe, A. (1998). Spike-and-Wave Oscillations Based on the Properties of GABAB Receptors. The Journal of Neuroscience, 18(21), 9099–9111.

Dienel, G. A. (2018). Brain Glucose Metabolism: Integration of Energetics with Function. Physiological Reviews, 99(1), 949–1045. https://doi.org/10.1152/physrev.00062.2017

Dutar, P., & Nicoll, R. A. (1988). Pre- and postsynaptic GABAB receptors in the hippocampus have different pharmacological properties. Neuron, 1(7), 585–591. http://dx.doi.org/10.1016/0896-6273(88)90108-0

Festing, M. F. W. (1979). Inbred Strains of Rats. In M. F. W. Festing (Ed.), Inbred Strains in Biomedical Research (pp. 267–296). Macmillan Education UK. https://doi.org/10.1007/978-1-349-03816-9_14

Flory, J., & Lipska, K. (2019). Metformin in 2019. JAMA, 321(19), 1926–1927. https://doi.org/10.1001/jama.2019.3805

Fogerson, P. M., & Huguenard, J. R. (2016). Tapping the Brakes: Cellular and Synaptic Mechanisms that Regulate Thalamic Oscillations. Neuron, 92(4), 687–704. http://dx.doi.org/10.1016/j.neuron.2016.10.024

French, J. A., & Pedley, T. A. (2009, June 6). Initial Management of Epilepsy (world) [N-clinical-practice]. Http://Dx.Doi.Org/10.1056/NEJMcp0801738; Massachusetts Medical Society. https://doi.org/10.1056/NEJMcp0801738

Furuse, T., Mizuma, H., Hirose, Y., Kushida, T., Yamada, I., Miura, I., Masuya, H., Funato, H., Yanagisawa, M., Onoe, H., & Wakana, S. (2019). A new mouse model of GLUT1 deficiency syndrome exhibits abnormal sleep-wake patterns and alterations of glucose kinetics in the brain. Disease Models & Mechanisms, 12(9). https://doi.org/10.1242/dmm.038828

Garriga-Canut, M., Schoenike, B., Qazi, R., Bergendahl, K., Daley, T. J., Pfender, R. M., Morrison, J. F., Ockuly, J., Stafstrom, C., Sutula, T., & Roopra, A. (2006). 2-Deoxy-D-glucose reduces epilepsy progression by NRSF-CtBP-dependent metabolic regulation of chromatin structure. Nature Neuroscience, 9(11), 1382–1387. https://doi.org/10.1038/nn1791

Gelisse, P., Genton, P., Kuate, C., Pesenti, A., Baldy-Moulinier, M., & Crespel, A. (2004). Worsening of seizures by oxcarbazepine in juvenile idiopathic generalized epilepsies. Epilepsia, 45(10), 1282–1286. https://doi.org/10.1111/j.0013-9580.2004.19704.x

Gibbs, F. A., Gibbs, E. L., & Lennox, W. G. (1939). Influence of the blood sugar on the wave and spike formation in petit mal epilepsy. Archives of Neurology & Psychiatry, 41(6), 1111–1116. https://doi.org/10.1001/archneurpsyc.1939.02270180039002

Giménez-Cassina, A., Martínez-François, J. R., Fisher, J. K., Szlyk, B., Polak, K., Wiwczar, J., Tanner, G. R., Lutas, A., Yellen, G., & Danial, N. N. (2012). BAD-Dependent Regulation of Fuel Metabolism and KATP Channel Activity Confers Resistance to Epileptic Seizures. Neuron, 74(4), 719–730. http://dx.doi.org/10.1016/j.neuron.2012.03.032

Göransson, O., McBride, A., Hawley, S. A., Ross, F. A., Shpiro, N., Foretz, M., Viollet, B., Hardie, D. G., & Sakamoto, K. (2007). Mechanism of Action of A-769662, a Valuable Tool for Activation of AMP-activated Protein Kinase. Journal of Biological Chemistry, 282(45), 32549–32560. https://doi.org/10.1074/jbc.M706536200

Groomes, L. B., Pyzik, P. L., Turner, Z., Dorward, J. L., Goode, V. H., & Kossoff, E. H. (2011). Do Patients With Absence Epilepsy Respond to Ketogenic Diets? Journal of Child Neurology, 26(2), 160–165. https://doi.org/10.1177/0883073810376443

Herzig, S., & Shaw, R. J. (2018). AMPK: Guardian of metabolism and mitochondrial homeostasis. Nature Reviews Molecular Cell Biology, 19(2), 121–135. https://doi.org/10.1038/nrm.2017.95

Hosford, D. A., Clark, S., Cao, Z., Wilson, W. A., Lin, F. H., Morrisett, R. A., & Huin, A. (1992). The role of GABAB receptor activation in absence seizures of lethargic (lh/lh) mice. Science, 257(5068), 398–401. https://doi.org/10.1126/science.1321503

Huang, W., Castelino, R. L., & Peterson, G. M. (2017). Lactate Levels with Chronic Metformin Use: A Narrative Review. Clinical Drug Investigation, 37(11), 991–1007. https://doi.org/10.1007/s40261-017-0564-6

Huguenard, J. R., & McCormick, D. A. (2007). Thalamic synchrony and dynamic regulation of global forebrain oscillations. Trends Neurosci, 30(7), 350–356. http://dx.doi.org/10.1016/j.tins.2007.05.007

Kadowaki, A., Sada, N., Juge, N., Wakasa, A., Moriyama, Y., & Inoue, T. (2017). Neuronal inhibition and seizure suppression by acetoacetate and its analog, 2-phenylbutyrate. Epilepsia, 58(5), 845–857. https://doi.org/10.1111/epi.13718

Kahn, B. B., Alquier, T., Carling, D., & Hardie, D. G. (2005). AMP-activated protein kinase: Ancient energy gauge provides clues to modern understanding of metabolism. Cell Metabolism, 1(1), 15–25. https://doi.org/10.1016/j.cmet.2004.12.003

Kandel, A., & Buzsáki, G. (1997). Cellular–Synaptic Generation of Sleep Spindles, Spike-and-Wave Discharges, and Evoked Thalamocortical Responses in the Neocortex of the Rat. Journal of Neuroscience, 17(17), 6783–6797. https://doi.org/10.1523/JNEUROSCI.17-17-06783.1997

Karschin, A., Brockhaus, J., & Ballanyi, K. (1998). KATP channel formation by the sulphonylurea receptors SUR1 with Kir6.2 subunits in rat dorsal vagal neurons in situ. The Journal of Physiology, 509(Pt 2), 339–346. https://doi.org/10.1111/j.1469-7793.1998.339bn.x

Kim, E.-K., Miller, I., Aja, S., Landree, L. E., Pinn, M., McFadden, J., Kuhajda, F. P., Moran, T. H., & Ronnett, G. V. (2004). C75, a Fatty Acid Synthase Inhibitor, Reduces Food Intake via Hypothalamic AMP-activated Protein Kinase. Journal of Biological Chemistry, 279(19), 19970–19976. https://doi.org/10.1074/jbc.M402165200

Kim, U., Sanchez-Vives, M. V., & McCormick, D. A. (1997). Functional Dynamics of GABAergic Inhibition in the Thalamus. Science, 278(5335), 130–134. https://doi.org/10.1126/science.278.5335.130

Kleiman-Weiner, M., Beenhakker, M. P., Segal, W. A., & Huguenard, J. R. (2009). Synergistic roles of GABAA receptors and SK channels in regulating thalamocortical oscillations. Journal of Neurophysiology, 102(1), 203–213. https://doi.org/10.1152/jn.91158.2008

Knake, S., Hamer, H. M., Schomburg, U., Oertel, W. H., & Rosenow, F. (1999). Tiagabine-induced absence status in idiopathic generalized epilepsy. Seizure, 8(5), 314–317. https://doi.org/10.1053/seiz.1999.0303

Konagaya, Y., Terai, K., Hirao, Y., Takakura, K., Imajo, M., Kamioka, Y., Sasaoka, N., Kakizuka, A., Sumiyama, K., Asano, T., & Matsuda, M. (2017). A Highly Sensitive FRET Biosensor for AMPK Exhibits Heterogeneous AMPK Responses among Cells and Organs. Cell Reports, 21(9), 2628–2638. https://doi.org/10.1016/j.celrep.2017.10.113

Kong, D., Dagon, Y., Campbell, J. N., Guo, Y., Yang, Z., Yi, X., Aryal, P., Wellenstein, K., Kahn, B. B., Sabatini, B. L., & Lowell, B. B. (2016). A Postsynaptic AMPK→p21-Activated Kinase Pathway Drives Fasting-Induced Synaptic Plasticity in AgRP Neurons. Neuron, 91(1), 25–33. https://doi.org/10.1016/j.neuron.2016.05.025

Kristopher, J. B., & Carl, E. S. (2010). The Ketogenic Diet. In Epilepsy (pp. 417–439). CRC Press.

Krosigk, M. von, Bal, T., & McCormick, D. A. (1993). Cellular mechanisms of a synchronized oscillation in the thalamus. Science, 261(5119), 361–364. https://doi.org/10.1126/science.8392750

Kulik, Á., Nakadate, K., Nyíri, G., Notomi, T., Malitschek, B., Bettler, B., & Shigemoto, R. (2002). Distinct localization of GABAB receptors relative to synaptic sites in the rat cerebellum and ventrobasal thalamus. European Journal of Neuroscience, 15(2), 291–307. https://doi.org/10.1046/j.0953-816x.2001.01855.x

Kuramoto, N., Wilkins, M. E., Fairfax, B. P., Revilla-Sanchez, R., Terunuma, M., Tamaki, K., Iemata, M., Warren, N., Couve, A., Calver, A., Horvath, Z., Freeman, K., Carling, D., Huang, L., Gonzales, C., Cooper, E., Smart, T. G., Pangalos, M. N., & Moss, S. J. (2007). Phospho-Dependent Functional Modulation of GABAB Receptors by the Metabolic Sensor AMP-Dependent Protein Kinase. Neuron, 53(2), 233–247. https://doi.org/10.1016/j.neuron.2006.12.015

Laker, R. C., Drake, J. C., Wilson, R. J., Lira, V. A., Lewellen, B. M., Ryall, K. A., Fisher, C. C., Zhang, M., Saucerman, J. J., Goodyear, L. J., Kundu, M., & Yan, Z. (2017). Ampk phosphorylation of Ulk1 is required for targeting of mitochondria to lysosomes in exercise-induced mitophagy. Nature Communications, 8(1), 548. https://doi.org/10.1038/s41467-017-00520-9

Leary, L. D., Wang, D., Nordli, D. R., Engelstad, K., & De Vivo, D. C. (2003). Seizure Characterization and Electroencephalographic Features in Glut-1 Deficiency Syndrome. Epilepsia, 44(5), 701–707. https://doi.org/10.1046/j.1528-1157.2003.05302.x

Lee, K., Dixon, A. K., Richardson, P. J., & Pinnock, R. D. (1999). Glucose-receptive neurones in the rat ventromedial hypothalamus express KATP channels composed of Kir6.1 and SUR1 subunits. The Journal of Physiology, 515(Pt 2), 439–452. https://doi.org/10.1111/j.1469-7793.1999.439ac.x

Lee, K., Li, B., Xi, X., Suh, Y., & Martin, R. J. (2005). Role of Neuronal Energy Status in the Regulation of Adenosine 5′-Monophosphate-Activated Protein Kinase,

Orexigenic Neuropeptides Expression, and Feeding Behavior. Endocrinology, 146(1), 3–10. https://doi.org/10.1210/en.2004-0968

Leiva-Salinas, C., Quigg, M., Elias, W. J., Patrie, J. T., Flors, L., Fountain, N. B., & Rehm, P. K. (2017). Earlier seizure onset and longer epilepsy duration correlate with the degree of temporal hypometabolism in patients with mesial temporal lobe sclerosis. Epilepsy Research, 138, 105–109. https://doi.org/10.1016/j.eplepsyres.2017.10.023

Li, J., Deng, J., Sheng, W., & Zuo, Z. (2012). Metformin attenuates Alzheimer's disease-like neuropathology in obese, leptin-resistant mice. Pharmacology Biochemistry and Behavior, 101(4), 564–574. https://doi.org/10.1016/j.pbb.2012.03.002

Li Jun, Zeng Zhiyuan, Viollet Benoit, Ronnett Gabriele V., & McCullough Louise D. (2007). Neuroprotective Effects of Adenosine Monophosphate- Activated Protein Kinase Inhibition and Gene Deletion in Stroke. Stroke, 38(11), 2992–2999. https://doi.org/10.1161/STROKEAHA.107.490904

Liu, H., Yang, Y., Wang, Y., Tang, H., Zhang, F., Zhang, Y., & Zhao, Y. (2018). Ketogenic diet for treatment of intractable epilepsy in adults: A meta-analysis of observational studies. Epilepsia Open, 3(1), 9–17. https://doi.org/10.1002/epi4.12098

Liu, L., Zheng, T., Morris, M. J., Wallengren, C., Clarke, A. L., Reid, C. A., Petrou, S., & O'Brien, T. J. (2006). The mechanism of carbamazepine aggravation of absence seizures. The Journal of Pharmacology and Experimental Therapeutics, 319(2), 790–798. https://doi.org/10.1124/jpet.106.104968

Liu, Z., Vergnes, M., Depaulis, A., & Marescaux, C. (1992). Involvement of intrathalamic GABAb neurotransmission in the control of absence seizures in the rat. Neuroscience, 48(1), 87–93. https://doi.org/10.1016/0306-4522(92)90340-8

López-Gambero, A. J., Martínez, F., Salazar, K., Cifuentes, M., & Nualart, F. (2018). Brain Glucose-Sensing Mechanism and Energy Homeostasis. Molecular Neurobiology. https://doi.org/10.1007/s12035-018-1099-4

Lu, A. C., Lee, C. K., Kleiman-Weiner, M., Truong, B., Wang, M., Huguenard, J. R., & Beenhakker, M. P. (2020). Nonlinearities between inhibition and T-type calcium channel activity bidirectionally regulate thalamic oscillations. ELife, 9, e59548. https://doi.org/10.7554/eLife.59548

Lutas, A., & Yellen, G. (2013). The ketogenic diet: Metabolic influences on brain excitability and epilepsy. Trends Neurosci, 36(1), 32–40. https://doi.org/10.1016/j.tins.2012.11.005

Ma, T. C., Buescher, J. L., Oatis, B., Funk, J. A., Nash, A. J., Carrier, R. L., & Hoyt, K. R. (2007). Metformin therapy in a transgenic mouse model of Huntington's disease. Neuroscience Letters, 411(2), 98–103. https://doi.org/10.1016/j.neulet.2006.10.039

Ma, W., Berg, J., & Yellen, G. (2007). Ketogenic Diet Metabolites Reduce Firing in Central Neurons by Opening KATP Channels. The Journal of Neuroscience, 27(14), 3618–3625. https://doi.org/10.1523/jneurosci.0132-07.2007

Manning, J.-P. A., Richards, D. A., Leresche, N., Crunelli, V., & Bowery, N. G. (2004). Cortical-area specific block of genetically determined absence seizures by ethosuximide. Neuroscience, 123(1), 5–9. https://doi.org/10.1016/j.neuroscience.2003.09.026

Martínez-François, J. R., Fernández-Agüera, M. C., Nathwani, N., Lahmann, C., Burnham, V. L., Danial, N. N., & Yellen, G. (2018). BAD and KATP channels regulate neuron excitability and epileptiform activity. ELife, 7, e32721. https://doi.org/10.7554/eLife.32721

Matricardi, S., Verrotti, A., Chiarelli, F., Cerminara, C., & Curatolo, P. (2014). Current Advances in Childhood Absence Epilepsy. Pediatric Neurology, 50(3), 205–212. http://dx.doi.org/10.1016/j.pediatrneurol.2013.10.009

McCafferty, C., David, F., Venzi, M., Lőrincz, M. L., Delicata, F., Atherton, Z., Recchia, G., Orban, G., Lambert, R. C., Di Giovanni, G., Leresche, N., & Crunelli, V. (2018). Cortical drive and thalamic feed-forward inhibition control thalamic output synchrony during absence seizures. Nature Neuroscience, 21(5), 744–756. https://doi.org/10.1038/s41593-018-0130-4

McCormick, D. A., & Contreras, D. (2001). On The Cellular and Network Bases of Epileptic Seizures. Annual Review of Physiology, 63(1), 815–846. https://doi.org/10.1146/annurev.physiol.63.1.815

McCrimmon, R. J., Fan, X., Ding, Y., Zhu, W., Jacob, R. J., & Sherwin, R. S. (2004). Potential Role for AMP-Activated Protein Kinase in Hypoglycemia Sensing in the Ventromedial Hypothalamus. Diabetes, 53(8), 1953–1958. https://doi.org/10.2337/diabetes.53.8.1953

McNally, M. A., & Hartman, A. L. (2012). Ketone Bodies in Epilepsy. Journal of Neurochemistry, 121(1), 28–35. https://doi.org/10.1111/j.1471-4159.2012.07670.x

Meeren, H. K. M., Pijn, J. P. M., Van Luijtelaar, E. L. J. M., Coenen, A. M. L., & Lopes da Silva, F. H. (2002a). Cortical Focus Drives Widespread Corticothalamic Networks during Spontaneous Absence Seizures in Rats. The Journal of Neuroscience, 22(4), 1480–1495.

Meeren, H. K. M., Pijn, J. P. M., Van Luijtelaar, E. L. J. M., Coenen, A. M. L., & Lopes da Silva, F. H. (2002b). Cortical Focus Drives Widespread Corticothalamic Networks during Spontaneous Absence Seizures in Rats. The Journal of Neuroscience, 22(4), 1480–1495.

Mehrabi, S., Sanadgol, N., Barati, M., Shahbazi, A., Vahabzadeh, G., Barzroudi, M., Seifi, M., Gholipourmalekabadi, M., & Golab, F. (2018). Evaluation of metformin effects in the chronic phase of spontaneous seizures in pilocarpine model of temporal lobe epilepsy. Metabolic Brain Disease, 33(1), 107–114. https://doi.org/10.1007/s11011-017-0132-z

Mergenthaler, P., Lindauer, U., Dienel, G. A., & Meisel, A. (2013). Sugar for the brain: The role of glucose in physiological and pathological brain function. Trends in Neurosciences, 36(10), 587–597. https://doi.org/10.1016/j.tins.2013.07.001

Mullen, S. A., & Berkovic, S. F. (2018). Genetic generalized epilepsies. Epilepsia, 59(6), 1148–1153. https://doi.org/10.1111/epi.14042

Osorio, I., Reed, R. C., & Peltzer, J. N. (2000). Refractory Idiopathic Absence Status Epilepticus: A Probable Paradoxical Effect of Phenytoin and Carbamazepine. Epilepsia, 41(7), 887–894. https://doi.org/10.1111/j.1528-1157.2000.tb00258.x

Padgett, C. L., & Slesinger, P. A. (2010). GABAB Receptor Coupling to G-proteins and Ion Channels. In P. B. Thomas (Ed.), Advances in Pharmacology: Vol. Volume 58 (pp. 123–147). Academic Press.

Panayiotopoulos, C. P. (1999). Typical absence seizures and their treatment. Archives of Disease in Childhood, 81(4), 351–355. https://doi.org/10.1136/adc.81.4.351

Panayiotopoulos, C. P., Agathonikou, A., Sharoqi, I. A., & Parker, A. P. (1997). Vigabatrin aggravates absences and absence status. Neurology, 49(5), 1467. https://doi.org/10.1212/wnl.49.5.1467

Parker, A. P., Agathonikou, A., Robinson, R. O., & Panayiotopoulos, C. P. (1998). Inappropriate use of carbamazepine and vigabatrin in typical absence seizures. Developmental Medicine and Child Neurology, 40(8), 517–519. https://doi.org/10.1111/j.1469-8749.1998.tb15409.x

Pernicova, I., & Korbonits, M. (2014). Metformin—Mode of action and clinical implications for diabetes and cancer. Nature Reviews Endocrinology, 10(3), 143–156. https://doi.org/10.1038/nrendo.2013.256

Ramamurthy, S., & Ronnett, G. V. (2006). Developing a head for energy sensing: AMP-activated protein kinase as a multifunctional metabolic sensor in the brain. The Journal of Physiology, 574(1), 85–93. https://doi.org/10.1113/jphysiol.2006.110122

Rehni, A. K., & Dave, K. R. (2018). Impact of Hypoglycemia on Brain Metabolism During Diabetes. Molecular Neurobiology, 55(12), 9075–9088. https://doi.org/10.1007/s12035-018-1044-6

Reid, C. A., Kim, T. H., Berkovic, S. F., & Petrou, S. (2011). Low blood glucose precipitates spike-and-wave activity in genetically predisposed animals. Epilepsia, 52(1), 115–120. https://doi.org/10.1111/j.1528-1167.2010.02911.x

Routh, V. H., Hao, L., Santiago, A. M., Sheng, Z., & Zhou, C. (2014). Hypothalamic glucose sensing: Making ends meet. Frontiers in Systems Neuroscience, 8, 236. https://doi.org/10.3389/fnsys.2014.00236

Rubio Osornio, M. del C., Custodio Ramírez, V., Calderón Gámez, D., Paz Tres, C., Carvajal Aguilera, K. G., & Phillips Farfán, B. V. (2018). Metformin Plus Caloric Restriction Show Anti-epileptic Effects Mediated by mTOR Pathway Inhibition. Cellular and Molecular Neurobiology, 38(7), 1425–1438. https://doi.org/10.1007/s10571-018-0611-8

Scanziani, M. (2000). GABA Spillover Activates Postsynaptic GABAB Receptors to Control Rhythmic Hippocampal Activity. Neuron, 25(3), 673–681. https://doi.org/10.1016/S0896-6273(00)81069-7

Schapel, G., & Chadwick, D. (1996). Tiagabine and non-convulsive status epilepticus. Seizure, 5(2), 153–156. https://doi.org/10.1016/S1059-1311(96)80111-7

Schousboe, A., Bak, L. K., Sickmann, H. M., Sonnewald, U., & Waagepetersen, H. S. (2007). Energy substrates to support glutamatergic and GABAergic synaptic function: Role of glycogen, glucose and lactate. Neurotoxicity Research, 12(4), 263–268. https://doi.org/10.1007/BF03033909

Sherwin, R. S., Hendler, R. G., & Felig, P. (1976). Effect of Diabetes Mellitus and Insulin on the Turnover and Metabolic Response to Ketones in Man. Diabetes, 25(9), 776–784. https://doi.org/10.2337/diab.25.9.776

Simpson, I. A., Appel, N. M., Hokari, M., Oki, J., Holman, G. D., Maher, F., Koehler-Stec, E. M., Vannucci, S. J., & Smith, Q. R. (1999). Blood—Brain Barrier Glucose Transporter. Journal of Neurochemistry, 72(1), 238–247. https://doi.org/10.1046/j.1471-4159.1999.0720238.x

Simpson, I. A., Carruthers, A., & Vannucci, S. J. (2007). Supply and demand in cerebral energy metabolism: The role of nutrient transporters. J Cereb Blood Flow Metab, 27(11), 1766–1791. http://www.nature.com/jcbfm/journal/v27/n11/suppinfo/9600521s1.html

Slusser, P. G., & Ritter, R. C. (1980). Increased feeding and hyperglycemia elicited by intracerebroventricular 5-thioglucose. Brain Research, 202(2), 474–478. https://doi.org/10.1016/0006-8993(80)90158-4

Smith, K. A., & Fisher, R. S. (1996). The selective GABAB antagonist CGP-35348 blocks spike-wave bursts in the cholesterol synthesis rat absence epilepsy model. Brain Research, 729(2), 147–150. https://doi.org/10.1016/0006-8993(96)00174-6

Sodickson, D. L., & Bean, B. P. (1996). GABAB Receptor-Activated Inwardly Rectifying Potassium Current in Dissociated Hippocampal CA3 Neurons. Journal of Neuroscience, 16(20), 6374–6385. https://doi.org/10.1523/JNEUROSCI.16-20-06374.1996

Soto-Insuga, V., López, R. G., Losada-Del Pozo, R., Rodrigo-Moreno, M., Cayuelas, E. M., Giráldez, B. G., Díaz-Gómez, E., Sánchez-Martín, G., García, L. O., & Serratosa, J. M. (2019). Glut1 deficiency is a rare but treatable cause of childhood absence epilepsy with atypical features. Epilepsy Research, 154, 39–41. https://doi.org/10.1016/j.eplepsyres.2019.04.003

Sprenger, J. U., Perera, R. K., Götz, K. R., & Nikolaev, V. O. (2012). FRET Microscopy for Real-time Monitoring of Signaling Events in Live Cells Using Unimolecular Biosensors. JoVE (Journal of Visualized Experiments), 66, e4081. https://doi.org/10.3791/4081

Stewart, L. S., Wu, Y., Eubanks, J. H., Han, H., Leschenko, Y., Perez Velazquez, J. L., Cortez, M. A., & Snead Iii, O. C. (2009). Severity of atypical absence phenotype in GABAB transgenic mice is subunit specific. Epilepsy & Behavior, 14(4), 577–581. http://dx.doi.org/10.1016/j.yebeh.2009.01.019

Tanner, G. R., Lutas, A., Martínez-François, J. R., & Yellen, G. (2011). Single KATP Channel Opening in Response to Action Potential Firing in Mouse Dentate Granule Neurons. The Journal of Neuroscience, 31(23), 8689–8696. https://doi.org/10.1523/jneurosci.5951-10.2011

Thammongkol, S., Vears, D. F., Bicknell-Royle, J., Nation, J., Draffin, K., Stewart, K. G., Scheffer, I. E., & Mackay, M. T. (2012). Efficacy of the ketogenic diet: Which epilepsies respond? Epilepsia, 53(3), e55–e59. https://doi.org/10.1111/j.1528-1167.2011.03394.x

Ting, J. T., Daigle, T. L., Chen, Q., & Feng, G. (2014). Acute Brain Slice Methods for Adult and Aging Animals: Application of Targeted Patch Clamp Analysis and Optogenetics. In M. Martina & S. Taverna (Eds.), Patch-Clamp Methods and Protocols (pp. 221–242). Springer New York. https://doi.org/10.1007/978-1-4939-1096-0_14

Titchenell, P. M., Lazar, M. A., & Birnbaum, M. J. (2017). Unraveling the Regulation of Hepatic Metabolism by Insulin. Trends in Endocrinology and Metabolism: TEM, 28(7), 497–505. https://doi.org/10.1016/j.tem.2017.03.003

Tokarz, V. L., MacDonald, P. E., & Klip, A. (2018). The cell biology of systemic insulin function. The Journal of Cell Biology, 217(7), 2273–2289. https://doi.org/10.1083/jcb.201802095

Tsou, P., Zheng, B., Hsu, C.-H., Sasaki, A. T., & Cantley, L. C. (2011). A Fluorescent Reporter of AMPK activity and Cellular Energy Stress. Cell Metabolism, 13(4), 476–486. https://doi.org/10.1016/j.cmet.2011.03.006

van Luijtelaar, E. L., & Coenen, A. M. (1986). Two types of electrocortical paroxysms in an inbred strain of rats. Neuroscience Letters, 70(3), 393–397.

Vergnes, M., Boehrer, A., Simler, S., Bernasconi, R., & Marescaux, C. (1997). Opposite effects of GABAB receptor antagonists on absences and convulsive seizures. European Journal of Pharmacology, 332(3), 245–255. http://dx.doi.org/10.1016/S0014-2999(97)01085-6

Vinué, Á., & González-Navarro, H. (2015). Glucose and Insulin Tolerance Tests in the Mouse. In V. Andrés & B. Dorado (Eds.), Methods in Mouse Atherosclerosis (pp. 247–254). Springer. https://doi.org/10.1007/978-1-4939-2929-0_17

von Krosigk, M., Bal, T., & McCormick, D. (1993). Cellular mechanisms of a synchronized oscillation in the thalamus. Science, 261(5119), 361. https://doi.org/10.1126/science.8392750

Wang, D., Pascual, J. M., & De Vivo, D. (1993). Glucose Transporter Type 1 Deficiency Syndrome. In M. P. Adam, H. H. Ardinger, R. A. Pagon, S. E. Wallace, L. J. Bean, K. Stephens, & A. Amemiya (Eds.), GeneReviews®. University of Washington, Seattle. http://www.ncbi.nlm.nih.gov/books/NBK1430/

Wick, A. N., Drury, D. R., Nakada, H. I., Wolfe, J. B., & Grabowski, W. the technical assistance of B. B. and R. (1957). Localization of the Primary Metabolic Block Produced by 2-Deoxyglucose. Journal of Biological Chemistry, 224(2), 963–969.

Yang, Y., Zhu, B., Zheng, F., Li, Y., Zhang, Y., Hu, Y., & Wang, X. (2017). Chronic metformin treatment facilitates seizure termination. Biochemical and Biophysical Research Communications, 484(2), 450–455. https://doi.org/10.1016/j.bbrc.2017.01.157

Yellen, G. (2008). Ketone bodies, glycolysis, and K(ATP) channels in the mechanism of the ketogenic diet. Epilepsia, 49(Suppl 8), 80–82. https://doi.org/10.1111/j.1528-1167.2008.01843.x

Zhao, R., Xu, X., Xu, F., Zhang, W., Zhang, W., Liu, L., & Wang, W. (2014). Metformin protects against seizures, learning and memory impairments and oxidative damage induced by pentylenetetrazole-induced kindling in mice. Biochemical and Biophysical Research Communications, 448(4), 414–417. https://doi.org/10.1016/j.bbrc.2014.04.130

Zhou, G., Myers, R., Li, Y., Chen, Y., Shen, X., Fenyk-Melody, J., Wu, M., Ventre, J., Doebber, T., Fujii, N., Musi, N., Hirshman, M. F., Goodyear, L. J., & Moller, D. E. (2001). Role of AMP-activated protein kinase in mechanism of metformin action. The Journal of Clinical Investigation, 108(8), 1167–1174. https://doi.org/10.1172/JCI13505

Chapter 3: Out of thin air: hyperventilation triggered seizures

Kathryn A. Salvati

Mark P. Beenhakker

Published:

Brain Research

1703: 41-52 (2019)

KAS wrote the manuscript with MPB. KAS and MPB crafted all the figures. Copyright permission granted for illustrations reproduced in original manuscript for figures 1,5,6. Herein, the text has been condensed to highlight the evidence for the midline thalamus as a critical node that precipitates absence seizures. Afterwards, the review addresses potential mechanisms that may underlie hyperventilation triggered absences seizures. KAS edited the text and added relevant references.

Abstract

Voluntary hyperventilation triggers seizures in the vast majority of people with absence epilepsy. The mechanisms that underlie this phenomenon remain unknown. Herein, we review observations – many made long ago – that provide insight into the relationship between breathing and absence seizures.

Hyperventilation triggers absence seizures

SWDs are triggered by voluntary hyperventilation in over 90% of patients with absence epilepsy (Panayiotopoulos, 2008), a phenomenon initially documented in the early 20th century (Foerster, 1924; Giannakodimos S, 1995; Watemberg et al., 2015). The use of hyperventilation to unequivocally and quickly diagnose patients with absence epilepsy is now commonplace, and largely obviates the need for a protracted EEG recording procedure to capture spontaneous seizures (Adams & Lueders, 1981). The effectiveness of this diagnostic tool even provides fodder for the suggestion that a diagnosis of absence epilepsy "*should be seriously questioned [if one] does not have an attack on hyperventilation*" (Holowach et al., 1962).

Hyperventilation elicits high-amplitude, slow and rhythmic brain activity even in *nonepileptic* individuals (Lum et al., 2002a; Nims, 1940a). This phenomenon, known as *Hyperventilation-Induced, High-Amplitude Rhythmic Slowing* (HIHARS), is often confused with spike-wave discharge (SWD) activity in the EEG. HIHARS and SWDs are both observed on most cortical recording electrodes, reflecting a generalized EEG pattern. HIHARS also evokes many of the automatisms – staring, eye opening/eyelid fluttering, yawning – observed during absence seizures (Epstein et al., 1994; Lum et al., 2002a). Electrographically, however, HIHARS and seizure-associated SWDs are distinct EEG events. HIHARS consists of slow (2-5Hz), high-amplitude (>100mV) electrical activity reminiscent of delta waves observed during slow-wave sleep (Lum et al., 2002b;

Nasreddine et al., 2020). In contrast, spontaneous and hyperventilation-triggered SWDs observed in absence patients consist of the canonical 3Hz, high-amplitude, nearly sinusoidal EEG wave that is punctuated by an abrupt and rapid spike during each cycle of the oscillation (see **Chapter 1, Figure 1**). Thus, while hyperventilation can clearly alter brain activity in healthy individuals, it is also clear that such rapid breathing evokes distinct electrical activity patterns in absence patients.

Physiological response to hyperventilation

To understand how hyperventilation alters EEG patterns, it is important to understand the relationship between breathing and blood pH, a relationship that is critically dependent on carbon dioxide (CO_2) in the blood. Indeed, in 1942, Gibbs et al. admonished brain researchers by suggesting that "*students of cerebral function have, in general, paid too little attention to carbon dioxide*" (Gibbs et al., 1942). In that spirit, we begin by directing our attention to CO_2.

CO_2 is a waste product of *aerobic respiration*, the series of biochemical events utilized by cells to convert glucose metabolites into energy (see Figure 1). Once produced, CO_2 diffuses out of the tissue and into the blood plasma. Most plasma CO_2 enters red blood cells, where it associates with water to produce bicarbonate and a hydrogen ion, a reaction catalyzed by carbonic anhydrase. Plasma CO_2 that does not enter red blood cells is converted into carbonic acid (H_2CO_3), an uncatalyzed reaction. Carbonic acid, in turn, *dissociates* into bicarbonate and hydrogen ions. The concentration of the free hydrogen ions ($[H^+]$), in turn, determines blood plasma pH. Naturally, this reaction can proceed in the reverse direction such that bicarbonate and a hydrogen ion *associate* to form carbonic acid. When this reverse reaction is favored, $[H^+]$ drops and the blood becomes more alkaline. The reverse reaction is favored when the partial pressure of CO_2 (PCO_2) drops.

Taking into account the aforementioned bicarbonate buffering system present in the blood plasma, we can begin to understand how hyperventilation alters blood pH (Figure 2). Rapid breathing causes CO_2 levels in the plasma to drop; in short, the individual *blows off* CO_2. The drop in free CO_2 in the blood plasma is called *hypocapnia* and promotes the reverse reaction in which carbonic acid dissociates into CO_2 and water. The resultant drop in carbonic acid, in turn, promotes the association of bicarbonate and H^+ ions to replenish depleted carbonic acid, a reaction that removes free H^+ ions. *In toto*, as CO_2 drops, the $[H^+]$ in the blood also drops, causing the blood to become more alkaline. This process during which rapid breathing alkalizes the blood is called *respiratory alkalosis*.

An important consideration regarding respiratory alkalosis is that rapid breathing occurs when metabolic activity is low. Accordingly, the CO_2-producing, biochemical process of cellular aerobic respiration occurs at low rates. Under conditions of low CO_2 production and high respiratory CO_2 elimination, the PCO_2 of blood drops and the blood alkalizes, as described above (see Fig. 1, purple). In contrast, elevated breathing during exercise, a phenomenon known as *hyperpnoea*, is associated with increased metabolic demands. Under such conditions, high CO_2 elimination is matched by high CO_2 production (Fig. 1, green). As the PCO_2 of blood is relatively stable during hyperpnoea, the pH of blood does not change. The distinction between hyperventilation and hyperpnoea is relevant, as the latter does not trigger seizures in absence patients (Esquivel et al., 1991), suggesting that absence seizures are specifically sensitive to blood pH.

Homeostatic mechanisms are in place to compensate for changes in blood pH. Namely, the vasculature responds when blood pH changes. Vessels normally dilate when blood acidifies, and constrict when blood alkalizes. The mechanisms by which vascular tone (i.e. dilation versus constriction) is modulated by blood pH are well-documented; as such, we direct the interested reader towards excellent reviews on the subject (Boron & Boulpaep, 2016; Cipolla, 2009; Kontos H A et al., 1977). Suffice to say, vascular tone is a

highly regulated process that involves complex interactions between the endothelial cells that line the inner walls of blood vessels and the smooth muscle cells that contract or relax to change vessel diameter. The canonical vasodilatory effect of nitric oxide (NO) underscores the intimate interaction between endothelial cells and muscle cells: sheer stress sensed by transient receptor potential (TRP) channels on endothelial cells triggers the production of endothelial nitric oxide synthase (eNOS) to catalyze the production of NO, a diffusible molecule that relaxes nearby muscle cells (Boron & Boulpaep, 2016). Vascular tone is also directly regulated by pH, a process that involves internal calcium stores, calcium-activated potassium (BK) channels (Koide & Wellman, 2015) and, possibly, TRP channels (Sonkusare et al., 2012).

Regardless of the specific mechanism, it is clear that vascular tone responds to blood CO_2 and pH in healthy individuals. Interestingly, Nims et al showed that inherent differences in this response likely exist between individuals with absence epilepsy and those without absence epilepsy (Nims et al., 1940b). Specifically, the authors measured the CO_2 content and pH of the carotid artery and jugular vein blood supplies, thereby enabling them to compare the physiochemical properties of blood entering and exiting the brain, respectively. The authors observed a standard response to hyperventilation in both epileptic and non-epileptic cohorts insofar that arterial blood CO_2 dropped to comparable levels. However, following hyperventilation, the drop in CO_2 content and concurrent alkalization of the jugular blood in absence epileptic individuals was consistently larger and persisted longer than that of healthy individuals. Taken together, the data indicate that (1) the blood *supplying* the brain is normal in absence patients, (2) the blood *returning* from the brain is different in absence patients, and (3) hyperventilation unmasks this difference. Thus, not only does voluntary hyperventilation trigger seizures in absence patients, but the brain's response to hypocapnic episodes is also different. Although Nims et al. published their findings more than 75 years ago, it remains unclear if the two

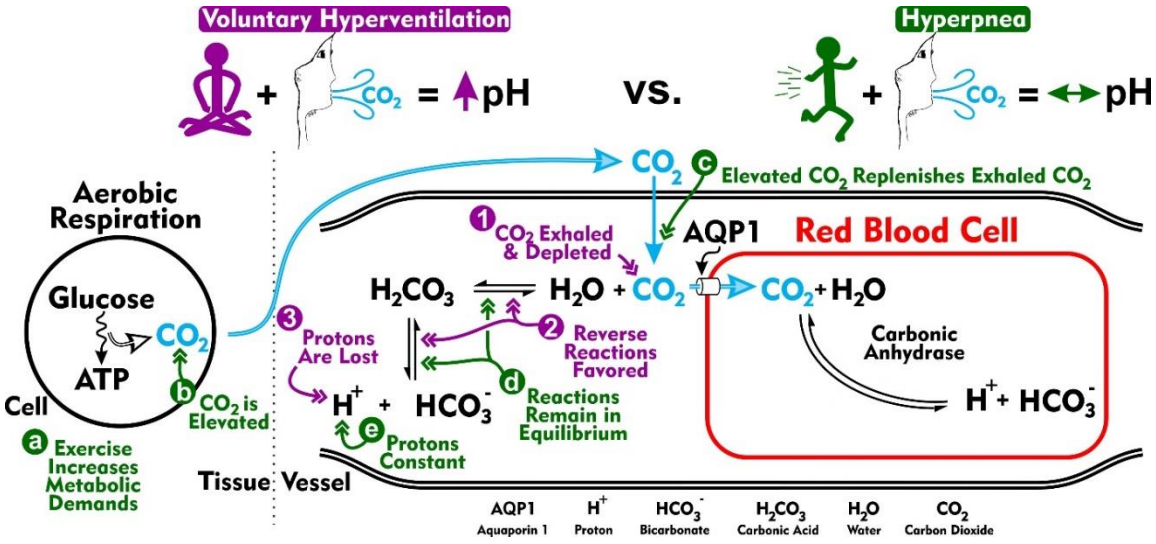

Figure 1. Acid-base blood physiology during rapid breathing. The schematic depicts biochemical reactions largely responsible for establishing blood pH. On the left is shown a cell situated in the tissue undergoing aerobic respiration, the process of converting glucose into ATP. Carbon dioxide (CO_2) is produced during this conversion process. CO_2 then diffuses into capillary plasma, after which the bulk is primarily transported into erythrocytes (red blood cells) via aquaporin 1 (AQP1) channels[114]. Within the red blood cell, CO_2 associates with H_2O (water) to produce H^+ (proton) and HCO_3^- (bicarbonate), a reaction catalyzed by carbonic anhydrase. Carbonic anhydrase is found in abundance in red blood cells, but not in the plasma. The dissociated proton acidifies the red blood cell and, in doing so, promotes the dissociation of hemoglobin and oxygen. A small portion of CO_2 entering the capillary remains in the plasma. As in the red blood cell, plasma CO_2 is also converted into H^+ and HCO_3^-, but this reaction is primarily *not* catalyzed by carbonic anhydrase [i.e. an *uncatalyzed* reaction (however, some carbonic anhydrase isoforms are localized to the extracellular surface of many cells[115,116], including red blood cells, and contribute to the catalyzed production of H^+ and HCO_3^- from CO_2 and H_2O[116])]. The uncatalyzed reaction reversibly proceeds through H_2CO_3 (carbonic acid) and occurs at low

basal rates. ***Purple (1-3)***. Acid-base physiology during voluntary hyperventilation. Voluntary hyperventilation is defined by excessive breathing (high rate and quantity) leading to the pronounced ventilation of CO_2 and ensuing respiratory alkalosis, a phenomenon in which blood plasma becomes alkaline. **(1)** Excessive ventilation reduces plasma concentrations of CO_2. **(2)** CO_2 depletion promotes the association of plasma H^+ and HCO_3^- to replenish, via H_2CO_3, CO_2. **(3)** Favoring the reverse reactions reduces the concentration of plasma H^+, thereby making the blood more alkaline. ***Green (a-e)***. Acid-base physiology during exercise-related hyperventilation (i.e. hyperpnoea). **(a)** Unlike during voluntary hyperventilation, hyperpnoea occurs during times of heightened metabolic demand. **(b)** Aerobic respiration associated with high metabolic demands produces high levels of CO_2. **(c)** Increased CO_2 production and subsequent diffusion into capillaries balances the increased CO_2 exhalation. **(d)** The equilibria underlying CO_2-H_2O biochemical reactions remain unperturbed. **(e)** As these biochemical reactions remain in equilibrium, plasma protons are not lost and plasma pH is stable. Importantly, absence seizures are triggered by voluntary hyperventilation, but not hyperpnoea.

phenomena are related. The observation that CO_2 inhalation can temporarily abolish absence seizures (Lennox, 1928; Yang et al., 2014) suggests an interdependent relationship.

At present, no consensus exists regarding whether the observed EEG changes in response to hyperventilation result from hypocapnia, the concomitant change in brain pH, or a combination of the two. An explanation will likely require a better understanding of pH-sensitivity among specific elements within the neural circuits that generate absence seizures. Below, we begin by describing results that highlight how crosstalk between structures in the cortex and in the thalamus, a subcortical structure, may precipitate seizures in response to hyperventilation. Then, we detail the neural circuits involved in absence epilepsy. Finally, we summarize evidence supporting the hypothesis that specific nodes within thalamic circuits are pH-sensitive.

Absence seizures: crosstalk between the thalamus and cortex

Decades of research highlight how reciprocal interactions between cortical and thalamic circuits act as critical architects of absence seizure generation (Massimo Avoli, 2012). As early as 1935 clinicians noted that highly synchronized seizure activity could be simultaneously recorded from EEG electrodes placed throughout the cortex, leading to the prescient postulation that subcortical structures with widespread cortical connectivity are likely involved (Jasper & Kershman, 1941; Penfield et al., 1941). The structure receiving early attention was the thalamus.

Besides serving as a relay station for vision, proprioception and hearing (Jones, 2007), the thalamus houses critical neural circuity responsible for electrical oscillations observed during sleep (McCormick & Bal, 1997; Steriade & Llinás, 1988) and seizures. Morison and Dempsey (Dempsey & Morison, 1942a, 1942b; Morison & Dempsey, 1942) as well as Jasper and colleagues (Hanbery & Jasper, 1953; Hunter & Jasper, 1949; Jasper

& Droogleever-Fortuyn, 1947; Jasper & Kershman, 1941), provided several key lines of evidence in support of the hypothesis that thalamic circuits play an important role in SWD generation. *First*, recordings from depth electrodes placed in the thalamus of cats reveal that thalamic circuits are highly oscillatory (Dempsey & Morison, 1942b; Morison & Dempsey, 1942). *Second*, electrical stimulation of the cat thalamus evokes generalized, cortical SWDs (Hunter & Jasper, 1949; Jasper & Droogleever-Fortuyn, 1947). *Third*, severing thalamus-cortex connections mitigates the capacity of thalamic stimulation to evoke SWDs (Hanbery & Jasper, 1953). Following these insightful studies, Fisher and Prince (Fisher & Prince, 1977), as well as Avoli and colleagues (Avoli et al., 1983; Avoli & Gloor, 1982a, 1982b), used the feline generalized penicillin model of epilepsy (FGPE) to assess, on a more granular level, thalamic contribution to SWDs. The FGPE is an experimental epilepsy model in which a large, intramuscular injection of penicillin reliably evokes SWDs (Prince & Farrell, 1969). By closely examining temporal relationships of neuronal activity throughout the brain in the FGPE, it was possible to determine that excessive, hypersynchronous cortical activity likely initiates the SWD (Avoli et al., 1983; Avoli & Gloor, 1982a). A similar conclusion was later derived in an inbred rat model of absence epilepsy (van Heukelum et al., 2016; van Luijtelaar & Coenen, 1986). Thus, decades of work underscore the notion that a “close coupling” of activity produced by the thalamus and cortex contributes to the onset and maintenance of the SWD (Avoli & Gloor, 1982a).

The riddle in the middle: midline structures of the thalamus

The pioneering studies of Rose and Woolsey prompted an era dedicated to organizing the thalamic nuclei based upon structure and function (Jones, 2007). Using anatomical and electrophysiological methods, their work revealed that the cortex receives inputs from specific subdivisions of the dorsal thalamus (Jones, 2007). Rose and Woolsey

divided the dorsal thalamus into two distinct divisions: *extrinsic* and *intrinsic*. The *extrinsic* nuclei included the anterior and ventral thalamic groups as well as the geniculate bodies. They proposed that these *extrinsic* structures projected to specific cortical areas, including motor, sensory and limbic areas. The *intrinsic* nuclei, consisting of the midline, intralaminar and posterior thalamic groups, were thought to receive only intrathalamic projections. However, the distinction between *extrinsic* and *intrinsic* was highly speculative and subsequent studies failed to demonstrate the existence of purely intrathalamic connectivity among thalamic nuclei.

Later, Morison and Dempsey proposed a second classification scheme to distinguish among the dorsal thalamic nuclei. They used the term *specific* to describe dorsal thalamic nuclei with distinct, topographically-mapped connections to the cortex (Dempsey & Morison, 1942a, 1942b). In contrast, the term *non-specific* was used to describe those nuclei, primarily the midline and intralaminar nuclei, with diffuse projections throughout the cortex (Dempsey & Morison, 1942a, 1942b). These non-specific nuclei are collectively called the *non-specific thalamic projecting system* (NSTPS) and include the mediodorsal nucleus, central medial (CM) nucleus, as well as other nuclei of the intralaminar complex (Jones, 2007). We illustrate the organization of the specific and non-specific thalamic nuclei in Figure 3. Special attention will be given to the NSTPS, as this system appears to play a critical role in hyperventilation-induced changes in EEG patterns.

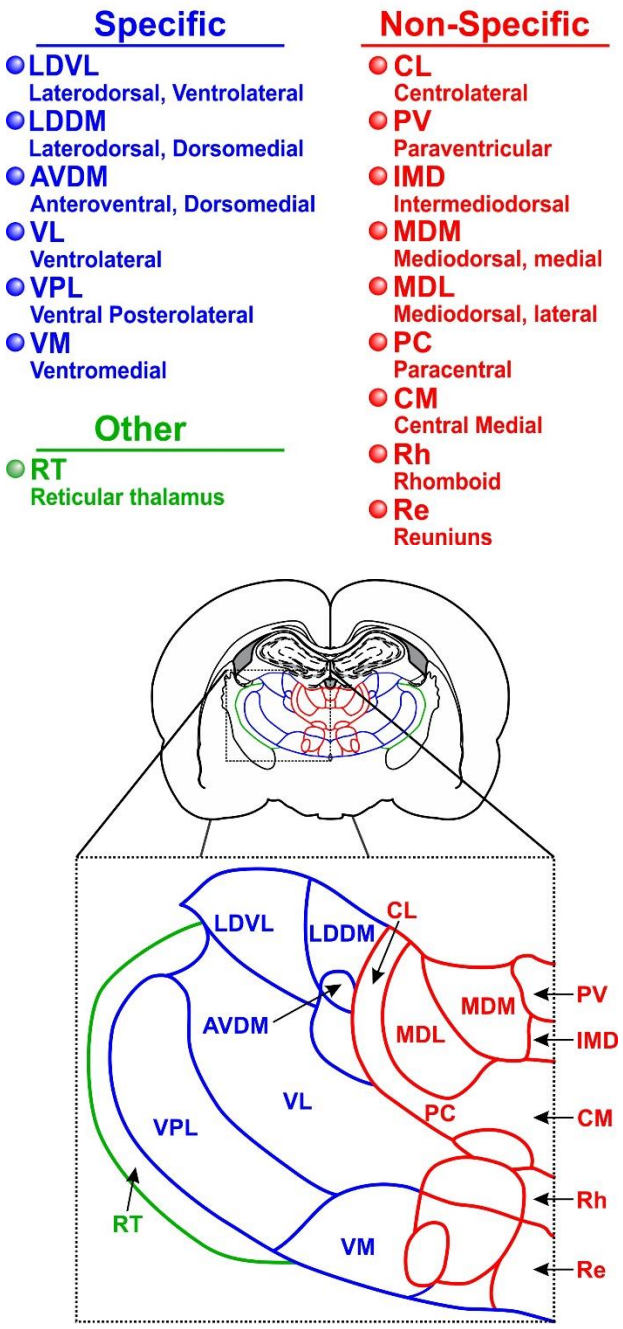

Figure 2. Specific and non-specific nuclei of the thalamus. On top is shown a coronal section of a rat brain (Paxinos & Watson, 2007). An expanded view of nuclei from the thalamus on one side is shown directly below the full coronal section. Nuclei abbreviations are found below the expanded view. Structures outlined in blue represent the specific

thalamic nuclei, whereas the structures outlined in red represent the non-specific nuclei. Collectively, specific and non-specific nuclei comprise the dorsal thalamus. The reticular nucleus (green), a member of the ventral thalamus, forms a thin, shell-like structure that surrounds the dorsal thalamus. Nuclei along the midline are considered members of the Non-Specific Thalamic Projection System (NSTPS). The following structures are not labeled: submedius thalamic nucleus (dorsal and ventral), anteromedial thalamic nucleus, ventral reuniens, mammillothalamic tract.

Morison and Dempsey first demonstrated that electrical stimulation of specific and non-specific thalamic nuclei in the anesthetized cat evoked divergent cortical responses. Stimulation of the specific nuclei evoked a localized, multiphasic response consisting of an early *primary response* and a later *augmenting response.* The latter response was so-called because it became larger after repetitive stimulation (Fig. 3A). In contrast, stimulation of the NSTPS evoked widespread responses in the cortex (Dempsey & Morison, 1942a, 1942b; Morison & Dempsey, 1942), consistent with the diffuse nature of NSTPS projections. Interestingly, successive NSTPS stimuli delivered at 6-12Hz often produced robust, high amplitude cortical responses that grew during the repetitive stimulus train (Fig. 3B). This latter feature led Morison and Dempsey to introduce the term *recruiting response*. There are several important characteristics that distinguish the recruiting response from the augmenting response (see Figure 3): (1) the latency from stimulus to event onset is much longer for the recruiting response; (2) the recruiting response waxes and wanes with repetitive stimulation; (3) the recruiting response spreads throughout the cortex, while the augmenting response is highly localized; (4) the recruiting response is not preceded by the primary response.

The phenomenon of the NSTPS-evoked recruiting response was subsequently confirmed in great detail by Jasper and colleagues (Hanbery & Jasper, 1953; Hunter & Jasper, 1949; Jasper & Droogleever-Fortuyn, 1947; Jasper & Kershman, 1941). Moreover, Jasper and colleagues demonstrated that even brief stimulation of the NSTPS in lightly anesthetized (Jasper & Droogleever-Fortuyn, 1947) or unanesthetized (Hunter & Jasper, 1949) cats evokes behavioral arrest and synchronized SWDs throughout the cortex that long outlasts the stimulus. The capacity for NSTPS stimulation to evoke either the recruiting response or prolonged SWDs accompanied with behavioral arrest likely depends on the state of anesthesia: recruiting responses are observed in anesthetized animals, while seizures are observed in awake animals. This observation firmly placed

the NSTPS at the forefront of possible structures that drive absence seizures, even prompting Jasper to conclude that this collection of nuclei serves as the “diencephalic basis for [absence epilepsy], or a diencephalic pacemaker for its characteristic cortical discharge” (Hunter & Jasper, 1949).

Following these seminal findings, Dominick Purpura set out to determine how the NSTPS drives widespread cortical activity. He focused much of his efforts on intrinsic thalamic connectivity (Jones, 2007). By performing intracellular recordings of neurons in the specific and non-specific thalamic nuclei of anesthetized cats, Purpura and colleagues revealed complex, bidirectional interactions between the NSTPS and the specific thalamic nuclei (Desiraju & Purpura, 1970; Purpura & Cohen, 1962). Their findings also provided a glimpse into how these interactions may contribute to the aforementioned recruiting response. Many of their studies focused on the CM nucleus, a member of the NSTPS.

Purpura and colleagues show that CM stimulation in the cat evoked post-synaptic potentials (PSPs) in neurons localized to several specific thalamic nuclei, including the ventral group of the dorsal thalamus and the reticular nucleus (Figure 4). The evoked PSPs follow a complex pattern[82]. CM stimulation evokes putative short-latency excitatory post-synaptic potentials (EPSPs) in neurons of the ventral group (i.e. ventromedial thalamus), followed by long-duration, inhibitory post-synaptic potentials (IPSPs) (Figure 4). The short

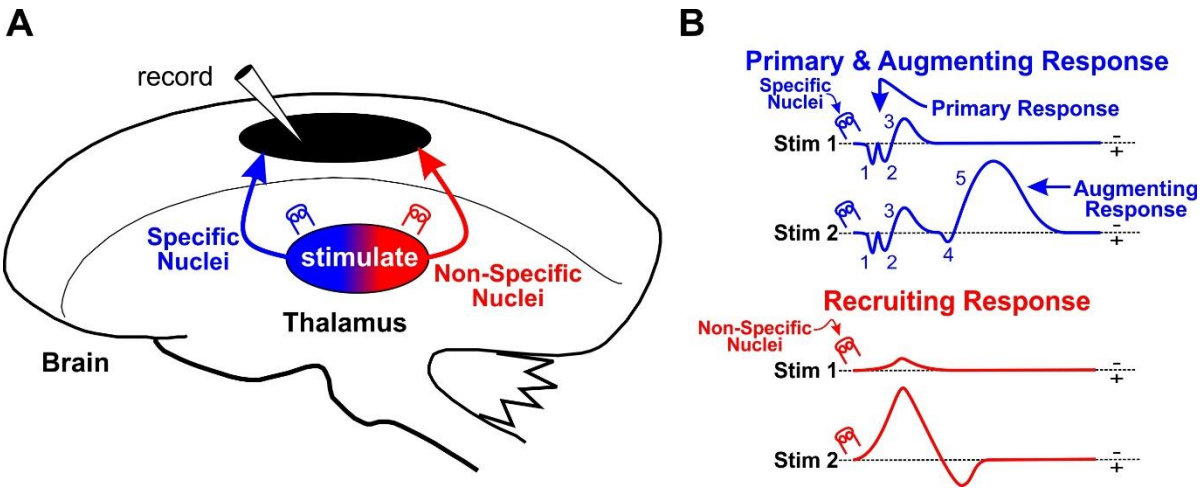

Figure 3. **Electrophysiological cortical response to electrical stimulation of specific versus non-specific thalamic nuclei. (A)** Schematic representing experiment. Field responses are recorded in the cortex (e.g. anterior sigmoid gyrus, visual cortex). Electrical stimuli are delivered to either the lateral thalamic nuclei (blue), or the midline thalamic nuclei (red). **(B)** A single electrical stimulation of the lateral thalamic nuclei evokes events known as the primary and augmenting responses (top, blue). The primary response is collectively composed of two positive deflections (1 & 2), followed by a larger negative component. Repetitive lateral nuclei stimulation produces a secondary component known as the *augmenting* response. In contrast to lateral nuclei stimulation, a single electrical stimulation of the midline thalamic nuclei evokes a single, small, negative component (bottom, red). Successive midline stimuli yield a progressively larger event known as the *recruiting* response. Schematized responses are based on those described in *The Thalamus* (Jones, 2007).

latency of the putative EPSPs led Purpura to posit that CM provided direct excitation to the ventral group.

The origin of CM-evoked IPSPs was more puzzling. When Purpura and Cohen recorded neurons of the reticular thalamus (RT), an inhibitory structure, the picture became clearer: CM stimulation activated RT neurons. As RT neurons inhibit many thalamic structures (Fuentealba & Steriade, 2005), a likely origin of the CM-evoked IPSPs observed in neurons of the ventral group was from the RT nucleus. Thus, it was proposed that CM provides direct excitation, as well as indirect, disynaptic inhibition, to neurons of the ventral group. The observed inhibition of ventral group neurons was quite robust and included a strong, long-lasting component indicative of activation of metabotropic, B-type, GABA ($GABA_B$) receptors. $GABA_B$ receptor antagonists effectively inhibit experimentally-induced absence seizures (Vergnes et al., 1997).

Purpura and Cohen ultimately attempted to relate the progression of CM-evoked EPSPs-IPSPs observed in ventral group neurons to the CM-evoked recruiting response. They proposed that the initial, large component of the recruiting response associates with ventral group EPSPs, while the ensuing, secondary component of the response associates with ventral group IPSPs. Moreover, special attention was paid to the potential synchronizing effect neurons of the RT nucleus had on thalamic activity. In sum, these experiments provided an unprecedented, macroscopic understanding of the structures involved in generating absence seizures. Left unaddressed was whether the NSTPS was involved in hyperventilation-triggered absence seizures.

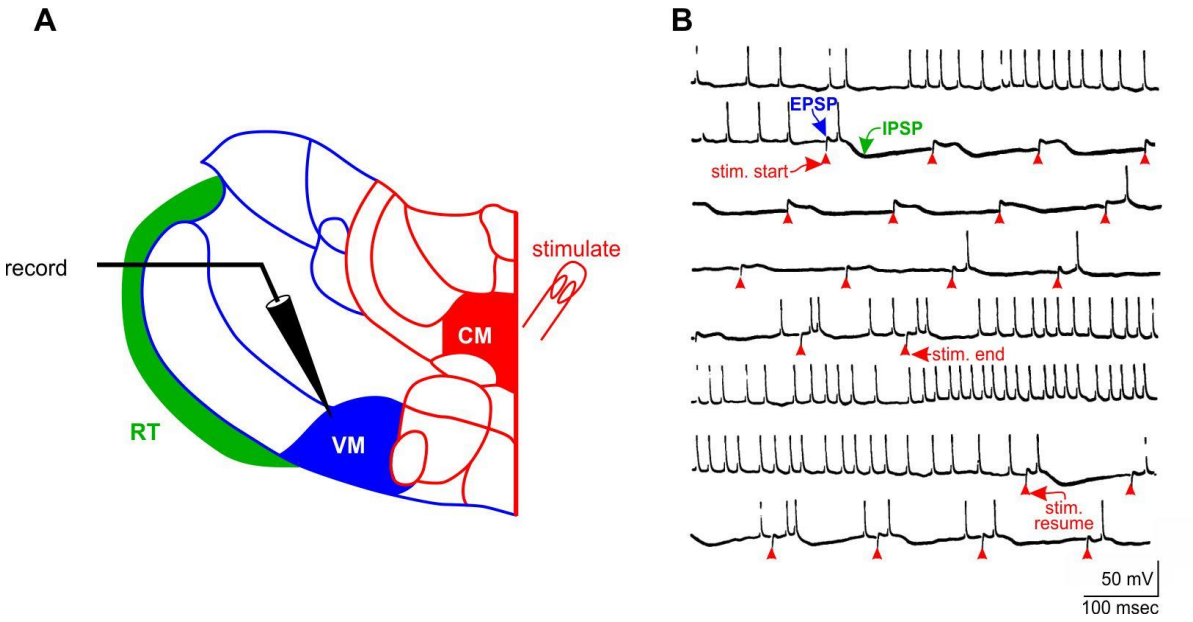

Figure 4. The central medial (i.e. non-specific) nucleus of the thalamus is functionally connected to specific and reticular thalamic nuclei. Shown are experimental results from Purpura and Cohen[82]. **(A)** Experimental preparation. *In vivo* experiments were performed in the cat. The central medial (CM) nucleus was stimulated with an extracellular stimulating electrode. Responses to such stimulation were recorded in neurons of the ventromedial (VM) using intracellular recording pipettes. Thalamic structures that are likely involved in the VM neuron responses are filled in with red, blue or green. **(B)** An example, intracellular recording of a VM neuron. Each red arrowhead represents a single electrical stimulus delivered to CM. Prior to CM stimulation, action potentials are spontaneously generated by the VM neuron. The first electrical stimulus elicits a putative excitatory postsynaptic potential (EPSP, blue) with a short latency in the recorded neuron. The putative EPSP is followed by a longer latency inhibitory postsynaptic potential (IPSP, green). Purpura and Cohen speculated that rapid EPSP occurred as a result of direct, monosynaptic connectivity between CM and VM nuclei. The IPSP, in contrast, likely resulted from an indirect, disynaptic connection that initially involved excitation of GABAergic neurons of the reticular thalamic (RT) nucleus, followed by RT-

mediated inhibition of VM neurons. This EPSP-IPSP combination is observed to differing extents with subsequent CM stimulation. Following CM stimulation (i.e. stim. end) results in a phase of slow VM neuron depolarization. Resumption of CM stimulation again evokes the EPSP-IPSP combination.

A basic modulation of the thalamus

Despite the long-established documentation of hyperventilation-induced (i.e. respiratory alkalosis-induced) absence seizures, few studies have attempted to experimentally recapitulate this phenomenon. Experiments performed by Ira Sherwin in the 1960s represent some of the few attempts to do so. Sherwin proposed two key questions in his experiments: (1) what brain structures are recruited by hyperventilation to increase the occurrence of SWDs (Sherwin, 1965, 1967), and (2) do these structures possess a specific, element that is responsive to respiratory-induced changes in pH?

In the first study (Sherwin, 1965), Sherwin demonstrated that hyperventilating a cat elicits high amplitude, rhythmic slowing in the cortical EEG comparable to activity observed during HIHARS (see Figure 5). Stimulating the cortex during HIHARS further transformed the activity to include generalized cortical seizures similar to SWDs. To determine how the coupling of HIHARS and cortical stimulation evokes seizures, Sherwin used a common procedure at the time to assess cortical excitability: the direct cortical response (DCR, Fig. 5A). Briefly, local electrical field potentials are evoked and recorded in one area of the cortex by stimulating another area of the cortex. The activation of excitatory synapses formed between thalamocortical and cortical neurons is thought to contribute to the DCR. Using this assay of cortical excitability, Sherwin showed that the DCR was enhanced during hyperventilation. Severing connections between the cortex and subcortical structures (i.e. isolating the cortex) abolished this hyperventilation-induced DCR enhancement. These findings prompted Sherwin to conclude that some subcortical structure capable of enhancing cortical excitability was recruited during hyperventilation. A few years later, Sherwin performed experiments designed to identify this structure.

Following, in 1967, Sherwin presented a study that demonstrated a critical role for the NSTPS in modulating cortical excitability (Sherwin, 1967). Sherwin specifically examined the contribution of the central lateral (CL) nucleus, a member of the NSTPS, to

hyperventilation-induced changes in cortical excitability and HIHARS. Sherwin demonstrated that HIHARS was abolished after lesioning the CL (see Fig. 5B), thereby presenting the strongest available data that provide an explanation for how hyperventilation alters cortical EEG patterns. At the time he could only postulate that the observed changes in cortical activity resulted from an element, likely in the thalamus, that is both chemoreceptive and capable of enhancing cortical activity (Sherwin, 1967). The conclusions drawn by Sherwin were never pursued further in the context of absence epilepsy. Nonetheless, the few-yet-critical results documented by Sherwin uncovered the interesting possibility that the thalamus acts as a potential pH-sensor (or contains pH sensing pathways to the cortex). It remains uncertain how the NSTPS engages with other rhythmic microcircuits in the thalamus during hyperventilation-induced SWDs.

We have described only a small subset of the rich dataset, accumulated over many decades, that highlights the critical role that thalamocortical circuits play in the generation of absence seizures. But what of pH sensitivity in these circuits? For the remainder of this review, we attempt to describe more specifically how pH alters thalamocortical circuits to possibly trigger absence seizures.

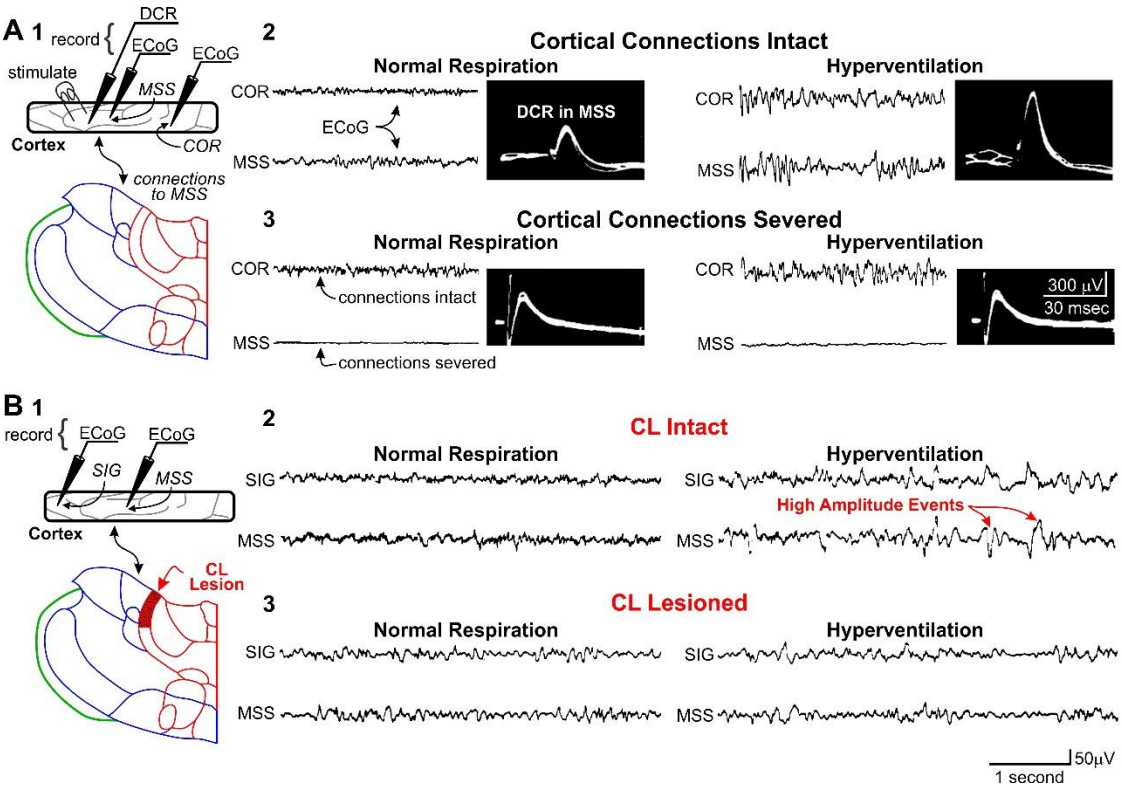

Figure 5. Hyperventilation-induced, high-amplitude slowing of cortical activity depends on non-specific thalamic nuclei. Panels A and B represent experimental observations from two *in vivo* cat studies performed by Ira Sherwin[85,86]. **(A)** In the first study, electrophysiological recordings were obtained from the cortex (1). Electrocorticogram (ECoG) recordings, similar to EEG recordings, were used to measure large-scale cortical activity in the mid-suprasylvian gyrus (MSS) and the coronal gyrus (COR). Local field recordings recorded in the MSS reveal the direct cortical response (DCR) evoked by a nearby electrical stimulating electrode. Importantly, the DCR is hypothesized to arise from direct activation of afferents that originate from the thalamus[118-120]. The experiment compared ECoG and DCR responses during hyperventilation before and after subcortical connections to the MSS were selectively severed. Cortical responses recorded before (2) and after (3) severing connections between the cortex and thalamus. With intact thalamus-cortex connectivity, normal respiration was associated with low-amplitude ECoG activity, as well as an evoked DCR of moderate amplitude.

Hyperventilation produced high-amplitude, slow ECoG activity in both the MSS and COR. Also, the evoked DCR was larger. After severing thalamus-MSS connections, hyperventilation did not alter ECoG activity recorded in the MSS. Importantly, after severing connections, hyperventilation also did not augment the DCR. **(B)** In the second study, the effects of CL lesion on hyperventilation-induced, high amplitude ECoG signals were assessed (1). As in panel A, hyperventilation elicits ECoG signals that consist of high amplitude events in the intact sigmoid gyrus (SIG) and MSS. (2). After CL lesion, these hyperventilation-induced events are not observed (3).

pH sensitivity in the thalamus

Despite a considerable void in literature detailing pH sensitive mechanisms in the NSTPS, evidence demonstrates that certain neurons of the specific thalamic nuclei possess pH-sensitive ion channels that contribute to the resting membrane potential of thalamic neurons. We focus on two such channels: the HCN channel responsible for the so-called h-current (I_h) (Soltesz et al., 1991), and TASK 1/3 channels responsible for a resting potassium current (I_{TASK}) (Meuth et al., 2006).

Meuth et al. revealed a complex, pH-sensitive interaction between I_h and I_{TASK} in thalamocortical (TC) neurons of the dorsal lateral geniculate nucleus, a "specific" thalamic nucleus that receives visual information from the retina (Meuth et al., 2006). The authors demonstrate that I_h and I_{TASK} exert opposing effects on TC neuron resting membrane potential. I_h is a mixed cationic (Na^+ and K^+) current that is activated at relatively hyperpolarized membrane potentials (Biel et al., 2009). The reversal potential of I_h is around -20 mV, meaning that when I_h is active, a neuron will typically depolarize towards -20 mV. Because the resting membrane potential of TC neurons is relatively hyperpolarized (~-70 mV), partial activation of I_h is observed at rest and contributes to TC neuron resting membrane potential. Evidence for this last point comes from the more hyperpolarized resting membrane potential observed in TC neurons when I_h is pharmacologically or genetically removed: the resting membrane potential shifts towards -80 mV (Meuth et al., 2006). I_{TASK}, in contrast, is a K^+ current and, as such, has a reversal potential of around -90 mV, meaning that when I_{TASK} is active, a neuron will typically hyperpolarize towards -90 mV. I_{TASK} is often described as a background current because it is usually active at rest and contributes significantly to the resting membrane potential of neurons.

I_h and I_{TASK} are both pH-sensitive in TC neurons (Meuth et al., 2006). Extracellular acidification blocks both currents. Because these two currents have functionally opposing

actions – I_h depolarizes cells while I_{TASK} hyperpolarizes cells – the net result of extracellular acidification is minimal; the resting membrane potential of TC neurons does not change much during extracellular acidification. The action potential firing properties of TC neurons are also unchanged during extracellular acidification. The results of Meuth et al. suggest that, functionally, TASK 1/3 and HCN expression levels are commensurate in TC neurons (Meuth et al., 2006). If such expression levels were mismatched in a sub-population of TC neurons, then changes in pH would likely significantly impact TC neuron activity. Also, it remains formally possible that extracellular alkalization, as might occur during hyperventilation, might preferentially modulate one current (e.g. I_h) over another (e.g. I_{TASK}), thereby significantly changing TC neuron firing behavior. To date, this possibility remains purely speculative. It remains entirely unclear to what extent pH sensitivity in the so-called "specific" nuclei contribute to hyperventilation-induced absence seizures. After all, much of the aforementioned work suggests that the NSTPS plays a major role in absence seizures triggered by respiratory alkalosis.

Conclusion

Herein, we highlight the potential link among thalamocortical networks, hyperventilation, and absence epilepsy. Specifically, we focus on studies indicating that the NSTPS of the thalamus may be capable of evoking hyperventilation-induced absence seizures. This conclusion is derived from demonstrations that the NSTPS appears critically involved in both SWDs and hyperventilation-triggered cortical activity patterns. Moreover, some thalamocortical circuit elements appear to be endowed with pH-sensitive proteins. What remains unclear is whether these observations point to a common mechanism accounting for hyperventilation-triggered absence seizures, a striking phenomenon shared by over 90% of absence patients. Perhaps the next few decades of thalamic research will shed light on this possibility.

References

Adams, D. J., & Lueders, H. (1981). Hyperventilation and 6-hour EEG recording in evaluation of absence seizures. *Neurology*, *31*(9), 1175–1177. https://doi.org/10.1212/wnl.31.9.1175

Avoli, Massimo. (2012). A brief history on the oscillating roles of thalamus and cortex in absence seizures. *Epilepsia*, *53*(5), 779–789. https://doi.org/10.1111/j.1528-1167.2012.03421.x

Avoli, M., Gloor, P., Kostopoulos, G., & Gotman, J. (1983). An analysis of penicillin-induced generalized spike and wave discharges using simultaneous recordings of cortical and thalamic single neurons. *Journal of Neurophysiology*, *50*(4), 819–837. https://doi.org/10.1152/jn.1983.50.4.819

Avoli, Massimo, & Gloor, P. (1982a). Role of the thalamus in generalized penicillin epilepsy: Observations on decorticated cats. *Experimental Neurology*, *77*(2), 386–402. http://dx.doi.org/10.1016/0014-4886(82)90252-7

Avoli, Massimo, & Gloor, P. (1982b). Interaction of cortex and thalamus in spike and wave discharges of feline generalized penicillin epilepsy. *Experimental Neurology*, *76*(1), 196–217. http://dx.doi.org/10.1016/0014-4886(82)90112-1

Biel, M., Wahl-Schott, C., Michalakis, S., & Zong, X. (2009). Hyperpolarization-Activated Cation Channels: From Genes to Function. *Physiological Reviews*, *89*(3), 847–885. https://doi.org/10.1152/physrev.00029.2008

Boron, W. F., & Boulpaep, E. (2016). *Medical Physiology—3rd Edition*. Elsevier Academic Press Inc. https://www.elsevier.com/books/medical-physiology/boron/978-1-4557-4377-3

Cipolla, M. J. (2009). Control of Cerebral Blood Flow. In *The Cerebral Circulation*. Morgan & Claypool Life Sciences. https://www.ncbi.nlm.nih.gov/books/NBK53082/

Dempsey, E., & Morison, R. (1942a). The interaction of certain spontaneous and induced cortical potentials. *American Journal of Physiology*, *135*, 301–308.

Dempsey, E., & Morison, R. (1942b). The production of rhythmically recurrent cortical potentials after localized thalamic stimulation. *American Journal of Physiology*, *135*, 293–300.

Desiraju, T., & Purpura, D. P. (1970). Organization of specific-nonspecific thalamic internuclear synaptic pathways. *Brain Research*, *21*(2), 169–181. http://dx.doi.org/10.1016/0006-8993(70)90361-6

Epstein, M. A., Duchowny, M., Jayakar, P., Resncik, T. J., & Alvarez, L. A. (1994, November). *Altered Responsiveness During Hyperventilation-Induced EEG Slowing: A Non-Epileptic Phenomenon in Normal Children—Epstein—1994—Epilepsia—Wiley Online Library*. https://onlinelibrary.wiley.com/doi/abs/10.1111/j.1528-1157.1994.tb01790.x?sid=nlm%3Apubmed

Esquivel, E., Chaussain, M., Plouin, P., Ponsot, G., & Arthuis, M. (1991). Physical exercise and voluntary hyperventilation in childhood absence epilepsy. *Electroencephalography and Clinical Neurophysiology*, *79*(2), 127–132. http://dx.doi.org/10.1016/0013-4694(91)90050-E

Fisher, R., & Prince, D. (1977). Spike-Wave rhythms in cat cortex induced by parenteral penicillin II. Cellular Features. *Electroencephalogr. Clin. Neurophysiol.*, *42*, 625–639.

Foerster, O. (1924). Hyperventilationsepilepsie. *Deut Ztschr Nervenheilk*, *83*, 347–356.

Fuentealba, P., & Steriade, M. (2005). The reticular nucleus revisited: Intrinsic and network properties of a thalamic pacemaker. *Progress in Neurobiology*, *75*(2), 125–141. http://dx.doi.org/10.1016/j.pneurobio.2005.01.002

Giannakodimos S, F. C. (1995). Qualitative and quantitative abnormalities of breath counting during brief generalized 3 Hz spike and slow wave “subclinical” discharges. *Clin. Electroencephalogr.*, *26*(4), 200–203.

Gibbs, E. L., Lennox, W. G., Gibbs, F. A., & Nims, L. F. (1942). Regulation of cerebral carbon dioxide. *Archives of Neurology and Psychiatry*, *47*(6), 879–889.

Hanbery, J., & Jasper, H. (1953). Independence of Diffuse Thalamocortical Projection System Shown by Specific Nuclear Destructions. *Journal of Neurophysiology*, 252–271.

Holowach, J., Thurston, D., & O’Leary, J. L. (1962). Petit Mal Epilepsy. *Pediatrics*, *30*, 893–901.

Hunter, J., & Jasper, H. H. (1949). Effects of thalamic stimulation in unanaesthetised animals: The arrest reaction and petit Mal-like seizures, activation patterns and generalized convulsions. *Electroencephalography and Clinical Neurophysiology*, *1*(1–4), 305–324. http://dx.doi.org/10.1016/0013-4694(49)90196-0

Jasper, H. H., & Droogleever-Fortuyn, J. (1947). Experimental studies of the functional anatomy of petit mal epilepsy. *Res. Publ. Assoc. Res. Nerve Ment. Dis.*, *26*, 272–298.

Jasper, Herbet H., & Kershman, J. (1941). Electroencephalographic classification of the epilepsies. *Arch Neurol Psychiatry*, *45*, 903–943.

Jones, E. G. (2007). *The Thalamus* (Vol. 1). Cambridge University Press.

Koide, M., & Wellman, G. C. (2015). Activation of TRPV4 channels does not mediate inversion of neurovascular coupling after SAH. *Acta Neurochirurgica. Supplement*, *120*, 111–116. https://doi.org/10.1007/978-3-319-04981-6_19

Kontos H A, Raper A J, & Patterson J L. (1977). Analysis of vasoactivity of local pH, PCO2 and bicarbonate on pial vessels. *Stroke*, *8*(3), 358–360. https://doi.org/10.1161/01.STR.8.3.358

Lennox, W. G. (1928). The effect on epileptic seizures of varying composition of respired air. *J. Clin. Investigation*, *6*, 6–23.

Lum, L. M., Connolly, M. B., Farrell, K., & Wong, P. K. H. (2002a). Hyperventilation-induced High-amplitude Rhythmic Slowing with Altered Awareness: A Video-EEG Comparison with Absence Seizures. *Epilepsia (Series 4)*, *43*(11), 1372–1378. https://doi.org/10.1046/j.1528-1157.2002.35101.x

Lum, L. M., Connolly, M. B., Farrell, K., & Wong, P. K. H. (2002b). Hyperventilation-induced High-amplitude Rhythmic Slowing with Altered Awareness: A Video-EEG Comparison with Absence Seizures. *Epilepsia (Series 4)*, *43*(11), 1372–1378. https://doi.org/10.1046/j.1528-1157.2002.35101.x

McCormick, D. A., & Bal, T. (1997). SLEEP AND AROUSAL: Thalamocortical Mechanisms. *Annual Review of Neuroscience*, *20*(1), 185–215. https://doi.org/10.1146/annurev.neuro.20.1.185

Meuth, S. G., Kanyshkova, T., Meuth, P., Landgraf, P., Munsch, T., Ludwig, A., Hofmann, F., Pape, H.-C., & Budde, T. (2006). Membrane Resting Potential of Thalamocortical Relay Neurons Is Shaped by the Interaction Among TASK3 and HCN2 Channels. *Journal of Neurophysiology*, *96*(3), 1517–1529. https://doi.org/10.1152/jn.01212.2005

Morison, R., & Dempsey, E. (1942). Mechanism of Thalamocortical Augmentation and Repetition. *Amer J Physiology*.

Nasreddine, W., Fakhredin, M., Makke, Y., Hmaimess, G., Sabbagh, S., Beaini, S., El Tourjuman, O., & Beydoun, A. (2020). Hyperventilation-induced high-amplitude rhythmic slowing: A mimicker of absence seizures in children. *Epilepsy & Behavior*, *103*, 106510. https://doi.org/10.1016/j.yebeh.2019.106510

Nims, L. F. (1940a). Adjustment of Acid-Base Balance of Patients with Petit Mal Epilepsy to Overventilation. *Archives of Neurology and Psychiatry*, *43*(2), 262–269.

Nims, L. F., Gibbs, E. L., Lennox, W. G., Gibbs, F. A., & Williams, D. (1940b). Adjustment of Acid-Base Balance of Patients with Petit Mal Epilepsy to Overventilation. *Archives of Neurology and Psychiatry*, *43*(2), 262–269.

Panayiotopoulos, C. P. (2008). Typical absence seizures and related epileptic syndromes: Assessment of current state and directions for future research. *Epilepsia*, *49*(12), 2131–2139. https://doi.org/10.1111/j.1528-1167.2008.01777.x

Paxinos, G., & Watson, C. (2007). *The Rat Brain In Sterotaxic Coordinates* (6th ed.). Elsevier.

Penfield, W., Erickson, T. C., Jasper, H. H., & Harrower, M. (1941). *Epilepsy and cerebral localization: A study of the mechanism, treatment and prevention of epileptic seizures*. Springfield : C.C. Thomas.

Prince, D. A., & Farrell, D. (1969). “Centrencephalic” spike-wave discharges following parenteral penicillin injection in the cat. *Neurology*, *19*, 309–310.

Purpura, D. P., & Cohen, B. (1962). INTRACELLULAR RECORDING FROM THALAMIC NEURONS DURING RECRUITING RESPONSES. *Journal of Neurophysiology*, *25*(5), 621–635.

Sherwin, I. (1965). Differential effects of hyperventillation on the excitability of intact and isolated cortex. *Electroencephalography and Clinical Neurophysiology*, *18*(6), 599–607. https://doi.org/10.1016/0013-4694(65)90077-5

Sherwin, I. (1967). Alterations in the non-specific cortical afference during hyperventilation. *Electroencephalography and Clinical Neurophysiology*, *23*(6), 532–538. https://doi.org/10.1016/0013-4694(67)90019-3

Soltesz, I., Lightowler, S., Leresche, N., Jassik-Gerschenfeld, D., Pollard, C. E., & Crunelli, V. (1991). Two inward currents and the transformation of low-frequency oscillations of rat and cat thalamocortical cells. *The Journal of Physiology*, *441*(1), 175–197. https://doi.org/10.1113/jphysiol.1991.sp018745

Sonkusare, S. K., Bonev, A. D., Ledoux, J., Liedtke, W., Kotlikoff, M. I., Heppner, T. J., Hill-Eubanks, D. C., & Nelson, M. T. (2012). Elementary Ca2+ signals through endothelial TRPV4 channels regulate vascular function. *Science (New York, N.Y.)*, *336*(6081), 597–601. https://doi.org/10.1126/science.1216283

Steriade, M., & Llinás, R. R. (1988). The functional states of the thalamus and the associated neuronal interplay. *Physiological Reviews*, *68*(3), 649–742.

van Heukelum, S., Kelderhuis, J., Janssen, P., van Luijtelaar, G., & Lüttjohann, A. (2016). Timing of high-frequency cortical stimulation in a genetic absence model. *Neuroscience*, *324*, 191–201. https://doi.org/10.1016/j.neuroscience.2016.02.070

van Luijtelaar, E. L., & Coenen, A. M. (1986). Two types of electrocortical paroxysms in an inbred strain of rats. *Neuroscience Letters*, *70*(3), 393–397.

Vergnes, M., Boehrer, A., Simler, S., Bernasconi, R., & Marescaux, C. (1997). Opposite effects of GABAB receptor antagonists on absences and convulsive seizures. *European Journal of Pharmacology*, *332*(3), 245–255. https://doi.org/10.1016/S0014-2999(97)01085-6

Watemberg, N., Farkash, M., Har-Gil, M., Sezer, T., Goldberg-Stern, H., & Alehan, F. (2015). Hyperventilation During Routine Electroencephalography: Are Three Minutes Really Necessary? *Pediatric Neurology*, *52*(4), 410–413. http://dx.doi.org/10.1016/j.pediatrneurol.2014.12.003

Yang, X.-F., Shi, X.-Y., Ju, J., Zhang, W.-N., Liu, Y.-J., Li, X.-Y., & Zou, L.-P. (2014). 5% CO2 inhalation suppresses hyperventilation-induced absence seizures in children. *Epilepsy Research*, *108*(2), 345–348. http://dx.doi.org/10.1016/j.eplepsyres.2013.11.012

Chapter 4: Respiratory alkalosis provokes spike-wave discharges in a rat model of absence epilepsy

Kathryn A. Salvati

George M.P.R. Souza

Adam C. Lu

Matthew L. Ritger

Patrice G. Guyenet

Stephen B. Abbott

Mark P. Beenhakker

K.A.S. and M.P.B. wrote the manuscript and crafted all figures. K.A.S. performed all experiments with additional aid from G.M.P.R.S., A.C.L., M.L.R., M.P.B. P.G.G., S.B.A., and G.M.P.R.S helped design experiments and interpret the data.

Abstract

Hyperventilation reliably provokes seizures in patients diagnosed with absence epilepsy. Despite this predictable patient response, the mechanisms that enable hyperventilation to powerfully activate absence seizure-generating circuits remain entirely unknown. Using the WAG/Rij rat, an established rodent model of absence epilepsy, we demonstrate that absence seizures are highly sensitive to arterial carbon dioxide, suggesting that seizure-generating circuits are sensitive to pH. Moreover, hyperventilation consistently activated neurons within the intralaminar nuclei of the thalamus, a structure implicated in seizure generation. We show that intralaminar thalamus also contains pH-sensitive neurons. Collectively, these observations suggest that hyperventilation activates pH-sensitive neurons of the intralaminar nuclei to provoke absence seizures.

Introduction

Epilepsy is a common neurological disorder characterized by recurrent and spontaneous seizures. Yet, accumulating evidence indicates that seizures are not necessarily unpredictable events (Amengual-Gual et al., 2019; Bartolini & Sander, 2019; Baud et al., 2018; Ferlisi & Shorvon, 2014). Several factors affect seizure occurrence, including metabolism (Lusardi et al., 2015; Masino et al., 2012; Masino & Rho, 2012, 2019), sleep (Bazil, 2019; Fountain et al., 1998; Malow et al., 1999; Nobili et al., 2001), catamenia (Herzog & Frye, 2014; Joshi & Kapur, 2019; Reddy et al., 2001), light (Padmanaban et al., 2019) and circadian rhythm (Amengual-Gual et al., 2019; Debski et al., 2020; Smyk & van Luijtelaar, 2020; Stirling et al., 2021). In extreme cases, stimuli immediately provoke seizures, a condition known as reflex epilepsy (Kasteleijn-Nolst Trenité, 2012; Koepp et al., 2016). The mechanisms that render certain seizure-generating networks susceptible to external factors remain unknown.

A highly reliable seizure trigger associated with childhood absence epilepsy is hyperventilation. Between 87-100% of all children diagnosed with the common Genetic Generalized Epilepsy produce spike-wave seizures upon voluntary hyperventilation (Hughes, 2009; Ma et al., 2011; Sadleir et al., 2009). Indeed, hyperventilation serves as a powerful tool for diagnosing this childhood epilepsy (Adams & Lueders, 1981; Holowach et al., 1962; Sadleir et al., 2006; Watemberg et al., 2015). Remarkably, as no single genetic etiology drives absence epilepsy (Chen et al., 2013; Crunelli & Leresche, 2002; Helbig, 2015; Koeleman, 2018; Robinson et al., 2002; Xie et al., 2019), hyperventilation appears to recruit fundamental seizure-generating mechanisms shared by virtually all patients.

Exhalation of CO_2 during hyperventilation causes hypocapnia, a state of decreased arterial CO_2 partial pressure ($PaCO_2$), and respiratory alkalosis, a state of elevated arterial pH (Laffey & Kavanagh, 2002). Hyperventilation also causes rapid arterial vasoconstriction (Raichle & Plum, 1972) and increased cardiac output (Donevan et al., 1962). Recent work demonstrates that inspiration of 5% CO_2 blunts hyperventilation-provoked spike-wave seizures in humans (Yang et al., 2014). Collectively, these observations suggest that respiratory alkalosis serves as the primary trigger for hyperventilation-provoked absence seizures.

Spike-wave seizures associated with absence epilepsy arise from hypersynchronous neural activity patterns within interconnected circuits between the thalamus and the cortex (Avoli, 2012; Beenhakker & Huguenard, 2009; Huguenard & McCormick, 2007; McCafferty et al., 2018; McCormick & Contreras, 2001; Meeren et al., 2002). The crux of the prevailing model describing absence seizure generation includes an initiating bout of synchronous activity within the somatosensory cortex that recruits rhythmically active circuits in the thalamus (Meeren et al., 2002; Sarrigiannis et al., 2018). With widespread connectivity to the cortex, the thalamus then rapidly generalizes spike-

wave seizures to other brain structures. The extent to which thalamocortical circuits respond to shifts in pH during hyperventilation-induced respiratory alkalosis is unknown.

Herein, we test the hypothesis that respiratory alkalosis regulates the occurrence of spike-wave seizures. We demonstrate that hyperventilation-provoked absence seizures observed in humans can be mimicked in an established rodent model, the WAG/Rij rat (Coenen, 2003; Coenen et al., 1992; Russo et al., 2016; van Luijtelaar & Coenen, 1986). We first show that hyperventilation induced with hypoxia reliably evokes respiratory alkalosis and increases spike-wave seizure count in the WAG/Rij rat. When supplemented with 5% CO_2 to offset respiratory alkalosis, hypoxia did not increase spike-wave seizure count. Moreover, hypercapnia alone (high $PaCO_2$) reduced spike-wave seizure count despite a robust increase in respiration rate. We also show that optogenetic stimulation of brainstem respiratory centers to produce respiratory alkalosis during normoxia induces CO_2-sensitive spike-wave seizures. Collectively, these results identify respiratory alkalosis as the primary seizure trigger in absence epilepsy following hyperventilation. Finally, we show that structures of the intralaminar thalamic nuclei are both (1) activated during respiratory alkalosis, and (2) pH-sensitive. Thus, our data demonstrate that respiratory alkalosis provokes spike-wave seizures and shine a spotlight on the poorly understood intralaminar thalamus in the pathophysiology of spike-wave seizures.

Results

Hypoxia triggers spike-wave seizures in the WAG/Rij rat

We first set out to determine if an accepted rat model of absence epilepsy, the WAG/Rij rat, recapitulates hyperventilation-provoked absence seizures, as observed in humans. We combined whole-body plethysmography and electrocorticography/electromyography (ECoG/EMG) recordings in awake WAG/Rij rats to assess respiration and spike-wave seizure occurrence while exposing animals to

different gas mixtures of O_2, CO_2 and N_2 (Figs. 1A-B). We only considered spike-wave seizures that persisted for a minimum of two seconds and occurred concomitantly with behavioral arrest in the animal. Spike-wave seizures are distinguishable from non-REM sleep based on the appearance of 5-8 Hz frequency harmonics in the power spectrogram (see Figure 1B, expanded trace).

We first compared respiration and ECoG/EMG activity in rats exposed to atmospheric conditions (i.e., normoxia: 21% O_2; 0% CO_2; 79% N_2) and hypoxia (10% O_2; 0% CO_2; 90% N_2). Hypoxia reliably stimulates rapid breathing, blood alkalosis and hypocapnia in rats (Basting et al., 2015; Souza et al., 2019). We cycled rats between 40-minute epochs of normoxia and 20-minute epochs of hypoxia. O2 levels were measured from the outflow of the plethysmography chamber for confirmation of gas exchange (Figure 1B, top). Hypoxia evoked a robust increase in respiratory rate (Figure 1B, expanded) and reliably provoked seizures. A peristimulus time histogram (PSTH) aligned to the onset of gas exchange shows spike-wave seizure counts during the 15 minutes immediately before and during hypoxia (Fig. 1C1); the PSTH shows the contribution of each rat in stacked histogram format. Respiratory rates confirmed that hypoxia increased ventilation (Figs. 1C2, 3). To quantify the effect of hypoxia on seizures, we calculated the mean spike-wave seizure count across all bins for each rat. Relative to normoxia, spike-wave seizure count during hypoxia was nearly 2-fold higher ($p = 4.5 \times 10\text{-}7$, $n = 15$; Fig. 1D) and respiratory rate increased by 30% ($p = 1.6 \times 10\text{-}5$, $n = 15$; Fig. 1E).

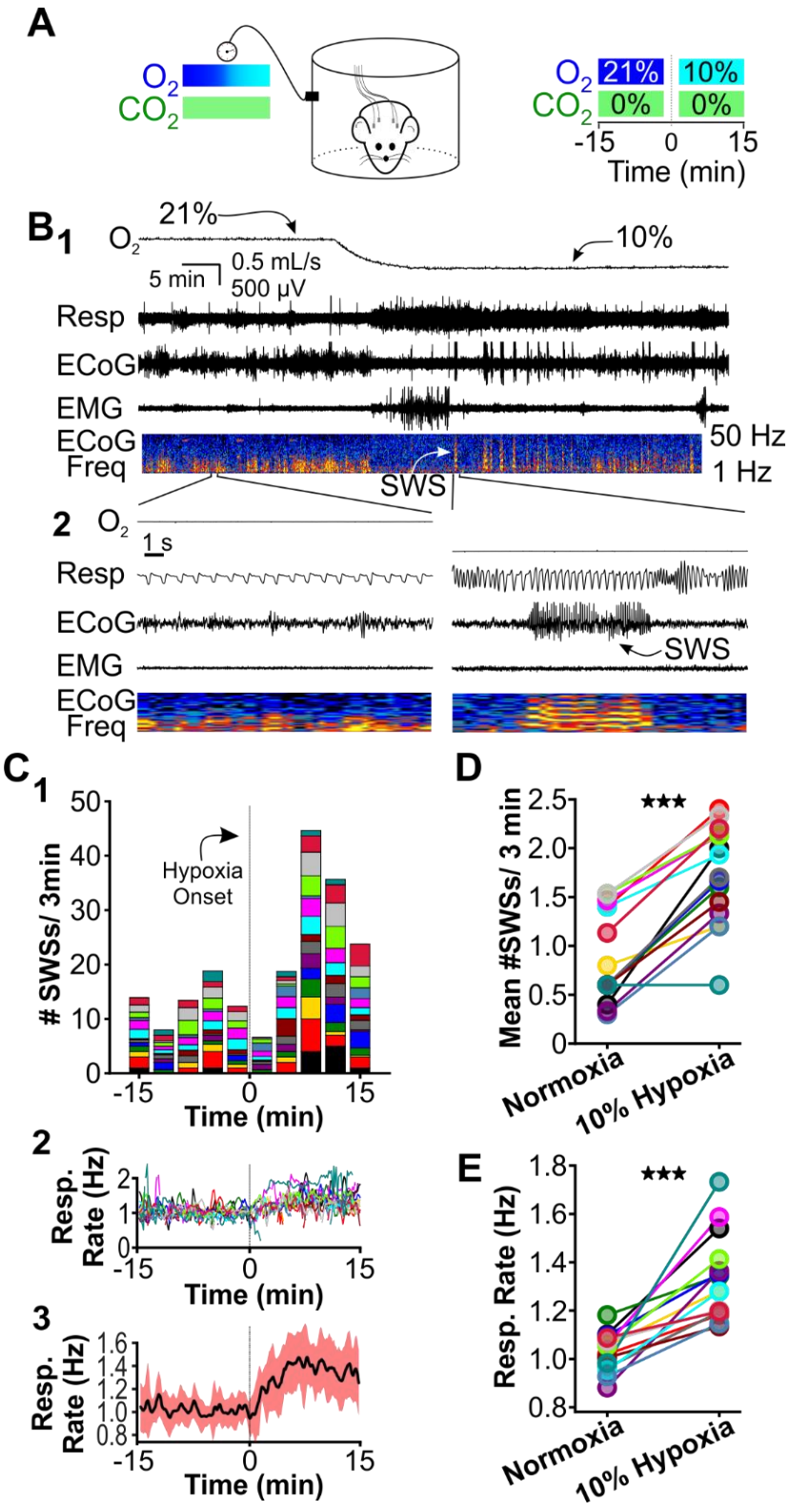
A
O2
CO2
O2 21% 10%
CO2 0% 0%
-15 0 15
Time (min)
B1
21%
O2
10%
5 min
0.5 mL/s
500 µV
Resp
ECoG
EMG
ECoG Freq
50 Hz
1 Hz
SWS
2
O2
1 s
Resp
ECoG
EMG
SWS
ECoG Freq
C1
SWSs/ 3min
Hypoxia Onset
Time (min)
2
Resp. Rate (Hz)
Time (min)
3
Resp. Rate (Hz)
Time (min)
D
Mean #SWSs/ 3 min
***
Normoxia
10% Hypoxia
E
Resp. Rate (Hz)
***
Normoxia
10% Hypoxia

Figure 1. Hypoxia provokes hyperventilation-associated spike-wave seizures in WAG/Rij rats.

(A) Experiment Paradigm. Left: Plethysmography chambers recorded ventilation and ECoG/EMG signals in rats exposed to normoxia (i.e., 21% O_2) and hypoxia (i.e., 10% O_2). Right: Example gas exchange protocol used to generate the peristimulus time histogram in panel C. Spike-wave seizure count was measured during the 15 minutes before and after gas exchange at t = 0 min. **(B)** Representative recordings during transition from normoxia to hypoxia. (1) From top to bottom: chamber O_2, respiration, ECoG, EMG, and ECoG power spectrogram. White arrow points to spike-wave seizure. (2) Bottom: expanded view B1. Spectrogram reveals 5-8 Hz frequency harmonics associated with spike-wave seizures. **(C)** Spike-wave seizure (SWS) and respiration quantification. (1) Stacked histogram illustrating spike-wave seizure count for each animal before and after the onset of hypoxia; each color is a different rat. Arrow points to gas exchange at t = 0 min. (2) Corresponding respiratory rate for each animal shown in panel C1. (3) Mean respiratory rate for all animals. **(D)** Mean spike-wave seizure count per bin and (E) respiratory rate before and after gas exchange. See Tables 1 & 2 for detailed statistics. ***$p < 0.001$.

Recent work shows that spike-wave seizures commonly occur in several rat strains, including those that are generally not considered epileptic (Taylor et al., 2017, 2019). While between 62% (Vergnes et al., 1982) and 84% (Robinson & Gilmore, 1980) of Wistar rats do not have seizures, we nonetheless tested whether hypoxia can unmask seizure-generating potential in this strain, as Wistar and WAG/Rij rats share the same genetic background (Festing, 1979). In normoxia, seizures were absent in all four Wistar rats we tested, consistent with the infrequent spike-wave seizure occurrence reported for this strain. Relative to normoxia in Wistar rats, hypoxia induced hyperventilation, hypocapnia and blood alkalization but did not provoke spike- wave seizures (Figure 2; see Table 3). Instead, hypoxia primarily triggered arousal in Wistar rats, as revealed in EEG spectrograms by the reduction in sleep-related frequencies. Therefore, we hypothesize that hypoxia-provoked spike-wave seizures are unique to seizure-prone rodent models, just as hyperventilation does not provoke absence seizures in otherwise healthy humans.

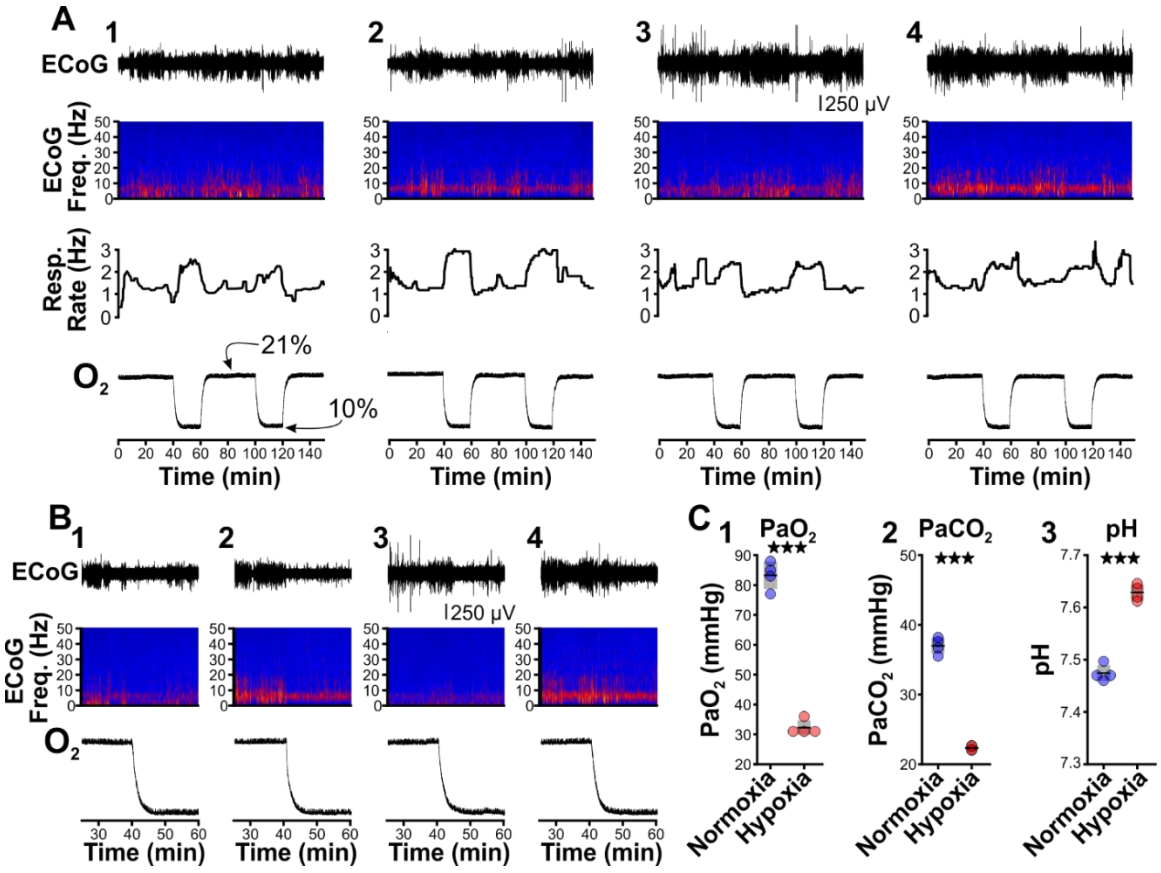

Figure 2. Hypoxia does not provoke hyperventilation-associated spike-wave seizures in Wistar rats. **(A)** Plethysmography chambers recorded ventilation and ECoG/EMG signals in four Wistar rats exposed to normoxia (i.e., 21% O_2) and hypoxia (i.e., 10% O_2). Panels 1-4 include responses from four Wistar rats, respectively, and show from top to bottom: ECoG, ECoG power spectrogram, respiratory rate, and chamber O_2. During the 2.5-hour recording session, rats were challenged twice with hypoxia. No spike-wave seizures were observed during either normoxia or hypoxia. **(B)** Expanded views of the first transition from normoxia to hypoxia shown in panel A. Increased low frequency power during normoxia in some rats (e.g., panel B2) represents sleep. Hypoxia in Wistar rats generally increased arousal. **(C)** Arterial measurements in the same rats show that

hypoxia challenges produced a predictable drop in arterial (1) O_2 and (2) CO_2, as well as (3) alkalosis. See Table 3 for detailed statistics. ***$p < 0.001$.

CO_2 suppresses spike-wave seizures

Hyperventilation promotes hypocapnia, a state of low $PaCO_2$. As dissolved CO_2 is acidic, hyperventilation-triggered hypocapnia is also associated with respiratory alkalosis. To test the hypothesis that hypocapnia specifically provokes seizures, we next determined whether supplemental CO_2 (5%) blunts the spike-wave seizure-provoking effects of hypoxia. We performed ECoG/plethysmography experiments as before but alternated between two test trials: hypoxia and hypoxia/hypercapnia (10% O_2, 5% CO_2; 85% N_2). Test trials were interleaved with 40-minute periods of normoxia to allow blood gases to return to baseline levels (Fig. 3A). As before, hypoxia increased spike-wave seizure count by nearly 2-fold ($p = 1.76 \times 10\text{-}6$, $n = 9$; Figs. 3B1-C) and increased respiratory rate by 27% ($p = 6.59 \times 10\text{-}4$, $n = 9$; Figs. 3B3, D). In the same rats, supplementing hypoxia with 5% CO_2 suppressed the spike-wave seizure response insofar that hypoxia/hypercapnia did not change spike-wave seizure count relative to normoxia ($p = 0.18$, $n = 9$; Figs. 3E1 and 3F) despite a predictable and robust elevation in respiratory rate ($p = 2.71 \times 10\text{-}4$, $n = 9$; Figs. 3E2, 3 and 3G).

In a separate cohort of rats, we collected arterial blood samples to measure blood $PaCO_2$, PaO_2 and pH during normoxia, hypoxia and hypoxia/hypercapnia (see Table 4). We observed a considerable change in PaO_2 [$F (1.056, 5.281) = 406.4$, $p = 3.0 \times 10\text{-}6$], $PaCO_2$ [$F (1.641, 8.203) = 338.9$, $p = 1.9 \times 10\text{-}8$] and pH [$F (1.938, 9.688) = 606$, $p = 7.2 \times 10\text{-}11$] values among the three conditions. Hypoxia decreased $PaCO_2$ ($p = 2.1 \times 10\text{-}6$; $n = 6$; Figure 3H2) and concomitantly alkalized the blood ($p = 7.0 \times 10\text{-}6$, $n = 6$; Figure 3H3). We also observed a decrease in PaO_2 ($p = 6.0 \times 10\text{-}6$; $n = 6$; Figure 3H1). Supplemental CO_2 returned blood pH ($p = 0.008$, $n = 6$; Fig. 3H3) and PaCO2 ($p = 0.42$, $n = 6$; Fig. 3H2) to normoxia levels. However, heightened respiratory rate in supplemental CO_2 raised PaO2 ($p = 00013$, $n = 6$; Fig. 3H1). Collectively, these data support the hypothesis that blood pH powerfully regulates spike-wave seizure activity.

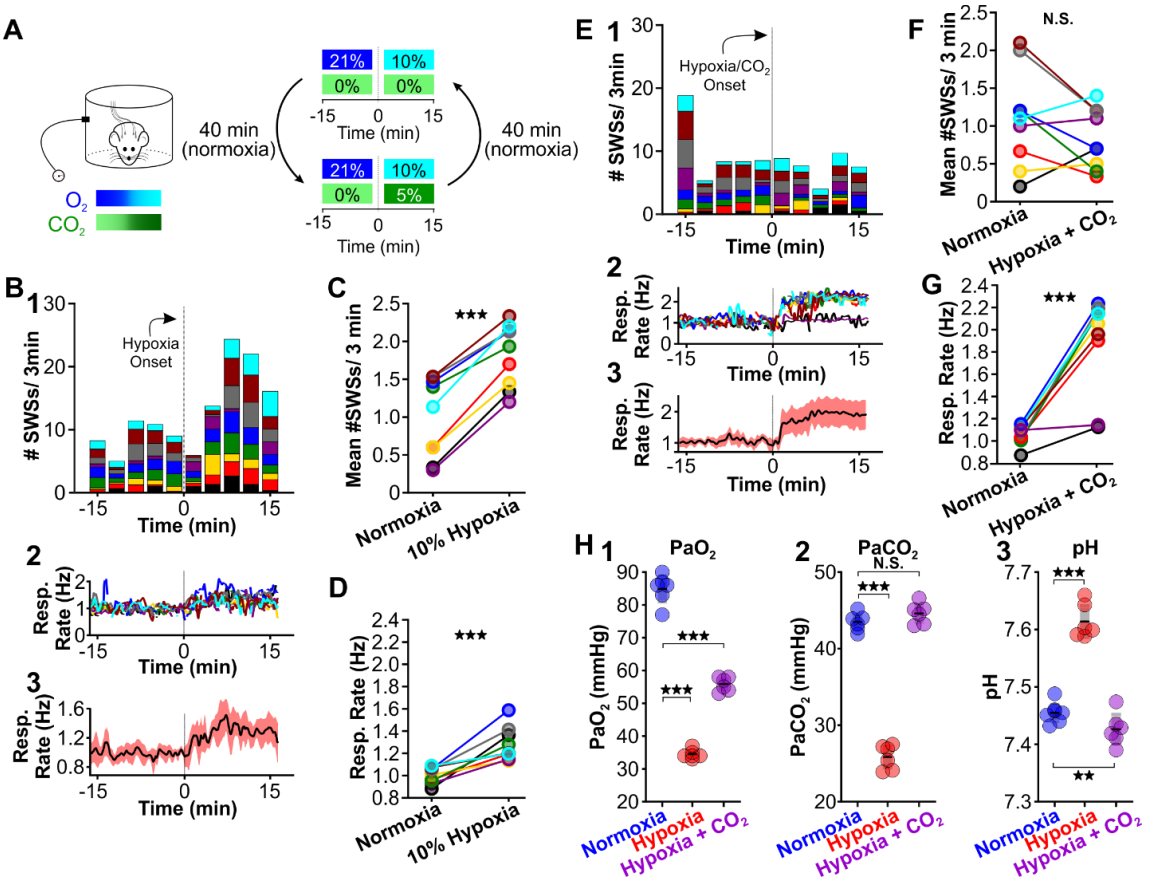

Figure 3. Supplemental CO_2 suppresses hypoxia-provoked spike-wave seizures.

(A) Experimental approach. Plethysmography chambers recorded ventilation and ECoG/EMG signals in WAG/Rij rats exposed to normoxia (i.e., 21% O_2) and then alternately challenged with hypoxia (i.e., 10% O_2) or hypoxia + CO_2, (i.e., 10% O_2, 5% CO_2). (B-D) Hypoxia challenge. **(B)** Spike-wave seizure (SWS) and respiration quantification. (1) Stacked histogram illustrating spike-wave seizure count for each animal before and after the onset of hypoxia. (2) Corresponding respiratory rate for each animal shown in panel B1. (3) Mean respiratory rate for all animals. **(C)** Mean spike-wave seizure count per bin and **(D)** respiratory rate before and after hypoxia exchange. **(E-G)** Hypoxia + CO_2 challenge. **(E)** SWS and respiration quantification. (1) Stacked histogram illustrating spike-wave seizure count for each animal before and after the onset of hypoxia + CO_2. (2)

Corresponding respiratory rate for each animal shown in panel E1. (3) Mean respiratory rate for all animals. **(F)** Mean spike-wave seizure count per bin and **(G)** respiratory rate before after hypoxia + CO_2 exchange. **(H)** Arterial measurements in the same rats show that hypoxia produced a predictable drop in arterial (1) O_2 and (2) CO_2, as well as (3) respiratory alkalosis (as in Wistar rats). Supplementing the chamber with 5% CO_2 normalizes arterial CO_2 and pH. Elevated arterial O_2 during hypoxia + CO_2 relative to hypoxia reflects a powerful inhalation response during the former condition (c.f., panels D and G). See Tables 1, 2 and 4 for detailed statistics. **p<0.01, ***p < 0.001.

Next, we tested whether supplementing normoxia with 5% CO_2 is sufficient to reduce spike-wave seizure counts. Respiration during high CO_2 causes hypercapnia, a condition that increases blood $PaCO_2$ and acidifies the blood (Eldridge et al., 1984). As with hypoxia, hypercapnia also triggers hyperventilation (Guyenet et al., 2019). We performed ECoG/plethysmography experiments in rats that cycled through trials of normoxia and hypercapnia (21% O_2; 5% CO_2; 74% N_2) and compared the mean number of seizures observed during the two conditions. Relative to normoxia, the number of spike-wave seizures was lower during 5% CO_2 ($p = 0.0028$, $n = 8$; Figs. 4B1 and 4C); hypercapnia also induced a powerful respiratory response ($p = 3.78 \times 10\text{-}5$, $n = 8$; Figs. 4B2, 3 and 4D). Blood gas measurements revealed that 5% hypercapnia increased $PaCO_2$ ($p = 0.022$, $n = 6$; Fig. 4E2) and slightly acidified blood pH ($p = 0.00063$, $n = 6$; Figure 4E3). These results provide further support for the hypothesis that the neural circuits that produce spike-wave seizures are CO_2-sensitive, and thus pH-sensitive. Moreover, the results demonstrate that neither the mechanics of elevated ventilation, nor increased arousal, is sufficient to provoke spike-wave seizures.

Optogenetic stimulation of the retrotrapezoid nucleus provokes spike-wave seizures

In addition to inducing hyperventilation and hypocapnia, hypoxia also lowers PaO_2 (see Fig. 3H1), an effect that stimulates the carotid body, the principal peripheral chemoreceptor that initiates hyperventilation during hypoxic conditions (Lindsey et al., 2018; López-Barneo et al., 2016; Semenza & Prabhakar, 2018). Carotid body activity recruits neurons of the nucleus tractus solitarius (NTS) that then excite neurons of the central respiratory pattern generator to drive a respiratory response (Guyenet, 2014; López-Barneo et al., 2016).

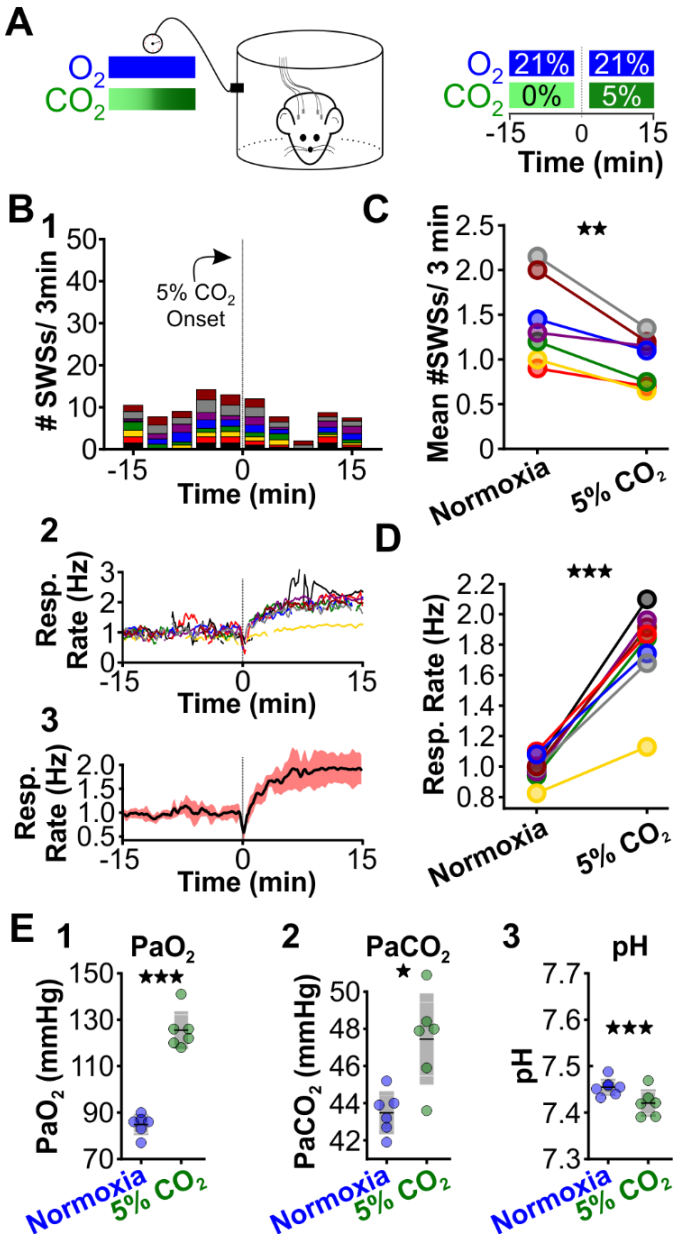

Figure 4. Supplemental CO_2 suppresses spontaneous spike-wave seizures.

(A) Experimental approach. Plethysmography chambers recorded ventilation and ECoG/EMG signals in WAG/Rij rats exposed to normoxia (i.e., 21% O_2) and hypercapnia (i.e., 21% O_2, 5% CO_2). **(B)** Spike-wave seizure (SWS) and respiratory quantification. (1) Stacked histogram illustrating spike-wave seizure count for each animal before and after the onset of hypercapnia. (2) Corresponding respiratory rate for each animal shown in panel B1. (3) Mean respiratory rate for all animals. **(C)** Mean spike-wave seizure count

per bin and **(D)** respiratory rate before and after hypercapnia exchange. **(E)** Arterial measurements in the same rats show that hypercapnia produced a predictable increase in arterial (1) O_2 and (2) CO_2, as well as (3) respiratory acidosis. Increase arterial O_2 reflects robust ventilatory response during hypercapnia. See Tables 1, 2 and 4 for detailed statistics. *$p < 0.05$, **$p < 0.01$, ***$p < 0.001$.

To evaluate the capacity of hyperventilation to provoke seizures in the absence of hypoxia (and, therefore, in the absence of carotid body activation), we utilized an alternative approach to induce hyperventilation. Under physiological conditions, chemosensitive neurons of the retrotrapezoid nucleus (RTN), a brainstem respiratory center, are activated during an increase in $PaCO_2$ and a consequent drop in arterial pH (Guyenet et al., 2016, 2019; Guyenet & Bayliss, 2015) that then stimulate respiration. Optogenetic activation of RTN neurons in normoxia is sufficient to evoke a powerful hyperventilatory response that alkalizes the blood (Abbott et al., 2011; Souza et al., 2020). Importantly, PaO_2 remains stable (or is slightly elevated) during optogenetically-induced respiration. Therefore, hyperventilation evoked by optogenetic RTN activation during normoxia both (1) promotes respiratory alkalosis without hypoxia and (2) is a more clinically relevant approximation of voluntary hyperventilation than hypoxia-induced hyperventilation.

We selectively transduced RTN neurons of WAG/Rij rats with a lentiviral approach using the PRSX8 promoter to drive channelrhodopsin expression (Abbott et al., 2009; Hwang et al., 2001; Lonergan et al., 2005). Once channelrhodopsin was expressed, we challenged rats with two test trials: RTN photostimulation during normoxia and RTN photostimulation during hypercapnia (Fig. 5A); in a subset of animals, we cycled rats between the two conditions. In both trials, the laser was pulsed at 20 Hz (10msec pulse) once every four seconds for two seconds. Laser stimulation during normoxia provoked spike-wave seizures ($p = 0.002$; $n = 10$; Figs. 5B, 5C1 and 5D) and also increased ventilation ($p = 0.019$; $n = 10$; Figs. 5C2, 3 and 5E). In contrast, laser stimulation during hypercapnia in the same animals did not alter spike-wave seizure count ($p = 0.86$; $n = 6$; Figs. 5F1 and 5G), despite the induction of a strong hyperventilatory response ($p = 0.031$; $n = 6$; Fig. 5F2, 3 and 5H). In sum, these results support the hypothesis that

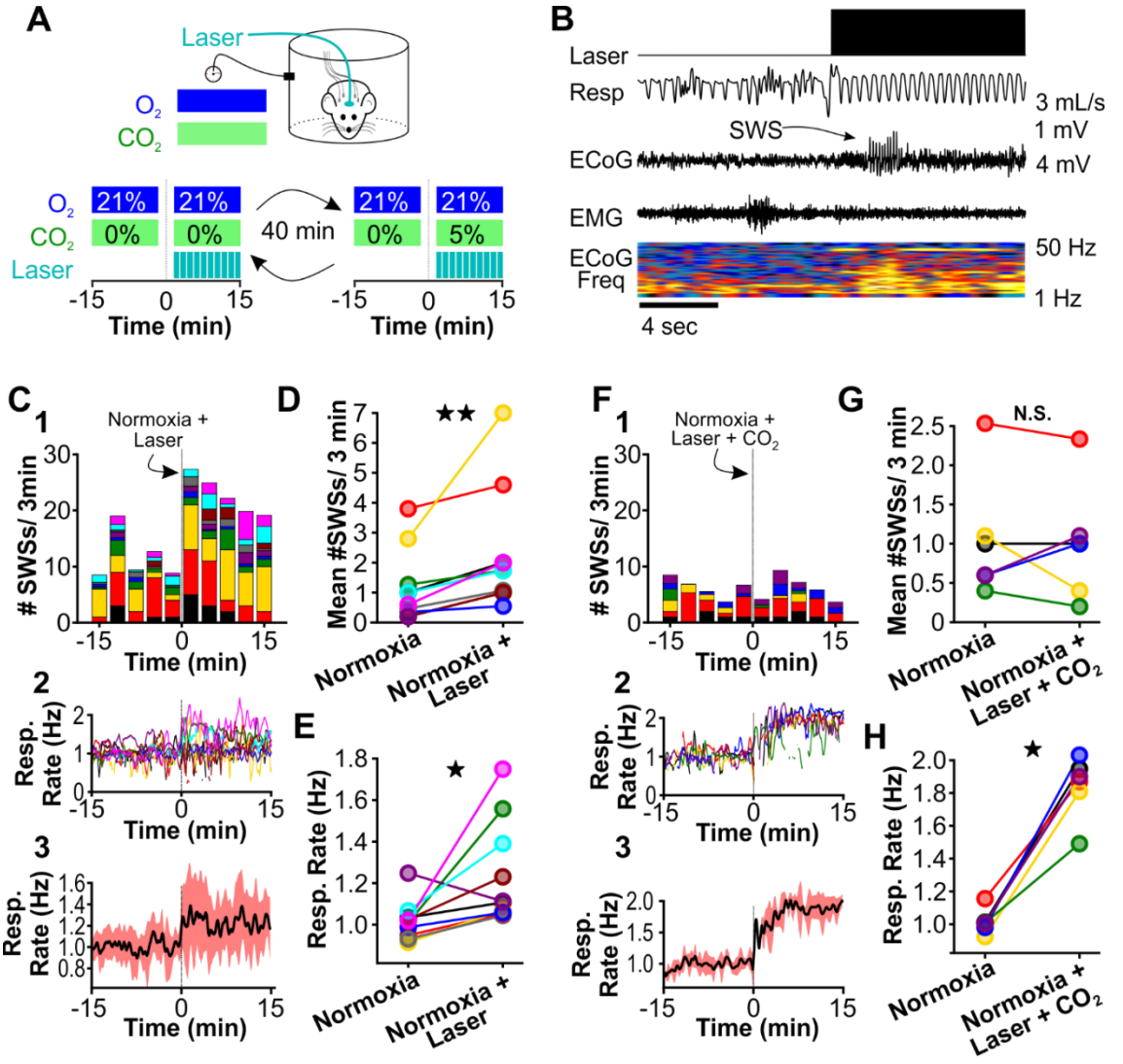

Figure 5. Normoxic hyperventilation provokes CO_2-sensitive spike-wave seizures.

(A) Experimental approach. Plethysmography chambers recorded ventilation and ECoG/EMG signals in WAG/Rij rats exposed to normoxia (i.e., 21% O_2) and normoxia + CO_2, (i.e., 10% O_2, 5% CO_2). Channelrhodopsin-mediated photostimulation of the retrotrapezoid nucleus (RTN) was used to increase ventilation. **(B)** Example of ventilatory response and spike-wave seizure during normoxic RTN photostimulation (C-E) RTN photostimulation during normoxia. **(C)** Spike-wave seizure (SWS) and respiration quantification. (1) Stacked histogram illustrating spike-wave seizure count for each animal before and after normoxia photostimulation onset. (2) Corresponding respiratory rate for

each animal shown in panel C1. (3) Mean respiratory rate for all animals. **(D)** Mean spike-wave seizure count per bin and **(E)** respiration rate before and after normoxia photostimulation onset. **(F-H)** RTN photostimulation during hypercapnia (i.e., 21% O_2, 5% CO_2). **(F)** Spike-wave seizure and respiratory quantification. (1) Stacked histogram illustrating spike-wave seizure count for each animal before and after hypercapnic photostimulation onset. (2) Corresponding respiratory rate for each animal shown in panel F1. (3) Mean respiratory rate for all animals. **(G)** Mean spike-wave seizure count per bin and **(H)** respiratory rate before and after hypercapnic photostimulation onset. See Tables 1, 2 and 4 for detailed statistics. *$p < 0.05$, **$p < 0.01$, not significant (n.s.).

respiratory alkalosis is necessary to provoke seizures during hyperventilation and excludes carotid body activation as a contributing factor.

Hypoxia-induced hyperventilation activates neurons of the intralaminar thalamus

Thus far, our results demonstrated that respiratory alkalosis (i.e., hyperventilation that promotes a net decrease in $PaCO_2$) provokes spike-wave seizures in the WAG/Rij rat. Next, we sought to identify brain structures activated during respiratory alkalosis that may contribute to spike-wave seizure provocation. We used the neuronal activity marker cFos to identify such structures in WAG/Rij rats. To isolate activation specifically associated with respiratory alkalosis, we first administered ethosuximide (200mg/kg, i.p.) to suppress spike-wave seizures; respiration and ECoG/EMG signals confirmed ventilatory responses and spike-wave seizure suppression. Ethosuximide-injected rats were exposed to either hypoxia, normoxia or hypoxia/hypercapnia for 30 minutes and then transcardially perfused 90 minutes later. Brains were harvested and evaluated for cFos immunoreactivity. Surprisingly, in rats exposed to hypoxia we observed heightened immunoreactivity in the intralaminar nuclei, a group of higher-order thalamic nuclei that, unlike first-order thalamic nuclei, do not receive peripheral sensory information (Saalmann, 2014) (Figs. 6A, B). Indeed, cFos immunoreactivity was largely absent from first-order thalamic nuclei and cortex, and was blunted in rats treated with normoxia and hypoxia/hypercapnia (Fig. 6B). Importantly, the latter condition elevates respiration but normalizes arterial pH (see Figs. 3G-H). Immunoreactivity quantification revealed that the number of cFos-positive cells within the intralaminar thalamic nuclei was highest following hypoxia [ANOVA: $F(2, 6) = 31.59$, $p = 0.00019$, Fig. 6C].

As heightened cFos immunoreactivity was observed primarily following hypoxia that results in pronounced respiratory alkalosis, we next tested the hypothesis that

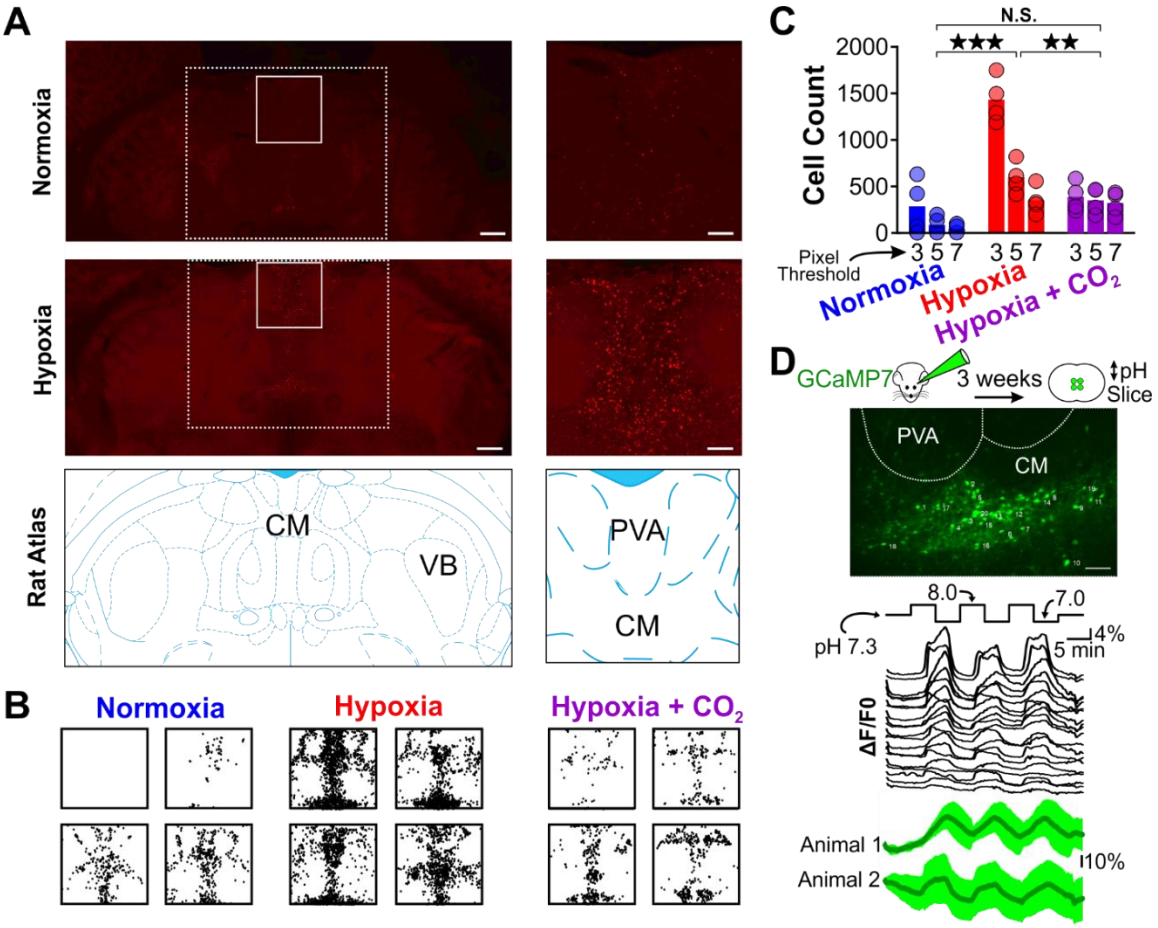

Figure 6. Hypoxia-induced hyperventilation activates intralaminar thalamic neurons. (A) cFos immunohistochemistry in horizontal sections of the WAG/Rij rat. Dashed lines highlight the medial region of the thalamus containing the intralaminar nuclei. Solid lines demarcate regions containing elevated cFos expression and are expanded on right. Top images are collected from a rat exposed to 30 minutes of normoxia. Middle images are collected from a rat exposed to 30 minutes of hypoxia. Bottom images are taken from Paxinos and Watson (Paxinos & Watson, 2007) and show the structural landmarks in the top and middle images. The central median nucleus (CM, intralaminar thalamus) and ventrobasal complex (VB, first-order thalamus) are labeled. **(B)** cFos density plots show immunoreactivity in each of four rats exposed to either normoxia, hypoxia or hypoxia + CO_2. Each black dot represents a cFos-positive cell, as identified with ImageJ (see Methods). Plots are aligned to expanded views in panel A. **(C)**

Quantification of cFos labeled cells at different ImageJ thresholding values. **(D)** GCaMP7 was stereotaxically delivered to the intralaminar nuclei. Later, fluorescence changes were measured during extracellular alkaline challenges in acute slices containing the intralaminar nuclei. Individual ROIs show fluorescence changes during alkalosis (black traces). Mean responses from two animals are shown in green. $^{**}p < 0.01$, $^{***}p < 0.001$. See Table 5 for detailed statistics. Scale bars are 500 µm (left) and 100 µm (right).

neurons of the intralaminar nuclei are pH-sensitive. We stereotaxically delivered the pan-neuronal expressing GCaMP7s (pGP-AAV-syn-jGCaMP7s-WPRE) to the intralaminar nuclei and harvested acute brain sections three weeks later (Fig. 6D). Recording fluorescence changes in brain sections revealed that extracellular alkalosis quickly and reversibly activated neurons of the intralaminar nuclei (Fig. 6D). Collectively, these results support the hypothesis that respiratory alkalosis activates pH-sensitive neurons of the intralaminar thalamic nuclei in the WAG/Rij rat.

Discussion

Hyperventilation-provoked seizures associated with absence epilepsy were first formally described in 1928 by William Lennox (Lennox, 1928) and despite the clinical ubiquity of utilizing hyperventilation to diagnose the common form of childhood epilepsy, no animal studies have attempted to resolve the physiological events that enable hyperventilation to reliably provoke spike-wave seizures. To resolve events and relevant brain structures recruited during this phenomenon, we first utilized the WAG/Rij rat to establish a rodent model that mimics hyperventilation-provoked spike-wave seizures in humans. With this model, we show that hyperventilation only provokes spike-wave seizures in seizure-prone, not generally seizure-free, rats. We then show that supplemental CO_2, by mitigating respiratory alkalosis, suppresses spike-wave seizures triggered by hyperventilation during either hypoxia or direct activation of brainstem respiratory centers. Moreover, supplemental CO_2, by producing respiratory acidosis, suppresses spontaneous spike-wave seizures (i.e., those occurring during normoxia) despite a compensatory increase in respiratory rate. These data demonstrate that spike-wave seizures are yoked to arterial CO_2/pH. Finally, we demonstrate that respiratory alkalosis activates neurons of the intralaminar thalamic nuclei, also in a CO_2-dependent manner; activation of these neurons is also pH-sensitive. With these observations, we

propose a working model wherein respiratory alkalosis activates pH-sensitive neurons of the intralaminar nuclei that in turn engage seizure-generating neural circuits to produce spike-wave seizures (Figure 7).

Cortical EEG Patterns Evoked by Hyperventilation

Hyperventilation produces stereotypical EEG patterns in both healthy children and children with absence epilepsy (Barker et al., 2012). In healthy children, hyperventilation can evoke an EEG pattern known *as Hyperventilation-Induced, High-Amplitude Rhythmic Slowing* (HIHARS) that is often associated with altered awareness (Barker et al., 2012; Lum et al., 2002). Electrographically, HIHARS is distinct from spike-wave seizures insofar the EEG lacks epilepsy-associated spikes and resembles slow-wave sleep. Nonetheless, similarities between HIHARS and absence seizures exist. Both events are associated with children of the same age (Mattozzi et al., 2021). Behaviorally, eye opening/staring and fluttering, as well as oral automatisms, are observed during both events, albeit with different frequencies (Lum et al., 2002). Finally, the mean latencies from the onset of hyperventilation to the onset of electrographic HIHARS in healthy children, or spike-wave seizures in absence patients, are also similar (Lum et al., 2002; Mattozzi et al., 2021).
Recent work suggests that spike-wave seizures may limit or preclude the generation of HIHARs in children with absence epilepsy, thereby supporting the hypothesis that HIHARS and spike-wave seizures borrow from similar neural circuit mechanisms (Mattozzi et al., 2021). In this model, hyperventilation engages brain structures that initiate and/or support widespread, synchronous cortical activity. However, the trajectory of this engagement ultimately bifurcates such that either HIHARS or a spike-wave seizure is produced, but not both. When viewed alongside work performed in the 1960s by Ira Sherwin (Sherwin, 1965, 1967), our results support this model. Sherwin demonstrated that hyperventilation evokes HIHARS in cats (Sherwin, 1965), and that the stereotyped EEG

pattern requires an intact central lateral nucleus of the thalamus (Sherwin, 1967). Together with the central medial (CM) and paracentral thalamic nuclei, the central lateral nucleus belongs to the anterior group of the intralaminar nuclei (Saalmann, 2014), the location of cFos immunoreactivity associated with respiratory alkalosis and pH-sensitivity (Figure 6). Indeed, at the time Sherwin postulated that the intralaminar nuclei of the thalamus are both chemoreceptive and capable of engaging widespread cortical activity (Sherwin, 1967). We now postulate that these nuclei are also instrumental for provoking spike-wave seizures during hyperventilation. If true, then resolving how and where the mechanisms that produce HIHARS diverge from those that produce spike-wave seizures becomes a central goal.

Thalamocortical circuit involvement in spike-wave seizures

Decades of work have culminated in a canonical model wherein interconnected circuits between the cortex and thalamus support the initiation and maintenance of generalized spike-wave seizures (Avoli, 2012; Beenhakker & Huguenard, 2009; Huguenard & McCormick, 2007; McCafferty et al., 2018; McCormick & Contreras, 2001; Meeren et al., 2002). By recording from multiple sites in the WAG/Rij rat, Meeren et al. (Meeren et al., 2002) concluded that the peri-oral region of somatosensory cortex provides the bout of hypersynchronous activity that initiates a spike-wave seizure. This activity then rapidly recruits additional somatosensory cortices and the lateral dorsal thalamus, a higher-order thalamic nucleus involved in spatial learning and memory (Bezdudnaya & Keller, 2008). Finally, first-order thalamic nuclei that encode somatosensory information (i.e., the ventrobasal complex) are recruited. This stereotyped succession of events occurs within the first 500 milliseconds of the spike-wave seizure, after which the temporal relationships among cortical and thalamic structures are more unpredictable (Meeren et al., 2002). Additional studies support the hypothesis that cortical hyperactivity initiates

spike-wave seizures (Pinault, 2003; Pinault et al., 1998) and have motivated what is generally referred to as the cortical focus theory for spike-wave seizure initiation (Meeren et al., 2005).

While resolving how seizures initiate and propagate through brain structures is of critical importance, this understanding does not necessarily address the mechanisms that drive the highly rhythmic and hypersynchronous activity associated with ongoing spike-wave seizures. Extensive work on acute brain slice preparations clearly demonstrates that circuits between first-order thalamic nuclei and the reticular thalamic nucleus are sufficient to sustain rhythmic network activities, including those comparable to absence seizures (Bal et al., 1995; Bal & McCormick, 1993; McCormick & Contreras, 2001; von Krosigk et al., 1993). In this model, feedforward inhibition provided by reticular neurons evokes robust, hypersynchronous post-inhibitory rebound bursts among thalamocortical neurons that then relay activity back to reticular thalamus and to cortex. Reticular neuron-mediated feedforward inhibition of thalamocortical neurons, coupled with reciprocal excitation from thalamocortical neurons to reticular neurons, forms the basis of a rhythmogenic circuit that is proposed to maintain spike-wave seizures. While this model very likely accounts for rhythmicity in the acute brain slice preparation, it is becoming less clear how first-order thalamocortical neurons actively contribute to the maintenance of spike-wave seizures recorded in vivo (Huguenard, 2019; McCafferty et al., 2018). Moreover, most current models of spike-wave initiation and maintenance neglect the potential contribution of the intralaminar nuclei to seizure initiation and maintenance despite several observations to the contrary.

In an effort to resolve structures capable of evoking spike-wave seizures, Jasper and colleagues electrically stimulated several thalamic nuclei in cats while recording EEG. By doing so in both lightly anesthetized (Jasper & Droogleever-Fortuyn, 1947) and unanesthetized (Hunter & Jasper, 1949) animals, the authors concluded that stimulation

of the anterior intralaminar nuclei (i.e., central lateral, central medial and paracentral nuclei) was sufficient to evoke spike-wave seizures that outlasted the stimulus; stimulation also produced behavioral repertoires associated with absence seizures. However, stimulation of first-order thalamic nuclei did not evoke spike-wave seizures, nor did it evoke seizure-like behaviors. Consistent with these observations, lesions to the intralaminar nuclei abolish pharmacologically-induced spike-wave seizures in Sprague-Dawley rats (Banerjee & Snead, 1994); seizures persist following lesions to first-order nuclei. More recently, an EEG-fMRI study in human patients also implicates the intralaminar nuclei in the initiation of spontaneous spike-wave seizures (Tyvaert et al., 2009). Regrettably, Meeren et al. (Meeren et al., 2002) did not include intralaminar thalamic recordings during their study of spike-wave seizure propagation in the WAG/Rij rat. Nonetheless, proposing the hypothesis that the intralaminar nuclei, not cortical structures, initiate spike-wave seizures, including those occurring spontaneously (i.e., not during hyperventilation), seems premature. Indeed, the possibility that activation of cortically projecting intralaminar neurons during hyperventilation recruits cortical structures to, in turn, initiate spike-wave seizures is equally plausible (see Figure 7).

Thalamic pH sensitivity

First-order thalamic neurons express several pH-sensitive ion channels and receptors. TASK-1 and TASK-3, two TWIK-related acid-sensitive potassium channels, with the hyperpolarization-activated cyclic nucleotide–gated (HCN) ion channel, collectively play a critical role in stabilizing the resting membrane potential of first-order

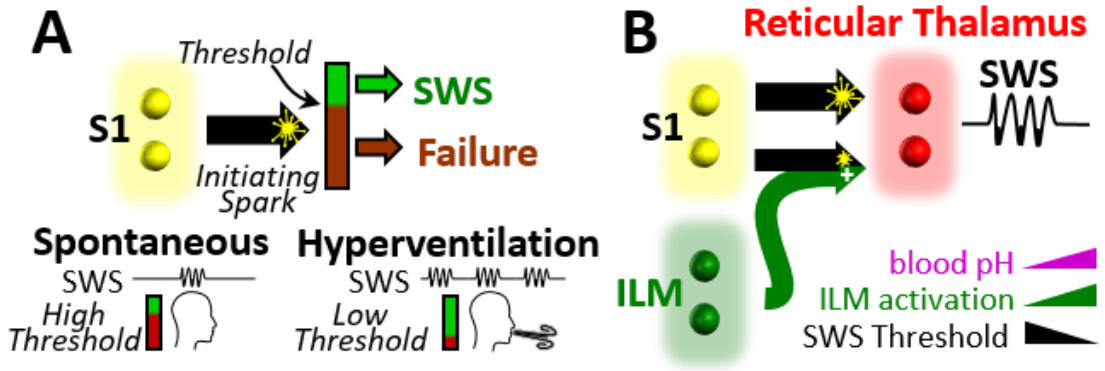

Figure 7. Working model. (A) Spike-wave seizures only occur if initiating activity from S1 somatosensory cortex successfully overcomes a threshold, consistent with the cortical focus theory (H. K. M. Meeren et al., 2002). Hyperventilation-associated alkalosis reduces spike-wave seizure (SWS) threshold. **(B)** S1 initiating activity is proposed to overcome a seizure node formed by circuits in reticular thalamus to generate an spike-wave seizure (Paz & Huguenard, 2015). We propose that hyperventilation-evoked respiratory alkalosis activates the intralaminar nuclei (ILM) to reduce the threshold for S1 activity required to evoke a spike-wave seizure.

thalamic neurons (Meuth et al., 2003, 2006). When activated, TASK channels hyperpolarize the membrane potential of thalamocortical neurons. In contrast, HCN channels depolarize thalamocortical neuron membrane potential. As extracellular acidification inhibits the activity of both channels, the opposing actions of TASK and HCN channels are simultaneously downregulated to yield no net effect on thalamocortical neuron membrane potential (Meuth et al., 2006), thereby stabilizing the membrane potential during acidic conditions. While not yet directly tested, the opposing actions of TASK and HCN channels also presumably stabilize thalamocortical membrane potential during alkaline conditions. Thus, while first-order thalamocortical neurons express pH-sensitive ion channels, these neurons are presumed to maintain stable membrane potentials during extracellular pH fluctuations. If true, then first-order thalamic nuclei are unlikely to support an active role in initiating hyperventilation-provoked spike-wave seizures. The extent to which higher-order thalamic nuclei express TASK and HCN channels remains unknown.

Importantly, intralaminar neurons recruited during hyperventilation-mediated alkalosis may not reflect intrinsic pH sensitivity. Instead, activation of intralaminar neurons during alkalosis may result from increased excitatory synaptic input. Intralaminar neurons receive significant, monosynaptic excitation from the midbrain reticular formation (Ropert & Steriade, 1981; Steriade & Glenn, 1982); first-order thalamic nuclei only do so negligibly (Edwards & de Olmos, 1976). Several reticular nuclei are critically important for respiration (Guyenet & Bayliss, 2015; Smith et al., 2013) and therefore provide clear rationale for testing the hypothesis that reticular-mediated excitation of the intralaminar nuclei drive hyperventilation-associated cFos expression (i.e., Figure 6). Notably, cFos expression was only observed during respiratory alkalosis (i.e., hypoxia) and not during hyperventilation associated with a normalized arterial pH (i.e., hypoxia-hypercapnia; c.f. Figs. 3H and 6B). Thus, if reticular-mediated excitation of intralaminar neurons plays a

role in hyperventilation-provoked spike-wave seizures, then it does so only during conditions of respiratory alkalosis. Finally, the possibility that the synaptic terminals of intralaminar-projecting afferents are pH-sensitive also warrants examination. Notably, solute carrier family transporters (SLC) shuttle H^+ and HCO_3^+ across neuronal membranes and are proposed to regulate seizures, including spike-wave seizures (Cox et al., 1997; Sander et al., 2002; Sinning & Hübner, 2013). Alkaline conditions enhance excitatory synaptic transmission, an effect attributed to Slc4a8, a Na^+-Driven Cl-/Bicarbonate Exchanger (Sinning et al., 2011; Sinning & Hübner, 2013), that is expressed in the presynaptic terminals of excitatory neurons, including those in the thalamus (Lein et al., 2007). Thus, the potentiation of intralaminar neuron excitation remains a plausible candidate mechanism to explain the observed cFos expression during respiratory alkalosis.

Conclusion

In aggregate, our data support the hypothesis that spike-wave seizures are yoked to arterial pH. The observation that respiratory alkalosis activates intralaminar thalamic neurons, and that such neurons are activated by alkaline conditions, reignites a 70-year-old hypothesis wherein intralaminar neurons actively participate in the initiation and maintenance of spike-wave seizures.

Materials and Methods

Study Design

The goal of this study was to parameterize the effect of blood gases on spike-wave seizures. To do so, we adapted a clinically observed human phenomenon in absence epilepsy patients to a rodent model of spike-wave seizures. We demonstrate that spike-wave seizure occurrence correlates with rising or falling values of $PaCO_2$ and pH.

Significantly, we show that neurons of the midline thalamus become activated after brief exposure to low $PaCO_2$ conditions. We propose that activity among pH-sensitive neurons in the thalamus, responsive to hyperventilation-induced hypocapnia, trigger spike-wave seizures. All physiology and ECoG/EMG recordings were performed in freely behaving WAG/Rij or Wistar rats. To reduce the number of animals, rats were exposed to multiple conditions. Experimenters were blinded to the condition for all respiration and ECoG/EMG data analysis. Group and sample size were indicated in the results section.

Animals

All procedures conformed to the National Institutes of Health Guide for Care and Use of Laboratory Animals and were approved by the University of Virginia Animal Care and Use Committee (Charlottesville, VA, USA). Unless otherwise stated, animals were housed at 23-25°C under an artificial 12 h light-dark cycle with food and water ad libitum. A colony of Wistar Albino Glaxo/from Rijswik (WAG/Rij rats) were kindly provided by Dr. Edward Bertram, University of Virginia) and maintained in the animal facilities at The University of Virginia Medical Center. Male Wistar IGS Rats were purchased from Charles River (Strain Code: #003). Plethysmography, EEG, blood gas measurements and cFos immunohistochemistry experiments were performed in 100+-day old WAG/Rij and Wistar rats as these ages correspond to when spike-wave seizures become robust in the WAG/Rij rat. Male and female rats were used in all experiments – no noticeable differences were observed. Of note, only male rats were used in optogenetic manipulations, as female rats were less likely to recover from surgery.

Animal Preparation

All surgical procedures were conducted under aseptic conditions. Body temperature was maintained at 37°C. Animals were anesthetized with 1-3% isoflurane or

a mixture of ketamine (75 mg/kg), xylazine (5 mg/kg) and acepromazine (1 mg/kg) administered intra-muscularly. Depth of anesthesia was monitored by lack of reflex response to a firm toe and tail pinch. Additional anesthetic was administered during surgery (25% of original dose) if warranted. All surgeries, except the arterial catheter implantation, were performed on a stereotaxic frame (David Kopf Instruments, Tujunga, CA, USA). Post-operative antibiotic (ampicillin, 125 mg/kg) and analgesia (ketoprofen, 3-5 mg/kg, subcutaneously) were administered and as needed for 3 days. Animals recovered for 1-4 weeks before experimentation.

Electrocorticogram (ECoG) and electromyography (EMG) electrode implantation

Commercially available rat recording devices were purchased from Plastics One (Roanoke, VA, USA). Recording electrodes were fabricated by soldering insulated stainless-steel wire (A-M system, Sequim, WA, USA) to stainless-steel screws (Plastics One) and gold pins (Plastics One). On the day of surgery, a small longitudinal incision was made along the scalp. Small burr holes were drilled in the skill and ECoG recording electrodes were implanted bilaterally in the cortex. Reference electrodes were placed in the cerebellum. A twisted-looped stainless-steel wire was sutured to the superficial neck muscles for EMG recordings. The recording device was secured to the skull with dental cement and incisions were closed with absorbable sutures and/or steel clips.

PRSX-8 lentivirus preparation

The lentivirus, PRSX8-hCHR2(H134R)-mCherry, was designed and prepared as described previously (Abbott et al., 2009). Lentivirus vectors were produced by the Salk Institute Viral Vector Core. The titer for the PRSX8-hCHR2(H134R)-mCherry lentivirus was diluted to a working concentration of 1.5 x 1010 TU/mL. The same batch of virus was used for all experiments included in this study.

Virus injection and fiber optic ferrule implantation

Borosilicate glass pipettes were pulled to an external tip diameter of 25 μm and backfilled with the lentivirus, PRSX8-hCHR2(H134R)-mCherry. Unilateral virus injections in the RTN were made under electrophysiological guidance of the antidromic potential of the facial nucleus (see Abbott et al., 2009; Souza et al., 2018). A total of 400 nL was delivered at three rostro caudal sites separated by 200 or 300 μm in the RTN. Illumination of the RTN was performed by placing a 200-μm-diameter fiber optic (Thor Labs, #BFL37-200; Newton, NJ, USA) and ferrule (Thor Labs, #CFX128-10) vertically through the cerebellum between 300-1000 μm dorsal to RTN ChR2-expressing neurons. These animals were also implanted with ECoG/EMG recording electrodes, as detailed above. All hardware was secured to the skill with dental cement. Animals recovered for 4 weeks, as this provided sufficient time for lentivirus expression in the RTN. Virus injection location was verified post-hoc. Only animals that responded to optical stimulation, demonstrated by an increase in respiratory frequency, were included in the results.

Physiology experiments in freely behaving rats

All experiments were performed during the dark cycle (hours 0-4) at ambient room temperature of 27°C-28°C. Rats were habituated to experimental conditions for a minimum of 4 hours, 1-2 d before experiment start. On the day of recordings, rats were briefly anesthetized with 3% isoflurane for < 5min to connect the ECoG/EMG recording head stage to a recording cable and, when necessary, to connect the fiber optic ferrule to a fiber optic cord (multimode 200 μm core, 0.39 nA) attached to a 473 nm blue laser (CrystaLaser model BC-273-060-M, Reno, NV, USA). Laser power was set to 14mW measured at the junction between the connecting fiber and the rat. Rats were then placed

immediately into a whole-body plethysmography chamber (5L, EMKA Technologies, Falls Church, VA, USA). Recordings began after 1 h of habituation. The plethysmography chamber was continuously perfused with room air or protocols cycling through specific gas mixtures of O_2, N_2 and CO_2 (total flow: 1.5 L/min). Mass flow controllers, operated by a custom-written Python script, regulated gas exchange. Respiratory flow was recorded with a differential pressure transducer. The respiratory signal was filtered and amplified at 0.1-100 Hz, X 500 (EMKA Technologies). Respiratory signals were digitized at 200 Hz (CED Instruments, Power1401, Cambridge, England). ECoG and EMG signals were amplified (X1000, Harvard Apparatus, Holliston, MA, USA; Model 1700 Differential Amplifier, A-M Systems), bandpass filtered (ECoG: 0.1-100 Hz; EMG: 100-300 Hz) and digitized at 200 Hz. Respiratory flow, ECoG/EMG recordings, O_2 flow and the laser pulse protocol were captured using Spike2, 7.03 software (CED Instruments). Spike-wave seizure occurrence before and during specific conditions is shown as a peri-stimulus time histogram aligned at time = 0 at gas exchange onset or laser-on for optogenetic stimulations. Spike-wave seizure counts were quantified in 3 bins beginning +/- 15 minutes of gas exchange or laser onset. Total spike-wave seizure counts were obtained by summing the number of spike-wave seizures between -15 and 0 minutes (control) and 0 and +15 minutes (manipulation). Respiratory frequency (fR, in breaths/minute) was derived from the respiration trace. The respiration trace was divided into individual windows, each 10 seconds in duration, and a fast Fourier transform (FFT) was computed on each discrete window. The respiratory rate for each window was defined by the FFT frequency with the maximal power density. Once derived for each window, we then applied a 30-second moving average to smooth the trace. RTN neurons were optically stimulated with 10 ms pulses delivered at 20 Hz for 2 seconds, followed by 2 seconds rest. This stimulation protocol was repeated for 20 minutes.

Femoral artery catheterization, blood gases and pH measurements.

Arterial blood samples for blood gas measurements through an arterial catheter during physiological experiments. One day prior to the experiments, rats anesthetized with isoflurane (2% in pure O_2) and a polyethylene catheter (P-10 to P-50, Clay Adams, Parsippany, NJ, USA) was introduced into the femoral artery by a small skin incision towards the abdominal aorta. The catheter was then tunneled under the skin and exteriorized between the scapulae with two inches of exposed tubing anchored with a suture. On the day of the experiment, animals were briefly anesthetized with 1-2% isoflurane to attach tubing for blood collection before placement into the plethysmography recording chamber. Arterial blood gases and pH were measured using a hand-held iStat configured with CG8+ cartridges (Abbott Instruments, Lake Bluff, USA).

cFos Histology

After exposing WAG/Rij rats to 30 minutes of hypoxia (10% O_2; 90% N_2) or hypoxia/hypercapnia (10% O_2; 5% CO_2; 75% N_2) rats were deeply anesthetized and perfused transcardially with 4% paraformaldehyde (pH 7.4). Brains were removed and post-fixed for 12-16 h at 4 °C. 40µm horizontal sections of the thalamus (D/V depth -5.3 mm to 6.0 mm) were obtained using a Leica VT 1000S microtome (Leica Biostystems, Buffalo Grove, IL, USA) and collected in 0.1 M phosphate buffer (PB) with 0.1% sodium azide (Millipore-Sigma, St. Louis, MO, USA). Sections were then transferred to a 0.1M PB solution containing 20% sucrose for 1hr, snap-frozen and transferred to 0.1% sodium borohydride for 15 minutes. Slices were washed 2x in phosphate buffered saline (PBS). All blocking and antibody solutions were prepared in an incubation buffer of 0.1% sodium azide, 0.5% Triton X-100 and 2% normal goat serum. Sections were blocked for 4hrs at room temperature or overnight at 4°C in incubation buffer. Sections were washed 3x with PBS between primary and secondary antibody solutions. Primary antibody solutions

containing rabbit anti-cFos (1:2000; Cell Signaling Technology Cat# 2250, RRID: AB_2247211, Danvers, MA, USA) and biotin (1:200, Jackson ImmunoResearch, West Grove, PA; RRID: AB_2340595) were prepared in incubation buffer and incubated overnight at 4°C. Sections were then incubated overnight in secondary antibody solutions containing donkey strepavidin-Cy3 (1:1000, Jackson ImmunoResearch; RRID: AB_2337244). Immunohistochemical controls were run in parallel on spare sections by omitting the primary antisera and/or the secondary antisera. Sections from each well were mounted and air-dried overnight. Slides were cover-slipped with VectaShield (VectorLabs, Burlingame, CA) with the addition of a DAPI counterstain. All images were captured with a Z1 Axio Imager (Zeiss Microscopy, Thornwood, NY, USA) with computer-driven stage (Neurolucida, software version 10; MicroBrightfield, Inc., Colchester, VT, USA). Immunological sections were examined with a 10x objective under epifluorescence (Cy3). All sections were captured with similar exposure settings. Images were stored in TIFF format and imported into ImageJ (NIH). Images were adjusted for brightness and contrast to reflect the true rendering as much as possible.

Calcium Imaging

pGP-AAV-syn-jGCaMP7s-WPRE (Addgene #104487-AAV9) was stereotaxically delivered to the central median thalamic nucleus in P20-30 rats with sterile microliter calibrated glass pipettes. A picospritzer (Picospritzer III, Parker Hannifin) was used to deliver 100-200 nL of virus. Three weeks later, animals were sacrificed and their brains harvested for acute brain slice preparation. Animals were deeply anesthetized with pentobarbital and then transcardially perfused with an ice-cold protective recovery solution containing the following (in mm): 92 NMDG, 26 $NaHCO_3$, 25 glucose, 20 HEPES, 10 $MgSO_4$, 5 Na-ascorbate, 3 Na-pyruvate, 2.5 KCl, 2 thiourea, 1.25 NaH_2PO_4, 0.5 $CaCl_2$, titrated to a pH of 7.3–7.4 with HCl (Ting et al., 2014). Horizontal slices (250 μm) containing

the intralaminar thalamic nuclei were cut in ice-cold protective recovery solution using a vibratome (VT1200, Leica Biosystems) and then transferred to protective recovery solution maintained at 32–34°C for 12 min. Brain slices were kept in room temperature artificial cerebrospinal fluid (ACSF) containing (in mm): 3 KCl, 140 NaCl, 10 HEPES, 10 Glucose, 2 $MgCl_2$, 2 $CaCl_2$. The solution was bubbled with 100% O2 and the pH was set by adding varied amounts KOH. Fluorescence signals were measured with a spinning disk confocal microscope outfitted with an sCMOS camera (ORCA-Flash4.0, Hamamatsu).

Data analysis and statistics

Statistical analyses were performed in GraphPad Prism v7 (San Diego, CA, USA). All data were tested for normality before additional statistical testing. Statistical details, including sample size, are found in the results section and corresponding supplemental tables. Either parametric or non-parametric statistical analyses were performed. A significance level was set at 0.05. Data are expressed as mean ± SEM.

Supplementary Material

Table 1. Spike-wave seizure count.

Figure	Comparison	Bin Count (Mean ± S.E.)	n	p value
1D	Normoxia Hypoxia	0.89 ± 0.12 1.73 ± 0.13	15	4.5 x 10-7
3C	Normoxia Hypoxia	0.99 ± 0.18 1.82 ± 0.14	9	1.76 x 10-6
3F	Normoxia Hypoxia + CO_2	1.09 ± 0.22 0.84 ± 0.13	9	0.18
4C	Normoxia Normoxia + CO_2	1.36 ± 0.17 0.95 ± 0.10	8	0.0028
5D	Normoxia Normoxia + Photostim.	1.17 ± 0.38 2.27 ± 0.63	10	0.002
5G	Normoxia Normoxia + Photostim. + CO_2	1.04 ± 0.32 1.01 ± 0.30	6	0.86

Table 2. Respiratory Rate.

Figure	Comparison	Resp. Rate (Hz) (Mean ± S.E.)	n	p value
1E	Normoxia Hypoxia	1.03 ± 0.02 1.33 ± 0.05	15	1.67 x 10-5
3D	Normoxia Hypoxia	1.00 ± 0.02 1.28 ± 0.05	9	6.59 x 10-4
3G	Normoxia Hypoxia + CO_2	1.06 ± 0.03 1.88 ± 0.15	9	2.71 x 10-4
4D	Normoxia Normoxia + CO_2	0.99 ± 0.03 1.78 ± 0.10	9	3.78 x 10-5
5E	Normoxia Normoxia + Photostim.	1.02 ± 0.03 1.24 ± 0.08	10	0.019
5H	Normoxia Normoxia + Photostim.+ CO_2	1.01 ± 0.03 1.84 ± 0.08	6	0.031

Table 3. Arterial measurements in Wistar rats.

Figure	Parameter	Comparison	Value	n	p value
3H1	PaO_2	Normoxia Hypoxia	84.93 ± 1.82 34.50 ± 0.56	6	6.0 x 10-6
		Normoxia Hypoxia +CO_2	84.93 ± 0.02 55.83 ± 0.87	6	0.000134
3H2	$PaCO_2$	Normoxia Hypoxia	43.48 ± 0.47 25.83 ± 0.65	6	2.1 x 10-6
		Normoxia Hypoxia +CO_2	43.48 ± 0.47 44.60 ± 0.55	6	0.42
3H3	pH	Normoxia Hypoxia	7.45 ± 0.01 7.61 ± 0.01	6	7.0 x 10-6
		Normoxia Hypoxia +CO_2	7.45 ± 0.01 7.43 ± 0.01	6	0.008
4E1	PaO_2	Normoxia 5% CO_2	84.93 ± 1.82 34.50 ± 0.56	6	0.00019
4E2	$PaCO_2$	Normoxia 5% CO_2	43.48 ± 0.47 25.83 ± 0.65	6	0.022
4E3	pH	Normoxia 5% CO_2	7.45 ± 0.01 7.42 ± 0.01	6	0.00063

Table 4. Arterial measurements in WAG/Rij rats.

Figure	Parameter	Comparison	Value	n	p value
2C1	PaO_2	Normoxia Hypoxia	83.25 ± 2.32 32.25 ± 1.25	4	0.0002
2C2	$PaCO_2$	Normoxia Hypoxia	37.0 ± 0.59 22.33 ± 0.16	4	6.6 x 10-5
2C3	pH	Normoxia Hypoxia	7.47 ± 0.01 7.63 ± 0.01	4	4.5 x 10-5

Table 5. cFos-positive cells in WAG/Rij rats.

Figure	Threshold	Comparison	Counts (Mean ± S.E.)	n	p value
6C	3	Normoxia Hypoxia	282 ± 148.2 1370 ± 137	4	1.5 x 10-7
		Normoxia Hypoxia + CO_2	282 ± 148.2 385.5 ± 78.7	4	0.55
		Hypoxia Hypoxia + CO_2	1370 ± 137 385.5 ± 78.7	4	4.3 x 10-7
	5	Normoxia Hypoxia	112.3 ± 57.1 595.3 ± 85.0	4	0.0005
		Normoxia Hypoxia + CO_2	112.3 ± 57.1 348 ± 68.9	4	0.045
		Hypoxia Hypoxia + CO_2	595.3 ± 85.0 348 ± 68.9	4	0.061
	7	Normoxia Hypoxia	57.3 ± 29.2 349 ± 75.0	4	0.021
		Normoxia Hypoxia + CO_2	57.3 ± 29.2 319.5 ± 63.1	4	0.036
		Hypoxia Hypoxia + CO_2	349 ± 75.0 319.5 ± 63.1	4	0.95

References

Abbott, S. B. G., Stornetta, R. L., Coates, M. B., & Guyenet, P. G. (2011). Phox2b-Expressing Neurons of the Parafacial Region Regulate Breathing Rate, Inspiration, and Expiration in Conscious Rats. *Journal of Neuroscience*, *31*(45), 16410–16422. https://doi.org/10.1523/JNEUROSCI.3280-11.2011

Abbott, S. B. G., Stornetta, R. L., Fortuna, M. G., Depuy, S. D., West, G. H., Harris, T. E., & Guyenet, P. G. (2009). Photostimulation of Retrotrapezoid Nucleus Phox2b-Expressing Neurons In Vivo Produces Long-Lasting Activation of Breathing in Rats. *Journal of Neuroscience*, *29*(18), 5806–5819. https://doi.org/10.1523/JNEUROSCI.1106-09.2009

Adams, D. J., & Lueders, H. (1981). Hyperventilation and 6-hour EEG recording in evaluation of absence seizures. *Neurology*, *31*(9), 1175–1177. https://doi.org/10.1212/wnl.31.9.1175

Amengual-Gual, M., Sánchez Fernández, I., & Loddenkemper, T. (2019). Patterns of epileptic seizure occurrence. *Brain Research*, *1703*, 3–12. https://doi.org/10.1016/j.brainres.2018.02.032

Avoli, M. (2012). A brief history on the oscillating roles of thalamus and cortex in absence seizures. *Epilepsia*, *53*(5), 779–789. https://doi.org/10.1111/j.1528-1167.2012.03421.x

Bal, T., & McCormick, D. A. (1993). Mechanisms of oscillatory activity in guinea-pig nucleus reticularis thalami in vitro: A mammalian pacemaker. *The Journal of Physiology*, *468*(1), 669–691. https://doi.org/10.1113/jphysiol.1993.sp019794

Bal, T., von Krosigk, M., & McCormick, D. A. (1995). Role of the ferret perigeniculate nucleus in the generation of synchronized oscillations in vitro. *The Journal of Physiology*, *483*(3), 665–685. https://doi.org/10.1113/jphysiol.1995.sp020613

Banerjee, P. K., & Snead, O. C. (1994). Thalamic mediodorsal and intralaminar nuclear lesions disrupt the generation of experimentally induced generalized absence-like seizures in rats. *Epilepsy Research*, *17*(3), 193–205. https://doi.org/10.1016/0920-1211(94)90050-7

Barker, A., Ng, J., Rittey, C. D. C., Kandler, R. H., & Mordekar, S. R. (2012). Outcome of children with hyperventilation-induced high-amplitude rhythmic slow activity with altered awareness. *Developmental Medicine and Child Neurology*, *54*(11), 1001–1005. https://doi.org/10.1111/j.1469-8749.2012.04337.x

Bartolini, E., & Sander, J. W. (2019). Dealing with the storm: An overview of seizure precipitants and spontaneous seizure worsening in drug-resistant epilepsy. *Epilepsy & Behavior*, *97*, 212–218. https://doi.org/10.1016/j.yebeh.2019.05.036

Basting, T. M., Burke, P. G. R., Kanbar, R., Viar, K. E., Stornetta, D. S., Stornetta, R. L., & Guyenet, P. G. (2015). Hypoxia Silences Retrotrapezoid Nucleus Respiratory Chemoreceptors via Alkalosis. *The Journal of Neuroscience*, *35*(2), 527–543. https://doi.org/10.1523/jneurosci.2923-14.2015

Baud, M. O., Kleen, J. K., Mirro, E. A., Andrechak, J. C., King-Stephens, D., Chang, E. F., & Rao, V. R. (2018). Multi-day rhythms modulate seizure risk in epilepsy. *Nature Communications*, *9*(1), 1–10. https://doi.org/10.1038/s41467-017-02577-y

Bazil, C. W. (2019). Seizure modulation by sleep and sleep state. *Brain Research*, *1703*, 13–17. https://doi.org/10.1016/j.brainres.2018.05.003

Beenhakker, M. P., & Huguenard, J. R. (2009). Neurons that Fire Together Also Conspire Together: Is Normal Sleep Circuitry Hijacked to Generate Epilepsy? *Neuron*, *62*(5), 612–632. http://dx.doi.org/10.1016/j.neuron.2009.05.015

Bezdudnaya, T., & Keller, A. (2008). Laterodorsal Nucleus of the Thalamus: A Processor of Somatosensory Inputs. *The Journal of Comparative Neurology*, *507*(6), 1979–1989. https://doi.org/10.1002/cne.21664

Chen, T. T., Klassen, T. L., Goldman, A. M., Marini, C., Guerrini, R., & Noebels, J. L. (2013). Novel brain expression of ClC-1 chloride channels and enrichment of CLCN1 variants in epilepsy. *Neurology*, *80*(12), 1078–1085. https://doi.org/10.1212/WNL.0b013e31828868e7

Coenen, A. M. (2003). Genetic animal models for absence epilepsy: A review of the WAG/Rij strain of rats. *Behavior Genetics*, *33*(6), 635–655.

Coenen, A. M., Drinkenburg, W. H., Inoue, M., & van Luijtelaar, E. L. (1992). Genetic models of absence epilepsy, with emphasis on the WAG/Rij strain of rats. *Epilepsy Res.*, *12*, 75–86.

Cox, G. A., Lutz, C. M., Yang, C.-L., Biemesderfer, D., Bronson, R. T., Fu, A., Aronson, P. S., Noebels, J. L., & Frankel, W. N. (1997). Sodium/Hydrogen Exchanger Gene Defect in Slow-Wave Epilepsy Mutant Mice. *Cell*, *91*(1), 139–148. https://doi.org/10.1016/S0092-8674(01)80016-7

Crunelli, V., & Leresche, N. (2002). Childhood absence epilepsy: Genes, channels, neurons and networks. *Nat Rev Neurosci*, *3*(5), 371–382.

Debski, K. J., Ceglia, N., Ghestem, A., Ivanov, A. I., Brancati, G. E., Bröer, S., Bot, A. M., Müller, J. A., Schoch, S., Becker, A., Löscher, W., Guye, M., Sassone-Corsi, P., Lukasiuk, K., Baldi, P., & Bernard, C. (2020). The circadian dynamics of the hippocampal transcriptome and proteome is altered in experimental temporal lobe epilepsy. *Science Advances*, *6*(41), eaat5979. https://doi.org/10.1126/sciadv.aat5979

Donevan, R. E., Anderson, N. M., Sekelj, P., Papp, O., & McGregor, M. (1962). Influence of voluntary hyperventilation on cardiac output. *Journal of Applied Physiology*, *17*(3), 487–491. https://doi.org/10.1152/jappl.1962.17.3.487

Edwards, S. B., & de Olmos, J. S. (1976). Autoradiographic studies of the projections of the midbrain reticular formation: Ascending projections of nucleus cuneiformis.

The Journal of Comparative Neurology, *165*(4), 417–431. https://doi.org/10.1002/cne.901650403

Eldridge, F. L., Kiley, J. P., & Millhorn, D. E. (1984). Respiratory effects of carbon dioxide-induced changes of medullary extracellular fluid pH in cats. *The Journal of Physiology*, *355*, 177–189. https://doi.org/10.1113/jphysiol.1984.sp015413

Ferlisi, M., & Shorvon, S. (2014). Seizure precipitants (triggering factors) in patients with epilepsy. *Epilepsy & Behavior: E&B*, *33*, 101–105. https://doi.org/10.1016/j.yebeh.2014.02.019

Festing, M. F. W. (1979). Inbred Strains of Rats. In M. F. W. Festing (Ed.), *Inbred Strains in Biomedical Research* (pp. 267–296). Macmillan Education UK. https://doi.org/10.1007/978-1-349-03816-9_14

Fountain, N. B., Kim, J. S., & Lee, S. I. (1998). Sleep Deprivation Activates Epileptiform Discharges Independent of the Activating Effects of Sleep. *Journal of Clinical Neurophysiology*, *15*(1), 69–75.

Guyenet, P. G. (2014). Regulation of Breathing and Autonomic Outflows by Chemoreceptors. *Comprehensive Physiology*, *4*(4), 1511–1562. https://doi.org/10.1002/cphy.c140004

Guyenet, P. G., & Bayliss, D. A. (2015). Neural Control of Breathing and CO2 Homeostasis. *Neuron*, *87*(5), 946–961. http://dx.doi.org/10.1016/j.neuron.2015.08.001

Guyenet, P. G., Bayliss, D. A., Stornetta, R. L., Ludwig, M.-G., Kumar, N. N., Shi, Y., Burke, P. G. R., Kanbar, R., Basting, T. M., Holloway, B. B., & Wenker, I. C. (2016). Proton detection and breathing regulation by the retrotrapezoid nucleus. *The Journal of Physiology*, *594*(6), 1529–1551. https://doi.org/10.1113/JP271480

Guyenet, P. G., Stornetta, R. L., Souza, G. M. P. R., Abbott, S. B. G., Shi, Y., & Bayliss, D. A. (2019). The Retrotrapezoid Nucleus: Central Chemoreceptor and Regulator

of Breathing Automaticity. *Trends in Neurosciences*, *42*(11), 807–824. https://doi.org/10.1016/j.tins.2019.09.002

Helbig, I. (2015). Genetic Causes of Generalized Epilepsies. *Seminars in Neurology*, *35*(03), 288–292. https://doi.org/10.1055/s-0035-1552922

Herzog, A. G., & Frye, C. A. (2014). Allopregnanolone levels and seizure frequency in progesterone-treated women with epilepsy. *Neurology*, *83*(4), 345–348. https://doi.org/10.1212/WNL.0000000000000623

Holowach, J., Thurston, D., & O'Leary, J. L. (1962). Petit Mal Epilepsy. *Pediatrics*, *30*, 893–901.

Hughes, J. R. (2009). Absence seizures: A review of recent reports with new concepts. *Epilepsy & Behavior*, *15*(4), 404–412. https://doi.org/10.1016/j.yebeh.2009.06.007

Huguenard, J. (2019). Current Controversy: Spikes, Bursts, and Synchrony in Generalized Absence Epilepsy: Unresolved Questions Regarding Thalamocortical Synchrony in Absence Epilepsy. *Epilepsy Currents*, *19*(2), 105–111. https://doi.org/10.1177/1535759719835355

Huguenard, J. R., & McCormick, D. A. (2007). Thalamic synchrony and dynamic regulation of global forebrain oscillations. *Trends in Neurosciences*, *30*(7), 350–356. https://doi.org/10.1016/j.tins.2007.05.007

Hunter, J., & Jasper, H. H. (1949). Effects of thalamic stimulation in unanaesthetised animals: The arrest reaction and petit Mal-like seizures, activation patterns and generalized convulsions. *Electroencephalography and Clinical Neurophysiology*, *1*(1–4), 305–324. http://dx.doi.org/10.1016/0013-4694(49)90196-0

Hwang, D. Y., Carlezon, W. A., Isacson, O., & Kim, K. S. (2001). A high-efficiency synthetic promoter that drives transgene expression selectively in noradrenergic

neurons. *Human Gene Therapy*, *12*(14), 1731–1740. https://doi.org/10.1089/104303401750476230

Jasper, H. H., & Droogleever-Fortuyn, J. (1947). Experimental studies of the functional anatomy of petit mal epilepsy. *Res. Publ. Assoc. Res. Nerve Ment. Dis.*, *26*, 272–298.

Joshi, S., & Kapur, J. (2019). Neurosteroid regulation of GABAA receptors: A role in catamenial epilepsy. *Brain Research*, *1703*, 31–40. https://doi.org/10.1016/j.brainres.2018.02.031

Kasteleijn-Nolst Trenité, D. G. A. (2012). Provoked and reflex seizures: Surprising or common? *Epilepsia*, *53 Suppl 4*, 105–113. https://doi.org/10.1111/j.1528-1167.2012.03620.x

Koeleman, B. P. C. (2018). What do genetic studies tell us about the heritable basis of common epilepsy? Polygenic or complex epilepsy? *Neuroscience Letters*, *667*, 10–16. https://doi.org/10.1016/j.neulet.2017.03.042

Koepp, M. J., Caciagli, L., Pressler, R. M., Lehnertz, K., & Beniczky, S. (2016). Reflex seizures, traits, and epilepsies: From physiology to pathology. *The Lancet. Neurology*, *15*(1), 92–105. https://doi.org/10.1016/S1474-4422(15)00219-7

Laffey, J. G., & Kavanagh, B. P. (2002). Hypocapnia. *New England Journal of Medicine*, *347*(1), 43–53. https://doi.org/10.1056/NEJMra012457

Lein, E. S., Hawrylycz, M. J., Ao, N., Ayres, M., Bensinger, A., Bernard, A., Boe, A. F., Boguski, M. S., Brockway, K. S., Byrnes, E. J., Chen, L., Chen, L., Chen, T.-M., Chi Chin, M., Chong, J., Crook, B. E., Czaplinska, A., Dang, C. N., Datta, S., … Jones, A. R. (2007). Genome-wide atlas of gene expression in the adult mouse brain. *Nature*, *445*(7124), 168–176. https://doi.org/10.1038/nature05453

Lennox, W. G. (1928). The effect on epileptic seizures of varying composition of respired air. *J. Clin. Investigation*, *6*, 23–24.

Lindsey, B. G., Nuding, S. C., Segers, L. S., & Morris, K. F. (2018). Carotid Bodies and the Integrated Cardiorespiratory Response to Hypoxia. *Physiology*, *33*(4), 281–297. https://doi.org/10.1152/physiol.00014.2018

Lonergan, T., Teschemacher, A. G., Hwang, D. Y., Kim, K.-S., Pickering, A. E., & Kasparov, S. (2005). Targeting brain stem centers of cardiovascular control using adenoviral vectors: Impact of promoters on transgene expression. *Physiological Genomics*, *20*(2), 165–172. https://doi.org/10.1152/physiolgenomics.00120.2004

López-Barneo, J., Macías, D., Platero-Luengo, A., Ortega-Sáenz, P., & Pardal, R. (2016). Carotid body oxygen sensing and adaptation to hypoxia. *Pflugers Archiv: European Journal of Physiology*, *468*(1), 59–70. https://doi.org/10.1007/s00424-015-1734-0

Lum, L. M., Connolly, M. B., Farrell, K., & Wong, P. K. H. (2002). Hyperventilation-induced High-amplitude Rhythmic Slowing with Altered Awareness: A Video-EEG Comparison with Absence Seizures. *Epilepsia (Series 4)*, *43*(11), 1372–1378. https://doi.org/10.1046/j.1528-1157.2002.35101.x

Lusardi, T. A., Akula, K. K., Coffman, S. Q., Ruskin, D. N., Masino, S. A., & Boison, D. (2015). Ketogenic diet prevents epileptogenesis and disease progression in adult mice and rats. *Neuropharmacology*, *99*, 500–509. http://dx.doi.org/10.1016/j.neuropharm.2015.08.007

Ma, X., Zhang, Y., Yang, Z., Liu, X., Sun, H., Qin, J., Wu, X., & Liang, J. (2011). Childhood absence epilepsy: Electroclinical features and diagnostic criteria. *Brain and Development*, *33*(2), 114–119. http://dx.doi.org/10.1016/j.braindev.2010.02.004

Malow, B. A., Selwa, L. M., Ross, D., & Aldrich, M. S. (1999). Lateralizing value of interictal spikes on overnight sleep-EEG studies in temporal lobe epilepsy.

Epilepsia, *40*(11), 1587–1592. https://doi.org/10.1111/j.1528-1157.1999.tb02044.x

Masino, S. A., Kawamura Jr, M., Ruskin, D. N., Geiger, J. D., & Boison, D. (2012). Purines and neuronal excitability: Links to the ketogenic diet. *Epilepsy Research*, *100*(3), 229–238. http://dx.doi.org/10.1016/j.eplepsyres.2011.07.014

Masino, S. A., & Rho, J. M. (2012). Mechanisms of Ketogenic Diet Action. In J. L. Noebels, M. Avoli, M. A. Rogawski, R. W. Olsen, & A. V. Delgado-Escueta (Eds.), *Jasper's Basic Mechanisms of the Epilepsies* (4th ed.). National Center for Biotechnology Information (US). http://www.ncbi.nlm.nih.gov/books/NBK98219/

Masino, S. A., & Rho, J. M. (2019). Metabolism and epilepsy: Ketogenic diets as a homeostatic link. *Brain Research*, *1703*, 26–30. https://doi.org/10.1016/j.brainres.2018.05.049

Mattozzi, S., Cerminara, C., Sotgiu, M. A., Carta, A., Coniglio, A., Roberto, D., Simula, D. M., Luca Pruneddu, G., Dell'Avvento, S., Muzzu, S. S., Fadda, M., Luzzu, G. M., Sotgiu, S., & Casellato, S. (2021). Occurrence of hyperventilation-induced high amplitude rhythmic slowing with altered awareness after successful treatment of typical absence seizures and a network hypothesis. *Clinical Neurophysiology Practice*, *6*, 185–188. https://doi.org/10.1016/j.cnp.2021.03.009

McCafferty, C., David, F., Venzi, M., Lőrincz, M. L., Delicata, F., Atherton, Z., Recchia, G., Orban, G., Lambert, R. C., Di Giovanni, G., Leresche, N., & Crunelli, V. (2018). Cortical drive and thalamic feed-forward inhibition control thalamic output synchrony during absence seizures. *Nature Neuroscience*, *21*(5), 744–756. https://doi.org/10.1038/s41593-018-0130-4

McCormick, D. A., & Contreras, D. (2001). On The Cellular and Network Bases of Epileptic Seizures. *Annual Review of Physiology*, *63*(1), 815–846. https://doi.org/10.1146/annurev.physiol.63.1.815

Meeren, H. K. M., Pijn, J. P. M., Van Luijtelaar, E. L. J. M., Coenen, A. M. L., & Lopes da Silva, F. H. (2002). Cortical Focus Drives Widespread Corticothalamic Networks during Spontaneous Absence Seizures in Rats. *The Journal of Neuroscience*, *22*(4), 1480–1495.

Meeren, H., van Luijtelaar, G., Lopes da Silva, F., & Coenen, A. (2005). Evolving concepts on the pathophysiology of absence seizures: The cortical focus theory. *Archives of Neurology*, *62*(3), 371–376. https://doi.org/10.1001/archneur.62.3.371

Meuth, S. G., Budde, T., Kanyshkova, T., Broicher, T., Munsch, T., & Pape, H.-C. (2003). Contribution of TWIK-Related Acid-Sensitive K+ Channel 1 (TASK1) and TASK3 Channels to the Control of Activity Modes in Thalamocortical Neurons. *The Journal of Neuroscience*, *23*(16), 6460–6469.

Meuth, S. G., Kanyshkova, T., Meuth, P., Landgraf, P., Munsch, T., Ludwig, A., Hofmann, F., Pape, H.-C., & Budde, T. (2006). Membrane Resting Potential of Thalamocortical Relay Neurons Is Shaped by the Interaction Among TASK3 and HCN2 Channels. *Journal of Neurophysiology*, *96*(3), 1517–1529. https://doi.org/10.1152/jn.01212.2005

Nobili, L., Baglietto, M. G., Beelke, M., De Carli, F., Veneselli, E., & Ferrillo, F. (2001). Temporal relationship of generalized epileptiform discharges to spindle frequency activity in childhood absence epilepsy. *Clinical Neurophysiology: Official Journal of the International Federation of Clinical Neurophysiology*, *112*(10), 1912–1916. https://doi.org/10.1016/s1388-2457(01)00624-1

Padmanaban, V., Inati, S., Ksendzovsky, A., & Zaghloul, K. (2019). Clinical advances in photosensitive epilepsy. *Brain Research*, *1703*, 18–25. https://doi.org/10.1016/j.brainres.2018.07.025

Paxinos, G., & Watson, C. (2007). *The Rat Brain In Sterotaxic Coordinates* (6th ed.). Elsevier.

Paz, J. T., & Huguenard, J. R. (2015). Microcircuits and their interactions in epilepsy: Is the focus out of focus? *Nat Neurosci*, *18*(3), 351–359. https://doi.org/10.1038/nn.3950

Pinault, D. (2003). Cellular interactions in the rat somatosensory thalamocortical system during normal and epileptic 5–9 Hz oscillations. *The Journal of Physiology*, *552*(3), 881–905. https://doi.org/10.1113/jphysiol.2003.046573

Pinault, D., Leresche, N., Charpier, S., Deniau, J.-M., Marescaux, C., Vergnes, M., & Crunelli, V. (1998). Intracellular recordings in thalamic neurones during spontaneous spike and wave discharges in rats with absence epilepsy. *The Journal of Physiology*, *509*(2), 449–456. https://doi.org/10.1111/j.1469-7793.1998.449bn.x

Raichle, M. E., & Plum, F. (1972). Hyperventilation and Cerebral Blood Flow. *Stroke*, *3*(5), 566–575. https://doi.org/10.1161/01.STR.3.5.566

Reddy, D. S., Kim, H.-Y., & Rogawski, M. A. (2001). Neurosteroid Withdrawal Model of Perimenstrual Catamenial Epilepsy. *Epilepsia*, *42*(3), 328–336. https://doi.org/10.1046/j.1528-1157.2001.10100.x

Robinson, P. F., & Gilmore, S. A. (1980). Spontaneous generalized spike-wave discharges in the electrocorticograms of albino rats. *Brain Research*, *201*(2), 452–458. https://doi.org/10.1016/0006-8993(80)91052-5

Robinson, R., Taske, N., Sander, T., Heils, A., Whitehouse, W., Goutières, F., Aicardi, J., Lehesjoki, A.-E., Siren, A., Laue Friis, M., Kjeldsen, M. J., Panayiotopoulos,

C., Kennedy, C., Ferrie, C., Rees, M., & Gardiner, R. M. (2002). Linkage analysis between childhood absence epilepsy and genes encoding GABAA and GABAB receptors, voltage-dependent calcium channels, and the ECA1 region on chromosome 8q. *Epilepsy Research*, *48*(3), 169–179. https://doi.org/10.1016/S0920-1211(01)00335-7

Ropert, N., & Steriade, M. (1981). Input-output organization of midbrain reticular core. *Journal of Neurophysiology*, *46*(1), 17–31. https://doi.org/10.1152/jn.1981.46.1.17

Russo, E., Citraro, R., Constanti, A., Leo, A., Lüttjohann, A., van Luijtelaar, G., & De Sarro, G. (2016). Upholding WAG/Rij rats as a model of absence epileptogenesis: Hidden mechanisms and a new theory on seizure development. *Neuroscience & Biobehavioral Reviews*, *71*, 388–408. https://doi.org/10.1016/j.neubiorev.2016.09.017

Saalmann, Y. B. (2014). Intralaminar and medial thalamic influence on cortical synchrony, information transmission and cognition. *Frontiers in Systems Neuroscience*, *8*. https://doi.org/10.3389/fnsys.2014.00083

Sadleir, L. G., Farrell, K., Smith, S., Connolly, M. B., & Scheffer, I. E. (2006). Electroclinical features of absence seizures in childhood absence epilepsy. *Neurology*, *67*(3), 413. https://doi.org/10.1212/01.wnl.0000228257.60184.82

Sadleir, L. G., Scheffer, I., Smith, S., Carstensen, B., Farrell, K., & Connolly, M. B. (2009). EEG features of absence seizures in idiopathic generalized epilepsy: Impact of syndrome, age, and state. *Epilepsia*, *50*(6), 1572–1578. https://doi.org/10.1111/j.1528-1167.2008.02001.x

Sander, T., Toliat, M. R., Heils, A., Leschik, G., Becker, C., Rüschendorf, F., Rohde, K., Mundlos, S., & Nürnberg, P. (2002). Association of the 867Asp variant of the human anion exchanger 3 gene with common subtypes of idiopathic generalized

epilepsy. *Epilepsy Research*, *51*(3), 249–255. https://doi.org/10.1016/S0920-1211(02)00152-3

Sarrigiannis, P. G., Zhao, Y., He, F., Billings, S. A., Baster, K., Rittey, C., Yianni, J., Zis, P., Wei, H., Hadjivassiliou, M., & Grünewald, R. (2018). The cortical focus in childhood absence epilepsy; evidence from nonlinear analysis of scalp EEG recordings. *Clinical Neurophysiology*, *129*(3), 602–617. https://doi.org/10.1016/j.clinph.2017.11.029

Semenza, G. L., & Prabhakar, N. R. (2018). The role of hypoxia-inducible factors in carotid body (patho) physiology. *The Journal of Physiology*, *596*(15), 2977–2983. https://doi.org/10.1113/JP275696

Sherwin, I. (1965). Differential effects of hyperventillation on the excitability of intact and isolated cortex. *Electroencephalography and Clinical Neurophysiology*, *18*(6), 599–607. https://doi.org/10.1016/0013-4694(65)90077-5

Sherwin, I. (1967). Alterations in the non-specific cortical afference during hyperventilation. *Electroencephalography and Clinical Neurophysiology*, *23*(6), 532–538. https://doi.org/10.1016/0013-4694(67)90019-3

Sinning, A., & Hübner, C. A. (2013). Minireview: PH and synaptic transmission. *FEBS Letters*, *587*(13), 1923–1928. https://doi.org/10.1016/j.febslet.2013.04.045

Sinning, A., Liebmann, L., Kougioumtzes, A., Westermann, M., Bruehl, C., & Hubner, C. A. (2011). Synaptic Glutamate Release Is Modulated by the Na+-Driven Cl-/HCOFormula Exchanger Slc4a8. *Journal of Neuroscience*, *31*(20), 7300–7311. https://doi.org/10.1523/JNEUROSCI.0269-11.2011

Smith, J. C., Abdala, A. P. L., Borgmann, A., Rybak, I. A., & Paton, J. F. R. (2013). Brainstem respiratory networks: Building blocks and microcircuits. *Trends in Neurosciences*, *36*(3), 152–162. https://doi.org/10.1016/j.tins.2012.11.004

Smyk, M. K., & van Luijtelaar, G. (2020). Circadian Rhythms and Epilepsy: A Suitable Case for Absence Epilepsy. *Frontiers in Neurology*, *11*. https://doi.org/10.3389/fneur.2020.00245

Souza, G. M. P. R., Kanbar, R., Stornetta, D. S., Abbott, S. B. G., Stornetta, R. L., & Guyenet, P. G. (2018). Breathing regulation and blood gas homeostasis after near complete lesions of the retrotrapezoid nucleus in adult rats. *The Journal of Physiology*, *596*(13), 2521–2545. https://doi.org/10.1113/JP275866

Souza, G. M. P. R., Stornetta, R. L., Stornetta, D. S., Abbott, S. B. G., & Guyenet, P. G. (2019). Contribution of the Retrotrapezoid Nucleus and Carotid Bodies to Hypercapnia- and Hypoxia-induced Arousal from Sleep. *The Journal of Neuroscience: The Official Journal of the Society for Neuroscience*, *39*(49), 9725–9737. https://doi.org/10.1523/JNEUROSCI.1268-19.2019

Souza, G. M. P. R., Stornetta, R. L., Stornetta, D. S., Abbott, S. B. G., & Guyenet, P. G. (2020). Differential Contribution of the Retrotrapezoid Nucleus and C1 Neurons to Active Expiration and Arousal in Rats. *The Journal of Neuroscience: The Official Journal of the Society for Neuroscience*, *40*(45), 8683–8697. https://doi.org/10.1523/JNEUROSCI.1006-20.2020

Steriade, M., & Glenn, L. L. (1982). Neocortical and caudate projections of intralaminar thalamic neurons and their synaptic excitation from midbrain reticular core. *Journal of Neurophysiology*, *48*(2), 352–371. https://doi.org/10.1152/jn.1982.48.2.352

Stirling, R. E., Cook, M. J., Grayden, D. B., & Karoly, P. J. (2021). Seizure forecasting and cyclic control of seizures. *Epilepsia*, *62*(S1), S2–S14. https://doi.org/10.1111/epi.16541

Taylor, J. A., Reuter, J. D., Kubiak, R. A., Mufford, T. T., Booth, C. J., Dudek, F. E., & Barth, D. S. (2019). Spontaneous Recurrent Absence Seizure-like Events in

Wild-Caught Rats. *Journal of Neuroscience*, *39*(24), 4829–4841. https://doi.org/10.1523/JNEUROSCI.1167-18.2019

Taylor, J. A., Rodgers, K. M., Bercum, F. M., Booth, C. J., Dudek, F. E., & Barth, D. S. (2017). Voluntary Control of Epileptiform Spike–Wave Discharges in Awake Rats. *The Journal of Neuroscience*, *37*(24), 5861–5869. https://doi.org/10.1523/JNEUROSCI.3235-16.2017

Ting, J. T., Daigle, T. L., Chen, Q., & Feng, G. (2014). Acute Brain Slice Methods for Adult and Aging Animals: Application of Targeted Patch Clamp Analysis and Optogenetics. In M. Martina & S. Taverna (Eds.), *Patch-Clamp Methods and Protocols* (pp. 221–242). Springer New York. https://doi.org/10.1007/978-1-4939-1096-0_14

Tyvaert, L., Chassagnon, S., Sadikot, A., LeVan, P., Dubeau, F., & Gotman, J. (2009). Thalamic nuclei activity in idiopathic generalized epilepsy: An EEG-fMRI study. *Neurology*, *73*(23), 2018–2022. https://doi.org/10.1212/WNL.0b013e3181c55d02

van Luijtelaar, E. L., & Coenen, A. M. (1986). Two types of electrocortical paroxysms in an inbred strain of rats. *Neuroscience Letters*, *70*(3), 393–397.

Vergnes, M., Marescaux, Ch., Micheletti, G., Reis, J., Depaulis, A., Rumbach, L., & Warter, J. M. (1982). Spontaneous paroxysmal electroclinical patterns in rat: A model of generalized non-convulsive epilepsy. *Neuroscience Letters*, *33*(1), 97–101. https://doi.org/10.1016/0304-3940(82)90136-7

von Krosigk, M., Bal, T., & McCormick, D. (1993). Cellular mechanisms of a synchronized oscillation in the thalamus. *Science*, *261*(5119), 361. https://doi.org/10.1126/science.8392750

Watemberg, N., Farkash, M., Har-Gil, M., Sezer, T., Goldberg-Stern, H., & Alehan, F. (2015). Hyperventilation During Routine Electroencephalography: Are Three

Minutes Really Necessary? *Pediatric Neurology*, *52*(4), 410–413. http://dx.doi.org/10.1016/j.pediatrneurol.2014.12.003

Xie, H., Su, W., Pei, J., Zhang, Y., Gao, K., Li, J., Ma, X., Zhang, Y., Wu, X., & Jiang, Y. (2019). De novo SCN1A, SCN8A, and CLCN2 mutations in childhood absence epilepsy. *Epilepsy Research*, *154*, 55–61. https://doi.org/10.1016/j.eplepsyres.2019.04.005

Yang, X.-F., Shi, X.-Y., Ju, J., Zhang, W.-N., Liu, Y.-J., Li, X.-Y., & Zou, L.-P. (2014). 5% CO2 inhalation suppresses hyperventilation-induced absence seizures in children. *Epilepsy Research*, *108*(2), 345–348. http://dx.doi.org/10.1016/j.eplepsyres.2013.11.012

Chapter 5: Mice harboring a non-functional *CILK1/ICK* allele fail to model the epileptic phenotype in patients carrying variant *CILK1/ICK*

Kathryn A. Salvati

Ashley J. Mason

Casey D. Gailey

Eric J. Wang

Zheng Fu

Mark P. Beenhakker

Published

International Journal of Molecular Sciences

22(16): 8875 (2021)

Conceptualization, M.P.B. and Z.F.; methodology, K.A.S., A.J.M., Z.F., and M.P.B.; software, K.A.S. and M.P.B.; validation, K.A.S., A.J.M., C.D.G., E.J.W., Z.F., and M.P.B.; formal analysis, K.A.S., A.J.M., and M.P.B.; investigation, K.A.S., A.J.M., C.D.G., E.J.W., Z.F., and M.P.B.; resources, M.P.B. and Z.F.; data curation, K.A.S., A.J.M., Z.F., and M.P.B.; writing—original draft preparation, K.A.S.; writing—review and editing, M.P.B. and Z.F.; visualization, K.A.S. and A.J.M.; supervision, M.P.B. and Z.F.; project administration, M.P.B. and Z.F.; funding acquisition, M.P.B. and Z.F. All authors have read and agreed to the published version of the manuscript.

Abstract

CILK1 (ciliogenesis associated kinase 1)/ICK (intestinal cell kinase) is a highly conserved protein kinase that regulates primary cilia structure and function. *CILK1* mutations cause a wide spectrum of human diseases collectively called ciliopathies. While several *CILK1* heterozygous variants have been recently linked to juvenile myoclonic epilepsy (JME), it remains unclear whether these mutations cause seizures. Herein, we investigated whether mice harboring either a heterozygous null *Cilk1* (*Cilk1*$^{+/-}$) mutation or a heterozygous loss-of-function *Cilk1* mutation (*Cilk1*$^{R272Q/+}$) have epilepsy. We first evaluated the spontaneous seizure phenotype of *Cilk1*$^{+/-}$ and *Cilk1*$^{R272Q/+}$ mice relative to wildtype littermates. We observed no electrographic differences among the three mouse genotypes during prolonged recordings. We also evaluated electrographic and behavioral responses of mice recovering from isoflurane anesthesia, an approach recently used to measure seizure-like activity. Again, we observed no electrographic or behavioral differences in control versus *Cilk1*$^{+/-}$ and *Cilk1*$^{R272Q/+}$ mice upon isoflurane recovery. These results indicate that mice bearing a non-functional copy of *Cilk1* fail to produce electrographic patterns resembling those of JME patients with a variant *CILK1* copy. Our findings argue against *CILK1* haploinsufficiency being the mechanism that links *CILK1* variants to JME.

Introduction

The primary cilium is a single solitary microtubule-based protrusion on the apical surface of most vertebrate cells that senses and transduces environmental and hormonal signals to regulate diverse cellular processes (Gerdes et al., 2009). The primary cilium is essential for tissue development and homeostasis. Defects in cilia have been linked to at least 35 human diseases collectively called ciliopathies that manifest as a constellation of

clinical features and deformities in various organ systems, including the brain (Reiter & Leroux, 2017).

Ciliogenesis-associated kinase 1 (CILK1), formerly known as intestinal cell kinase (ICK), is a highly conserved serine/threonine kinase that negatively regulates cilia length and ciliogenesis (Fu et al., 2019). Inactivating mutations in the human *CILK1* gene (R272Q) cause neonatal–lethal human ciliopathies, such as endocrine-cerebro-osteodysplasia (ECO) syndrome (Lahiry et al., 2009) and ECO-like syndromes (Oud et al., 2016; Paige Taylor et al., 2016). Similar to humans with ECO syndrome, homozygous *Cilk1* null mice and R272Q mutant mice are perinatal lethal (Chaya et al., 2014; Moon et al., 2014; Tong et al., 2017). Complete *Cilk1* deletion also recapitulates ciliopathy phenotypes and causes exuberant cilia growth, consistent with the role of CILK1 in restricting cilia formation and growth. In contrast, cells from heterozygous *Cilk1* null mice grow normal cilia and the mice develop normally (Chaya et al., 2014; Moon et al., 2014), thus indicating that at least one wildtype copy of the gene is sufficient for normal cilia growth. Collectively, these results support the general conclusion that CILK1 mutations causing exuberant cilia growth result in ciliopathy, whereas CILK1 mutations preserving normal cilia growth are associated with normal development.

Although ample evidence demonstrates that primary cilia critically regulate the development and patterning of the nervous system, cilia function in mature neurons remains poorly understood and underexplored (Youn & Han, 2018). Moreover, the role of CILK1 in regulating cilia growth and cellular function in postmitotic differentiated cells, such as neurons, remains unknown. Recently, an expansive genetic study linked multiple pathological *CILK1* point mutations to juvenile myoclonic epilepsy (JME) (Bailey et al., 2018), the most commonly diagnosed *Genetic Generalized Epilepsy*. The authors examined the genomes of 334 families whose members are afflicted with JME and identified 21 pathogenic *CILK1* variants in 22 of 310 JME patients. Notably, four *CILK1*

variants, K220E, K305T, A615T, and R632X, were strongly linked to JME. Mouse neocortices transfected with these four pathogenic variants and the *CILK1* variant, R272Q, exhibited impaired mitosis, cell-cycle exit, radial neuroblast migration, and increased apoptosis (Bailey et al., 2018). The authors also evaluated the spontaneous and isoflurane-provoked seizure phenotype of heterozygous *Cilk1* null (*Cilk1*$^{+/-}$) mice and concluded that the mutations are epileptogenic. These novel observations, however, diverge from previous reports on the lack of cilia and development phenotypes in the heterozygous *Cilk1* null mice.

In this study, we re-examine the hypothesis that CILK1 mutations contribute to JME. We evaluate the seizure phenotype of both heterozygous null *Cilk1* (*Cilk1*$^{+/-}$) mice and mice harboring the loss-of-function *Cilk1* variant, R272Q (*Cilk1*$^{R272Q/+}$) (Ding et al., 2018; Tong et al., 2017). By coupling video capture with electrocorticogram and electromyogram (ECoG/EMG) recordings, we first evaluated the spontaneous seizure phenotype of both *Cilk1* mutant mice. We captured no electrographic or behavioral tonic–clonic seizures in *Cilk1*$^{+/-}$ and *Cilk1*$^{R272Q/+}$ mice. Second, we investigated whether isoflurane exposure induces tonic–clonic seizures in *Cilk1*$^{+/-}$ and *Cilk1*$^{R272Q/+}$ mice, as previously reported (Bailey et al., 2018). Again, we observed no seizures during the recovery phase of isoflurane treatment. However, a subset of mice exhibited opisthotonos-like behavior during isoflurane recovery, a nonepileptic behavior that includes tonic full-body extension but is electrographically normal. In sum, our observations do not support the hypothesis that either *Cilk1*$^{+/-}$ or *Cilk1*$^{R272Q/+}$ mutations promote JME. These results challenge the recent conclusion that *CILK1* haploinsufficiency contributes to JME.

Results

Cilk1$^{+/-}$ *and Cilk1*$^{R272Q/+}$ *Mice do Not Exhibit Electrographic Seizures*

CILK1 has two structural domains, a catalytic N-terminal domain (amino acids 4-284) and a noncatalytic C-terminal domain (amino acids 285–632). *CILK1* variants associate with both JME [11] (Fig. 1A, red) and human ciliopathies (Lahiry et al., 2009; Oud et al., 2016; Paige Taylor et al., 2016) (Fig. 1A, purple). Notably, recent evidence calls into question the association between *CILK1* variants and JME (Lerche et al., 2019). Moreover, previous reports indicate that *Cilk1* heterozygote knockout (i.e., *Cilk1*$^{+/-}$) mice develop normally and exhibit normal cilia growth (Chaya et al., 2014; Moon et al., 2014). We were therefore motivated to re-evaluate the hypothesis that Cilk1+/- mice generate seizures associated with JME. We compared the seizure phenotype of Cilk1+/- mice to wildtype littermates as well as mice harboring the autosomal-recessive inactivating mutation *Cilk1* R272Q (i.e., heterozygous *Cilk1*$^{R272Q/+}$) associated with human ECO syndrome (Tong et al., 2017).

We first evaluated the spontaneous seizure phenotype of *Cilk1*$^{+/-}$ and *Cilk1*$^{R272Q/+}$ mutant mice with their respective wildtype littermates using chronic video-ECoG/EMG recordings. Common electrographic events observed in JME patients include myoclonic jerks, generalized tonic–clonic seizures, polyspikes, and absence seizures. These events have readily observable correlates in mice (Figure 1B). We also catalogued sleep spindles (Fig. 1B) to determine if *Cilk1* mutations contribute to abnormal sleep activity among the three mouse types (i.e., *Cilk1*$^{+/-}$, *Cilk1*$^{R272Q/+}$, and wildtype). Investigators were blinded to the genotype of mice throughout the experimental procedure and data analysis. By quantifying a 48-hour recording period, we concluded that a minority of *Cilk1*$^{+/-}$ and wildtype mice express a low frequency of JME-associated electrographic events. Between 14% (n = 1/7) and 29% (n = 2/7) of *Cilk1*$^{+/-}$ mice produced myoclonic

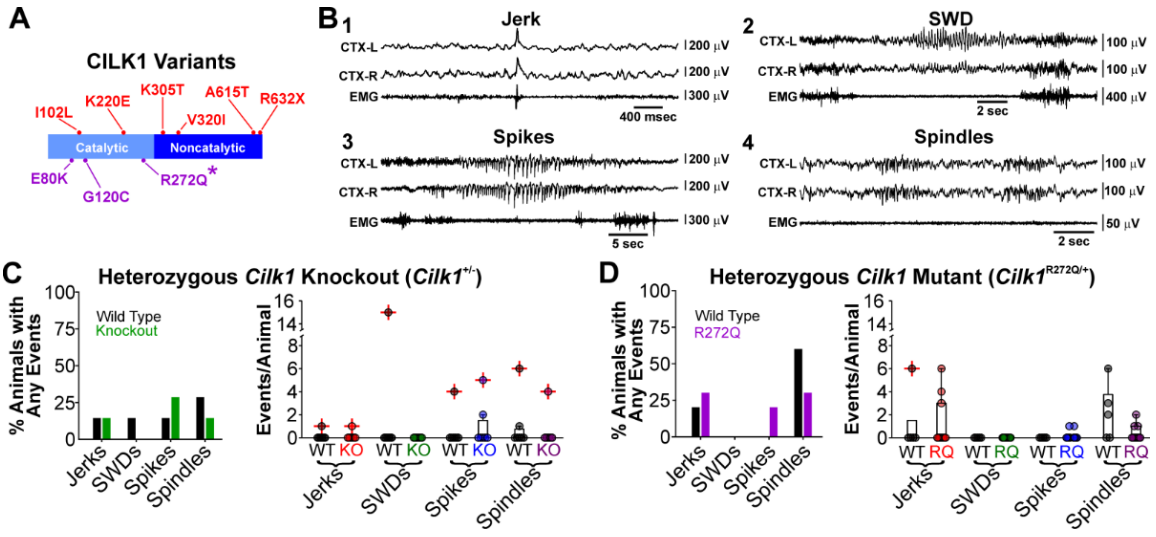

Figure 1. The seizure phenotype of *Cilk1*$^{+/-}$ and *Cilk1*$^{R272Q/+}$ mutants is indistinguishable from wildtype littermates. (A) *Cilk1* mutations associated with JME (red) and those associated with ciliopathies (purple). **(B)** Electrographic examples of seizure activity observed in mice: (1) myoclonic jerk, (2) spike-wave discharge (SWD), (3) spike run (associated with convulsions), and (4) sleep spindles. **(C)** Left. The percentage of *Cilk1*$^{+/-}$ and wildtype littermates that exhibited at least one electrographic jerk, SWD, spike run, or spindle. Right. The number of electrographic events per animal. **(D)** Left. The percentage of *Cilk1*$^{R272Q/+}$ and wildtype littermates that exhibited at least one electrographic jerk, SWD, spike run, or spindle. Right. The number of electrographic events per animal. Symbols marked with a red cross are considered to be outliers according to MATLAB based functions.

jerks and spikes, respectively, but no SWDs (n = 0/7). Similarly, 14% (1/7) of wildtype littermates exhibited myoclonic jerks and spikes; one mouse had an SWD (n = 1/7; Figure 1C, left). We also observed sleep spindles in 14% (n = 1/7) of *Cilk1*$^{+/-}$ and 29% (n = 2/7) of wildtype mice (Fig. 1C, left). Notably, sleep spindles are generally difficult to resolve in rodents and often require automated algorithms for detection (Uygun et al., 2019); as the primary goal of this study was to evaluate seizures, we did not utilize such spindle detection algorithms. Statistical comparisons revealed that the occurrence of all seizure subtypes did not differ between *Cilk1*$^{+/-}$ and wildtype littermates (myoclonic jerks, p = 1.0; SWDs, p = 0.37; spikes, p = 0.65, spindles, p = 0.68; see Fig. 1C, right).

Similarly, *Cilk1*$^{R272Q/+}$ and their wildtype littermates had minimal JME-associated electrographic activity. Between 30% (n = 2/10) and 20% (n = 3/10) of *Cilk1*$^{R272Q/+}$ mice had myoclonic jerks and spikes, respectively, and no SWDs (n = 0/7; Fig. 1D, left). Comparatively, 20% (n = 1/5) and 60% (n = 3/5) of wildtype littermates exhibited myoclonic jerks and spikes, respectively, and no SWDs (n = 0/7; Fig. 1D, left). Sleep spindles were observed in 29% (n = 2/7) of *Cilk1*$^{R272Q/+}$ and 57% (n = 4/7) of wildtype mice (Fig. 1D, right). Statistical measures revealed no difference in seizure phenotype between the *Cilk1*$^{R272Q/+}$ and wildtype littermates (myoclonic jerks, p = 0.94; SWDs, p = 1; spikes, p = 0.32). Sleep spindle occurrence was lower in *Cilk1*$^{R272Q/+}$ mice relative to their wildtype littermates (spindles, p = 0.047; see Fig. 1D, right). Importantly, we did not observe electrographic or behavioral generalized tonic–clonic seizures in any *Cilk1*$^{+/-}$ and *Cilk1*$^{R272Q/+}$ mice, or their wildtype littermates. We also did not observe such seizures while handling or caring for mice. In sum, our data suggest that *Cilk1*$^{+/-}$ and *Cilk1*$^{R272Q/+}$ mice do not have a higher occurrence in JME-like events relative to wildtype mice.

Isoflurane Does not Induce Generalized Tonic–Clonic Seizures in Cilk1$^{+/-}$ and Cilk1$^{R272Q/+}$ Mice

Isoflurane is a widely used volatile anesthetic for the induction and maintenance of general anesthesia in humans (Gupta et al., 2004; Purdon et al., 2015) and research animals (Stokes et al., 2009). Generally, isoflurane does not induce seizures in humans and, in fact, exhibits anticonvulsant properties. However, several studies report that emergence from isoflurane anesthesia in mice causes opisthotonos (Komatsu et al., 1988, 1996; Komatsu & Ogli, 1987), a behavioral repertoire that includes hyperextension of the neck, arching of the back, and tail extension. Importantly, opisthotonos is not considered to reflect epilepsy (Sadan et al., 2016). Indeed, opisthotonos in humans is often associated with psychogenic nonepileptic seizures (Delgado-Escueta, 2007; Kholi et al., 2020). Recently, *Cilk1*$^{+/-}$ mice were reported to generate tonic–clonic seizures upon recovery from isoflurane (Bailey et al., 2018), an assessment based entirely on behavioral measures. As tonic–clonic seizures and opisthotonos include similar behavioral features, we were motivated to test the hypothesis that *Cilk1*$^{+/-}$ mice generate opisthotonos, not seizures, upon isoflurane recovery, a distinction readily testable using ECoG/EMG recordings.

To record ECoG/EMG activity in behaving mice before and during isoflurane exposure, we used plethysmography chambers to reduce the variability of isoflurane gas exchange among mice. While recording ECoG/EMG signals in *Cilk1*$^{+/-}$ and *Cilk1*$^{R272Q/+}$ mice, and their respective wildtype littermate, we supplied plethysmography chambers with atmospheric oxygen (21% O2) containing 0% isoflurane. After recording the baseline activity for 45 min, we then switched to oxygen containing either 1.5% or 5% isoflurane; all mice were subjected to both 1.5% and 5% isoflurane, with sufficient rest time between exposures. To match the method of Bailey et al. (Bailey et al., 2018), 1.5% isoflurane was chosen, while 5% isoflurane was chosen to rapidly induce anesthesia and potentially increase the probability of an isoflurane-induced electrographic and behavioral

generalized tonic–clonic seizures. Isoflurane was delivered to mice until burst suppression was observed in the ECoG recording (e.g., Fig. 2B3), indicating that isoflurane was maximally effective. Once burst suppression was observed, isoflurane delivery was halted and the animal was allowed to recover (i.e., “isoflurane recovery”). As before, video and ECoG/EMG signals were simultaneously captured. Collectively, we observed nearly identical behavioral patterns among all mice subjected to isoflurane. In total, 50% (n = 2/4) of *Cilk1*$^{+/-}$, 15% (n = 2/13) of *Cilk1*$^{R272Q/+}$, 50% (n = 1/2) of WT littermate controls for *Cilk1*$^{+/-}$, and 50% (n = 1/2) of WT littermate controls for *Cilk1*$^{R272Q/+}$ exhibited moderate head bobbing, tail extension, and occasional back and/or neck arching. These behavioral reactions were similarly consistent with opisthotonos but did not associate with any particular genotype. Importantly, the opisthotonos-like behavior did not align with any corresponding electrographic activity consistent with generalized tonic–clonic seizures in the ECoG/EMG recordings (Figs. 2B-D); when present, generalized tonic–clonic seizures are readily apparent in the ECoG spectrogram. Thus, our data do not support the hypothesis that isoflurane induces generalized tonic–clonic seizures in either *Cilk1*$^{+/-}$ or *Cilk1*$^{R272Q/+}$ mice.

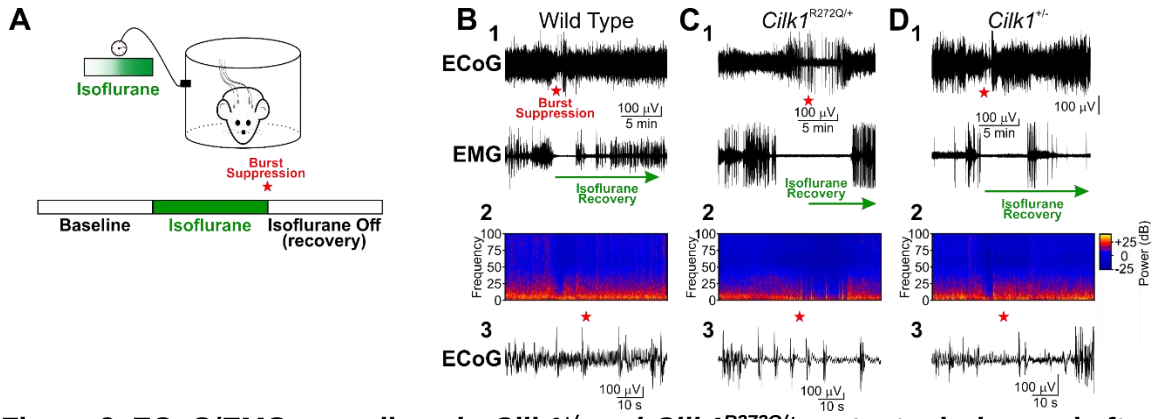

Figure 2. ECoG/EMG recordings in *Cilk1*$^{+/-}$ and *Cilk1*$^{R272Q/+}$ mutants during and after isoflurane exposure is consistent with opisthotonos, not JME. **(A)** Mice were placed in a plethysmography chamber that enabled controlled delivery of isoflurane. Baseline ECoG/EMG activity was recorded for 45 min, after which isoflurane (1.5% or 5%) was delivered to the chamber. Once burst suppression was observed in the ECoG, isoflurane delivery was halted and the animal was allowed to recover. Opisthotonos generally occurs within a few minutes of isoflurane recovery. **(B–D)** ECoG/EMG activity of a **(B)** wildtype, **(C)** *Cilk1*$^{+/-}$, and **(D)** *Cilk1*$^{R272Q/+}$ mouse before, during, and after 1.5% isoflurane exposure. (1) Compressed recordings of ECoG/EMG. Red star indicates occurrence of burst suppression. Green arrow indicates period of isoflurane recovery. Note the suppression of all muscle activity surrounding burst suppression occurrence. (2) Spectrogram of ECoG recording in (1). ECoG signals are generally enriched in low-frequency components indicative of resting or sleeping behaviors. The spectrograms show no generalized tonic–clonic activity. (3) Expanded ECoG trace showing burst suppression.

Discussion

Here, we investigated whether heterozygous *Cilk1* null mice, or mice harboring the non-functional *Cilk1* R272Q mutation, have seizure phenotypes consistent with JME. Chronic ECoG/EMG recordings revealed that *Cilk1*$^{+/-}$ and *Cilk1*$^{R272Q/+}$ mice do not generate spontaneous generalized tonic–clonic seizures but do occasionally produce electrographic JME-like events. However, these infrequent electrographic events occurred at the same rate as in wildtype littermates. We also tested the hypothesis that recovery from isoflurane induces tonic–clonic seizures in *Cilk1*$^{+/-}$ and *Cilk1*$^{R272Q/+}$ mice, as previously reported (Bailey et al., 2018). While some mice produced opisthotonos during isoflurane recovery, electrographic seizure activity was absent. In mice, opisthotonos is commonly associated with exposure to anesthesia (Komatsu & Ogli, 1987). In sum, our data do not support the hypothesis that heterozygous *Cilk1* null mice or mice heterozygous for a non-functional pathogenic *Cilk1* R272Q variant have JME.

Juvenile myoclonic epilepsy is the most common form of the *Genetic Generalized Epilepsies* and accounts for 12% to 30% of epilepsies cared for in hospitals and clinics (Delgado-Escueta, 2007). Imaging studies have revealed that the brains of JME patients present with altered structural connectivity (Vulliemoz et al., 2011), more cortical grey matter (Woermann et al., 1999), and abnormal hippocampal structure and function (Caciagli et al., 2019). Consistent with structural abnormalities, genetic screens have identified the cilia protein myoclonin1/EFHC1, a microtubule-associated protein involved in regulation of cell division, as the most frequent cause of JME (Delgado-Escueta, 2007; Medina et al., 2008; Suzuki et al., 2004). Recent evidence linking *CILK1* mutations to JME underscores the potential importance of cilia in regulating the excitability of neural circuits. Bailey et al. recently identified several *CILK1* variants in JME patients and also showed that *Cilk1* haploinsufficiency in mice produces convulsions and electrographic events (i.e., spikes) associated with JME (Bailey et al., 2018); notably, only three recording days were

sufficient to resolve seizures in *Cilk1* mutant mice. By contrast, our data do not support a role for either *Cilk1* haploinsufficiency or *Cilk1*$^{R272Q/+}$ mutations as epileptogenic. While we only quantified EEG patterns from 48 continuous hours of recording, these data are representative of the ECoG/EMG activity observed over 7 days. While we did not observe a robust seizure phenotype in *Cilk1* mutant mice, we believe that concluding that *Cilk1* mutations do not form an underlying cause of JME is premature. First, differences in the mouse genetic background (i.e., BL6J versus BL6N substrains) can contribute to discrepant seizure phenotypes (Kang et al., 2019). However, seizure phenotype is nevertheless often clear across strains for highly penetrant mutations (Kang et al., 2019). Thus, one might expect that *CILK1* mutations strongly linked to JME, including those that impair mitosis, cell-cycle exit, and radial neuroblast migration, would also produce seizures in multiple mouse substrains. Second, not all *CILK1* mutations produce overt ciliary phenotypes. Notably, neither *Cilk1* haploinsufficiency nor *Cilk1*$^{R272Q/+}$ mutations affect cilia growth (Medina et al., 2008; Moon et al., 2014; Tong et al., 2017). An intriguing hypothesis is that only those *CILK1* mutations that alter cilia morphology produce JME.

CILK1 has a conserved role in the control of cilia formation and length (Fu et al., 2019). Knocking out both *Cilk1* alleles in mice is required to reproduce developmental phenotypes associated with altered cilia morphology and Hedgehog signaling (Chaya et al., 2014; Moon et al., 2014). In contrast, single *Cilk1* allele deletion does not produce an obvious molecular or cellular phenotype, a conclusion supported by our observation that the cortical activity of *Cilk1*$^{+/-}$ mice was normal.

We have recently demonstrated that overexpression of JME-associated *CILK1* variants causes exuberant cilia formation and growth in vitro (Wang et al., 2020), indicating that single residue mutations exert a dominant-negative effect on CILK1 function (wildtype CILK1 restrains cilia growth). We speculate that JME-associated phenotypes will primarily track with those *CILK1* mutations that produce overt morphological changes to cilia. Such

mutations are more likely to produce deficits in neuronal maturation and migration, thereby possibly resulting in improper neural circuit formation and epilepsy. Indeed, cilia dysfunction resulting from the selective loss of ciliary GTPase Arl13b affects cilia growth and also reduces the morphological complexity of parvalbumin-positive interneurons (Guo et al., 2017), a subset of inhibitory neurons implicated in multiple forms of epilepsy (Arkan et al., 2019; Magloire et al., 2019; Panthi & Leitch, 2019). Similarly, we hypothesize that *CILK1* variants that promote ciliary growth by dominant-negative mechanisms will promote similar interneuronal deficits that promote JME. Creating new rodent models harboring JME-associated *Cilk1* variants, and subsequently evaluating cilia morphology, interneuronal excitability, and seizure phenotype in these mice, will be necessary to test this hypothesis.

Conclusions

We are now learning that many gene mutations associated with epilepsy do not neatly fall into categories that obviously regulate neural excitability. Indeed, some have proposed that “entirely new mechanisms of epilepsy” may be identified by investigating the cell biology of epilepsy-associated genes that do not encode inhibitory or excitatory ion channels (Staley, 2015). *CILK1* represents such a gene. We anticipate future studies to resolve how a highly conserved protein critical for fundamental cell biological processes regulates cilia function in the brain and, ultimately, interneuron maturation and neural circuit excitability.

Materials and Methods

Animals

Unless otherwise stated, animals were housed at 23–25 °C under an artificial 12 h light–dark cycle with food and water provided ad libitum. *Cilk1*$^{R272Q/+}$ and *Cilk1*$^{+/-}$ mice [9,12] were maintained on a C57BL6/J background in the animal facilities at the University of Virginia Medical Center (Charlottesville, VA, USA). We performed experiments in mice aged P60–80. Mice of both sexes were used in all experiments—no noticeable differences were observed.

Electrocorticography (ECoG)/Electromyographic (EMG) Surgery

Mouse recording devices were assembled from parts purchased at Digikey (Thief River, MN, USA). Recording devices were outfitted with insulated stainless steel wire (A-M system, Sequim, WA, USA) and stainless steel screws (Plastics One, Roanoke, VA, USA). Recording electrodes were implanted bilaterally in the cortex under 1–3% isoflurane. A reference electrode was placed in the cerebellum. A singular wire was sutured to the superficial neck muscle to obtain EMG recordings. Recording devices were secured to the skull with dental cement, and incisions were closed with sutures. Following surgery, animals received a subcutaneous injection of ketaprofen (5 mg/kg) and recovered for a minimum of 1 week before video-ECoG/EMG recording.

Chronic Electrocorticography (ECoG)/Electromyographic (EMG) Recordings

Before experimentation, animals were habituated to recording cages for 48 h. ECoG/EMG signals were captured using a cable tethered to a rotating commutator (Adafruit, New York, NY). To reduce movement artifact, operational amplifiers (TL2274x Texas Instruments, Dallas, TX, USA) were fixed within the recording cable. ECoG and EMG signals were filtered between 0.3 and 100 Hz and between 100 and 1000 Hz, respectively, amplified with a Model 3500 amplifier (A-M Systems), and sampled at 200 Hz with a

PowerLab digitizer (ADI Instruments, Colorado Springs, CO, USA). ECoG/EMG recordings were captured using LabChart software (ADI Instruments). Video was captured using Webcam Zone Trigger software (Montreal, Quebec, CA). Chronic ECoG/EMG recordings were restarted after every 24 h for 3 days.

Electrocorticography (ECoG)/Electromyographic (EMG) Recording with Isoflurane

Mice were habituated to a vacuum-sealed plethysmography recording cage for 1–2 h before the day of experimentation. Recordings were performed during hours 0–12 of the 12 h light–dark cycle. On the experiment day, a 45 min baseline recording was performed with the mice exposed to room air. Subsequently, mice were exposed to two isoflurane treatments, 1.5% and 5%, interspersed with a 45 min recovery period. Isoflurane treatment stopped once burst suppression was observed in the ECoG recording. Isoflurane was rapidly expelled from the recording chamber with 100% O_2 and room air. ECoG/EMG signals and video were captured as stated previously.

References

Arkan, S., Kasap, M., Akman, Ö., Akpınar, G., Ateş, N., & Karson, A. (2019). The lower expression of parvalbumin in the primary somatosensory cortex of WAG/Rij rats may facilitate the occurrence of absence seizures. *Neuroscience Letters*, *709*, 134299. https://doi.org/10.1016/j.neulet.2019.134299

Bailey, J. N., Nijs, L. de, Bai, D., Suzuki, T., Miyamoto, H., Tanaka, M., Patterson, C., Lin, Y.-C., Medina, M. T., Alonso, M. E., Serratosa, J. M., Durón, R. M., Nguyen, V. H., Wight, J. E., Martínez-Juárez, I. E., Ochoa, A., Jara-Prado, A., Guilhoto, L., Molina, Y., … Delgado-Escueta, A. V. (2018). Variant Intestinal-Cell Kinase in Juvenile Myoclonic Epilepsy. *New England Journal of Medicine*. https://doi.org/10.1056/NEJMoa1700175

Caciagli, L., Wandschneider, B., Xiao, F., Vollmar, C., Centeno, M., Vos, S. B., Trimmel, K., Sidhu, M. K., Thompson, P. J., Winston, G. P., Duncan, J. S., & Koepp, M. J. (2019). Abnormal hippocampal structure and function in juvenile myoclonic epilepsy and unaffected siblings. *Brain: A Journal of Neurology*, *142*(9), 2670–2687. https://doi.org/10.1093/brain/awz215

Chaya, T., Omori, Y., Kuwahara, R., & Furukawa, T. (2014). ICK is essential for cell type-specific ciliogenesis and the regulation of ciliary transport. *The EMBO Journal*, *33*(11), 1227–1242. https://doi.org/10.1002/embj.201488175

Delgado-Escueta, A. V. (2007). Advances in Genetics of Juvenile Myoclonic Epilepsies. *Epilepsy Currents*, *7*(3), 61–67. https://doi.org/10.1111/j.1535-7511.2007.00171.x

Ding, M., Jin, L., Xie, L., Park, S. H., Tong, Y., Wu, D., Chhabra, A. B., Fu, Z., & Li, X. (2018). A Murine Model for Human ECO Syndrome Reveals a Critical Role of Intestinal Cell Kinase in Skeletal Development. *Calcified Tissue International*, *102*(3), 348–357. https://doi.org/10.1007/s00223-017-0355-3

Fu, Z., Gailey, C. D., Wang, E. J., & Brautigan, D. L. (2019). Ciliogenesis associated kinase 1 (CILK1): Targets and functions in various organ systems. *FEBS Letters*, *593*(21), 2990–3002. https://doi.org/10.1002/1873-3468.13600

Gerdes, J. M., Davis, E. E., & Katsanis, N. (2009). The Vertebrate Primary Cilium in Development, Homeostasis, and Disease. *Cell*, *137*(1), 32–45. https://doi.org/10.1016/j.cell.2009.03.023

Guo, J., Otis, J. M., Higginbotham, H., Monckton, C., Cheng, J., Asokan, A., Mykytyn, K., Caspary, T., Stuber, G. D., & Anton, E. S. (2017). Primary Cilia Signaling Shapes the Development of Interneuronal Connectivity. *Developmental Cell*, *42*(3), 286-300.e4. https://doi.org/10.1016/j.devcel.2017.07.010

Gupta, A., Stierer, T., Zuckerman, R., Sakima, N., Parker, S. D., & Fleisher, L. A. (2004). Comparison of recovery profile after ambulatory anesthesia with propofol, isoflurane, sevoflurane and desflurane: A systematic review. *Anesthesia and Analgesia*, *98*(3), 632–641, table of contents. https://doi.org/10.1213/01.ane.0000103187.70627.57

Kang, S. K., Hawkins, N. A., & Kearney, J. A. (2019). C57BL/6J and C57BL/6N substrains differentially influence phenotype severity in the Scn1a +/- mouse model of Dravet syndrome. *Epilepsia Open*, *4*(1), 164–169. https://doi.org/10.1002/epi4.12287

Kholi, H., Bellier, A., & Vercueil, L. (2020). PNESSE 1: Psychogenic status and status epilepticus: Could they be distinguished retrospectively? A survey among neurologists. *Epilepsy & Behavior*, *102*, 106665. https://doi.org/10.1016/j.yebeh.2019.106665

Komatsu, H., Izumikawa, N., Yoda, K., Morita, J., Chujo, K., Endo, S., Nogaya, J., Ueki, M., & Ogli, K. (1996). Clonic convulsive movements during and on emergence from sevoflurane anesthesia. *Journal of Anesthesia*, *10*, 72–75.

Komatsu, H., & Ogli, K. (1987). Opisthotonus during Exposure to Isoflurane, Enflurane, and Halothane in Mice. *Anesthesiology*, *67*(5), 771–774. https://doi.org/10.1097/00000542-198711000-00022

Komatsu, H., Yokono, S., & Ogli, K. (1988). The central nervous stimulating effect of four different halogenated ether anesthetics and halothane in mice. *Journal of Anesthesia*, *2*(1), 115–117. https://doi.org/10.1007/s0054080020115

Lahiry, P., Wang, J., Robinson, J. F., Turowec, J. P., Litchfield, D. W., Lanktree, M. B., Gloor, G. B., Puffenberger, E. G., Strauss, K. A., Martens, M. B., Ramsay, D. A., Rupar, C. A., Siu, V., & Hegele, R. A. (2009). A Multiplex Human Syndrome Implicates a Key Role for Intestinal Cell Kinase in Development of Central Nervous, Skeletal, and Endocrine Systems. *American Journal of Human Genetics*, *84*(2), 134–147. https://doi.org/10.1016/j.ajhg.2008.12.017

Lerche, H., Berkovic, S. F., Lowenstein, D. H., EuroEPINOMICS-CoGIE Consortium, EpiPGX Consortium, & Epi4K Consortium/Epilepsy Phenome/Genome Project. (2019). Intestinal-Cell Kinase and Juvenile Myoclonic Epilepsy. *The New England Journal of Medicine*, *380*(16), e24. https://doi.org/10.1056/NEJMc1805100

Magloire, V., Mercier, M. S., Kullmann, D. M., & Pavlov, I. (2019). GABAergic Interneurons in Seizures: Investigating Causality With Optogenetics. *The Neuroscientist: A Review Journal Bringing Neurobiology, Neurology and Psychiatry*, *25*(4), 344–358. https://doi.org/10.1177/1073858418805002

Medina, M. T., Suzuki, T., Alonso, M. E., Durón, R. M., Martínez-Juárez, I. E., Bailey, J. N., Bai, D., Inoue, Y., Yoshimura, I., Kaneko, S., Montoya, M. C., Ochoa, A., Prado, A. J., Tanaka, M., Machado-Salas, J., Fujimoto, S., Ito, M., Hamano, S., Sugita, K., … Delgado-Escueta, A. V. (2008). Novel mutations in Myoclonin1/EFHC1 in sporadic and familial juvenile myoclonic epilepsy.

Neurology, *70*(22 Part 2), 2137–2144. https://doi.org/10.1212/01.wnl.0000313149.73035.99

Moon, H., Song, J., Shin, J.-O., Lee, H., Kim, H.-K., Eggenschwiller, J. T., Bok, J., & Ko, H. W. (2014). Intestinal cell kinase, a protein associated with endocrine-cerebro-osteodysplasia syndrome, is a key regulator of cilia length and Hedgehog signaling. *Proceedings of the National Academy of Sciences of the United States of America*, *111*(23), 8541–8546. https://doi.org/10.1073/pnas.1323161111

Oud, M. M., Bonnard, C., Mans, D. A., Altunoglu, U., Tohari, S., Ng, A. Y. J., Eskin, A., Lee, H., Rupar, C. A., de Wagenaar, N. P., Wu, K. M., Lahiry, P., Pazour, G. J., Nelson, S. F., Hegele, R. A., Roepman, R., Kayserili, H., Venkatesh, B., Siu, V. M., … Arts, H. H. (2016). A novel ICK mutation causes ciliary disruption and lethal endocrine-cerebro-osteodysplasia syndrome. *Cilia*, *5*, 8. https://doi.org/10.1186/s13630-016-0029-1

Paige Taylor, S., Kunova Bosakova, M., Varecha, M., Balek, L., Barta, T., Trantirek, L., Jelinkova, I., Duran, I., Vesela, I., Forlenza, K. N., Martin, J. H., Hampl, A., Bamshad, M., Nickerson, D., Jaworski, M. L., Song, J., Ko, H. W., Cohn, D. H., Krakow, D., & Krejci, P. (2016). An inactivating mutation in intestinal cell kinase, ICK, impairs hedgehog signalling and causes short rib-polydactyly syndrome. *Human Molecular Genetics*, *25*(18), 3998–4011. https://doi.org/10.1093/hmg/ddw240

Panthi, S., & Leitch, B. (2019). The impact of silencing feed-forward parvalbumin-expressing inhibitory interneurons in the cortico-thalamocortical network on seizure generation and behaviour. *Neurobiology of Disease*, *132*, 104610. https://doi.org/10.1016/j.nbd.2019.104610

Purdon, P. L., Sampson, A., Pavone, K. J., & Brown, E. N. (2015). Clinical Electroencephalography for Anesthesiologists: Part I: Background and Basic

Signatures. *Anesthesiology*, *123*(4), 937–960. https://doi.org/10.1097/ALN.0000000000000841

Reiter, J. F., & Leroux, M. R. (2017). Genes and molecular pathways underpinning ciliopathies. *Nature Reviews. Molecular Cell Biology*, *18*(9), 533–547. https://doi.org/10.1038/nrm.2017.60

Sadan, O., Neufeld, M. Y., Parmet, Y., Rozenberg, A., & Kipervasser, S. (2016). Psychogenic seizures: Long-term outcome in patients with and without epilepsy. *Acta Neurologica Scandinavica*, *133*(2), 145–151. https://doi.org/10.1111/ane.12458

Staley, K. (2015). Molecular mechanisms of epilepsy. *Nature Neuroscience*, *18*(3), 367–372. https://doi.org/10.1038/nn.3947

Stokes, E. L., Flecknell, P. A., & Richardson, C. A. (2009). Reported analgesic and anaesthetic administration to rodents undergoing experimental surgical procedures. *Laboratory Animals*, *43*(2), 149–154. https://doi.org/10.1258/la.2008.008020

Suzuki, T., Delgado-Escueta, A. V., Aguan, K., Alonso, M. E., Shi, J., Hara, Y., Nishida, M., Numata, T., Medina, M. T., Takeuchi, T., Morita, R., Bai, D., Ganesh, S., Sugimoto, Y., Inazawa, J., Bailey, J. N., Ochoa, A., Jara-Prado, A., Rasmussen, A., … Yamakawa, K. (2004). Mutations in EFHC1 cause juvenile myoclonic epilepsy. *Nature Genetics*, *36*(8), 842–849. https://doi.org/10.1038/ng1393

Tong, Y., Park, S. H., Wu, D., Xu, W., Guillot, S. J., Jin, L., Li, X., Wang, Y., Lin, C.-S., & Fu, Z. (2017). An essential role of intestinal cell kinase in lung development is linked to the perinatal lethality of human ECO syndrome. *FEBS Letters*, *591*(9), 1247–1257. https://doi.org/10.1002/1873-3468.12644

Uygun, D. S., Katsuki, F., Bolortuya, Y., Aguilar, D. D., McKenna, J. T., Thankachan, S., McCarley, R. W., Basheer, R., Brown, R. E., Strecker, R. E., & McNally, J. M.

(2019). Validation of an automated sleep spindle detection method for mouse electroencephalography. *Sleep*, *42*(2). https://doi.org/10.1093/sleep/zsy218

Vulliemoz, S., Vollmar, C., Koepp, M. J., Yogarajah, M., O'Muircheartaigh, J., Carmichael, D. W., Stretton, J., Richardson, M. P., Symms, M. R., & Duncan, J. S. (2011). Connectivity of the supplementary motor area in juvenile myoclonic epilepsy and frontal lobe epilepsy. *Epilepsia*, *52*(3), 507–514. https://doi.org/10.1111/j.1528-1167.2010.02770.x

Wang, E. J., Gailey, C. D., Brautigan, D. L., & Fu, Z. (2020). Functional Alterations in Ciliogenesis-Associated Kinase 1 (CILK1) that Result from Mutations Linked to Juvenile Myoclonic Epilepsy. *Cells*, *9*(3), 694. https://doi.org/10.3390/cells9030694

Woermann, F. G., Free, S. L., Koepp, M. J., Sisodiya, S. M., & Duncan, J. S. (1999). Abnormal cerebral structure in juvenile myoclonic epilepsy demonstrated with voxel-based analysis of MRI. *Brain: A Journal of Neurology*, *122 (Pt 11)*, 2101–2108. https://doi.org/10.1093/brain/122.11.2101

Youn, Y. H., & Han, Y.-G. (2018). Primary Cilia in Brain Development and Diseases. *The American Journal of Pathology*, *188*(1), 11–22. https://doi.org/10.1016/j.ajpath.2017.08.031

Chapter 6: Conclusion

Research summary

My dissertation aimed to debunk the opinion that unpredictable shifts in neuronal activity cause a seizure. I sought to advance the hypothesis that certain external factors provoke *foreseeable* changes in neuronal activity patterns that precipitate seizures. Once aware of the underlying cause, one can then better anticipate or stop the forthcoming epileptic episode. The long-held belief that epilepsy arises from channelopathies or dysfunctional neurotransmission is no longer an acceptable dogma. Most clinically used anti-seizure drugs that target ion channels or neurotransmitter receptors fail to treat ~30% of epilepsy patients. Moreover, successful management of seizures in ~60% of patients is misleading as anti-seizure drugs have serious side-effects that diminish quality of life (French & Pedley, 2009; Manford, 2017).

With regards to childhood absence epilepsy, the anti-seizure drugs, ethosuximide, valproic acid and lamotrigine are generally effective when used alone or in combination (Glauser et al., 2013; Kim et al., 2015), yet 5-10% of absence patients remain refractory to these treatments. Unlike in focal epilepsies, like temporal lobe epilepsy, neurosurgeons cannot cut out a seizure focus in absence patients; hence, pharmacological intervention remains the only option. Sadly, absence seizure remission only hovers around 50% (Glauser et al., 2013; Kim et al., 2015; Matricardi et al., 2014) and the permanent effects blunt, pharmacological hammers have on young, developing brains warrants more attention. Why 5-10% of absence patients remain untreatable points to our limited knowledge of this idiopathic epilepsy syndrome. Indeed, more work still needs to be done, but how do we achieve better treatment options?

The necessity for better absence seizure therapies motivated me to re-examine neglected clinical observations that provided evidence for external factors capable of

provoking absence seizures. I chose two factors, metabolism and respiration. Although distinct, both changes in metabolism and respiration invoke the same neural networks to precipitate a spike-wave seizure. My studies have demonstrated that metabolism and respiration act on different, but critical, gateways of spike-wave seizure genesis within the thalamus.

My first project, detailed in **Chapter 2**, aimed to investigate a mechanism to elucidate why hypoglycemia triggers spike-wave seizures in absence epilepsy patients (Gibbs et al., 1939). Even more curious, hypoglycemia in the brain of GLUT1 deficient patients also sparks spike-wave seizures (Arsov et al., 2012; Mullen et al., 2010). I showed that hypoglycemia-induced seizures appear in two rodent models of spike-wave seizures, the DBA/2J mouse and the WAG/Rij rat. I demonstrated that this effect likely depends on the interaction between the cellular energy sensor AMPK and the $GABA_B$ receptor. As highlighted in **Chapter 1**, $GABA_B$ receptor signaling plays an essential role in facilitating hypersynchronous activity within the thalamocortical circuit (Crunelli & Leresche, 1991; Lu et al., 2020; Vergnes et al., 1997; von Krosigk et al., 1993). Based on this knowledge, I hypothesized that activated AMPK enhances $GABA_B$ receptor activity during instances of acute hypoglycemia and, thus, drives an increase in spike-wave seizures. My study was the first to demonstrate that an energy sensitive molecule has the ability to alter neuronal activity in spike-wave seizure circuits. Further implications of this study and potential future directions will be discussed at length below.

In parallel, I worked to adapt the human phenomenon of hyperventilation-induced seizures to a rat model of absence epilepsy, the WAG/Rij rat. I took advantage of being in a special scientific setting that possesses expertise in respiratory physiology, pH-modulation of neuronal activity, and epilepsy. Consequently, I was able to successfully combine plethysmography and electrocorticography (ECoG) recordings to produce hyperventilation-triggered seizures in the WAG/Rij rat. My new model allowed me to

assess whether respiratory alkalosis, incurred by hyperventilation, is sufficient to trigger spike-wave seizures. My results, described in **Chapter 4**, demonstrate that spike-wave seizures are likely PCO_2 sensitive. I observed that hypocapnia increased spike-wave seizure count and hypercapnia decreased seizure counts. Additionally, my data support the hypothesis that hyperventilation, without hypocapnia, does not aggravate spike-wave seizures. Significantly, hypocapnia was unable to precipitate spike-wave seizures in the non-epileptic Wistar rat, thereby suggesting that spike-wave seizure circuits in the WAG/Rij rat are inherently sensitive to hypocapnia. I concluded this study with provocative data showing that hypocapnia activated neurons of the midline thalamus. The midline thalamic nuclei have not been considered active participants in the origin of spike-wave seizures since the 1980s. I am excited to see future studies explore this intriguing observation.

Altogether, I used metabolism and respiration as a strategy to understand how specific factors can perturb normal thalamocortical circuit activity into a state that begets spike-wave seizures. Indeed, by using acute hypoglycemia, I have uncovered that AMPK and $GABA_B$ receptors act together, in an energy-dependent manner, to modulate thalamic neuron and thalamocortical circuit activity. Secondly, the conclusions gained from my exploration into hyperventilation-triggered seizures has once more brought the midline thalamus to the forefront as a key constituent in spike-wave seizure genesis. Furthermore, my data support the hypothesis that human spike-wave seizures are indeed sensitive to hypocapnia (Wirrell et al., 1996). I believe that my studies have created a launch point for future work to unveil new mechanisms that delineate how metabolism and respiration modulate spike-wave seizures. I am optimistic that my approach of using external factors will become more common in epilepsy research as others aim to demystify pro-seizure mechanisms in other epilepsy syndromes. In the following sections, I will discuss the

implications of my work and speculate on possible future directions that could complement my findings.

Implications: metabolism and absence epilepsy

The brain cannot function without glucose. Remarkably, the brain consumes 20% of the body's total calories at rest, which exceeds the demand of any other organ (Magistretti & Allaman, 2015; Rho et al., 2019). This amount is excessive relative to its size, yet this makes sense, as the central nervous system is likely the most active structure in our body, on par with the heart. Epileptic activity imposes greater demand on glucose metabolism due to brain network hyperexcitability. Seizures impose greater energetic demands on neuronal glucose metabolism as well as astrocytes, which help shuttle energy metabolites to neurons (Magistretti & Allaman, 2015). Epilepsy therapies that invoke metabolism as an anti-convulsive agent largely rely on limiting the pool of available glucose to feed excessive neuronal activity.

The most common metabolic therapy is the ketogenic diet. The ketogenic diet forces the brain to adapt to using ketone bodies as fuel instead of glucose (Kristopher & Carl, 2010). The impact of the ketogenic diet on brain metabolism is diverse (Yudkoff et al., 2012) and may different components of the diet have been considered to be anti-convulsive (Lutas & Yellen, 2013; Rho et al., 2019; Yudkoff et al., 2012). A second approach is 2-deoxyglucose (2-DG). Although not yet approved for clinical use, clinic trials in epilepsy patients (unpublished, Fountain et al., University of Virginia) and data from rodent models of epilepsy support 2-DG as an effective anti-seizure therapy (Garriga-Canut et al., 2006; Pan et al., 2019; Stafstrom et al., 2008). The last factor I will highlight is metformin and lactate. Repurposing metformin as an anti-seizure drug is a newer method of metabolic intervention to control seizures. However, metformin does have an FDA black-box warning as it can cause metformin-associated lactic acidosis (MALA)

(Boucaud-Maitre et al., 2016; DeFronzo et al., 2016) . Elevated lactate is also a marker of seizure activity in the brain. Conflicting evidence exists for the anti- or pro-convulsive actions of lactate. All these approaches were touched upon by my study in **Chapter 2.** Herein, I will address the implications of my findings and how they relate to the current literature.

The ketogenic diet

The effect of cellular metabolism on epilepsy is well-known but the cellular and circuit-level mechanisms that drive seizures during instances of metabolic dysfunction are unclear. However, not all elements of metabolism become pro-seizure. The clinical use of the ketogenic diet (a traditional high-fat, low carbohydrate diet) reduces seizures, even in refractory epilepsies, and stymies seizure progression (Masino & Rho, 2012; Ruskin & Masino, 2012; Wilder RM, 1921). I mention the ketogenic diet to highlight a paradox: low glucose abates seizures in many epilepsies, but my study and others demonstrate that low glucose exacerbated spike-wave seizures.

I believe that the acute effects of hypoglycemia on spike-wave seizures, as shown in my work, cannot be directly compared to evidence that supports the ketogenic diet as a moderately effective absence seizure therapy (Groomes et al., 2011; Ross et al., 1985; Thammongkol et al., 2012). However, I only examined spike-wave seizure activity following <u>acute</u> hypoglycemia induced by an overnight fast. I speculate that the pro-seizure actions of acute hypoglycemia recruit metabolic actions distinct from those during long-term adherence to the ketogenic diet. Moreover, many studies on epilepsy and the ketogenic diet demonstrate that ketone bodies have anti-convulsive effects (Masino & Rho, 2012; Rho et al., 2019), yet these observations were made in the context of limbic epilepsies (Ma et al., 2007; Tanner et al., 2011; Yellen, 2008).

My data, presented in **Chapter 2**, did not support the hypothesis that ketone bodies are seizure protective (Ma et al., 2007; Tanner et al., 2011; Yellen, 2008). However, I did not test ketone bodies independent of hypoglycemia. Future work from our lab and others should more thoroughly investigate ketone body metabolism within the thalamocortical circuit. On a final note, few studies, to my knowledge, have evaluated the efficacy of the ketogenic diet in rodent models of absence epilepsy. Unfortunately, the conclusions drawn from prior work are conflicting (Kovács et al., 2019; Nehlig et al., 2009), but may be attributed to the use of different rat models, the GAERS (Genetic Absence Epilepsy Rat from Strasbourg) versus the WAG/Rij rat.

All things considered, the mechanism(s) of action for the ketogenic diet are not well-understood and we need more clarity on how it behaves in all epilepsies. In light of my observations, I believe that the anti-convulsive properties of the ketogenic diet could be effective in treating absence seizures, but more studies in animal models must be pursued to elucidate how long-term ketosis affects energy metabolism in neurons and glia. Moreover, even if we learn that the ketogenic diet is *ineffective* in treating absence seizures, such knowledge would nonetheless likely provide new insights into thalamic neuron metabolism.

2-Deoxyglucose

A second prospective epilepsy therapy that invokes elements of glucose metabolism is 2-deoxyglucose (2-DG). Glycolysis powers neuronal activity to produce the necessary intermediaries for downstream oxidative metabolism (Bélanger et al., 2011; Brekke et al., 2015; Dienel, 2018) and 2-DG acts to inhibit glycolysis by preventing the conversion of glucose into glucose-6-phosphate (Wick et al., 1957). Consequently, 2-DG decreases glycolytic flux and reduces the main source of cellular energy, ATP. In the context of epilepsy, less available fuel would decrease the probability of seizure-like

activity to emerge. What makes the use of 2-DG more appealing than the ketogenic diet is that 2-DG mimics a low-glucose environment without inducing ketosis. Effectively, 2-DG avoids the many side-effects of the ketogenic diet and precludes adherence to a very restrictive diet. Another advantage of 2-DG is that it is primarily taken up in cells with the highest energy demand. In epilepsy, a proposed hypothesis suggests that 2-DG treatment would preferentially target seizure foci or brain structures that become hyperactive (Stafstrom et al., 2008, 2009).

The rationale for 2-DG being anti-convulsive stems mostly from *in vitro* and *in vivo* experiments performed in rodent models of epilepsy. When applied to a pharmacological model of seizure-like activity in acute hippocampal slices (high $[K^+]_o$), 2-DG reduced the frequency of ictal and inter-ictal epileptiform bursts in field recordings obtained from the CA3 region (Stafstrom et al., 2008). Another group demonstrated that 2-DG reduced excitatory transmission when applied in the same acute hippocampal slice model (Pan et al., 2019). Moreover, Pan et al., showed that 2-DG did not disrupt normal synaptic activity in “non-epileptic” slices (Pan et al., 2019). The effect of 2-DG reducing seizures *in vivo* is also encouraging in most animals models of temporal lobe epilepsy (Garriga-Canut et al., 2006; Stafstrom et al., 2008, 2009).

Notably, my study demonstrated 2-DG to be pro-seizure in a rat model of absence epilepsy. I draw attention to these controversial findings because my results in **Chapter 2** challenge the hypothesis that 2-DG is an anti-convulsant (see **Chapter 2, Figure 2**). I postulated that 2-DG would make spike-wave seizures worse, as low glucose aggravates spike-wave seizures. Moreover, I hypothesized that local 2-DG infusion in the thalamus would increase spike-wave seizures because 2-DG application likely boosts inhibition mediated by metabotropic $GABA_B$ receptors. One caveat in my experimental design is that I only examined the effect of 2-DG in the thalamus, one arm of the thalamocortical, spike-wave seizure network. My study did not address how 2-DG would affect activity in the

cortex. Perhaps, if simultaneously delivered to the cortex and thalamus, the net effect of 2-DG on thalamocortical circuit activity would be null.

In sum, low glucose, either driven by 2-DG, insulin or an overnight fast (data in **Chapter 2, Figures 1, 2**), exacerbated spike-wave seizures in the WAG/Rij rat. Taken together, hypoglycemia should be avoided in absence epilepsy patients. I propose that a dietary therapy for absence epilepsy may be akin to that of diabetes patients. Both patient populations should be cognizant of their blood glucose levels. Additionally, correlating instances of large blood glucose fluctuations to spike-wave seizure occurrence could help a patient preemptively act to avoid subsequent seizures.

Metformin and lactate

Metformin is used by 120 million people worldwide for the treatment of type 2 diabetes (Viollet et al., 2012). The ability of metformin to effectively control glucose metabolism has also become a viable therapy in cancer treatment, as it effectively starves tumors and prevents hyperinsulinemia (Viollet et al., 2012). The epilepsy field has started to investigate whether metformin can be repurposed to treat seizures. Several studies have tested the hypothesis that metformin can act as an anti-seizure drug, as its mechanism of action shares similarities to the ketogenic diet and 2-DG. In addition to metformin's ability to prevent unstable blood glucose levels, it also has anti-inflammatory and anti-oxidant properties, as well as the ability to activate AMPK. Recent work has shown that metformin suppresses tonic-clonic seizures (Hussein et al., 2019; Zhao et al., 2014) in the pentylenetetrazol (PTZ)-induced kindling model (Brueggeman et al., 2019; Hussein et al., 2019; Yang et al., 2017; Zhao et al., 2014) and the pilocarpine, intrahippocampal kainate and amygdala kindling models of temporal lobe epilepsy (Mehrabi et al., 2018; Rubio Osornio et al., 2018; Yang et al., 2017).

Nonetheless, the anti-convulsive actions of metformin stick to the common recurring theme in my work: what works for some seizures does not work for all. I used metformin, in my study, as a means to support the hypothesis that activated AMPK augments $GABA_B$-mediated synchronous activity in the thalamus (see **Chapter 2, Figure 4**). Indeed, metformin increased the duration of thalamic oscillations in acute thalamic slices and increased the expression of spike-wave seizures *in vivo*. As discussed previously (**Chapter 2,** *Discussion*), at high doses metformin also induced fatal, convulsive seizures (**Chapter 2, Figure 5**). I attributed this shocking result to metformin-associated lactic acidosis. I hypothesized that metformin's ability to activate AMPK and increase lactate lead to the robust seizure response observed in my study.

The implications for metformin and absence epilepsy are two-fold. First, metformin promotes functional coupling between $GABA_B$-receptors and GIRK channels in an AMPK-dependent manner (Kuramoto et al., 2007; see **Chapter 2, Figs. 3, 4**). Potentiation of $GABA_B$ receptor signaling in thalamocortical neurons promotes hypersynchronous activity and spike-wave seizures. Therefore, instances of cellular stress that activate AMPK, such as acute hypoglycemia, may contribute to more absence seizures. Second, the elevated lactate levels recorded after metformin injection (see **Chapter 2, Figure 5**) may also strengthen $GABA_B$ receptor signaling.

Recently, Abrantes et al., demonstrated that the lactate receptor HCAR1 augments $GABA_B$ receptor function (Abrantes et al., 2019). HCAR1 and $GABA_B$ receptors are both G_i-coupled GPCRS and are able to modify each other (Werry et al., 2003) and both act to inhibit neuronal activity. The authors discovered that HCAR1 and $GABA_B$ receptors interact at the $G_{i\alpha}$ and $G_{i\beta\gamma}$ subunits (Abrantes et al., 2019). We showed that application of the HCAR1 agonist, 3-chloro-5-hydroxybenzoic acid, prolonged thalamocortical oscillation duration (see **Chapter 2, Figure 5**). The novel findings described in **Chapter 2** are the first to explore the actions of lactate on the thalamocortical circuit.

Notably, acute hypoglycemia causes the brain to rely more on lactate for maintenance of neuronal activity (Magistretti & Allaman, 2018). Astrocytes breakdown glycogen to produce lactate as a fast intermediary to replenish pyruvate and NAD^+ levels (Bélanger et al., 2011). Regeneration of NAD^+ is needed to maintain glycolytic flux, and pyruvate is an intermediary necessary for aerobic respiration (Magistretti & Allaman, 2018). Indeed, it is hypothesized that patients with GLUT1 deficiency syndrome primarily rely on lactate and other monocarboxylates for brain fuel (Taher et al., 2016). I hypothesize that the increased demand for lactate, during hypoglycemia, leads to higher extracellular lactate as it is shuttled between astrocytes and neurons. Consequently, increased HCAR1 activation may be sufficient to augment $GABA_B$-receptor activity. Future investigation on the role of lactate in thalamic neurons is a path worth pursuing.

Future Directions

Below, I propose several experiments that aim to build on my findings. The potential avenues I recommend will lead to new observations that elucidate how energetic stress modulates thalamic neuron activity.

1. *Assess the response of hyperglycemia on spike-wave seizures*. Though elementary, my rational for this experiment is that (a) it's easily achievable and (b) it hones in on glucose being the metabolite that is most critical for spike-wave seizure expression. One should perform these experiments in a rodent model of absence epilepsy, like the WAG/Rij rat. Experimental design would include analyzing blood glucose, serum ketone bodies and spike-wave seizure occurrence in the EEG. Hyperglycemia can be achieved through glucose given via an oral gavage, i.p. injection or reverse microdialysis to target the thalamus exclusively.

2. *Reevaluate the effect of ketone bodies on thalamocortical neurons*. *In vivo* and *in vitro* methods can be used to address whether ketone bodies have any effect on thalamic neuron activity. For example, one can simultaneously infuse ketone bodies, like β-hydroxybutyrate, locally into the thalamus and record EEG. Based on my observations in **Chapter 2, Figs. 1, 2**, I hypothesize that there will be not much effect on spike-wave seizure occurrence. Second, one can employ intracellular patch-clamp recordings and/or field recordings in acute thalamic slices that will measure changes in thalamic neuron firing properties/resting membrane potential, etc. and thalamic oscillations, respectively, in the presence of β-hydroxybutyrate.

3. *Use monocarboxylate transporter (MCT) pharmacology to enhance or inhibit ketone body and/or lactate uptake in neurons*. Ketone bodies and lactate use MCT transporters to gain access across the membranes of neurons. Similar methodology can be used as described in (2). If experiments from (2) reject the hypothesis that ketone bodies modulate thalamic neuron and thalamic oscillations, then one can likely assume that only the degree of lactate transport is being evaluated.

4. *Test the hypothesis that lactate increases $GABA_B$-mediated current amplitude in thalamic neurons*. I posed the hypothesis that activation of the lactate receptor, HCAR1 may act to augment $GABA_B$ receptor function. $GABA_B$ receptor-mediated currents can be evoked in thalamocortical neurons either using methods detailed in **Chapter 2, Figure 3.** Alternatively, $GABA_B$ receptor mediated currents can be synaptically-evoked by electrically stimulating the internal capsule and/or the reticular thalamic nucleus (Beenhakker & Huguenard, 2010). Lactate or lactate receptor agonists can then be washed-on and -off through the perfusate. Current amplitude in control and lactate/HCAR1 activation condition(s) can be measured and compared.

5. *Inhibit lactate dehydrogenase (LDH) in thalamic neurons*. LDH is the critical enzyme that catalyzes the conversion of lactate into pyruvate. Inhibiting LDH *in vivo* or *in vitro* will test the hypothesis that thalamic neurons depend on lactate to maintain normal activity. I hypothesize that LDH inhibition would promote lactate accumulation in the intra- and extra-cellular compartments. This action may be sufficient to recruit the seizure-permissive actions of HCAR1. I recommend using experimental approaches described in (1 & 2).

6. *Test the hypothesis that AMPK acts on presynaptic $GABA_B$ receptors*. Thus far, I have only examined the action of post-synaptic $GABA_B$ receptors. Post-synaptic $GABA_B$ receptors primarily modulate GIRK channels to promote membrane hyperpolarization. Pre-synaptic $GABA_B$ receptors act to inhibit synaptic release of neurotransmitters via inhibition of voltage gated calcium channels. To test this possibility in thalamic neurons, one can measure the paired-pulse ratio (Regehr, 2012) of synaptically evoked $GABA_A$ IPSCs before and after bath application of AMPK activators. The addition of cesium to the internal solution of the recording pipette will block GIRK channels, i.e. $GABA_B$-mediated currents, in the recorded neuron. If IPSC amplitude ratio increases, then this result would support the hypothesis that activated AMPK modulates presynaptic $GABA_B$ receptors.

7. *Test the hypothesis that activated AMPK during acute hypoglycemia is necessary to augment $GABA_B$ receptor function*. Perhaps the most difficult but critical hypothesis to test is whether activated AMPK solely enhances $GABA_B$ receptor activity. First, one should inhibit the actions of lactate to isolate AMPK. Creation of a conditional AMPK knock-out mouse or rat model would permit the experimenter to target specific

populations of neurons in the thalamus. One could measure evoked $GABA_B$ receptor-mediated currents in thalamic neurons (use approach in (4) treated with either standard (10 mM glucose) or low glucose aCSF (5 mM to 1 mM) to mimic acute hyperglycemia. Additionally, one can record the frequency of spike-wave seizures in acute hypoglycemia. If AMPK is necessary to increase $GABA_B$-mediated spike-wave seizures during hypoglycemia, AMPK knock-out animals should have fewer seizures. Ideally, the strain of mouse or rat would already be a model of absence epilepsy, but spike-wave seizures can nonetheless be mimicked using low-dose PTZ or gamma butyrolactone (GBL). As an alternative approach, one could design a siRNA or shRNA to knock-down endogenous AMPK. The siRNA or shRNA can be packaged into a viral vector, like AAV, and injected into the thalamus. Moreover, the viral construct can be designed to target excitatory or inhibitory neurons within the thalamus. After allowing adequate time for robust viral transfection, one can measure spike-wave seizure occurrence. I suggest using the WAG/Rij rat or another rodent model of absence epilepsy.

In aggregate, these experiments will reveal greater insight into the novel properties of thalamic neuron metabolism and its effect on thalamocortical circuit activity. Subsequent studies can use the results from these suggested experiments to inform how new metabolic therapies can be applied to childhood absence epilepsy.

Implications: PCO_2 and spike-wave seizures

Neuronal activity gives rise to rapid changes in intra- and extracellular pH (Chesler, 1990, 2003; Chesler & Kaila, 1992). In turn, acidic or alkaline shifts in pH can modulate the activity of transporters and ion channels (Chesler, 1990, 2003; Chesler & Kaila, 1992). The pH-sensitive neurons of the midbrain and brainstem are critical examples of how pH-

dependent activity tightly controls the cardiorespiratory system (Del Negro et al., 2018; Guyenet et al., 2019; Guyenet & Bayliss, 2015; Guyenet & Mulkey, 2010; Pilowsky, 2014; Richerson, 2004). Moreover, several works support the hypothesis that dysfunction in these neuronal populations likely causes sudden unexpected death in epilepsy, (Aiba & Noebels, 2015; Jefferys et al., 2019; Kuo et al., 2019), congenital central hypoventilation syndrome (Goridis et al., 2010; Moreira et al., 2016; Rand et al., 2013) and sleep apnea (Guyenet & Abbott, 2013).

Below, I will reflect upon my study that focused on the relationship between absence seizures and hyperventilation (see **Chapter 4**). I will address how my findings support or clash with those of previous works that explored the effects of pH and blood gases on seizures. Moreover, I will address the hypothesis that neurons within the midline thalamus respond to changes in pH. In effect, my study has set-up the opportunity for future *in vivo* and *in vitro* experiments to explore thalamic pH-sensitivity and to unmask novel communication between the thalamus and pH-sensitive brain structures within the reticular activating system (Glenn & Steriade, 1982; Steriade & Glenn, 1982; Steriade, 1996, 1996).

Hyperventilation, hypocapnia and pH in epilepsy

Initially by chance, epilepsy provided the first glimpse into pH-modulation of brain activity. Seizure expression in the EEG provided a visual output to assess how varying blood gases altered seizures. Foerster and Rosett first observed that hyperventilation triggered absence seizures (Foerster, 1924; Rosett, 1924). Shortly thereafter, Lennox and colleagues recorded that inhalation of 10% CO_2 suppressed absence seizures in the EEG (Lennox, 1928; Lennox et al., 1936), thereby providing significant evidence that respiratory alkalosis (i.e. hypocapnia) is the likely trigger for absence seizures. Although hyperventilation associates most closely with absence seizures, I do direct your attention

to other evidence that associates hyperventilation as a trigger for partial complex seizures and temporal lobe seizures (Blume, 2006; Guaranha et al., 2005). However, hyperventilation does not evoke these seizures to nearly the same extent as it can in > 90% of absence epilepsy patients.

Hyperventilation rapidly induces hypocapnia and blood alkalosis in both epileptic and non-epileptic people and cats (Gibbs et al., 1940; Nims et al., 1940; Lavy & Carmon, 1967; Pirsch & McCrum, 1951; Sherwin, 1965), and induces delta-like oscillations in the EEG, an electrographic pattern known as HIHARS (Davis & Wallace, 1942; Lum et al., 2002; Yamatani et al., 1994). Additionally, hyperventilation causes hypocapnia. In the brain, hypocapnia slows cerebral blood flow and causes vasoconstriction (Achenbach-Ng et al., 1994; Meyer & Gotoh, 1960; Nwaigwe et al., 2000; Raichle & Plum, 1972). In contrast, hypercapnia increases blood flow and causes vasodilation (Bloch-Salisbury et al., 2000; Xu et al., 2011). The effects of hypocapnia and hypercapnia on neuronal activity are also distinct.

Neurophysiologists have found, in general, that hypocapnia increases excitation in the brain whereas hypercapnia suppresses activity (Balestrino & Somjen, 1988; Krnjević et al., 1965). Data from *in vitro* studies using acute brain slices have demonstrated that increasing CO_2 suppressed neuronal excitability (Dulla et al., 2005; Velísek et al., 1994). It is hypothesized that this result reflects pH-dependent modulation of voltage- and ligand-gated ion channels (Pasternack, 1995; Pasternack et al., 1996; Traynelis et al., 1995; Velísek et al., 1994) as well as purinergic signaling (Dulla et al., 2005, 2009).

Hypercapnia has proven very effective in the management of seizures. As I highlighted previously (**Chapter 4,** *Discussion*), the use of the carbonic anhydrase inhibitor, acetazolamide, has proven effective for the management of absence seizures and for seizures associated with other epilepsies (Reiss & Oles, 1996). The anti-seizure effects of CO_2 have also been demonstrated to reduce febrile seizures, temporal lobe

seizures and hypoxia-induced neonatal seizures in rodent models of these epilepsies (Ohmori et al., 2013; Schuchmann et al., 2006; Sun et al., 2016; Yang et al., 2016; Ziemann et al., 2008).

Based on these encouraging observations, how can CO_2 therapy be implemented in the clinic? A potential clinical application of CO_2 proposed by Tolner et al., is that CO_2 could be used as a means to arrest seizures in patients headed to the emergency room (Tolner et al., 2011). The authors showed that 5% CO_2 rapidly abated seizure progression shortly after seizure onset in 7 epilepsy patients (Tolner et al., 2011). A commentary on this study suggested that CO_2 could "prove to be an easy and inexpensive intervention for acute seizures in a hospital and at home" (Miller, 2011). I am optimistic that more clinical applications of CO_2 as an anti-convulsant will be discovered in the near future.

Coming back to my study presented in **Chapter 4**, my observations made from rats were consistent with prior studies that evaluated the connection between spike-wave seizures and blood gases in humans. I demonstrated that hypocapnia exacerbated and hypercapnia reduced seizures, respectively (see **Chapter 4, Figs. 1, 4**). Unlike the effect of low glucose on absence seizures (described in **Chapter 2**), the aforementioned evidence shows that hypercapnia/acidosis blunts spike-wave seizures as well as seizures related to other epilepsies. Although acidosis results in a similar outcome, I hypothesize that the cellular mechanisms invoked to respond to pH-changes within thalamocortical circuits are likely not identical to those of seizure nodes within the cortex and hippocampus.

At the moment, several mechanisms have been proposed that support acidosis as a seizure suppressant. First, in an elegant study by Dulla et al, the authors investigated the hypothesis that CO_2-mediated acidification suppresses epileptic activity by modulating purinergic signaling (Dulla et al., 2005). The authors showed that hypercapnia raised extracellular adenosine and led to enhanced activation of adenosine A_1 receptors.

Activated A_1 receptors limit excitation (Johansson et al., 2001; Masino & Dunwiddie, 1999) and reduce seizures (Boison et al., 2002). Indeed, hypercapnia enhanced A_1 receptor activation and lead to a reduction in epileptiform activity evoked in acute hippocampal slices (Dulla et al., 2005). Second, the authors tested whether the major metabolic source of adenosine, ATP, has any effect on reducing excitatory neurotransmission during hypercapnia. In blocking, P2X and P2Y receptors, hypercapnia-related inhibition of excitatory synaptic transmission was blunted. Collectively, these data advance the notion that hypercapnia exercises anti-seizure actions. Importantly, the authors also examined the effects of hypocapnia. They demonstrated that hypocapnia augmented neuronal excitation and epileptiform activity by inhibiting the actions of purines.

I emphasize this study in relation to my work because there is evidence for the purinergic system modulating thalamic network activity (Fontanez & Porter, 2006; Halassa, 2011; Ulrich & Huguenard, 1995). Detailing how purinergic signaling within the thalamus acts during hypocapnia to precipitate spike-wave seizures would be informative. I hypothesize that inhibition of adenosine signaling evoked by hypocapnia may lead to (1) enhanced glutamatergic transmission at thalamocortical synapses and (2) enhanced corticothalamic excitation onto reticular thalamic neurons and thalamocortical neurons. Both would increase the probability of a spike-wave seizure (Bal et al., 2000; Contreras et al., 1996). Of note, my hypothesis is largely based on work that used the accepted thalamocortical model of spike-wave seizures and not on activity observed within the midline thalamus. Nonetheless, any findings gleaned from studying modulation of thalamic purinergic signaling by hypocapnia would be novel.

Even though the above evidence supports acidosis as anti-seizure, I must address an important qualification: seizures cause extracellular acidosis (Siesjö et al., 1985; Somjen, 1984; Wang & Sonnenschein, 1955). For most epilepsies, seizure onset causes a rapid drop in extracellular pH that is sustained until seizure termination. Siesjö et al.

hypothesized that the initial acidification of the extracellular milieu results from spreading depolarization (Siesjö et al., 1985). Spreading depolarization causes a large flux in $[Na^+]_o$ that triggers Na^+/H^+ exchangers to extrude more H^+ into the extracellular space. The authors also propose that sustained extracellular acidosis stems from extracellular lactate pumped out by astrocytes. How then does acidosis work to inhibit seizures?

One proposed mechanism that depends on acidosis to terminate seizures is the acid-sensing ion channel, ASIC1α (Waldmann et al., 1997). Expression of ASIC1α in neurons (de la Rosa et al., 2003) and astrocytes (Yang et al., 2016) has been shown to terminate seizures in two mouse models of epilepsy (Yang et al., 2016; Ziemann et al., 2008). Moreover, when ASIC1α was knocked-down or knocked-out, seizures became worse (Yang et al., 2016; Ziemann et al., 2008). Whether ASIC1α channels function similarly in thalamocortical neurons during spike-wave seizures is unclear and worth investigating.

Many studies that have examined the buffering of CO_2/H^+ in the brain point to astrocytes as the principal pH gatekeepers. The balance of intra- and extra-cellular pH by astrocytes largely depends on the expression of the Na^+/HCO_3^- transporter, NBCe1 (Theparambil et al., 2017). The action of this transporter is hypothesized to be invoked during pH shifts associated with respiratory acidosis and alkalosis (Theparambil et al., 2017). A second work looked at the cooperative action between NBCe1 and the Na^+/Ca^{2+} transporter, NCX, in pH-sensitive astrocytes that reside in the ventral lateral medulla (Turovsky et al., 2016). For example, in instances of CO_2-induced intracellular acidosis, NBCe1 transports Na^+ and HCO_3^- into the astrocytes (Turovsky et al., 2016). In turn, this effect raises Na^+ inside the cell and causes NCX to activate in reverse mode, i.e. bringing Ca^{2+} in and Na^+ out (Turovsky et al., 2016). Increased intracellular Ca^{2+} consequently activates astrocytes and downstream gliotransmission that can modulate neuronal activity (Turovsky et al., 2016). I recommend that future studies target the function of astrocytes

in the midline thalamus to determine how pH-induced changes during hyperventilation influence astrocyte activity and their effects on thalamic neuron activity.

In effect, my study (**Chapter 4**) only scratches the surface of delineating a mechanism for hyperventilation-induced spike-wave seizures. Nonetheless, my creation of a rodent model that is capable of recapitulating the human response of hyperventilation-triggered spike-wave seizures is the first step to unlock the underlying mechanisms. Now with this model, many of the above hypotheses can be tested *in vivo* and *in vitro* to evaluate how hypercapnia and hypocapnia influence thalamic neuron and thalamocortical circuit activity.

Thalamic connectivity to pH sensitive structures of the reticular formation

Wakefulness, non-REM sleep and REM sleep characterize the three vigilance states of the brain and the thalamus actively participates in switching among these brain states. In early stages of sleep, thalamic neurons are generally hyperpolarized and fire in burst-mode to generate sleep-spindle oscillations (Steriade et al., 1993). Sleep-spindle oscillations are proposed to be modulated mainly by the synaptic activity among reticular thalamic neurons, thalamocortical neurons and neocortical neurons. In other brain states, the thalamus receives modulatory input from the ascending reticular activating system during wakefulness and REM sleep. Specifically, the intralaminar nuclei of the midline thalamus receive input from the ascending reticular activating system which originates within the brainstem reticular formation (Barth & MacDonald, 1996; Brown et al., 2012; Jones, 2020; Steriade, 1996a).

Indeed, the ascending reticular activating system has extremely diverse neuromodulatory input to the thalamus and these inputs stem from more than 50 brainstem and midbrain structures (Krout et al., 2002). Acetylcholine, norepinephrine, serotonin, histamine and glutamate are the five core neurotransmitters whose actions

transition thalamic activity into an “aroused state” (burst firing to tonic firing) (McCormick & Bal, 1997). I draw attention to the projections of the ascending reticular activating system because this system houses pH-sensitive structures. I hypothesize that input from these pH sensitive structures likely send projections to the same regions defined by my cFos staining following hyperventilation.

Anatomical studies have demonstrated that the chemosensitive structures, the dorsal and median raphé, send projections to nearly all of the midline and intralaminar nuclei (Krout et al., 2002; Krout & Loewy, 2000; Vertes, 1991). Thalamic neurons express a variety of 5-HT receptors (5-HT_{1A}, 5-HT_{2A}, 5-HT_{7} and likely others) whose downstream signaling acts on important ion channel conductances that modulate thalamic neuron membrane potential (Goaillard & Vincent, 2002; McCormick & Pape, 1990). Coincident with the expression of many different 5-HT receptors is the bidirectional actions of serotonin on thalamic neuron activity. Serotonin can be either excitatory or inhibitory depending on the cell-type and action of the target 5-HT receptor. In general, serotonin action in the thalamus evokes a hyperpolarizing response. However, there is evidence that serotonin depolarizes neurons as well. This effect is attributed to serotonin receptor signaling causing a shift in the voltage-dependence action of I_h (McCormick & Pape, 1990; Monckton & McCormick, 2002). Additionally, serotonin also can depolarize GABAergic interneurons (Monckton & McCormick, 2002). Markedly, neurons of the intralaminar and midline nuclei have the highest expression of the 5-HT_{7} receptor in the brain (Gustafson et al., 1996) and its expression facilitates tonic firing within these nuclei, which is an important activity mode necessary to induce arousal (Goaillard & Vincent, 2002). Taken together, serotonin release from the dorsal and median raphé have a considerable effect on thalamic neuron activity.

Special attention is directed to the dorsal and median raphé because they function as central chemoreceptors in the brain (Richerson, 2004; Severson et al., 2003). Like

neurons of the medullary raphé, midbrain raphé nuclei are also highly sensitive to changes in CO_2/pH and are stimulated by hypercapnia *in vivo* (Severson et al., 2003). How do pH changes modulate serotonergic input to the thalamus? I believe this is an important question to answer for two reasons. First, serotonergic projections localize to neurons within the midline and intralaminar nuclei wherein, cFos expression was increased after exposure to hypoxia-induced hyperventilation (**Chapter 4, Figure 6**). Second, the strength of serotonergic input from the dorsal and median raphé into the thalamus is likely affected by pH. How thalamic neuron activity is modulated by serotonin during instances of hypocapnia and hypercapnia is critical to understand, especially if these actions increase the likelihood for spike-wave seizures.

Future Directions

Undoubtedly, there are many different directions one can pursue based on my findings in **Chapter 4**. The implications of my work can initiate a range of projects from the cellular to the network level. Although my observations did not nail down a specific midline or intralaminar nucleus, I am hopeful that activity-dependent tools more sensitive than cFos can pinpoint the relevant structure(s). Below I suggest future directions that aim to parse the potential intrinsic pH-sensitive properties of midline thalamic neurons, the role of thalamic astrocytes in buffering pH changes and the crosstalk between the thalamus and the serotonergic inputs from the midbrain raphé. I believe these experiments will discern new mechanisms to explain the phenomenon of hyperventilation-induced spike-wave seizures.

1. *Measure intrathalamic PCO_2 and spike-wave seizures in WAG/Rij rats during different gas mixtures.* I propose that one adopts a multi-pronged approach that incorporates whole-body plethysmography, ECoG/EMG recordings and the use of a CO_2 probe that

can measure thalamic interstitial pH. Implanting a CO_2 probe into the midline thalamus will provide greater access to the changes in interstitial pH that occur with different gas mixtures. This experiment can be performed in the same gas conditions as described in **Chapter 4**. The design of this study was inspired by Jansen et al (Jansen et al., 2019). One can monitor real-time changes in pH on a time-scale concomitant with spike-wave seizure activity in the EEG. pH data gained from this study will inform one of the appropriate pH solutions to use for the experiments described in (2).

2. *Measure the effect of CO_2/pH on the intrinsic properties of midline thalamic neurons.* I suggest one analyze changes in thalamic neuron firing response, resting membrane potential, and input resistance in the pH conditions extracted from (1). This experiment will test the hypothesis that extracellular pH modulates the neuronal activity of midline thalamic neurons. Additionally, measuring the amplitude and frequency of spontaneous and mini post-synaptic excitatory and inhibitory currents will test the hypothesis that midline neurons are intrinsically pH sensitive and the hypothesis that their activity is modulated by synaptic excitation/inhibition from pH sensitive structures. To ensure that one is recording under the desired pH, neurons can be loaded with the pH-indicator BCECF-AM (Dulla et al., 2005; Ozkan & Mutharasan, 2002) before beginning the patch-clamp recording.

3. *Assess the functional expression of resident H^+ or HCO_3^+ exchangers/transporters in midline thalamic neurons.* As highlighted previously (**Chapter 4,** *Discussion*), the SLC family transporters have been demonstrated to enhance excitatory synaptic transmission in alkaline conditions (Sinning et al., 2011). Other works have associated other sodium exchangers with modulating epileptic activity (Cox et al., 1997; Sander et al., 2002; Sinning & Hübner, 2013). I suggest performing intracellular or perforated

patch-clamp recordings to evaluate ion flux in these transporters/channel in response to extracellular pH. Altering pH can be done by bubbling different gradients of CO_2 to mimic the changes in PCO_2 that reflect hypo- or hypercapnia.

4. *Assess bicarbonate buffer capacity of resident astrocytes in the midline thalamus.* Similar to the experiment outline in (3), one can examine the role of thalamic astrocytes in buffering interstitial pH. The primary transporters/exchangers to be evaluated are the Na^+/HCO_3^+, NBCe1, and the Na^+/Ca^{2+} calcium exchanger, NCX. I encourage one to adopt similar approaches that are detailed in these studies: Turovsky et al., 2016; Theparambil et al., 2017.

5. *Test the hypothesis that hypocapnia exacerbates spike-wave seizures through inhibition of purinergic signaling within the midline thalamus.* First, one can begin by evaluating the normal properties of purinergic signaling in the thalamus using pharmacological agonists and antagonists. Indeed, any insight gained from these preliminary experiments would be informative as this has not been well-characterized in midline thalamic neurons. I suggest using whole-cell patch-clamp recordings to evaluate the effect of adenosine on excitatory neurotransmission in midline thalamic neurons. Second, one would analyze the effects of hypocapnia and hypercapnia on adenosine-mediated excitatory neurotransmission using patch-clamp recording techniques done in a similar fashion as Dulla et al., 2005. Third, one can move *in vivo* to assess the effect of adenosine signaling on spike-wave seizure occurrence in the WAG/Rij rat independent of pH changes. This would address whether disruption in adenosine signaling is sufficient to precipitate spike-wave seizures.

6. *Test the hypothesis that activity changes in the midline thalamus are necessary to trigger hyperventilation-induced spike-wave seizures*. Using the inhibitory opsin, Archaerhodopsin, one can use optogenetics to inhibit midline thalamic neurons during hyperventilation. If photic inhibition of midline neurons suppresses the increase in seizures observed using 10 % hypoxia (see **Chapter 4, Figure 1**), then one can conclude that the midline thalamus is necessary to precipitate hypocapnic spike-wave seizures.

7. *Test the hypothesis the serotonergic input into the midline thalamus is necessary for hypercapnic suppression of spike-wave seizures.* I propose this experiment to first evaluate the effect of serotonergic input during instances of hypercapnia because the midbrain raphé is primarily sensitive to an increase in CO_2. The activity of midbrain raphé neurons during instances of hypocapnia is less-well understood. As in (6), one can use optogenetics to photo-inhibit neurons of the dorsal and median raphé during hypercapnia and evaluate the frequency of spike-wave seizures in the EEG. I hypothesize that the hypercapnic suppression of spike-wave seizures will be blunted. Alternatively, one can photo-activate the same neuronal populations in hypocapnia and assess whether this occludes hypocapnic-driven spike-wave seizures. Each experiment would be informative to understand whether members of the ascending reticular activating system can modulate spike-wave seizures.

Collectively, these experiments will initiate future projects that can use my rodent model of hyperventilation-induced spike-wave seizures. I am excited to learn what observations these forthcoming projects will discover regarding pH-dependent modulation of midline thalamic neurons and upon the greater activity of spike-wave seizure generating

thalamocortical circuits. Moreover, any revelations on how the ascending reticular activating system affects spike-wave seizures circuits will be groundbreaking.

Final remarks

My dissertation work is the first to study how environmental factors influence the probability of a patient having an absence seizure. I chose to evaluate the effects of metabolism and respiration on absence seizures as both factors had long-storied clinical observations of influencing absence seizure occurrence. My first study found that hypoglycemia likely invokes the action of activated AMPK to drive $GABA_B$ receptor-mediated activity to produce spike-wave seizures. Second, my foray into elucidating the mechanisms underlying spike-wave seizures provided evidence to support the observation that spike-wave seizures are modulated by CO_2. Moreover, I am the first to demonstrate that hyperventilation-induced seizures likely recruit neurons of the midline thalamus. Both investigations highlighted in my dissertation present novel findings on how daily fluctuations in dietary glucose and blood gases effect the probability of precipitating an absence seizure.

Though my observations mainly highlight how hypoglycemia and PCO_2 influence the basic properties of thalamic neuron and thalamocortical activity, I am hopeful that follow-up studies will take us a step-closer to developing new absence seizure therapies. If elements of metabolism and pH can be targeted directly to arrest spike-wave seizures, I believe this approach would help avoid the unfavorable side-effects of the currently available anti-absence seizure drugs.

References

Abrantes, H. de C., Briquet, M., Schmuziger, C., Restivo, L., Puyal, J., Rosenberg, N., Rocher, A.-B., Offermanns, S., & Chatton, J.-Y. (2019). The Lactate Receptor HCAR1 Modulates Neuronal Network Activity through the Activation of Gα and Gβγ Subunits. *Journal of Neuroscience*, *39*(23), 4422–4433. https://doi.org/10.1523/JNEUROSCI.2092-18.2019

Achenbach-Ng, J., Siao, T. C., Mavroudakis, N., Chiappa, K. H., & Kiers, L. (1994). Effects of routine hyperventilation on PCO2 and PO2 in normal subjects: Implications for EEG interpretations. *Journal of Clinical Neurophysiology: Official Publication of the American Electroencephalographic Society*, *11*(2), 220–225. https://doi.org/10.1097/00004691-199403000-00007

Aiba, I., & Noebels, J. L. (2015). Spreading depolarization in the brainstem mediates sudden cardiorespiratory arrest in mouse SUDEP models. *Science Translational Medicine*, *7*(282), 282ra46. https://doi.org/10.1126/scitranslmed.aaa4050

Arsov, T., Mullen, S. A., Rogers, S., Phillips, A. M., Lawrence, K. M., Damiano, J. A., Goldberg-Stern, H., Afawi, Z., Kivity, S., Trager, C., Petrou, S., Berkovic, S. F., & Scheffer, I. E. (2012). Glucose transporter 1 deficiency in the idiopathic generalized epilepsies. *Annals of Neurology*, *72*(5), 807–815. https://doi.org/10.1002/ana.23702

Bal, T., Debay, D., & Destexhe, A. (2000). Cortical feedback controls the frequency and synchrony of oscillations in the visual thalamus. *J. Neurosci.*, *20*, 7478–7488.

Balestrino, M., & Somjen, G. G. (1988). Concentration of carbon dioxide, interstitial pH and synaptic transmission in hippocampal formation of the rat. *The Journal of Physiology*, *396*, 247–266.

Barnes, N. M., & Sharp, T. (1999). A review of central 5-HT receptors and their function. *Neuropharmacology*, *38*(8), 1083–1152. https://doi.org/10.1016/s0028-3908(99)00010-6

Barth, D. S., & MacDonald, K. D. (1996). Thalamic modulation of high-frequency oscillating potentials in auditory cortex. *Nature*, *383*(6595), 78–81. https://doi.org/10.1038/383078a0

Beenhakker, M. P., & Huguenard, J. R. (2010). Astrocytes as Gatekeepers of GABAB Receptor Function. *Journal of Neuroscience*, *30*(45), 15262–15276. https://doi.org/10.1523/JNEUROSCI.3243-10.2010

Bélanger, M., Allaman, I., & Magistretti, P. J. (2011). Brain Energy Metabolism: Focus on Astrocyte-Neuron Metabolic Cooperation. *Cell Metabolism*, *14*(6), 724–738. https://doi.org/10.1016/j.cmet.2011.08.016

Bloch-Salisbury, E., Lansing, R., & Shea, S. A. (2000). Acute changes in carbon dioxide levels alter the electroencephalogram without affecting cognitive function. *Psychophysiology*, *37*(4), 418–426. https://doi.org/10.1111/1469-8986.3740418

Blume, W. T. (2006). Hyperventilation, More than Just Hot Air: *Epilepsy Currents*. https://journals.sagepub.com/doi/10.1111/j.1535-7511.2006.00103.x?url_ver=Z39.88-2003&rfr_id=ori%3Arid%3Acrossref.org&rfr_dat=cr_pub++0pubmed

Boison, D., Huber, A., Padrun, V., Déglon, N., Aebischer, P., & Möhler, H. (2002). Seizure Suppression by Adenosine-releasing Cells Is Independent of Seizure Frequency. *Epilepsia*, *43*(8), 788–796. https://doi.org/10.1046/j.1528-1157.2002.33001.x

Boucaud-Maitre, D., Ropers, J., Porokhov, B., Altman, J.-J., Bouhanick, B., Doucet, J., Girardin, E., Kaloustian, E., Lassmann Vague, V., & Emmerich, J. (2016). Lactic acidosis: Relationship between metformin levels, lactate concentration and

mortality. *Diabetic Medicine: A Journal of the British Diabetic Association*, *33*(11), 1536–1543. https://doi.org/10.1111/dme.13098

Brekke, E., Morken, T. S., & Sonnewald, U. (2015). Glucose metabolism and astrocyte–neuron interactions in the neonatal brain. *Neurochemistry International*, *82*, 33–41. https://doi.org/10.1016/j.neuint.2015.02.002

Brown, R. E., Basheer, R., McKenna, J. T., Strecker, R. E., & McCarley, R. W. (2012). Control of Sleep and Wakefulness. *Physiological Reviews*, *92*(3), 1087–1187. https://doi.org/10.1152/physrev.00032.2011

Brueggeman, L., Sturgeon, M. L., Martin, R. M., Grossbach, A. J., Nagahama, Y., Zhang, A., Howard, M. A., Kawasaki, H., Wu, S., Cornell, R. A., Michaelson, J. J., & Bassuk, A. G. (2019). Drug repositioning in epilepsy reveals novel antiseizure candidates. *Annals of Clinical and Translational Neurology*, *6*(2), 295–309. https://doi.org/10.1002/acn3.703

Chesler, M. (1990). The regulation and modulation of pH in the nervous system. *Progress in Neurobiology*, *34*(5), 401–427. http://dx.doi.org/10.1016/0301-0082(90)90034-E

Chesler, M. (2003). Regulation and Modulation of pH in the Brain. *Physiological Reviews*, *83*(4), 1183–1221. https://doi.org/10.1152/physrev.00010.2003

Chesler, M., & Kaila, K. (1992). Modulation of pH by neuronal activity. *Trends Neurosci*, *15*(10), 396–402. http://dx.doi.org/10.1016/0166-2236(92)90191-A

Contreras, D., Destexhe, A., Sejnowski, T. J., & Steriade, M. (1996). Control of Spatiotemporal Coherence of a Thalamic Oscillation by Corticothalamic Feedback. *Science*, *274*(5288), 771–774. https://doi.org/10.1126/science.274.5288.771

Cox, G. A., Lutz, C. M., Yang, C.-L., Biemesderfer, D., Bronson, R. T., Fu, A., Aronson, P. S., Noebels, J. L., & Frankel, W. N. (1997). Sodium/Hydrogen Exchanger

Gene Defect in Slow-Wave Epilepsy Mutant Mice. *Cell*, *91*(1), 139–148. https://doi.org/10.1016/S0092-8674(01)80016-7

Crunelli, V., & Leresche, N. (1991). A role for GABAB receptors in excitation and inhibition of thalamocortical cells. *Trends in Neurosciences*, *14*(1), 16–21. https://doi.org/10.1016/0166-2236(91)90178-W

Davis, H., & Wallace, W. McL. (1942). Factors affecting changes in the EEG by standardized hyperventilation. *Archives of Neurology and Psychiatry*, *47*, 606–625.

de la Rosa, D. A., Krueger, S. R., Kolar, A., Shao, D., Fitzsimonds, R. M., & Canessa, C. M. (2003). Distribution, subcellular localization and ontogeny of ASIC1 in the mammalian central nervous system. *The Journal of Physiology*, *546*(Pt 1), 77–87. https://doi.org/10.1113/jphysiol.2002.030692

DeFronzo, R., Fleming, G. A., Chen, K., & Bicsak, T. A. (2016). Metformin-associated lactic acidosis: Current perspectives on causes and risk. *Metabolism: Clinical and Experimental*, *65*(2), 20–29. https://doi.org/10.1016/j.metabol.2015.10.014

Del Negro, C. A., Funk, G. D., & Feldman, J. L. (2018). Breathing matters. *Nature Reviews Neuroscience*, *19*(6), 351–367. https://doi.org/10.1038/s41583-018-0003-6

Dienel, G. A. (2018). Brain Glucose Metabolism: Integration of Energetics with Function. *Physiological Reviews*, *99*(1), 949–1045. https://doi.org/10.1152/physrev.00062.2017

Dulla, C. G., Dobelis, P., Pearson, T., Frenguelli, B. G., Staley, K. J., & Masino, S. A. (2005). Adenosine and ATP Link P(CO(2)) to Cortical Excitability via pH. *Neuron*, *48*(6), 1011–1023. https://doi.org/10.1016/j.neuron.2005.11.009

Dulla, C. G., Frenguelli, B. G., Staley, K. J., & Masino, S. A. (2009). Intracellular Acidification Causes Adenosine Release During States of Hyperexcitability in the

Hippocampus. *Journal of Neurophysiology*, *102*(3), 1984–1993. https://doi.org/10.1152/jn.90695.2008

Foerster, O. (1924). Hyperventilationsepilepsie. *Deut Ztschr Nervenheilk*, *83*, 347–356.

Fontanez, D. E., & Porter, J. T. (2006). Adenosine A1 receptors decrease thalamic excitation of inhibitory and excitatory neurons in the barrel cortex. *Neuroscience*, *137*(4), 1177–1184. https://doi.org/10.1016/j.neuroscience.2005.10.022

French, J. A., & Pedley, T. A. (2009, June 6). *Initial Management of Epilepsy* (world) [N-clinical-practice]. Http://Dx.Doi.Org/10.1056/NEJMcp0801738; Massachusetts Medical Society. https://doi.org/10.1056/NEJMcp0801738

Garriga-Canut, M., Schoenike, B., Qazi, R., Bergendahl, K., Daley, T. J., Pfender, R. M., Morrison, J. F., Ockuly, J., Stafstrom, C., Sutula, T., & Roopra, A. (2006). 2-Deoxy-D-glucose reduces epilepsy progression by NRSF-CtBP-dependent metabolic regulation of chromatin structure. *Nature Neuroscience*, *9*(11), 1382–1387. https://doi.org/10.1038/nn1791

Gibbs, E., Lennox, W., & Gibbs, F. (1940). Variations in the cabon dioxide content of the blood in epilepsy. *Archives of Neurology and Psychiatry*, *43*, 223–239.

Gibbs, F. A., Gibbs, E. L., & Lennox, W. G. (1939). Influence of the blood sugar on the wave and spike formation in petit mal epilepsy. *Archives of Neurology & Psychiatry*, *41*(6), 1111–1116. https://doi.org/10.1001/archneurpsyc.1939.02270180039002

Glauser, T. A., Cnaan, A., Shinnar, S., Hirtz, D. G., Dlugos, D., Masur, D., Clark, P. O., & Adamson, P. C. (2013). Ethosuximide, valproic acid, and lamotrigine in childhood absence epilepsy: Initial monotherapy outcomes at 12 months. *Epilepsia*, *54*(1), 141–155. https://doi.org/10.1111/epi.12028

Glenn, L. L., & Steriade, M. (1982). Discharge rate and excitability of cortically projecting intralaminar thalamic neurons during waking and sleep states. *Journal of*

Neuroscience, *2*(10), 1387–1404. https://doi.org/10.1523/JNEUROSCI.02-10-01387.1982

Goaillard, J.-M., & Vincent, P. (2002). Serotonin suppresses the slow afterhyperpolarization in rat intralaminar and midline thalamic neurones by activating 5-HT7 receptors. *The Journal of Physiology*, *541*(2), 453–465. https://doi.org/10.1113/jphysiol.2001.013896

Goridis, C., Dubreuil, V., Thoby-Brisson, M., Fortin, G., & Brunet, J.-F. (2010). Phox2b, congenital central hypoventilation syndrome and the control of respiration. *Seminars in Cell & Developmental Biology*, *21*(8), 814–822. https://doi.org/10.1016/j.semcdb.2010.07.006

Groomes, L. B., Pyzik, P. L., Turner, Z., Dorward, J. L., Goode, V. H., & Kossoff, E. H. (2011). Do Patients With Absence Epilepsy Respond to Ketogenic Diets? *Journal of Child Neurology*, *26*(2), 160–165. https://doi.org/10.1177/0883073810376443

Guaranha, M. S. B., Garzon, E., Buchpiguel, C. A., Tazima, S., Yacubian, E. M. T., & Sakamoto, A. C. (2005). Hyperventilation revisited: Physiological effects and efficacy on focal seizure activation in the era of video-EEG monitoring. *Epilepsia*, *46*(1), 69–75. https://doi.org/10.1111/j.0013-9580.2005.11104.x

Gustafson, E. L., Durkin, M. M., Bard, J. A., Zgombick, J., & Branchek, T. A. (1996). A receptor autoradiographic and in situ hybridization analysis of the distribution of the 5-ht7 receptor in rat brain. *British Journal of Pharmacology*, *117*(4), 657–666.

Guyenet, P. G., & Abbott, S. B. G. (2013). Chemoreception and asphyxia-induced arousal. *Respiratory Physiology & Neurobiology*, *188*(3), 333–343. https://doi.org/10.1016/j.resp.2013.04.011

Guyenet, P. G., & Bayliss, D. A. (2015). Neural Control of Breathing and CO2 Homeostasis. *Neuron*, *87*(5), 946–961. http://dx.doi.org/10.1016/j.neuron.2015.08.001

Guyenet, P. G., & Mulkey, D. K. (2010). Retrotrapezoid nucleus and parafacial respiratory group. *Respiratory Physiology & Neurobiology*, *173*(3), 244–255. https://doi.org/10.1016/j.resp.2010.02.005

Guyenet, P. G., Stornetta, R. L., Souza, G. M. P. R., Abbott, S. B. G., Shi, Y., & Bayliss, D. A. (2019). The Retrotrapezoid Nucleus: Central Chemoreceptor and Regulator of Breathing Automaticity. *Trends in Neurosciences*, *42*(11), 807–824. https://doi.org/10.1016/j.tins.2019.09.002

Halassa, M. M. (2011). Thalamocortical dynamics of sleep: Roles of purinergic neuromodulation. *Seminars in Cell & Developmental Biology*, *22*(2), 245–251. https://doi.org/10.1016/j.semcdb.2011.02.008

Hussein, A. M., Eldosoky, M., El-Shafey, M., El-Mesery, M., Ali, A. N., Abbas, K. M., & Abulseoud, O. A. (2019). Effects of metformin on apoptosis and α-synuclein in a rat model of pentylenetetrazole-induced epilepsy. *Canadian Journal of Physiology and Pharmacology*, *97*(1), 37–46. https://doi.org/10.1139/cjpp-2018-0266

Jansen, N. A., Schenke, M., Voskuyl, Rob. A., Thijs, R. D., van den Maagdenberg, A. M. J. M., & Tolner, E. A. (2019). Apnea Associated with Brainstem Seizures in *Cacna1a* ^{S218L} Mice Is Caused by Medullary Spreading Depolarization. *The Journal of Neuroscience*, *39*(48), 9633–9644. https://doi.org/10.1523/JNEUROSCI.1713-19.2019

Jefferys, J. G. R., Arafat, M. A., Irazoqui, P. P., & Lovick, T. A. (2019). Brainstem activity, apnea, and death during seizures induced by intrahippocampal kainic acid in anaesthetized rats. *Epilepsia*, *60*(12), 2346–2358. https://doi.org/10.1111/epi.16374

Johansson, B., Halldner, L., Dunwiddie, T. V., Masino, S. A., Poelchen, W., Giménez-Llort, L., Escorihuela, R. M., Fernández-Teruel, A., Wiesenfeld-Hallin, Z., Xu, X.-

J., Hårdemark, A., Betsholtz, C., Herlenius, E., & Fredholm, B. B. (2001). Hyperalgesia, anxiety, and decreased hypoxic neuroprotection in mice lacking the adenosine A1 receptor. *Proceedings of the National Academy of Sciences*, *98*(16), 9407–9412. https://doi.org/10.1073/pnas.161292398

Jones, B. E. (2020). Arousal and sleep circuits. *Neuropsychopharmacology*, *45*(1), 6–20. https://doi.org/10.1038/s41386-019-0444-2

Kim, H. R., Kim, G.-H., Eun, S.-H., Eun, B.-L., & Byeon, J. H. (2015). Therapeutic Outcomes and Prognostic Factors in Childhood Absence Epilepsy. *J Clin Neurol*, *11*.

Kovács, Z., D'Agostino, D. P., Diamond, D. M., & Ari, C. (2019). Exogenous Ketone Supplementation Decreased the Lipopolysaccharide-Induced Increase in Absence Epileptic Activity in Wistar Albino Glaxo Rijswijk Rats. *Frontiers in Molecular Neuroscience*, *12*. https://doi.org/10.3389/fnmol.2019.00045

Kristopher, J. B., & Carl, E. S. (2010). The Ketogenic Diet. In *Epilepsy* (pp. 417–439). CRC Press.

Krnjević, K., Randić, M., & Siesjö, B. K. (1965). Cortical CO2 tension and neuronal excitability. *The Journal of Physiology*, *176*(1), 105–122.

Krout, K. E., Belzer, R. E., & Loewy, A. D. (2002). Brainstem projections to midline and intralaminar thalamic nuclei of the rat. *The Journal of Comparative Neurology*, *448*(1), 53–101. https://doi.org/10.1002/cne.10236

Krout, K. E., & Loewy, A. D. (2000). Parabrachial nucleus projections to midline and intralaminar thalamic nuclei of the rat. *The Journal of Comparative Neurology*, *428*(3), 475–494. https://doi.org/10.1002/1096-9861(20001218)428:3<475::AID-CNE6>3.0.CO;2-9

Kuo, F.-S., Cleary, C. M., LoTurco, J. J., Chen, X., & Mulkey, D. K. (2019). Disordered breathing in a mouse model of Dravet syndrome. *ELife*, *8*, e43387. https://doi.org/10.7554/eLife.43387

Kuramoto, N., Wilkins, M. E., Fairfax, B. P., Revilla-Sanchez, R., Terunuma, M., Tamaki, K., Iemata, M., Warren, N., Couve, A., Calver, A., Horvath, Z., Freeman, K., Carling, D., Huang, L., Gonzales, C., Cooper, E., Smart, T. G., Pangalos, M. N., & Moss, S. J. (2007). Phospho-Dependent Functional Modulation of GABAB Receptors by the Metabolic Sensor AMP-Dependent Protein Kinase. *Neuron*, *53*(2), 233–247. https://doi.org/10.1016/j.neuron.2006.12.015

Lavy, S., & Carmon, A. (1967). The effect of 5 per cent CO2 inhalation on the functional and metabolic activity of the cortex in cerveau isolé preparations. *Electroencephalography and Clinical Neurophysiology*, *22*(6), 590.

Lennox, W. G. (1928). The effect on epileptic seizures of varying composition of respired air. *J. Clin. Investigation*, *6*, 6–23.

Lennox, William G., Gibbs, F. A., & Gibbs, E. L. (1936). EFFECT ON THE ELECTRO-ENCEPHALOGRAM OF DRUGS AND CONDITIONS WHICH INFLUENCE SEIZURES. *Archives of Neurology & Psychiatry*, *36*(6), 1236–1250. https://doi.org/10.1001/archneurpsyc.1936.02260120083006

Lu, A. C., Lee, C. K., Kleiman-Weiner, M., Truong, B., Wang, M., Huguenard, J. R., & Beenhakker, M. P. (2020). Nonlinearities between inhibition and T-type calcium channel activity bidirectionally regulate thalamic oscillations. *ELife*, *9*, e59548. https://doi.org/10.7554/eLife.59548

Lum, L. M., Connolly, M. B., Farrell, K., & Wong, P. K. H. (2002). Hyperventilation-induced High-amplitude Rhythmic Slowing with Altered Awareness: A Video-EEG Comparison with Absence Seizures. *Epilepsia (Series 4)*, *43*(11), 1372–1378. https://doi.org/10.1046/j.1528-1157.2002.35101.x

Lutas, A., & Yellen, G. (2013). The ketogenic diet: Metabolic influences on brain excitability and epilepsy. *Trends Neurosci*, *36*(1), 32–40. https://doi.org/10.1016/j.tins.2012.11.005

Ma, W., Berg, J., & Yellen, G. (2007). Ketogenic Diet Metabolites Reduce Firing in Central Neurons by Opening KATP Channels. *The Journal of Neuroscience*, *27*(14), 3618–3625. https://doi.org/10.1523/jneurosci.0132-07.2007

Magistretti, P. J., & Allaman, I. (2015). A Cellular Perspective on Brain Energy Metabolism and Functional Imaging. *Neuron*, *86*(4), 883–901. https://doi.org/10.1016/j.neuron.2015.03.035

Magistretti, P. J., & Allaman, I. (2018). Lactate in the brain: From metabolic end-product to signalling molecule. *Nature Reviews Neuroscience*, *19*, 235. https://doi.org/10.1038/nrn.2018.19

Manford, M. (2017). Recent advances in epilepsy. *Journal of Neurology*, *264*(8), 1811–1824. https://doi.org/10.1007/s00415-017-8394-2

Masino, S. A., & Dunwiddie, T. V. (1999). Temperature-Dependent Modulation of Excitatory Transmission in Hippocampal Slices Is Mediated by Extracellular Adenosine. *Journal of Neuroscience*, *19*(6), 1932–1939. https://doi.org/10.1523/JNEUROSCI.19-06-01932.1999

Masino, S. A., & Rho, J. M. (2012). Mechanisms of Ketogenic Diet Action. In J. L. Noebels, M. Avoli, M. A. Rogawski, R. W. Olsen, & A. V. Delgado-Escueta (Eds.), *Jasper's Basic Mechanisms of the Epilepsies* (4th ed.). National Center for Biotechnology Information (US). http://www.ncbi.nlm.nih.gov/books/NBK98219/

Matricardi, S., Verrotti, A., Chiarelli, F., Cerminara, C., & Curatolo, P. (2014). Current Advances in Childhood Absence Epilepsy. *Pediatric Neurology*, *50*(3), 205–212. http://dx.doi.org/10.1016/j.pediatrneurol.2013.10.009

McCormick, D A, & Pape, H. C. (1990). Noradrenergic and serotonergic modulation of a hyperpolarization-activated cation current in thalamic relay neurones. *The Journal of Physiology*, *431*(1), 319–342. https://doi.org/10.1113/jphysiol.1990.sp018332

McCormick, David A., & Bal, T. (1997). SLEEP AND AROUSAL: Thalamocortical Mechanisms. *Annual Review of Neuroscience*, *20*(1), 185–215. https://doi.org/10.1146/annurev.neuro.20.1.185

Mehrabi, S., Sanadgol, N., Barati, M., Shahbazi, A., Vahabzadeh, G., Barzroudi, M., Seifi, M., Gholipourmalekabadi, M., & Golab, F. (2018). Evaluation of metformin effects in the chronic phase of spontaneous seizures in pilocarpine model of temporal lobe epilepsy. *Metabolic Brain Disease*, *33*(1), 107–114. https://doi.org/10.1007/s11011-017-0132-z

Meyer, J. S., & Gotoh, F. (1960). Hyperventilation and the electroencephalogram. Recording brain oxygen and carbon dioxide tensions, pH, EEG and blood flow during hyperventilation. *Transactions of the American Neurological Association*, *85*, 155–160.

Miller, J. W. (2011). Stopping Seizures With Carbon Dioxide. *Epilepsy Currents*, *11*(4), 114–115. https://doi.org/10.5698/1535-7511-11.4.114

Monckton, J. E., & McCormick, D. A. (2002). Neuromodulatory Role of Serotonin in the Ferret Thalamus. *Journal of Neurophysiology*, *87*(4), 2124–2136. https://doi.org/10.1152/jn.00650.2001

Moreira, T. S., Takakura, A. C., Czeisler, C., & Otero, J. J. (2016). Respiratory and autonomic dysfunction in congenital central hypoventilation syndrome. *Journal of Neurophysiology*, *116*(2), 742–752. https://doi.org/10.1152/jn.00026.2016

Mullen, S. A., Suls, A., Jonghe, P. D., Berkovic, S. F., & Scheffer, I. E. (2010). Absence epilepsies with widely variable onset are a key feature of familial GLUT1

deficiency. *Neurology*, *75*(5), 432–440. https://doi.org/10.1212/WNL.0b013e3181eb58b4

Nehlig, A., Dufour, F., Klinger, M., Willing, L. B., Simpson, I. A., & Vannucci, S. J. (2009). The ketogenic diet has no effect on the expression of spike-and-wave discharges and nutrient transporters in genetic absence epilepsy rats from Strasbourg. *Journal of Neurochemistry*, *109*, 207–213. https://doi.org/10.1111/j.1471-4159.2009.05938.x

Nims, L. F., Gibbs, E. L., Lennox, W. G., Gibbs, F. A., & Williams, D. (1940). Adjustment of Acid-Base Balance of Patients with Petit Mal Epilepsy to Overventilation. *Archives of Neurology and Psychiatry*, *43*(2), 262–269.

Nwaigwe, C. I., Roche, M. A., Grinberg, O., & Dunn, J. F. (2000). Effect of hyperventilation on brain tissue oxygenation and cerebrovenous PO2 in rats. *Brain Research*, *868*(1), 150–156. http://dx.doi.org/10.1016/S0006-8993(00)02321-0

Ohmori, I., Hayashi, K., Wang, H., Ouchida, M., Fujita, N., Inoue, T., Michiue, H., Nishiki, T., & Matsui, H. (2013). Inhalation of 10% carbon dioxide rapidly terminates Scn1a mutation-related hyperthermia-induced seizures. *Epilepsy Research*, *105*(1), 220–224. https://doi.org/10.1016/j.eplepsyres.2013.01.003

Ozkan, P., & Mutharasan, R. (2002). A rapid method for measuring intracellular pH using BCECF-AM. *Biochimica Et Biophysica Acta*, *1572*(1), 143–148. https://doi.org/10.1016/s0304-4165(02)00303-3

Pan, Y.-Z., Sutula, T. P., & Rutecki, P. A. (2019). 2-Deoxy-d-glucose reduces epileptiform activity by presynaptic mechanisms. *Journal of Neurophysiology*, *121*(4), 1092–1101. https://doi.org/10.1152/jn.00723.2018

Pasternack, M. (1995). Intracellular carbonic anhydrase and its role in GABA-induced acidosis in isolated rat hippocampal pyramidal neurons. *Act Physiol Scand*, *148*, 229–231.

Pasternack, M., Smirnov, S., & Kaila, K. (1996). Proton Modulation of Functionally Distinct GABAA Receptors in Acutely Isolated Pyramidal Neurons of Rat Hippocampus. *Neuropharmacology*, *35*(9), 1279–1288. https://doi.org/10.1016/S0028-3908(96)00075-5

Pilowsky, P. M. (2014). Peptides, serotonin, and breathing: The role of the raphe in the control of respiration. *Progress in Brain Research*, *209*, 169–189. https://doi.org/10.1016/B978-0-444-63274-6.00009-6

Pirsch, J. G., & McCrum, W. R. (1951). Effect of varied CO2 concentrations of respired air on the EEG of the cat. *Proceedings of the Society for Experimental Biology and Medicine. Society for Experimental Biology and Medicine (New York, N.Y.)*, *78*(2), 430–431. https://doi.org/10.3181/00379727-78-19093

Raichle, M. E., & Plum, F. (1972). Hyperventilation and Cerebral Blood Flow. *Stroke*, *3*(5), 566–575. https://doi.org/10.1161/01.STR.3.5.566

Rand, C. M., Patwari, P. P., Carroll, M. S., & Weese-Mayer, D. E. (2013). Congenital Central Hypoventilation Syndrome and Sudden Infant Death Syndrome: Disorders of Autonomic Regulation. *Seminars in Pediatric Neurology*, *20*(1), 44–55. https://doi.org/10.1016/j.spen.2013.01.005

Regehr, W. G. (2012). Short-Term Presynaptic Plasticity. *Cold Spring Harbor Perspectives in Biology*, *4*(7), a005702. https://doi.org/10.1101/cshperspect.a005702

Reiss, W. G., & Oles, K. S. (1996). Acetazolamide in the Treatment of Seizures. *Annals of Pharmacotherapy*, *30*(5), 514–519. https://doi.org/10.1177/106002809603000515

Rho, J. M., Shao, L.-R., & Stafstrom, C. E. (2019). 2-Deoxyglucose and Beta-Hydroxybutyrate: Metabolic Agents for Seizure Control. *Frontiers in Cellular Neuroscience*, *13*. https://doi.org/10.3389/fncel.2019.00172

Richerson, G. B. (2004). Serotonergic neurons as carbon dioxide sensors that maintain ph homeostasis. *Nat Rev Neurosci*, *5*(6), 449–461.

Rosett, J. (1924). The experimental production of rigidity, of abnormal involuntary movements and of abnormal states of consciousness in man. *Brain*, *47*, 293–336.

Ross, D. L., Swaiman, K. F., Torres, F., & Hansen, J. (1985). Early biochemical and EEG correlates of the ketogenic diet in children with atypical absence epilepsy. *Pediatric Neurology*, *1*(2), 104–108. http://dx.doi.org/10.1016/0887-8994(85)90045-1

Rubio Osornio, M. del C., Custodio Ramírez, V., Calderón Gámez, D., Paz Tres, C., Carvajal Aguilera, K. G., & Phillips Farfán, B. V. (2018). Metformin Plus Caloric Restriction Show Anti-epileptic Effects Mediated by mTOR Pathway Inhibition. *Cellular and Molecular Neurobiology*, *38*(7), 1425–1438. https://doi.org/10.1007/s10571-018-0611-8

Ruskin, D. N., & Masino, S. A. (2012). The nervous system and metabolic dysregulation: Emerging evidence converges on ketogenic diet therapy. *Frontiers in Neuroscience*, *6*. https://doi.org/10.3389/fnins.2012.00033

Sander, T., Toliat, M. R., Heils, A., Leschik, G., Becker, C., Rüschendorf, F., Rohde, K., Mundlos, S., & Nürnberg, P. (2002). Association of the 867Asp variant of the human anion exchanger 3 gene with common subtypes of idiopathic generalized epilepsy. *Epilepsy Research*, *51*(3), 249–255. https://doi.org/10.1016/S0920-1211(02)00152-3

Schuchmann, S., Schmitz, D., Rivera, C., Vanhatalo, S., Salmen, B., Mackie, K., Sipila, S. T., Voipio, J., & Kaila, K. (2006). Experimental febrile seizures are precipitated by a hyperthermia-induced respiratory alkalosis. *Nat Med*, *12*(7), 817–823. http://www.nature.com/nm/journal/v12/n7/suppinfo/nm1422_S1.html

Severson, C. A., Wang, W., Pieribone, V. A., Dohle, C. I., & Richerson, G. B. (2003). Midbrain serotonergic neurons are central pH chemoreceptors. *Nature Neuroscience*, *6*(11), 1139–1140. https://doi.org/10.1038/nn1130

Sherwin, I. (1965). Differential effects of hyperventillation on the excitability of intact and isolated cortex. *Electroencephalography and Clinical Neurophysiology*, *18*(6), 599–607. https://doi.org/10.1016/0013-4694(65)90077-5

Siesjö, B. K., von Hanwehr, R., Nergelius, G., Nevander, G., & Ingvar, M. (1985). Extra- and Intracellular pH in the Brain during Seizures and in the Recovery Period following the Arrest of Seizure Activity. *Journal of Cerebral Blood Flow & Metabolism*, *5*(1), 47–57. https://doi.org/10.1038/jcbfm.1985.7

Sinning, A., Liebmann, L., Kougioumtzes, A., Westermann, M., Bruehl, C., & Hubner, C. A. (2011). Synaptic Glutamate Release Is Modulated by the Na+-Driven Cl-/HCOFormula Exchanger Slc4a8. *Journal of Neuroscience*, *31*(20), 7300–7311. https://doi.org/10.1523/JNEUROSCI.0269-11.2011

Sinning, Anne, & Hübner, C. A. (2013). Minireview: PH and synaptic transmission. *FEBS Letters*, *587*(13), 1923–1928. https://doi.org/10.1016/j.febslet.2013.04.045

Somjen, G. G. (1984). Acidification of interstitial fluid in hippocampal formation caused by seizures and by spreading depression. *Brain Research*, *311*(1), 186–188. https://doi.org/10.1016/0006-8993(84)91416-1

Stafstrom, C. E., Ockuly, J. C., Murphree, L., Valley, M. T., Roopra, A., & Sutula, T. P. (2009). ANTICONVULSANT AND ANTIEPILEPTIC ACTIONS OF 2-DEOXY-

DGLUCOSE IN EPILEPSY MODELS. *Annals of Neurology*, *65*(4), 435–447. https://doi.org/10.1002/ana.21603

Stafstrom, C. E., Roopra, A., & Sutula, T. P. (2008). Seizure suppression via glycolysis inhibition with 2-deoxy-D-glucose (2DG). *Epilepsia*, *49*, 97–100. https://doi.org/10.1111/j.1528-1167.2008.01848.x

Steriade, M., & Glenn, L. L. (1982). Neocortical and caudate projections of intralaminar thalamic neurons and their synaptic excitation from midbrain reticular core. *Journal of Neurophysiology*, *48*(2), 352–371. https://doi.org/10.1152/jn.1982.48.2.352

Steriade, M., McCormick, D. A., & Sejnowski, T. J. (1993). Thalamocortical oscillations in the sleeping and aroused brain. *Science*, *262*(5134), 679–685. https://doi.org/10.1126/science.8235588

Steriade, Mircea. (1996a). Arousal—Revisiting the Reticular Activating System. *Science*, *272*(5259), 225–225. https://doi.org/10.1126/science.272.5259.225

Steriade, Mircea. (1996b). Awakening the brain. *Nature*, *383*(6595), 24–25. https://doi.org/10.1038/383024a0

Sun, H., Juul, H. M., & Jensen, F. E. (2016). Models of hypoxia and ischemia-induced seizures. *Journal of Neuroscience Methods*, *260*, 252–260. http://dx.doi.org/10.1016/j.jneumeth.2015.09.023

Taher, M., Leen, W. G., Wevers, R. A., & Willemsen, M. A. (2016). Lactate and its many faces. *European Journal of Paediatric Neurology*, *20*(1), 3–10. https://doi.org/10.1016/j.ejpn.2015.09.008

Tanner, G. R., Lutas, A., Martínez-François, J. R., & Yellen, G. (2011). Single KATP Channel Opening in Response to Action Potential Firing in Mouse Dentate Granule Neurons. *The Journal of Neuroscience*, *31*(23), 8689–8696. https://doi.org/10.1523/jneurosci.5951-10.2011

Thammongkol, S., Vears, D. F., Bicknell-Royle, J., Nation, J., Draffin, K., Stewart, K. G., Scheffer, I. E., & Mackay, M. T. (2012). Efficacy of the ketogenic diet: Which epilepsies respond? *Epilepsia*, *53*(3), e55–e59. https://doi.org/10.1111/j.1528-1167.2011.03394.x

Theparambil, S. M., Naoshin, Z., Defren, S., Schmaelzle, J., Weber, T., Schneider, H.-P., & Deitmer, J. W. (2017). Bicarbonate sensing in mouse cortical astrocytes during extracellular acid/base disturbances. *The Journal of Physiology*, *595*(8), 2569–2585. https://doi.org/10.1113/JP273394

Tolner, E. A., Hochman, D. W., Hassinen, P., Otáhal, J., Gaily, E., Haglund, M. M., Kubová, H., Schuchmann, S., Vanhatalo, S., & Kaila, K. (2011). 5% CO2 is a potent, fast acting inhalation anticonvulsant. *Epilepsia*, *52*(1), 104–114. https://doi.org/10.1111/j.1528-1167.2010.02731.x

Traynelis, S. F., Hartley, M., & Heinemann, S. F. (1995). Control of proton sensitivity of the NMDA receptor by RNA splicing and polyamines. *Science (New York, N.Y.)*, *268*(5212), 873–876. https://doi.org/10.1126/science.7754371

Turovsky, E., Theparambil, S. M., Kasymov, V., Deitmer, J. W., del Arroyo, A. G., Ackland, G. L., Corneveaux, J. J., Allen, A. N., Huentelman, M. J., Kasparov, S., Marina, N., & Gourine, A. V. (2016). Mechanisms of CO_2 /H^+ Sensitivity of Astrocytes. *The Journal of Neuroscience*, *36*(42), 10750–10758. https://doi.org/10.1523/JNEUROSCI.1281-16.2016

Ulrich, D., & Huguenard, J. R. (1995). Purinergic inhibition of GABA and glutamate release in the thalamus: Implications for thalamic network activity. *Neuron*, *15*(4), 909–918. https://doi.org/10.1016/0896-6273(95)90181-7

Velísek, L., Dreier, J. P., Stanton, P. K., Heinemann, U., & Moshé, S. L. (1994). Lowering of extracellular pH suppresses low-Mg(2+)-induces seizures in

combined entorhinal cortex-hippocampal slices. *Experimental Brain Research*, *101*(1), 44–52. https://doi.org/10.1007/BF00243215

Vergnes, M., Boehrer, A., Simler, S., Bernasconi, R., & Marescaux, C. (1997). Opposite effects of GABAB receptor antagonists on absences and convulsive seizures. *European Journal of Pharmacology*, *332*(3), 245–255. http://dx.doi.org/10.1016/S0014-2999(97)01085-6

Vertes, R. P. (1991). A PHA-L analysis of ascending projections of the dorsal raphe nucleus in the rat. *The Journal of Comparative Neurology*, *313*(4), 643–668. https://doi.org/10.1002/cne.903130409

Viollet, B., Guigas, B., Sanz Garcia, N., Leclerc, J., Foretz, M., & Andreelli, F. (2012). Cellular and molecular mechanisms of metformin: An overview. *Clinical Science (London, England : 1979)*, *122*(6), 253–270. https://doi.org/10.1042/CS20110386

von Krosigk, M., Bal, T., & McCormick, D. (1993). Cellular mechanisms of a synchronized oscillation in the thalamus. *Science*, *261*(5119), 361. https://doi.org/10.1126/science.8392750

Waldmann, R., Champigny, G., Bassilana, F., Heurteaux, C., & Lazdunski, M. (1997). A proton-gated cation channel involved in acid-sensing. *Nature*, *386*(6621), 173–177. https://doi.org/10.1038/386173a0

Wang, R. I. H., & Sonnenschein, R. R. (1955). PH OF CEREBRAL CORTEX DURING INDUCED CONVULSIONS. *Journal of Neurophysiology*, *18*(2), 130–137. https://doi.org/10.1152/jn.1955.18.2.130

Werry, T. D., Wilkinson, G. F., & Willars, G. B. (2003). Mechanisms of cross-talk between G-protein-coupled receptors resulting in enhanced release of intracellular Ca2+. *The Biochemical Journal*, *374*(Pt 2), 281–296. https://doi.org/10.1042/BJ20030312

Wick, A. N., Drury, D. R., Nakada, H. I., Wolfe, J. B., & Grabowski, W. the technical assistance of B. B. and R. (1957). Localization of the Primary Metabolic Block Produced by 2-Deoxyglucose. *Journal of Biological Chemistry*, *224*(2), 963–969.

Wilder RM. (1921). The effect of ketonemia on the course of epilepsy. *Mayo Clin Bulletin*, *2*, 2.

Wirrell, E. C., Camfield, P. R., Gordon, K. E., Camfield, C. S., Dooley, J. M., & Hanna, B. D. (1996). Will a Critical Level of Hyperventilation-Induced Hypocapnia Always Induce an Absence Seizure? *Epilepsia*, *37*(5), 459–462. https://doi.org/10.1111/j.1528-1157.1996.tb00592.x

Xu, F., Uh, J., Brier, M. R., Hart, J., Yezhuvath, U. S., Gu, H., Yang, Y., & Lu, H. (2011). The influence of carbon dioxide on brain activity and metabolism in conscious humans. *Journal of Cerebral Blood Flow & Metabolism*, *31*(1), 58–67. https://doi.org/10.1038/jcbfm.2010.153

Yamatani, M., Konishi, T., Murakami, M., & Okuda, T. (1994). Hyperventilation Activation on EEG Recording in Childhood. *Epilepsia*, *35*(6), 1199–1203. https://doi.org/10.1111/j.1528-1157.1994.tb01789.x

Yang, F., Sun, X., Ding, Y., Ma, H., Yang, T. O., Ma, Y., Wei, D., Li, W., Xu, T., & Jiang, W. (2016). Astrocytic Acid-Sensing Ion Channel 1a Contributes to the Development of Chronic Epileptogenesis. *Scientific Reports*, *6*(1), 31581. https://doi.org/10.1038/srep31581

Yang, Y., Zhu, B., Zheng, F., Li, Y., Zhang, Y., Hu, Y., & Wang, X. (2017). Chronic metformin treatment facilitates seizure termination. *Biochemical and Biophysical Research Communications*, *484*(2), 450–455. https://doi.org/10.1016/j.bbrc.2017.01.157

Yellen, G. (2008). Ketone bodies, glycolysis, and K(ATP) channels in the mechanism of the ketogenic diet. *Epilepsia*, *49*(Suppl 8), 80–82. https://doi.org/10.1111/j.1528-1167.2008.01843.x

Yudkoff, M., Daikhin, Y., Horyn, O., Nissim, I., & Nissim, I. (2012). *The Ketogenic Diet and Brain Metabolism Neural Metabolism In Vivo* (I.-Y. Choi & R. Gruetter, Eds.; Vol. 4, pp. 819–839). Springer US.

Zhao, R., Xu, X., Xu, F., Zhang, W., Zhang, W., Liu, L., & Wang, W. (2014). Metformin protects against seizures, learning and memory impairments and oxidative damage induced by pentylenetetrazole-induced kindling in mice. *Biochemical and Biophysical Research Communications*, *448*(4), 414–417. https://doi.org/10.1016/j.bbrc.2014.04.130

Ziemann, A. E., Schnizler, M. K., Albert, G. W., Severson, M. A., Howard, M. A., Welsh, M. J., & Wemmie, J. A. (2008). Seizure Termination by Acidosis Depends on ASIC1a. *Nature Neuroscience*, *11*(7), 816–822. https://doi.org/10.1038/nn.2132